

FDL-TDR-64-2  
PART I

# **PRESSURE AND HEAT TRANSFER MEASUREMENTS FOR MACH 8 FLOWS OVER A BLUNT PYRAMIDAL CONFIGURATION WITH AERODYNAMIC CONTROLS**

**PART I: PRESSURE DATA FOR DELTA WING SURFACE**

**DEPARTMENT OF AERONAUTICS  
U. S. Naval Postgraduate School  
Monterey, California**

TECHNICAL DOCUMENTARY REPORT No. FDL-TDR-64-2, PART I

JANUARY 1964

AIR FORCE FLIGHT DYNAMICS LABORATORY  
RESEARCH AND TECHNOLOGY DIVISION  
AIR FORCE SYSTEMS COMMAND  
WRIGHT-PATTERSON AIR FORCE BASE, OHIO

Project No. 8219, Task No. 821902

(Prepared under Contract No. AF 33(616)-8130 by the  
Research Department, Grumman Aircraft Engineering Corporation  
Bethpage, New York; Louis G. Kaufman II, author)

## NOTICES

When Government drawings, specifications, or other data are used for any purpose other than in connection with a definitely related Government procurement operation, the United States Government thereby incurs no responsibility nor any obligation whatsoever; and the fact that the Government may have formulated, furnished, or in any way supplied the said drawings, specifications, or other data, is not to be regarded by implication or otherwise as in any manner licensing the holder or any other person or corporation, or conveying any rights or permission to manufacture, use, or sell any patented invention that may in any way be related thereto.

Qualified requesters may obtain copies of this report from the Defense Documentation Center (DDC), (formerly ASTIA), Cameron Station, Bldg. 5, 5010 Duke Street, Alexandria 4, Virginia

This report has been released to the Office of Technical Services, U.S. Department of Commerce, Washington 25, D.C., in stock quantities for sale to the general public.

Copies of this report should not be returned to the Aeronautical Systems Division unless return is required by security considerations, contractual obligations, or notice on a specific document.

## FOREWORD

This report, written in four parts, presents the results of a portion of the experimental program for the investigation of hypersonic flow separation and control characteristics being conducted by the Research Department of Grumman Aircraft Engineering Corporation, Bethpage, New York. Messrs. Donald E. Hoak and Wilfred J. Klotzback of the Flight Control Division, Air Force Flight Dynamics Laboratory, Aeronautical Systems Division, located at Wright-Patterson Air Force Base, Ohio, are the Air Force Project Engineers for the program, which is being supported primarily under Contract AF33(616)8130, Air Force Task 821902.

The author wishes to express his appreciation to the staff of the von Karman Facility for their helpfulness in conducting the tests and particularly to Messrs. Schueler, Baer and Deitering for providing the machine plotted graphs of the experimental data included in this report. Ozalid reproducible copies of the tabulated data are available on loan from the Flight Control Division of the Air Force Flight Dynamics Laboratory.


The parts of this report are:

- Part I: Pressure Data for Delta Wing Surface
- Part II: Pressure Data for Dihedral Surfaces
- Part III: Heat Transfer Data for Delta Wing Surface
- Part IV: Heat Transfer Data for Dihedral Surfaces

## ABSTRACT

Pressure and heat transfer data were obtained for Mach 8 flows over a blunt pyramidal configuration composed of a 70 degree sweepback delta wing surface and two dihedral surfaces. Trailing edge flap deflections were varied up to 40 degrees on all surfaces, and the model was tested with and without canards and ventral fins. The model was pitched at angles of attack between  $\pm 54$  degrees and was tested at sideslip angles of 0 and 12 degrees for free stream Reynolds numbers, based on model length of 1.5 and 4.5 million.

This report has been reviewed and is approved.

  
CHARLES B. WESTBROOK  
Chief, Control Criteria Branch  
Flight Control Division  
Air Force Flight Dynamics Laboratory

## TABLE OF CONTENTS

<u>Item</u>	<u>Page</u>
Introduction .....	1
Model .....	1
Remote Control System for Flaps .....	3
Test Conditions .....	4
Data Reduction and Accuracy .....	5
Results .....	5
References .....	7

## LIST OF ILLUSTRATIONS

<u>Figure</u>	<u>Page</u>
1      General Outline of Models and Remarks for Over-all Program .....	19
2      Photographs of Model Installed in the AEDC 50-inch Mach 8 Tunnel .....	20
3      Model Instrumentation .....	22
4      Actuators for Remotely Controlled Flaps .....	25
5      Electrical Circuits for Remotely Controlled Flaps .....	26
6      Photograph of Flap Control and Indicator Panels ....	27
7-102   Pressure Coefficient Data Plots* .....	28

\*See Table II, p. 13, for figure numbers corresponding to particular test conditions.

# LIST OF SYMBOLS

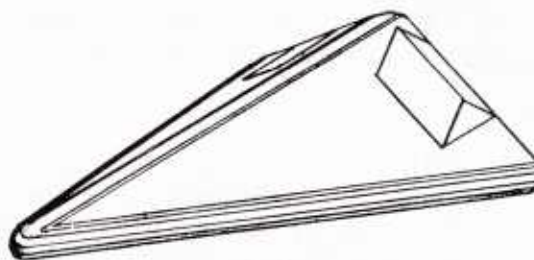
$C_p$	pressure coefficient, $C_p \equiv (p - p_\infty)/q_\infty$
$M_\infty$	free stream Mach number
$p$	pressure (psia)
$p_o$	stagnation pressure (psia)
$p_\infty$	free stream static pressure (psia)
$q_\infty$	free stream dynamic pressure (psia)
$Re_\infty/ft$	Reynolds number per foot, $Re_\infty/ft \equiv \rho_\infty U_\infty/\mu_\infty$
$T_o$	stagnation temperature ( $^{\circ}R$ )
$T_\infty$	free stream static temperature ( $^{\circ}R$ )
$U_\infty$	free stream velocity (ft/sec)
$X'$	nondimensional streamwise distance from virtual apex to planform projection (see Fig. 3)
$Y'$	nondimensional spanwise distance measured outboard from the model centerline
$\alpha$	angle of attack (degrees), positive for nose up
$\beta$	sideslip angle (degrees), positive for nose left
$\mu_\infty$	viscosity of air in the free stream (slugs/ft sec)
$\rho_\infty$	density of air in the free stream (slugs/ft <sup>3</sup> )



## INTRODUCTION

The experimental data generated for an investigation of hypersonic flow separation and aerodynamic control characteristics are to be presented in a series of reports, of which this is one. Pressure, heat transfer, and force data are to be obtained for hypersonic flows over "basic geometries," such as a wedge mounted on a flat plate, and for "typical" hypersonic flight configurations with aerodynamic control surfaces. The experimental portion of the program requires a total of 11 models (see Fig. 1, p. 19); 8 for tests in the von Karman Facility of the Arnold Engineering Development Center and 3 for tests in the Grumman Hypersonic Shock Tunnel (Refs. 1 and 2). Data obtained from AEDC tests of one of the models are given in this four part report (see Foreword).

This report (Part I) presents pressure data obtained in the AEDC 50-inch Mach 8 tunnel (Ref. 3) on the lower surface of a blunt pyramidal configuration having remotely controlled trailing edge flaps. Pressure data obtained on the dihedral surfaces of the model are presented in Part II, and heat transfer data obtained on the model are presented in Parts III and IV. The same model was tested in the AEDC 40-inch Supersonic Tunnel to obtain pressure distributions for Mach 5 flows (Ref. 4). A geometrically similar force model was tested at the same Mach numbers and at the same model length Reynolds numbers in both the 40-inch and 50-inch tunnels. A third geometrically similar model, with limited pressure and heat transfer instrumentation, is to be tested in the Grumman Hypersonic Shock Tunnel (see Fig. 1).



## MODEL

Photographs of the model installed in the 50-inch Mach 8 tunnel are shown in Fig. 2. The lower surface of the model is a blunt delta wing with 70 degree sweepback. The planar portions of the

---

Manuscript released by the author in November 1963  
for publication as an FDL Technical Documentary Report.



dihedral surfaces are right triangles and are connected by a cylindrical segment which forms the model's "ridge line." The three cylindrical leading edges and the spherical nose have the same radius (also the same as for Configuration "C" shown in Fig. 1). The cross-sectional shape is the same as one of the ASD — General Applied Sciences Laboratory pyramidal models tested in the AEDC Hotshot 2 hypervelocity facility (Ref. 5).

The model has four, remotely controlled, trailing edge flaps, one on each dihedral surface (both of which are deflected in Fig. 2), and two on the lower surface of the model. The two lower surface flaps are actuated as a pair and are always set at equal deflections. As shown in Fig. 3, the flaps have rectangular planforms, and their hinge lines are parallel to the base of the model (perpendicular to the ridge line). The chords of the remotely controlled flaps are 15 per cent of the virtual length of the model. The flaps are deflectable at angles between 0 and 40 degrees, measured in the planes normal to the flap hinge lines. In addition to the remotely controlled flaps, one pair of instrumented flaps having a set deflection of 20 degrees and a chord equal to 25 per cent of the model reference length are attachable to the lower surface of the model (see Fig. 3).

As indicated in Fig. 3, there are also attachable canards and a ventral fin for the model. The canards, shown attached to the model in Fig. 2, have cylindrical leading edges and 45 degree sweep-back. They are geometrically similar to the force model canards and have a planform area equal to that of the basic model from the nose to the trailing edge of the canards. The ventral fin is attachable in either of two positions on the lower surface of the model between the trailing edge flaps. The fin is wedge shaped (total wedge angle of 30 degrees), has a cylindrical leading edge, and is geometrically similar to the instrumented fin of Configuration "B" shown in Fig. 1. As indicated in Fig. 3, the fin can be set at fin (or rudder) deflection angles of 0 or +15 degrees (trailing edge left), and has a chord equal to 15 per cent of the model reference length.

Pressure tap and thermocouple locations are shown in Fig. 3. There are 5 streamwise lines of pressure taps on the lower surface; 8 taps are on the centerline of the lower surface and 10 taps are positioned along a streamwise line coincident with the flap centerline and extending forward to the leading edge of the model. There are four streamwise lines of thermocouples on the lower surface of the model. As indicated in Fig. 3, the attachable extended-chord flaps also are instrumented for pressure and temperature measurements. The upper surface of the model has a similar array of

pressure taps and thermocouples in lines parallel to the ridge line of the model. Eight pressure taps are on the ridge line; 10 taps are positioned along a line coincident with the flap centerline and extending forward to the leading edge of the model.

### Remote Control System for Flaps

The trailing edge flaps are actuated by bell cranks and push-pull rods connected to drive screws and 28 volt dc motors housed in a water cooled jacket mounted to the base of the model. The water cooled actuator housing contains three each: motors, drive screws, and potentiometers required to actuate the flaps and to determine the flap deflection angles (see Fig. 4). For the model discussed herein, one motor is used to actuate the pair of flaps on the lower surface of the model, and the other motors are used to actuate the flaps on the left and right dihedral surfaces. The same actuator housing is used for the other pressure and heat transfer models having remotely controlled flaps (Configurations "A", "C" and "D", Fig. 1).

The electrical circuits for the flaps are shown in Fig. 5. As indicated in the diagram, the flaps are driven by the 28 volt dc motors and the potentiometer readings, used to position the flaps, appear on Leeds and Northrup indicators. A "limit light" circuit is also shown in Fig. 5. Microswitches at both ends of each drive screw are calibrated to close when any flap is in a limiting position (either 0 or 40 degree deflection for the model considered herein). When in this limiting position, a limit lamp lights in the control room. Finally, the actuator housing also contains thermocouples used to monitor temperatures at three locations in the housing.

The temperature and potentiometer indicators are shown in Fig. 6. Also shown in Fig. 6, from left to right, are the limit lamp box, variable resistors used in calibrating the potentiometer readings, the flap motor control box, and an ammeter used to indicate the motor loads. Any excess motor loads, due, for example, to binding in the flap control linkage, would be apparent immediately by a high ammeter reading, and the motor could be stopped before causing further damage.

## TEST CONDITIONS

The pressure data presented herein were obtained from tests in the AEDC 50-inch Mach 8 tunnel made during the latter part of July 1963. The model was pitched from 54 degrees nose down to 54 degrees nose up for various flap settings and for free stream Reynolds numbers per foot of 1.1 and 3.3 million. Data were also obtained for selected flap settings for +12 degree sideslip and for changes in the basic geometry of the configuration (longer chord flaps on the lower surface, canards, and ventral fin). The test conditions for the pressure data are shown in Tables I and II. Flap deflection angles are considered positive when the flap trailing edge is deflected downward. Thus, the flaps on the lower surface were deflected at positive angles and the flaps on the upper, dihedral, surfaces were deflected at negative angles. The 15 degree ventral fin (rudder) setting is indicated in Fig. 3 and is set to trim at positive sideslip angle (nose left).

Flap deflections were set using Leeds and Northrup indicator readings of the potentiometers connected to the drive screws in the water cooled actuator housing. The potentiometer readings for the desired flap settings were calibrated using hand held templates. Flap settings were checked frequently while the tunnel was running by using a flood lamp and a surveyor's transit focused on scribe lines on the trailing edges of the flaps.

In order to minimize model cooling time, heat transfer data were obtained for a set of test conditions before obtaining pressure data for the same conditions. The flaps were set at the desired deflections, and the model was pitched to the desired angle of attack while inside the tunnel cooling shoes (shown retracted in Fig. 2). The cooling shoes were rapidly retracted (full retraction within 3/4 sec) and temperature readings recorded for every thermocouple every 0.05 seconds for 4.00 seconds. The shoes were then closed quickly, the model cooled to approximately 500°R and pitched to the next desired angle of attack. In this manner, the heat transfer data were obtained for a given configuration and value of  $Re_{\infty}/ft$  for the various angles of attack and flap settings while limiting the amount of heat absorbed by the model. The shoes were then left retracted while the pressure data, which require several minutes to stabilize for each set of test conditions, were obtained.

## DATA REDUCTION AND ACCURACY

All pressure data were reduced to standard coefficient form:

$$C_p = \frac{p - p_\infty}{q_\infty}$$

where  $p$  is the measured pressure;  $p_\infty$  is the free stream static pressure; and  $q_\infty$  is the free stream dynamic pressure. The inaccuracy in the measured pressure varies from  $\pm 0.003$  psia for pressures below 0.40 psia, to  $\pm 0.026$  psia for pressures greater than 15 psia. Pressure coefficient uncertainties vary, for example, from 0.004 for  $C_p < 0.3$  and  $Re_\infty/ft = 1.1$  million, to 0.013 for  $C_p = 2.0$  and  $Re_\infty/ft = 3.3$  million. At the higher pressure coefficients, the greatest part of the inaccuracy is due to fluctuations in the Mach 8 free stream dynamic pressure (Ref. 6).

The automatic plotting machines, used in presenting the data herein, introduce another source of possible error. The discrepancy in the plotted pressure coefficients due to this machine error should not exceed  $\pm 0.01$ . Nevertheless, there is always the possibility that a point will be completely misplotted. Each graph has been inspected and questionable points checked with the tabulated pressure coefficients.

The remotely controlled flap settings were estimated to be accurate to well within half a degree.

## RESULTS

Table II summarizes the Mach 8 pressure data obtained on the lower, delta wing, surface of the model and indicates the corresponding figure numbers where the sets of data are presented herein. The AEDC group number is presented in the last column of the Table. This number indicates the order in which the data were obtained and is to be used when referring to the tabulated data.

Streamwise and spanwise distributions of the pressures, in coefficient form, are presented in Figs. 7 through 102. The first part of each figure presents streamwise pressure distributions at



five spanwise stations and the second part of each figure presents spanwise pressure distributions at five streamwise stations. An outline of the model, showing the position of the streamwise and spanwise lines of pressure taps, appears on each full-page figure. As indicated in the figures,  $X'$  is the nondimensional streamwise distance from the planform virtual apex to the projection of a pressure tap on the planform, and  $Y'$  is the nondimensional spanwise distance of the planform projection of the tap measured outboard from the centerline (see Fig. 3 and Table III).

Some of the pressure tubes developed leaks during the tests. The corresponding pressure tap numbers, and the AEDC group numbers, are given in the tabulated data. The erroneous pressure coefficient values have been omitted from the graphs presented herein.

Although the accuracy of the plotted data should suffice for engineering purposes, ozalid reproducible copies of the tabulated data are available on loan (see Foreword). The plotted data may be read accurately using standard 20/inch grid, tracing graph paper overlays.

## REFERENCES

1. Kaufman, L.G. II, et al., A Review of Hypersonic Flow Separation and Control Characteristics, ASD-TDR-62-168, March 1962.
2. Evans, W.J., and Kaufman, L.G. II, Pretest Report on Hypersonic Flow Separation and Control Models for AEDC Tunnels A, B, Hotshot 2 and Grumman Hypersonic Shock Tunnel, Grumman Research Department Memorandum RM-209, July 1962.
3. Arnold Center, Test Facilities Handbook, Arnold Air Force Station, Tennessee, January 1961.
4. Kaufman, L.G. II, Pressure Measurements for Mach Five Flows over a Blunt Pyramidal Configuration with Aerodynamic Controls, to be published as a RTD Technical Documentary Report.
5. Wallace, A.R., and Swain, W.N., Pressure Distribution Tests on a 60° and 70° Delta Wing at Mach Numbers 20 to 22, AEDC-TN-61-14, February 1961, CONFIDENTIAL REPORT.
6. Kaufman, L.G. II, and Meckler, L.H., Pressure and Heat Transfer Measurements at Mach 5 and 8 for a Fin - Flat Plate Model, ASD-TDR-63-235, April 1963.
7. Kaufman, L.G. II, Pressure and Heat Transfer Measurements for Hypersonic Flows Over Expansion Corners and Ahead of Ramps, ASD-TDR-63-679, Part I: Mach 5 and 8 Data for Expansion Corner Flows, October 1963, Part II: Mach 5 Pressure Data for Flows Ahead of Ramps, September 1963, Part III: Mach 8 Pressure Data for Flows Ahead of Ramps, November 1963, Part IV: Mach 8 Heat Transfer Data for Flows Ahead of Ramps, to be published.
8. Kaufman, L.G. II, Pressure Measurements for Mach 8 Flows Over Expansion Corners and Ramps on an Internally Cooled Model, RTD-TDR-63-4044, Part I: Expansion Corner Flows, November 1963, Part II: Flows Over a Flat Plate with and without a Partial Span Ramp, December 1963, Part III: Flows Over Full Span Ramps Mounted on a Flat Plate, to be published.

9. Baer, A.L., An Investigation of Separated Flows on Two-Dimensional Models at Mach Numbers 5 and 8, AEDC-TDR-63-200, October 1963.
10. Kaufman, L.G. II, Pressure Distributions and Oil Film Photographs for Mach 5 Flows Past Fins Mounted on a Flat Plate, ASD-TDR-63-755, September 1963.
11. Kaufman, L.G. II, Pressure Measurements for Mach 5 Flows Over Winged Re-Entry Configurations with Aerodynamic Controls, to be published as a RTD Technical Documentary Report.
12. Hartofilis, S.A., Pressure Measurements at Mach 19 for a Winged Re-Entry Configuration, ASD-TDR-63-319, May 1963.
13. Lacey, J.J. Jr., Pressure Tests on a Blunt Delta Wing Vehicle at  $M = 19$ , AEDC-TDR-63-32, February 1963.
14. Meckler, L., Static Aerodynamic Characteristics at Mach 5 and 8 for an Aerodynamically Controllable Winged Re-Entry Configuration, to be published as a RTD Technical Documentary Report.



TABLE I  
TEST CONDITIONS  
(Sheet 1 of 4)

Tunnel Conditions		
$Re_{\infty}/10^6 \text{ ft}$	3.26*	1.09*
$M_{\infty}$	8.09	8.04
$p_{\infty}$ (psia)	0.0736	0.0250
$q_{\infty}$ (psia)	3.37	1.13
$p_o$ (psia)	773	254
$T_o$ (°R.)	1,345	1,340

\*The corresponding free stream Reynolds numbers, based on the model reference length, are 4.5 and 1.5 million.

TABLE I  
TEST CONDITIONS  
(Sheet 2 of 4)

BASIC PYRAMIDAL CONFIGURATION (without canards, without ventral fin, and with shorter chord (15% ref. length) flaps on lower surface) AT ZERO SIDESLIP ( $\beta = 0$ ) AND FOR $Re_{\infty}/10^6 \text{ ft} = 3.3$									
Flap Settings (deg)			Angles of Attack (deg)						
Bottom	Left	Right							
0	-40	-40	-54	-33	0	+14.3*	+45		
			-45	-12	+7		+33	+54	
0	-30	-30		-12	0	+14.3			
0	-20	-20	-45	-12	0	+14.3	+45		
0	-10	-10		-12	0	+14.3			
0	0	0	-54	-33	0	+14.3	+45		
			-45	-12			+33	+54	
+10	0	0		-12	0	+14.3			
+20	0	0		-12	0	+14.3	+45		
							+33	+54	
+30	0	0		-12	0	+14.3			
+40	0	0	-45	-12	0	+14.3	+45		
					+7		+33	+54	
0	-20	0		-12	0	+14.3			
0	-40	0		-12	0	+14.3			
0	0	-20		-12	0	+14.3			
0	0	-40		-12	0	+14.3			

\*Dihedral surfaces parallel to free stream flow at  $\alpha = 14.3^\circ$ .

TABLE I  
TEST CONDITIONS  
(Sheet 3 of 4)

BASIC PYRAMIDAL CONFIGURATION						
Flap Settings (deg)			Angles of Attack (deg) at zero sideslip			$\frac{Re_{\infty}}{10^6 \text{ ft}}$
Bottom	Left	Right				
0	-40	-40	-12	0	+14.3*	1.1
0	-20	-20	-12	0	+14.3	1.1
0	0	0	-12	0	+14.3	1.1
+20	0	0	-12	0	+14.3	1.1
+40	0	0	-12		+14.3	1.1
			Slideslip Angles (deg) at $\alpha = 0$			
0	-20	0		+12**		3.3
0	0	0		+12		3.3
+20	0	0		+12		3.3

BASIC + LONGER CHORD BOTTOM FLAPS (without canards, without ventral fin, and with longer chord (25% ref. length) flaps on lower surface)						
Flap Settings (deg)			Angles of Attack (deg) at zero sideslip			$\frac{Re_{\infty}}{10^6 \text{ ft}}$
Bottom	Left	Right				
+20	0	0	-12	0	+14.3	3.3
+20	0	0	-12	0	+14.3	1.1

\*Dihedral surfaces parallel to free stream flow at  $\alpha = 14.3^\circ$ .

\*\*Nose left.

TABLE I

## TEST CONDITIONS

(Sheet 4 of 4)

BASIC + CANARDS					
(without ventral fin and with shorter chord (15% ref. length) flaps on lower surface)					
FOR $Re_{\infty}/10^6 \text{ ft} = 3.3$					
Flap Settings (deg)			Angles of Attack (deg) at zero sideslip		
Bottom	Left	Right			
0	-20	-20	-12	0	+14.3*
0	0	0	-12	0	+14.3

BASIC + VENTRAL FIN					
(without canards and with shorter chord (15% ref. length) flaps on lower surface)					
FOR $Re_{\infty}/10^6 \text{ ft} = 3.3$					
Flap Settings (deg)			Fin (Rudder) Setting (deg)	Sideslip Angles (deg) at $\alpha = 0$	
Bottom	Left	Right			
0	0	0	0	0	+12**
+20	0	0	0	0	
0	0	0	+15***	0	+12

\*Dihedral surfaces parallel to free stream flow at  $\alpha = 14.3^\circ$ .

\*\*Nose Left.

\*\*\*Fin trailing edge left.

TABLE II

## TEST DATA FIGURE NUMBERS

(Sheet 1 of 5)

Configuration*	Flap Settings (deg)			$\alpha^*$ (deg)	$\beta^*$ (deg)	$\frac{Re_\infty}{10^6 ft}$	Figure Number	AEDC Group Number
	Bottom	Left	Right					
Basic	0	-40	-40	-54	0	3.3	7	295
	0	0	0	-54	0	3.3	8	291
	0	-40	-40	-45	0	3.3	9	293
	0	-20	-20	-45	0	3.3	10	292
	0	0	0	-45	0	3.3	11	290
	+40	0	0	-45	0	3.3	12	288
	0	-40	-40	-33	0	3.3	13	294
	0	0	0	-33	0	3.3	14	289
	0	-40	-40	-12	0	1.1	15	223
	0	-40	-40	-12	0	3.3	16	250
	0	-40	0	-12	0	3.3	17	260
	0	0	-40	-12	0	3.3	18	266
+ Canards	0	-30	-30	-12	0	3.3	19	249
	0	-20	-20	-12	0	1.1	20	222
	0	-20	-20	-12	0	3.3	21	244
	0	-20	0	-12	0	3.3	22	255
	0	0	-20	-12	0	3.3	23	261
	0	-20	-20	-12	0	3.3	24	209
	0	-10	-10	-12	0	3.3	25	254
	0	0	0	-12	0	1.1	26	213
	0	0	0	-12	0	3.3	27	226
	0	0	0	-12	0	3.3	28	206
	0	0	0	-12	0	3.3	29	206
	0	0	0	-12	0	3.3	30	206

\*See last sheet of Table for notes.

TABLE II

## TEST DATA FIGURE NUMBERS

(Sheet 2 of 5)

Configuration*	Flap Settings (deg)		$\alpha^*$ (deg)	$\beta^*$ (deg)	$\frac{Re_\infty}{10^6 \text{ ft}}$	Figure Number	AEDC Group Number
	Bottom	Left Right					
Basic	+10	0	-12	0	3.3	29	231
	+20	0	-12	0	1.1	30	217
	+20	0	-12	0	3.3	31	232
+ Longer Chord Flaps	+20	0	-12	0	1.1	32	203
	+20	0	-12	0	3.3	33	200
	+30	0	-12	0	3.3	34	237
Basic	+40	0	-12	0	1.1	35	218
	+40	0	-12	0	3.3	36	238
	+40	0	-12	0	1.1	37	224
	0	-40	0	0	3.3	38	251
	0	-40	0	0	3.3	39	259
	0	-40	0	0	3.3	40	265
	0	0	0	0	3.3	41	248
	0	-30	0	0	1.1	42	221
	0	-20	0	0	3.3	43	245
	0	-20	0	0	3.3	44	256
	0	-20	0	0	3.3	45	262
	0	0	0	0	3.3	46	210
+ Canards	0	-20	0	0	3.3	47	243
Basic	0	-10	0	0	1.1	48	212
	0	0	0	0	3.3	49	227
	0	0	0	0	3.3	50	207
+ Canards	0	0	0	0	3.3	51	271
+ Fin ( $\delta = 0$ )	0	0	0	0	3.3	52	267
+ Fin ( $\delta = 15^\circ$ )	0	0	0	0	3.3		

\*See last sheet of Table for notes.

TABLE II

## TEST DATA FIGURE NUMBERS

(Sheet 3 of 5)

Configuration*	Flap Settings (deg)		$\alpha^*$ (deg)	$\beta^*$ (deg)	$\frac{Re_\infty}{6}$ 10 ft	Figure Number	AEDC Group Number
	Bottom	Left Right					
Basic	+10	0	0	0	3.3	53	230
	+20	0	0	0	1.1	54	216
	+20	0	0	0	3.3	55	233
+ Fin ( $\delta = 0$ )	+20	0	0	0	3.3	56	269
+ Longer Chord Flaps	+20	0	0	0	1.1	57	204
Basic	+20	0	0	0	3.3	58	201
	+30	0	0	0	3.3	59	236
	+40	0	0	0	3.3	60	239
	0	-20	0	+12	3.3	61	274
	0	0	0	+12	3.3	62	273
	+20	0	0	+12	3.3	63	272
+ Fin ( $\delta = 0$ )	0	0	0	+12	3.3	64	270
+ Fin ( $\delta = 15^\circ$ )	0	0	0	+12	3.3	65	268
Basic	0	-40	+7	0	3.3	66	253
	+40	0	+7	0	3.3	67	240
	0	-40	+14.3	0	1.1	68	225
	0	-40	+14.3	0	3.3	69	252
	0	-40	+14.3	0	3.3	70	258
	0	0	+14.3	0	3.3	71	264
	0	-30	+14.3	0	3.3	72	247
	0	-20	+14.3	0	1.1	73	220
	0	-20	+14.3	0	3.3	74	246
	0	-20	+14.3	0	3.3	75	257
	0	0	+14.3	0	3.3	76	263
+ Canards	0	-20	+14.3	0	3.3	77	211

\*See last sheet of Table for notes.



TABLE II

## TEST DATA FIGURE NUMBERS

(Sheet 4 of 5)

Configuration*	Flap Settings (deg)		$\alpha^*$ (deg)	$\beta^*$ (deg)	$\frac{Re_\infty}{10^6 \text{ ft}}$	Figure Number	AEDC Group Number
	Bottom	Left Right					
Basic	0	-10	-10	0	3.3	78	242
	0	0	+14.3	0	1.1	79	214
	0	0	+14.3	0	3.3	80	228
+ Canards	0	0	+14.3	0	3.3	81	208
Basic	+10	0	+14.3	0	3.3	82	229
	+20	0	+14.3	0	1.1	83	215
	+20	0	+14.3	0	3.3	84	234
+ Longer Chord Flaps	+20	0	+14.3	0	1.1	85	205
	+20	0	+14.3	0	3.3	86	202
Basic	+30	0	+14.3	0	3.3	87	235
	+40	0	+14.3	0	1.1	88	219
	+40	0	+14.3	0	3.3	89	241
	0	-40	+33	0	3.3	90	286
	0	0	+33	0	3.3	91	275
	+20	0	+33	0	3.3	92	280
	+40	0	+33	0	3.3	93	281
	0	-40	+45	0	3.3	94	285
	0	-20	+45	0	3.3	95	287
	0	0	+45	0	3.3	96	276
	+20	0	+45	0	3.3	97	279
	+40	0	+45	0	3.3	98	282
	0	-40	+54	0	3.3	99	284
	0	0	+54	0	3.3	100	277
	+20	0	+54	0	3.3	101	278
	+40	0	+54	0	3.3	102	283

\*See last sheet of Table for notes.

TABLE II

TEST DATA FIGURE NUMBERS

(Sheet 5 of 5)

\*Notes:

- Basic configuration is without canards, without ventral fin, and with shorter chord (15% ref. length) flaps on the lower surface.
- + Canards is the basic configuration with canards.
- + Longer chord flaps is the basic configuration with the longer chord (25% ref. length) flaps on the lower surface.
- + Fin ( $\delta = 0$ ) is the basic configuration with the ventral fin undeflected (zero rudder angle).
- + Fin ( $\delta = 15^\circ$ ) is the basic configuration with the ventral fin deflected 15 degrees (fin trailing edge left).

Flap settings are measured in planes normal to the flap hinge lines; the bottom flaps always act as a pair and have equal settings.

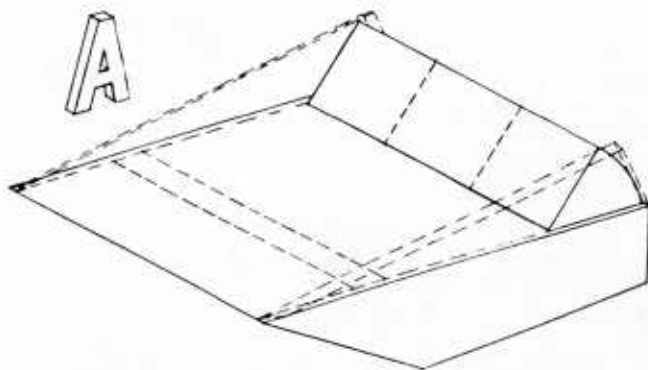
At  $\alpha = 14.3^\circ$  the dihedral surfaces are parallel to the free stream flow.

Positive sideslip angle ( $\beta = +12^\circ$ ) is nose left.

TABLE III  
COORDINATES OF PLANFORM PROJECTIONS  
OF PRESSURE TAPS

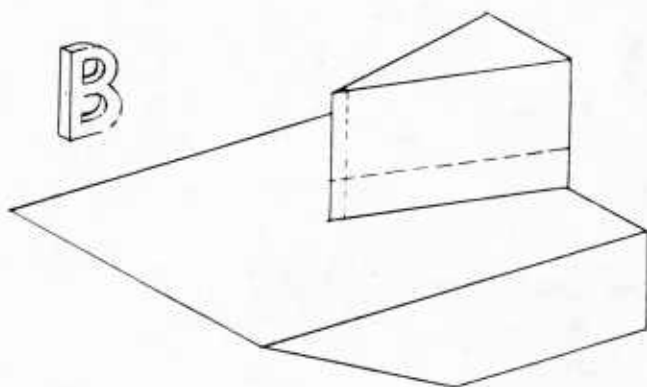
Tap Number	X'	Y'
5	0.3243	0
7	0.4144	↓
9	0.5045	
11	0.5946	
13	0.6847	
15	0.7748	↓
16	0.8198	
17	0.8799	0
25	0.7748	0.1218
26	0.8198	↓
27	0.8799	
28	0.9249	0.1218
33	0.6847	0.3090
35	0.7748	↓
437 & 37	0.8799	
438 & 38	0.9249	↓
439 & 39	0.9700	0.3090

Tap Number	X'	Y'
40	0.4297	0.4340
41	0.5946	↓
42	0.6396	
43	0.6847	
44	0.7297	
445 & 45	0.7748	
446 & 46	0.8198	
447 & 47	0.8799	↓
448 & 48	0.9249	
449 & 49	0.9700	0.4340
457 & 57	0.8799	0.5590
458 & 58	0.9249	0.5590
459 & 59	0.9700	0.5590



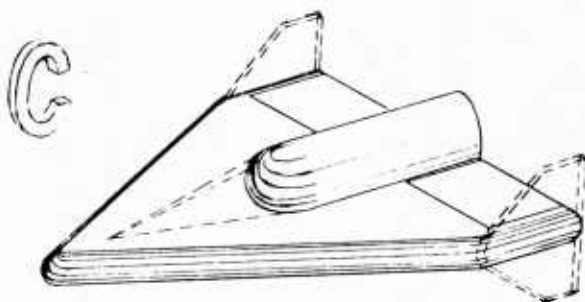
Separated Flows ahead of a Ramp  
Fore and aft flaps, end plates  
3 separate models:

- 1) Pressure and heat transfer, AEDC Tunnels A & B,  $M = 5$  &  $8$ , results in Refs. 7 and 9.
- 2) Controlled wall temperature, pressure, AEDC Tunnel B,  $M = 8$ , results in Refs. 8 and 9.
- 3) Pressure and heat transfer, Grumman Shock Tunnel,  $M = 13$  &  $19$ , results not available yet.



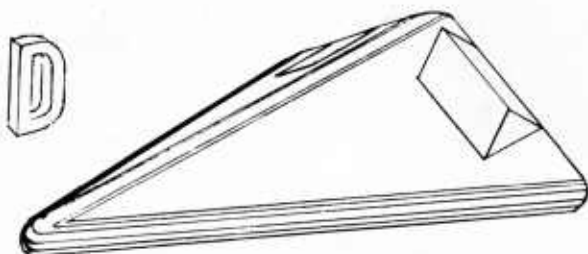
Wedge - Plate Interaction  
Small and large fins with sharp and blunt leading edges  
2 separate models:

- 1) Pressure and heat transfer, AEDC Tunnels A & B,  $M = 5$  &  $8$ , results in Refs. 6, 9 and 10.
- 2) Pressure and heat transfer, Grumman Shock Tunnel,  $M = 13$  &  $19$ , results not available yet.



Clipped Delta, Blunt L.E.  
Center body, T.E. flaps, drooped nose, spoiler, tip fins  
3 separate models:

- 1) Pressure and heat transfer, AEDC Tunnels A & B,  $M = 5$  &  $8$ , results in Ref. 11.
- 2) Pressure, AEDC Hotshot 2,  $M = 19$ , results in Refs. 12 and 13.
- 3) Six component force, AEDC Tunnels A & B,  $M = 5$  &  $8$ , results in Ref. 14.



Delta, Blunt L.E., Dihedral  
T.E. flaps, canard, ventral fin  
3 separate models:

- 1) Pressure and heat transfer, AEDC Tunnels A & B,  $M = 5$  &  $8$ , results in Ref. 4 and herein.
- 2) Pressure and heat transfer, Grumman Shock Tunnel,  $M = 19$ , results not available yet.
- 3) Six component force, AEDC Tunnels A & B,  $M = 5$  &  $8$ , results not available yet.

Fig. 1 General Outline of Models and Remarks for Over-all Program

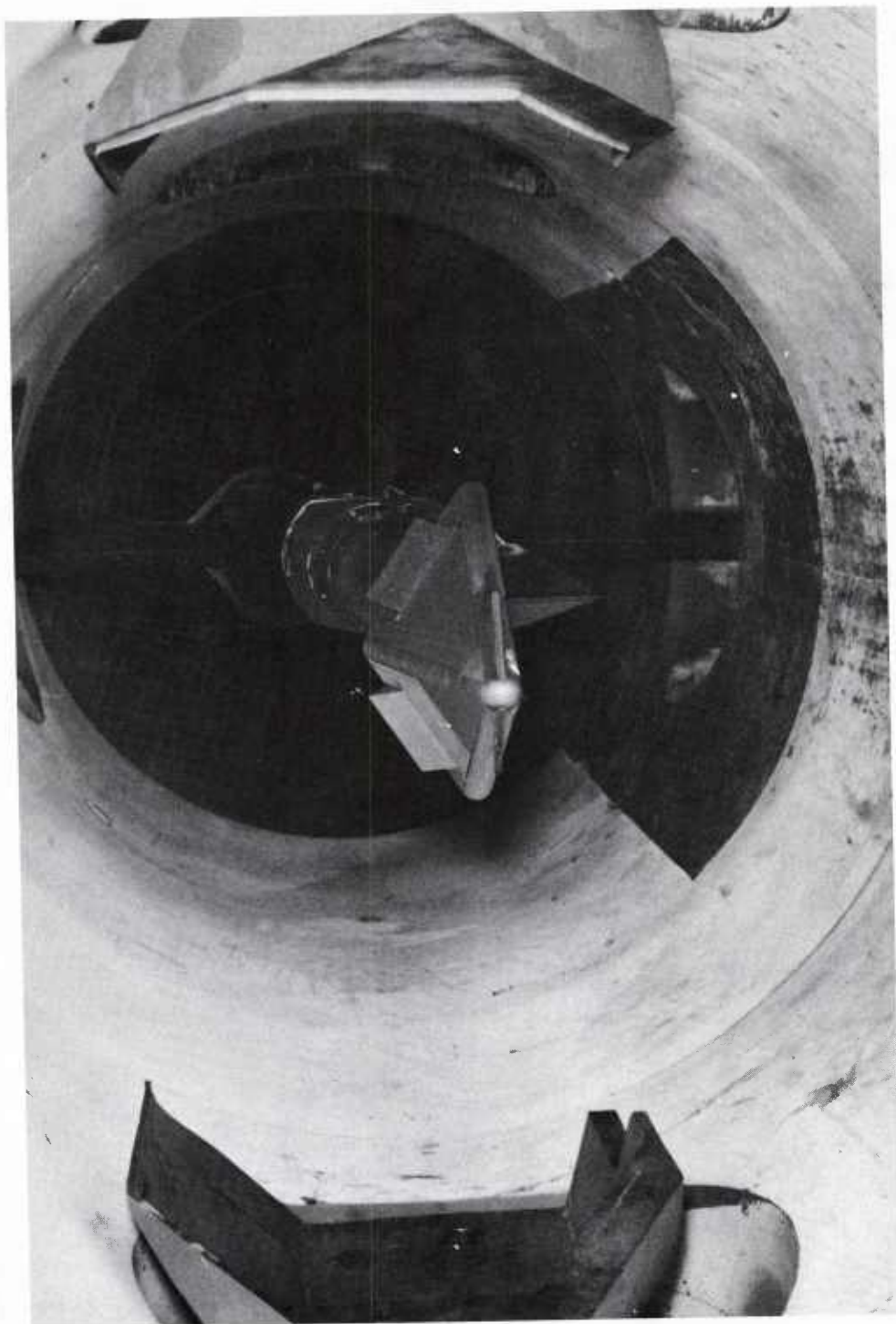


Fig. 2a Photograph of Model, with Canards and Upper (Dihedral) Flaps Deflected, Installed in the AEDC 50-inch Mach 8 Tunnel

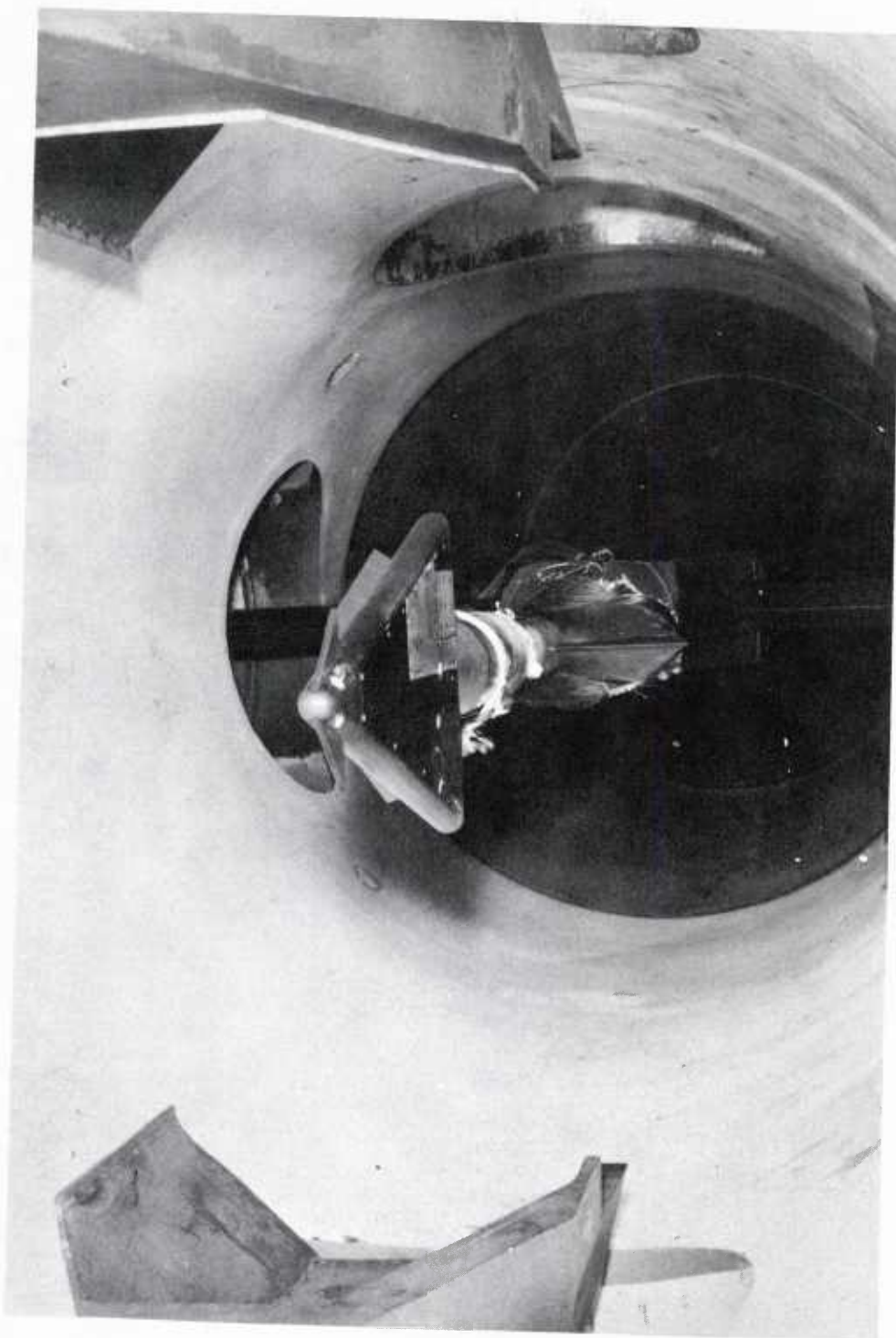


Fig. 2b Photograph of Model, with Canards and Upper (Dihedral) Flaps Deflected, Installed in the AEDC 50-inch Mach 8 Tunnel



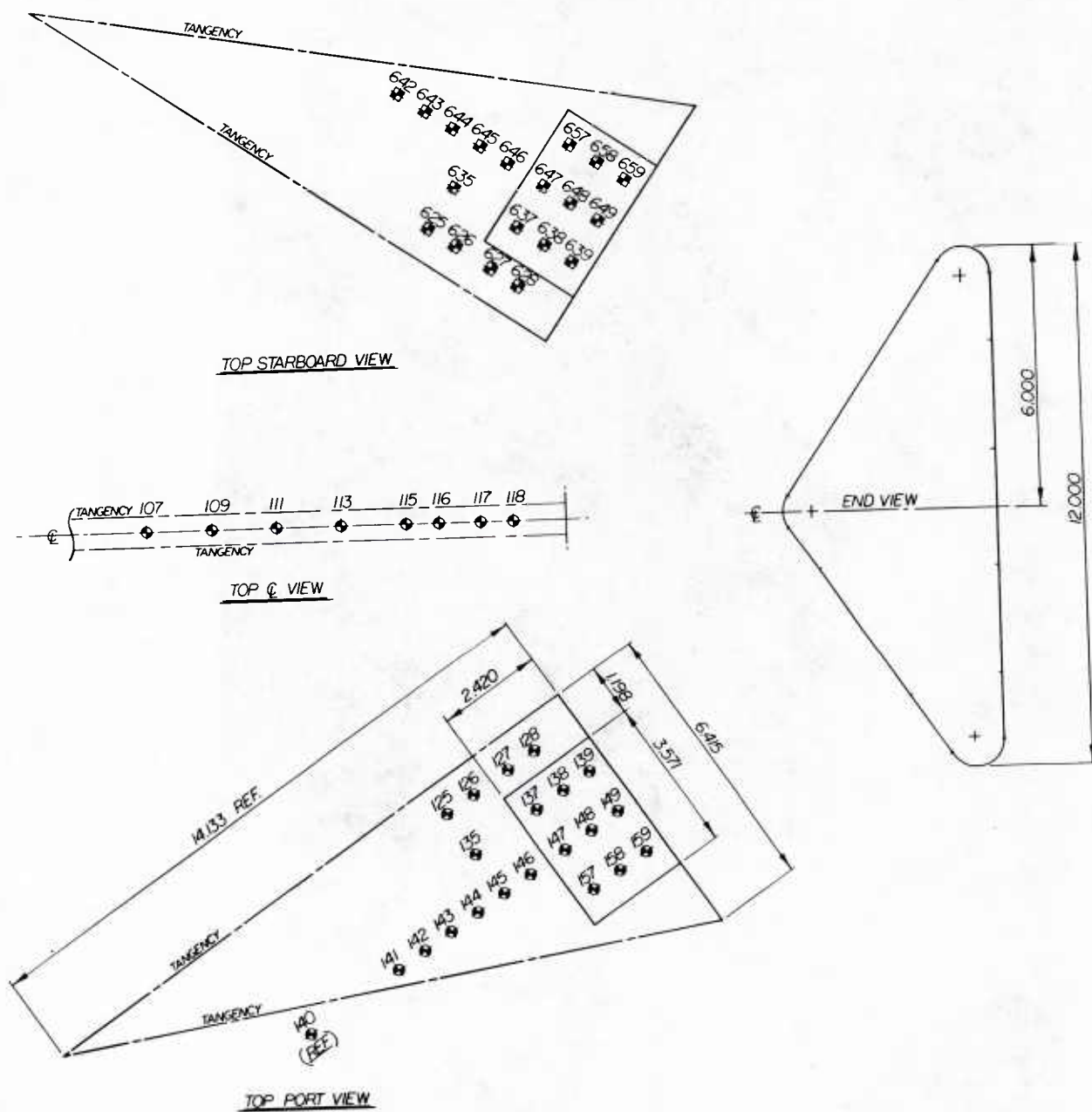


Fig. 3a Model Instrumentation (Sheet 1 of 3)







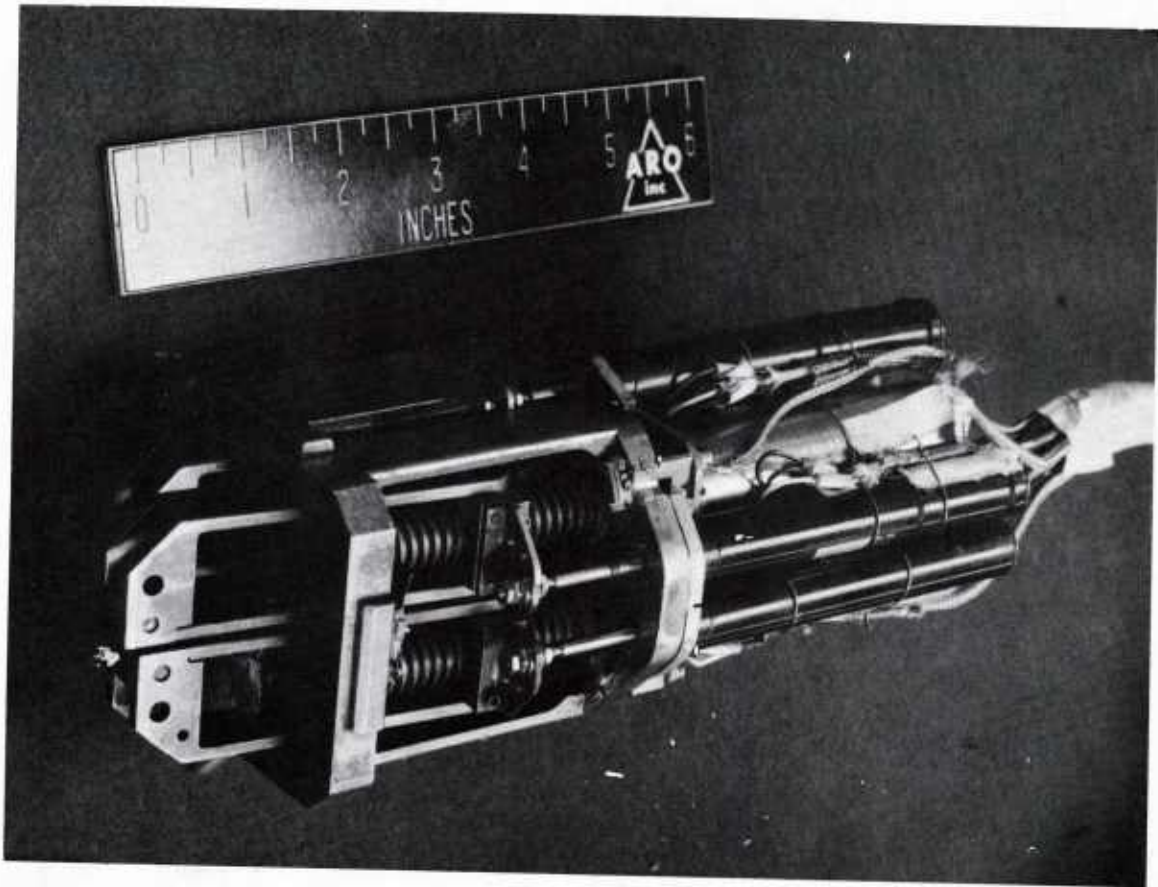
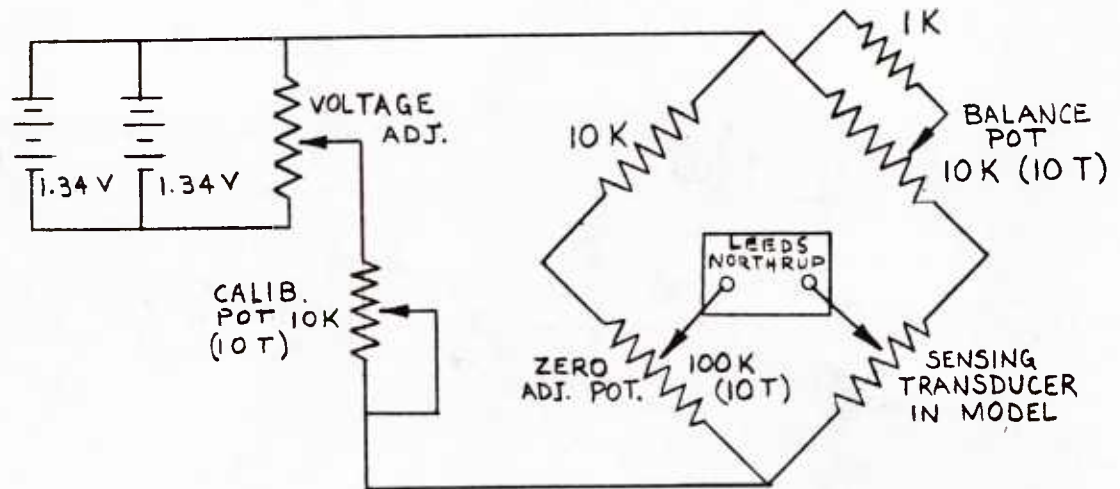
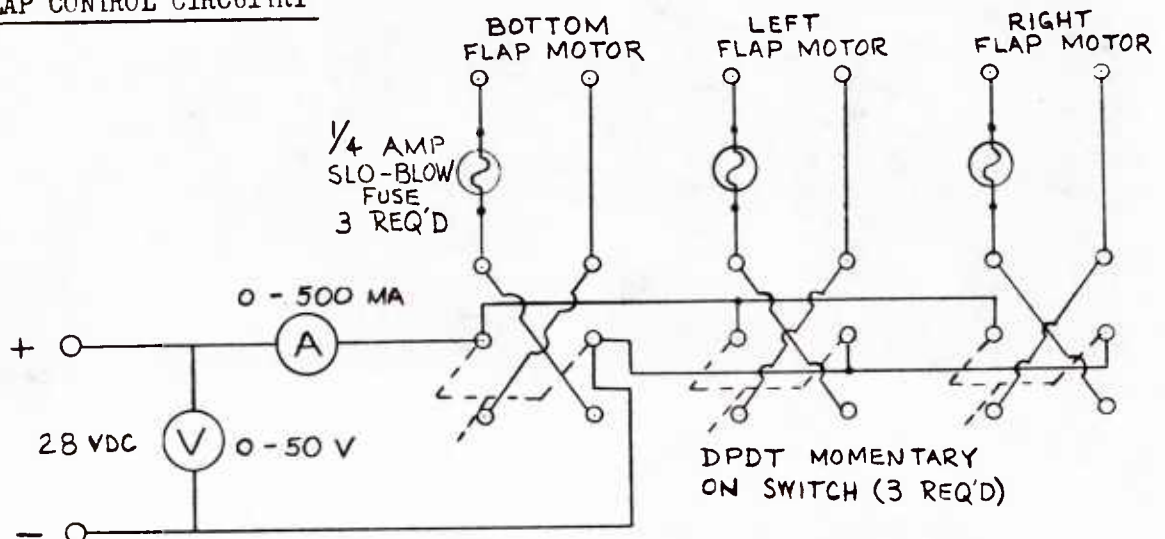


Fig. 4 Actuators for Remotely Controlled Flaps

### FLAP MEASURING CIRCUITRY



### FLAP CONTROL CIRCUITRY



### FLAP LIMIT LIGHT CIRCUITRY

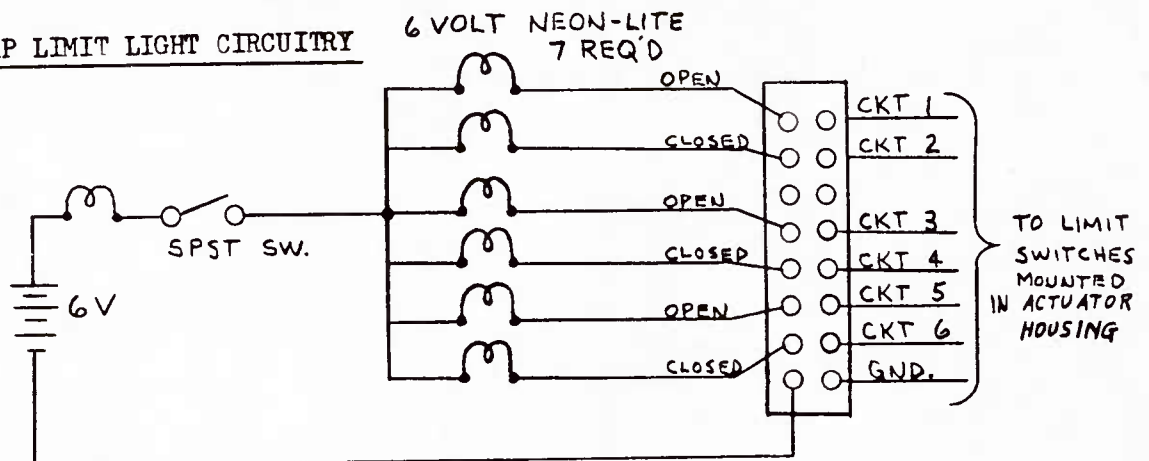


Fig. 5 Electrical Circuits for Remotely Controlled Flaps



Fig. 6 Photograph of Flap Control and Indicator Panels

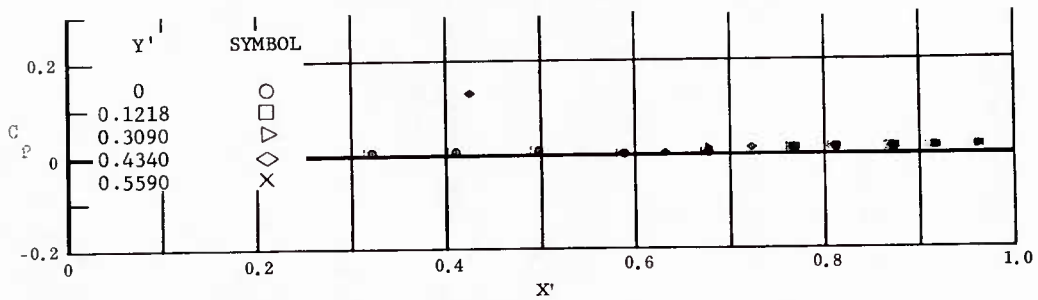


Fig. 7 Streamwise Distributions of Pressure Coefficients

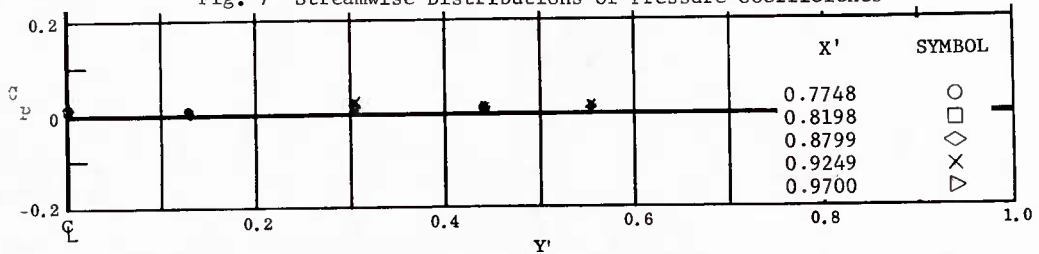


Fig. 7 Spanwise Distributions of Pressure Coefficients; Basic Configuration, Left and Right (Upper) Flaps Deflected  $-40^\circ$ ,  $\alpha = -54^\circ$ ,  $\beta = 0^\circ$ ,  $Re_\infty/ft = 3,300,000$ .

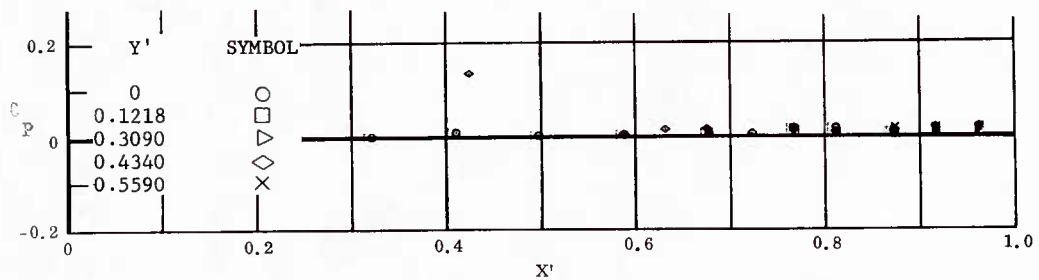


Fig. 8 Streamwise Distributions of Pressure Coefficients

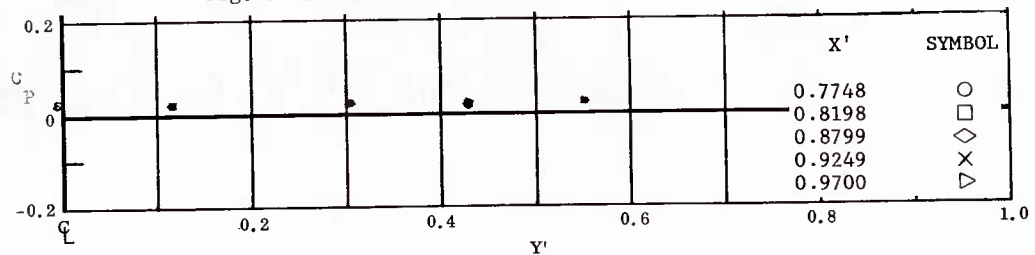


Fig. 8 Spanwise Distributions of Pressure Coefficients; Basic Configuration, No Flap Deflections,  $\alpha = -54^\circ$ ,  $\beta = 0^\circ$ ,  $Re_\infty/ft = 3,300,000$ .



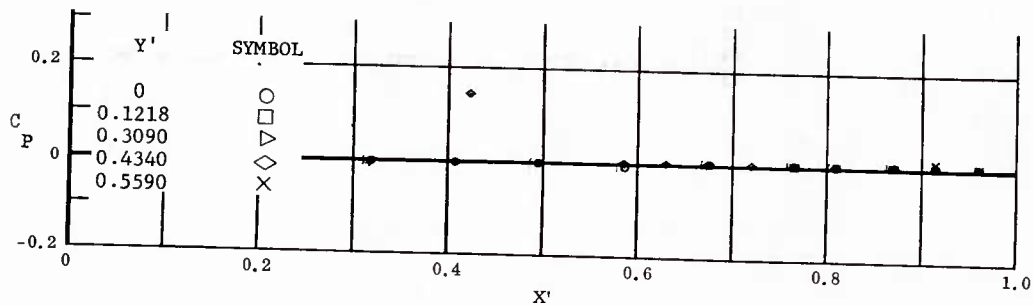


Fig. 9 Streamwise Distributions of Pressure Coefficients

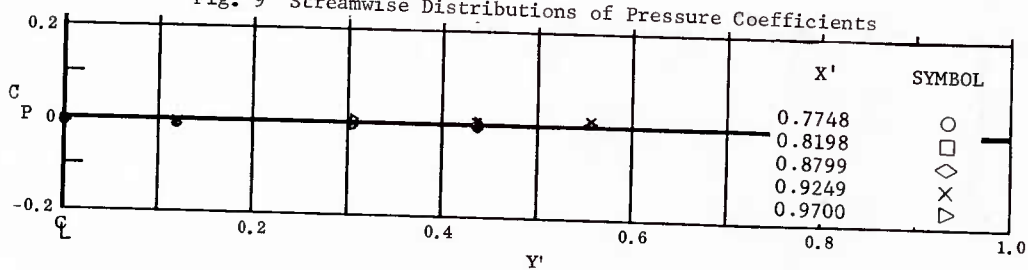


Fig. 9 Spanwise Distributions of Pressure Coefficients; Basic Configuration, Left and Right (Upper) Flaps Deflected  $-40^\circ$ ,  $\alpha = -45^\circ$ ,  $\beta = 0^\circ$ ,  $Re_\infty/ft = 3,300,000$ .

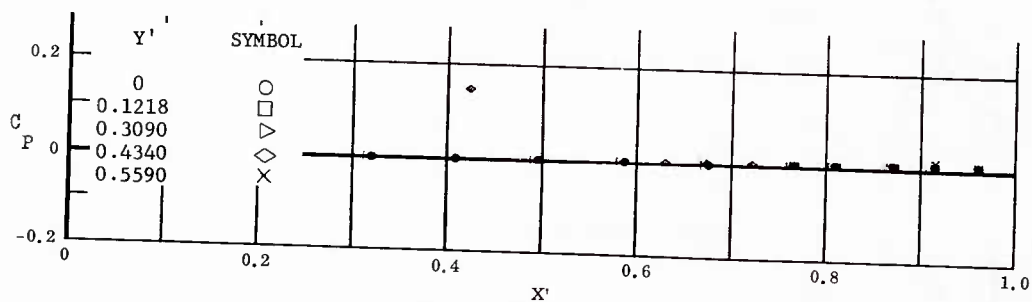


Fig. 10 Streamwise Distributions of Pressure Coefficients

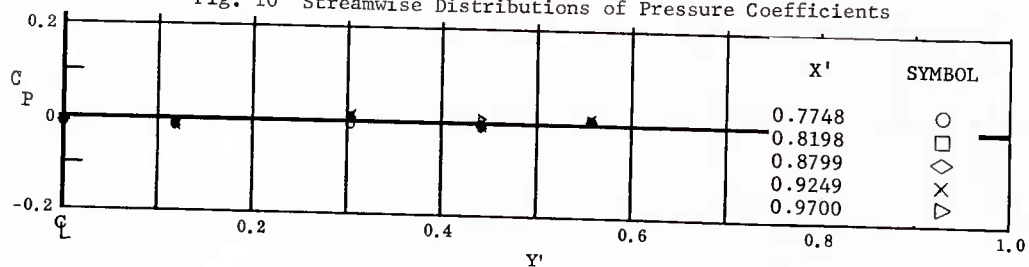


Fig. 10 Spanwise Distributions of Pressure Coefficients; Basic Configuration, Left and Right (Upper) Flaps Deflected  $-20^\circ$ ,  $\alpha = -45^\circ$ ,  $\beta = 0^\circ$ ,  $Re_\infty/ft = 3,300,000$ .



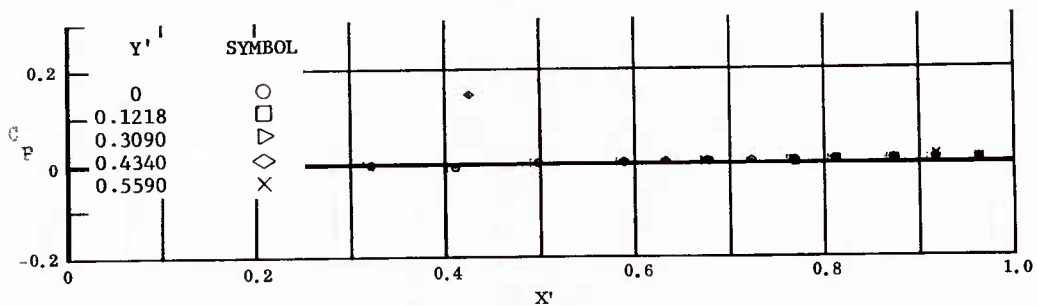


Fig. 11 Streamwise Distributions of Pressure Coefficients

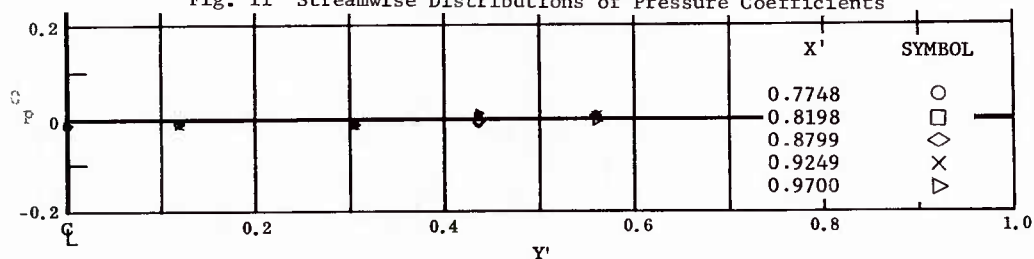


Fig. 11 Spanwise Distributions of Pressure Coefficients; Basic Configuration, No Flap Deflections,  $\alpha = -45^\circ$ ,  $\beta = 0^\circ$ ,  $Re_\infty/ft = 3,300,000$ .

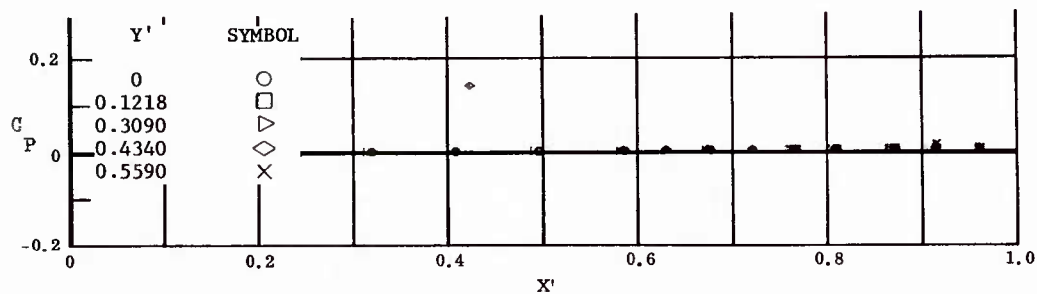


Fig. 12 Streamwise Distributions of Pressure Coefficients

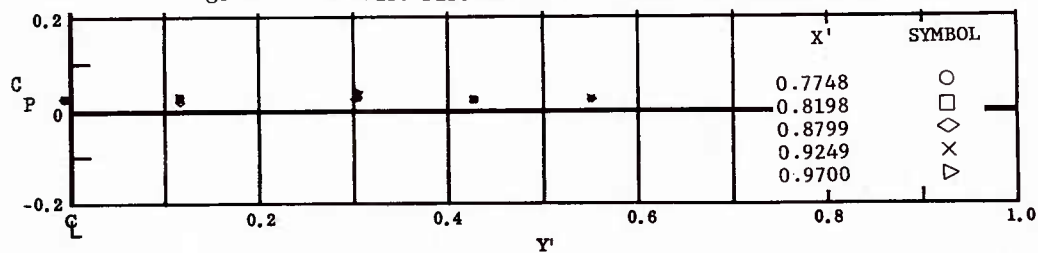


Fig. 12 Spanwise Distributions of Pressure Coefficients; Basic Configuration, Bottom Flaps Deflected  $+40^\circ$ ,  $\alpha = -45^\circ$ ,  $\beta = 0^\circ$ ,  $Re_\infty/ft = 3,300,000$ .

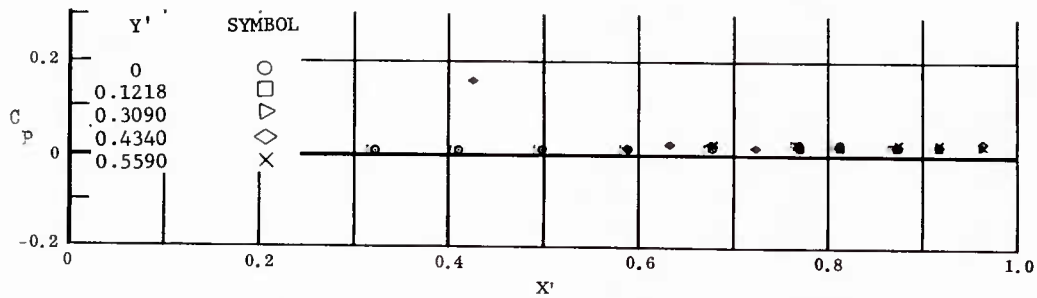


Fig. 13 Streamwise Distributions of Pressure Coefficients

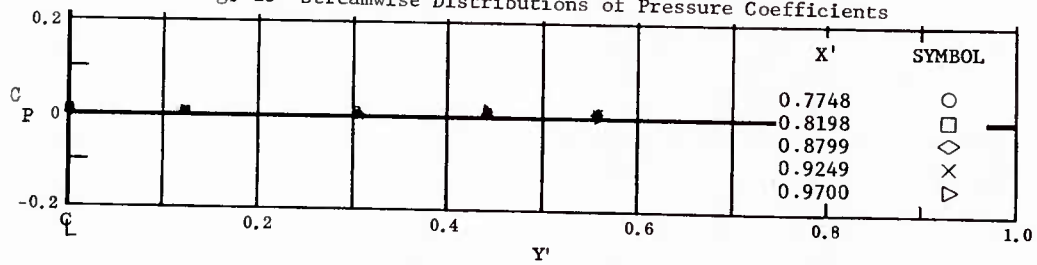


Fig. 13 Spanwise Distributions of Pressure Coefficients; Basic Configuration, Left and Right (Upper) Flaps Deflected  $-40^\circ$ ,  $\alpha = -33^\circ$ ,  $\beta = 0^\circ$ ,  $Re_\infty/ft = 3,300,000$ .

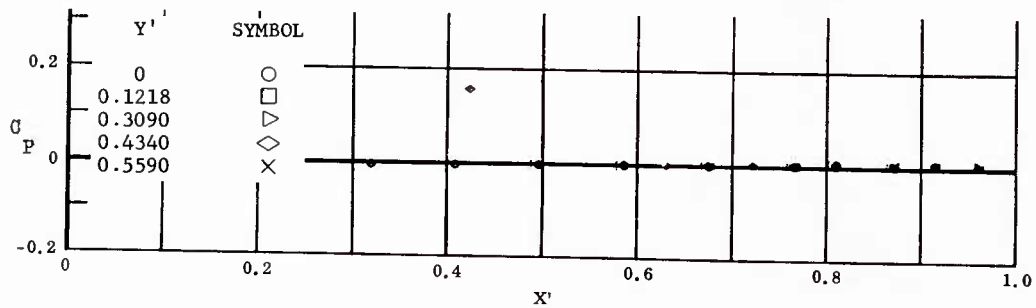


Fig. 14 Streamwise Distributions of Pressure Coefficients

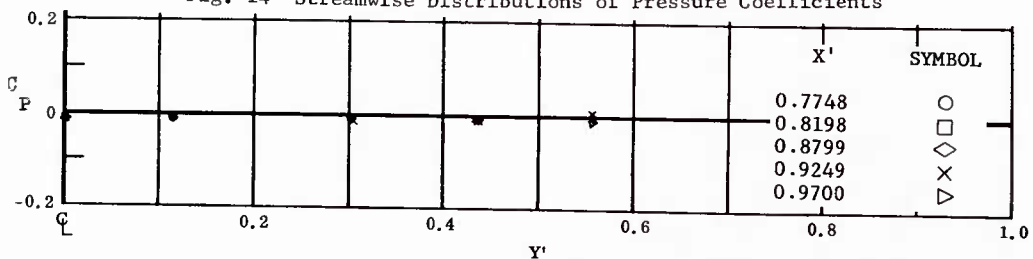


Fig. 14 Spanwise Distributions of Pressure Coefficients; Basic Configuration, No Flap Deflections,  $\alpha = -33^\circ$ ,  $\beta = 0^\circ$ ,  $Re_\infty/ft = 3,300,000$ .

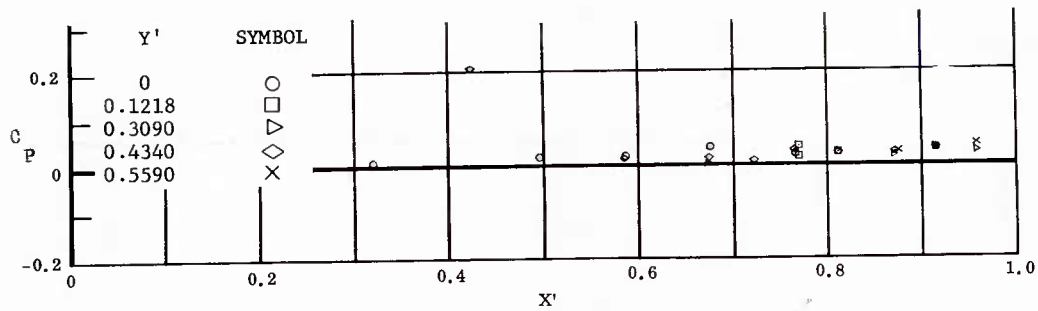


Fig. 15 Streamwise Distributions of Pressure Coefficients

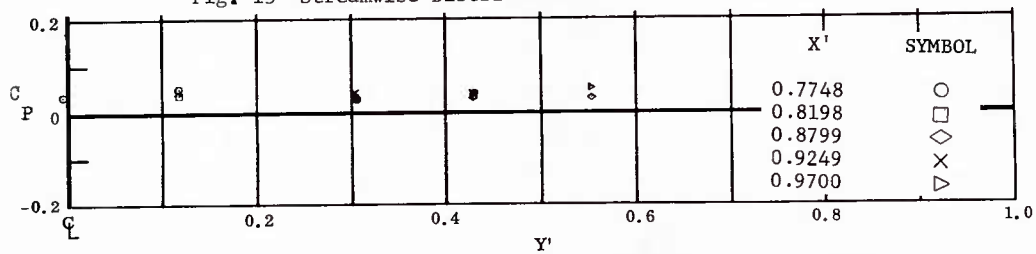


Fig. 15 Spanwise Distributions of Pressure Coefficients; Basic Configuration, Left and Right (Upper) Flaps Deflected  $-40^\circ$ ,  $\alpha = -12^\circ$ ,  $\beta = 0^\circ$ ,  $Re_\infty/ft = 1,100,000$ .

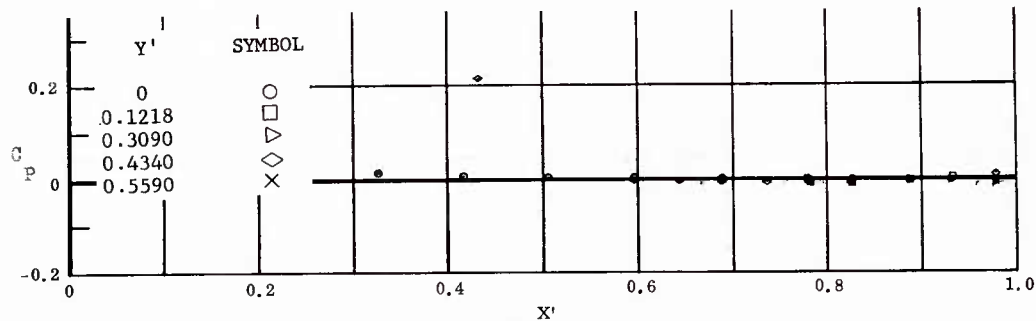


Fig. 16 Streamwise Distributions of Pressure Coefficients

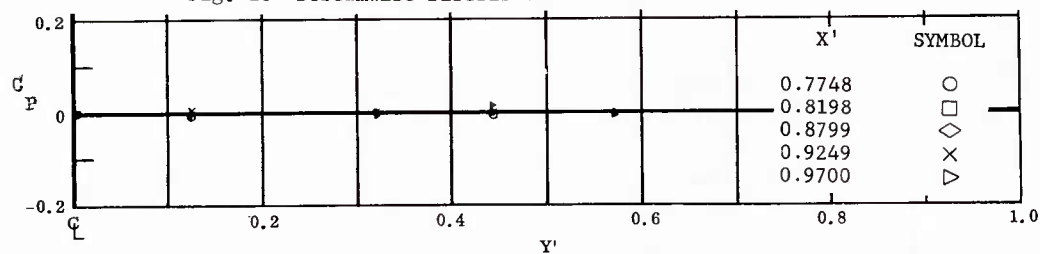


Fig. 16 Spanwise Distributions of Pressure Coefficients; Basic Configuration, Left and Right (Upper) Flaps Deflected  $-40^\circ$ ,  $\alpha = -12^\circ$ ,  $\beta = 0^\circ$ ,  $Re_\infty/ft = 3,300,000$ .

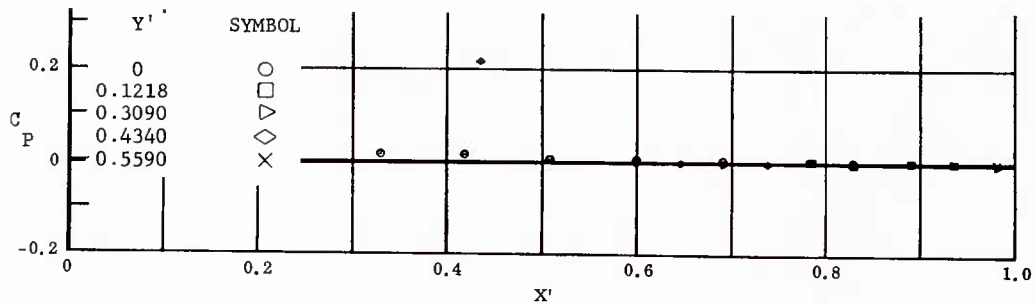


Fig. 17 Streamwise Distributions of Pressure Coefficients

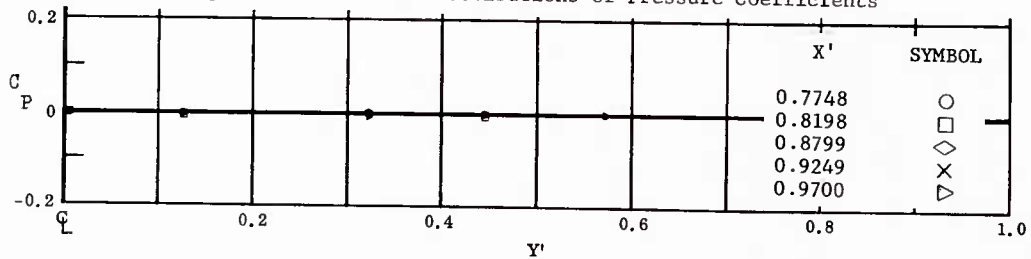


Fig. 17 Spanwise Distributions of Pressure Coefficients; Basic Configuration  
Left (Upper) Flap Deflected  $-40^\circ$ ,  $\alpha = -12^\circ$ ,  $\beta = 0^\circ$ ,  
 $Re_\infty/ft = 3,300,000$ .

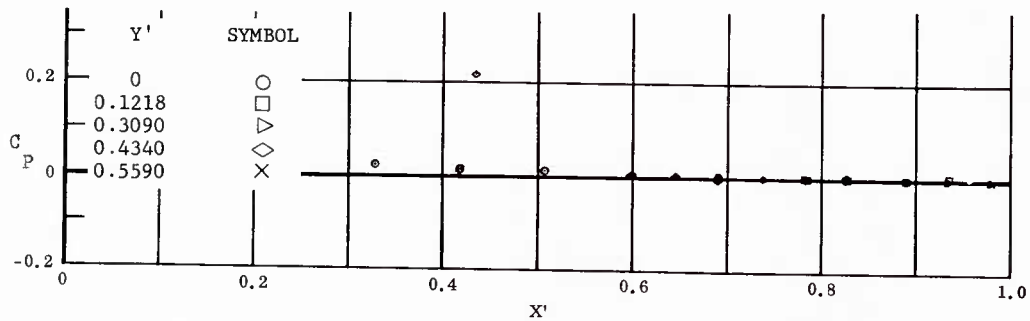


Fig. 18 Streamwise Distributions of Pressure Coefficients

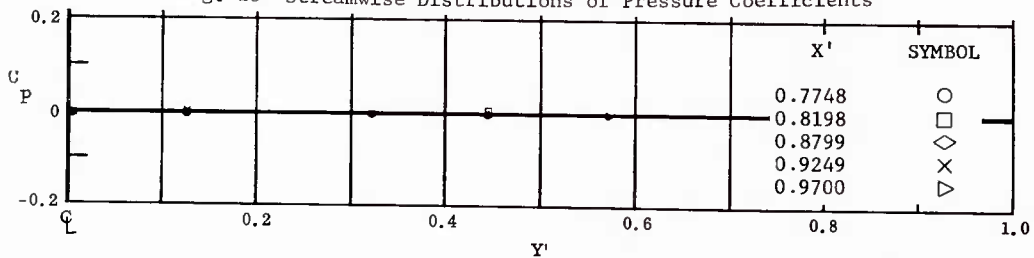


Fig. 18 Spanwise Distributions of Pressure Coefficients; Basic Configuration,  
Right (Upper) Flap Deflected  $-40^\circ$ ,  $\alpha = -12^\circ$ ,  $\beta = 0^\circ$ ,  
 $Re_\infty/ft = 3,300,000$ .

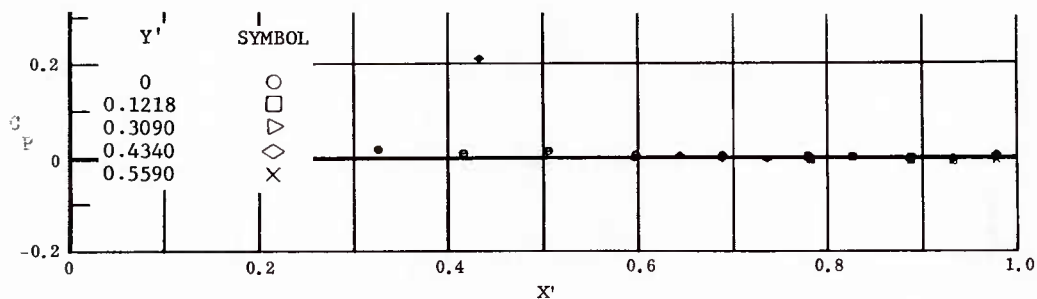


Fig. 19 Streamwise Distributions of Pressure Coefficients

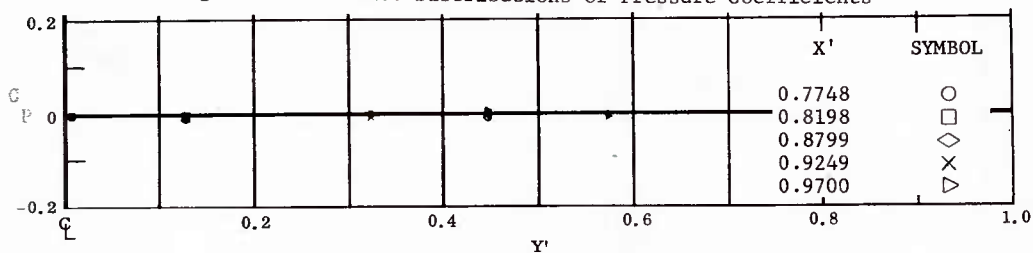


Fig. 19 Spanwise Distributions of Pressure Coefficients; Basic Configuration, Left and Right (Upper) Flaps Deflected  $-30^\circ$ ,  $\alpha = -12^\circ$ ,  $\beta = 0^\circ$ ,  $Re_\infty/ft = 3,300,000$ .

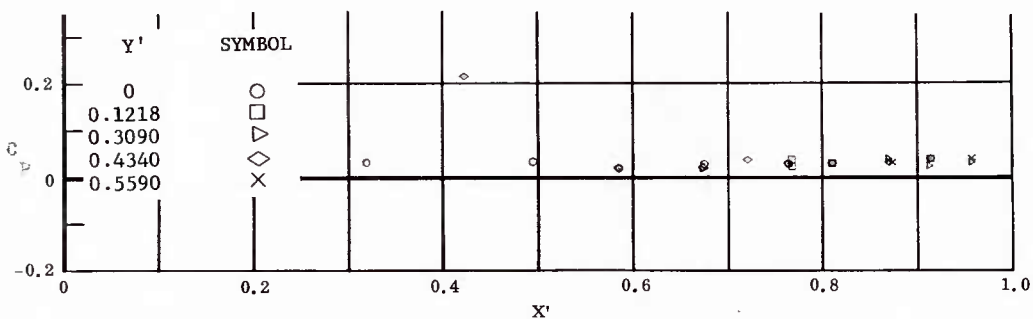


Fig. 20 Streamwise Distributions of Pressure Coefficients

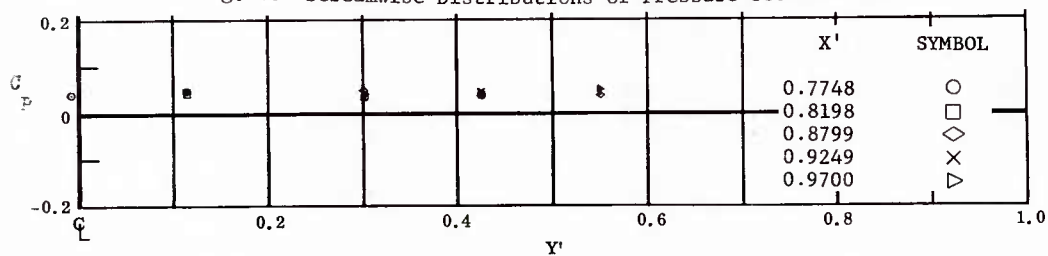


Fig. 20 Spanwise Distributions of Pressure Coefficients; Basic Configuration, Left and Right (Upper) Flaps Deflected  $-20^\circ$ ,  $\alpha = -12^\circ$ ,  $\beta = 0^\circ$ ,  $Re_\infty/ft = 1,100,000$ .

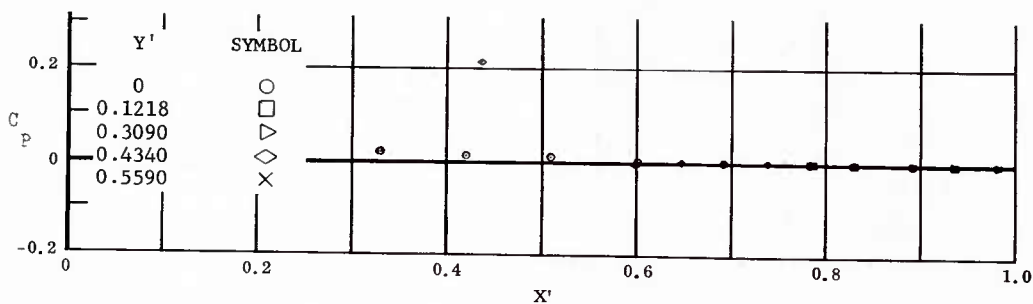


Fig. 21 Streamwise Distributions of Pressure Coefficients

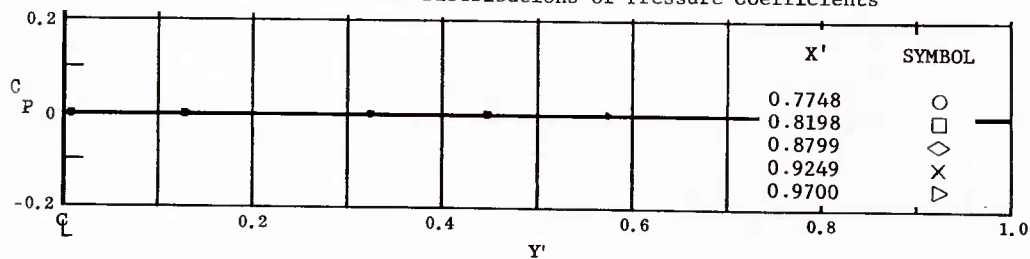


Fig. 21 Spanwise Distributions of Pressure Coefficients; Basic Configuration, Left and Right (Upper) Flaps Deflected  $-20^\circ$ ,  $\alpha = -12^\circ$ ,  $\beta = 0^\circ$ ,  $Re_\infty/ft = 3,300,000$ .

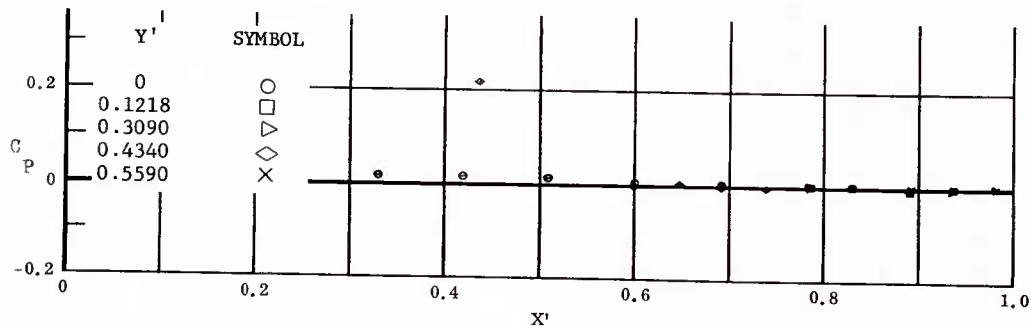


Fig. 22 Streamwise Distributions of Pressure Coefficients

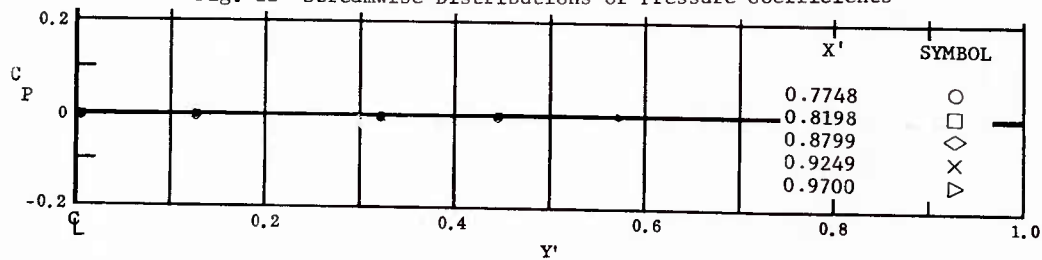


Fig. 22 Spanwise Distributions of Pressure Coefficients; Basic Configuration, Left (Upper) Flap Deflected  $-20^\circ$ ,  $\alpha = -12^\circ$ ,  $\beta = 0^\circ$ ,  $Re_\infty/ft = 3,300,000$ .

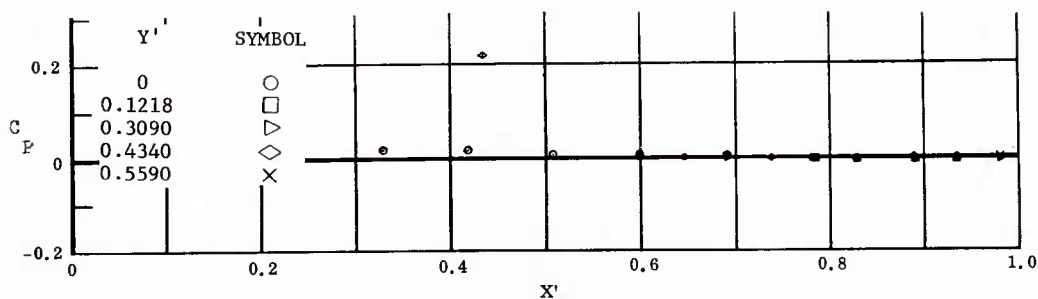


Fig. 23 Streamwise Distributions of Pressure Coefficients

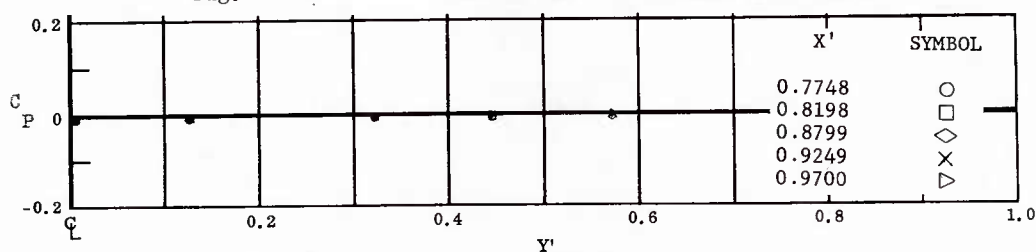


Fig. 23 Spanwise Distributions of Pressure Coefficients; Basic Configuration, Right (Upper) Flap Deflected  $-20^\circ$ ,  $\alpha = -12^\circ$ ,  $\beta = 0^\circ$ ,  $Re_\infty/ft = 3,300,000$ .

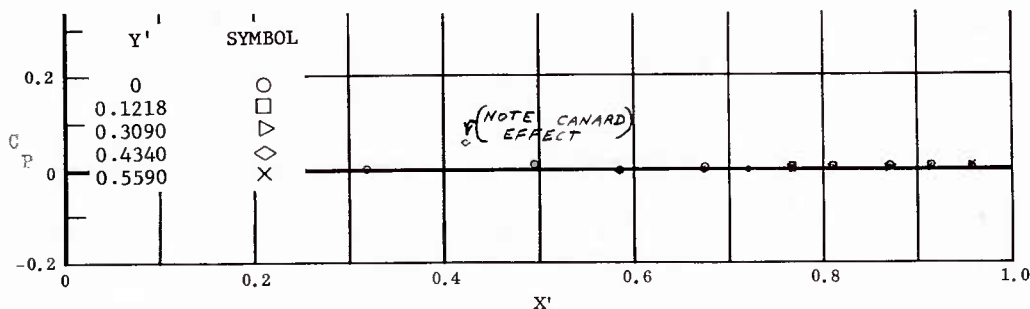


Fig. 24 Streamwise Distributions of Pressure Coefficients

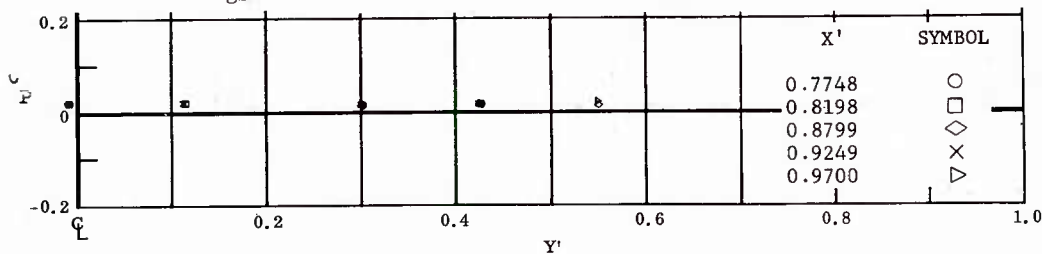


Fig. 24 Spanwise Distributions of Pressure Coefficients; Basic Configuration + Canards, Left and Right (Upper) Flaps Deflected  $-20^\circ$ ,  $\alpha = -12^\circ$ ,  $\beta = 0^\circ$ ,  $Re_\infty/ft = 3,300,000$ .



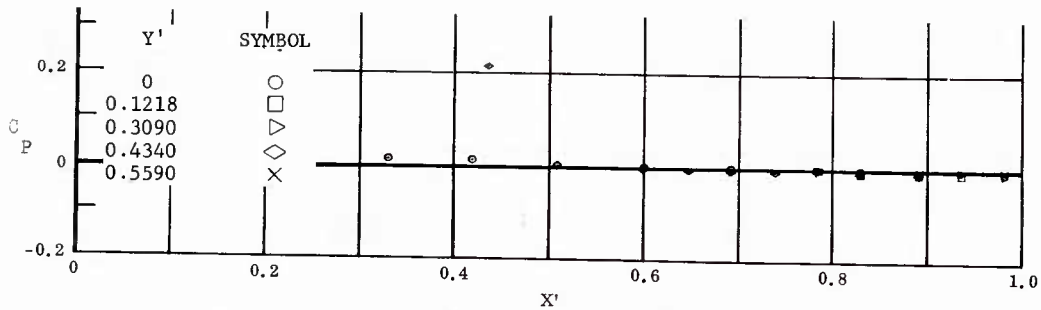


Fig. 25 Streamwise Distributions of Pressure Coefficients

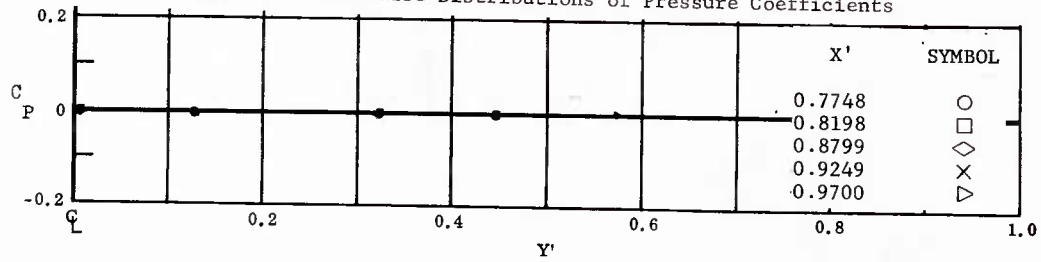


Fig. 25 Spanwise Distributions of Pressure Coefficients; Basic Configuration, Left and Right (Upper) Flaps Deflected  $-10^\circ$ ,  $\alpha = -12^\circ$ ,  $\beta = 0^\circ$ ,  $Re_\infty/ft = 3,300,000$ .

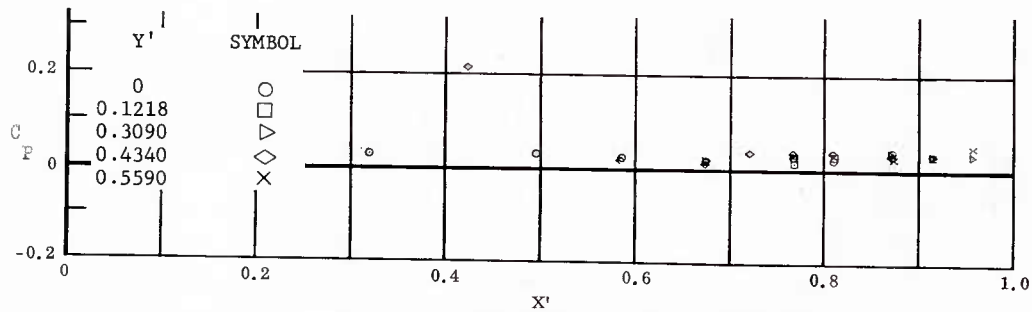


Fig. 26 Streamwise Distributions of Pressure Coefficients

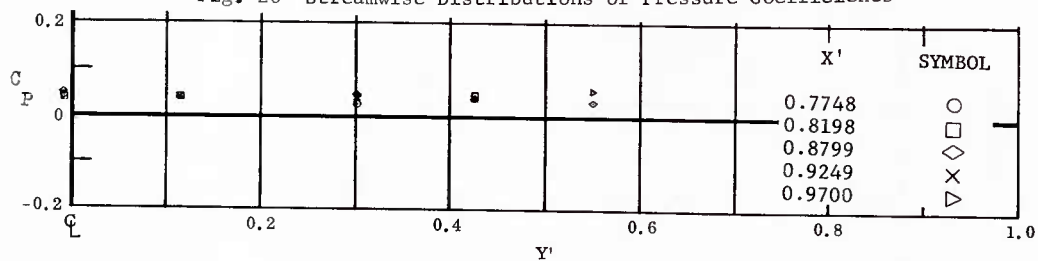


Fig. 26 Spanwise Distributions of Pressure Coefficients; Basic Configuration, No Flap Deflections,  $\alpha = -12^\circ$ ,  $\beta = 0^\circ$ ,  $Re_\infty/ft = 1,100,000$ .

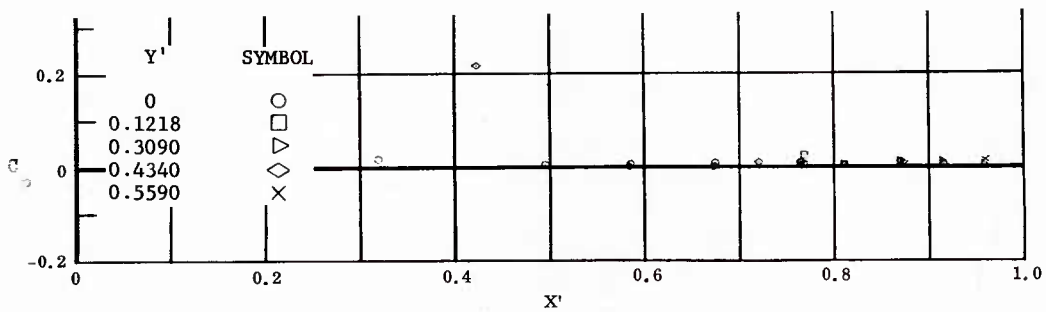


Fig. 27 Streamwise Distributions of Pressure Coefficients

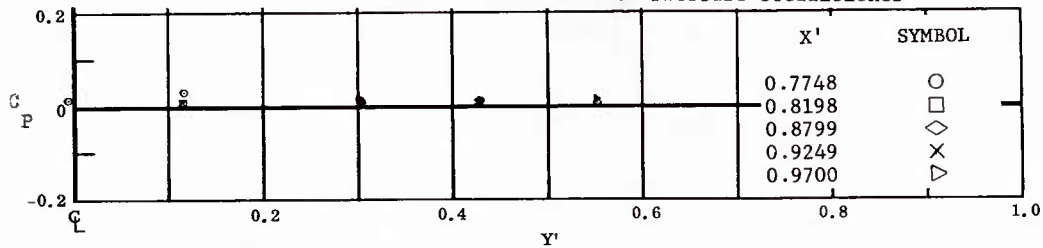


Fig. 27 Spanwise Distributions of Pressure Coefficients; Basic Configuration, No Flap Deflections,  $\alpha = -12^\circ$ ,  $\beta = 0^\circ$ ,  $Re_\infty / ft = 3,300,000$ .

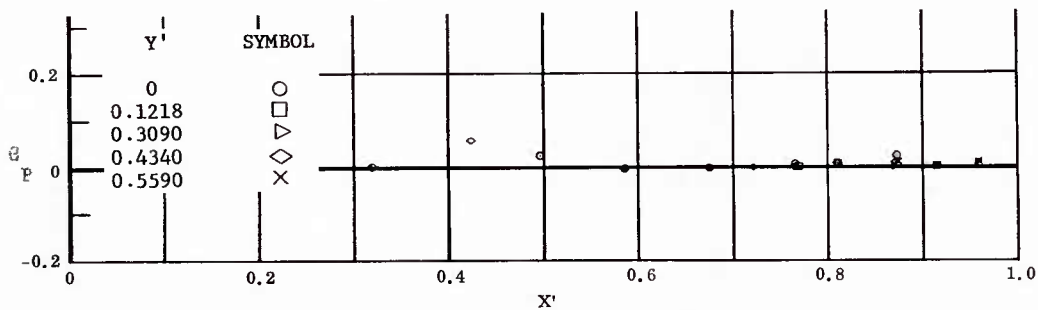


Fig. 28 Streamwise Distributions of Pressure Coefficients

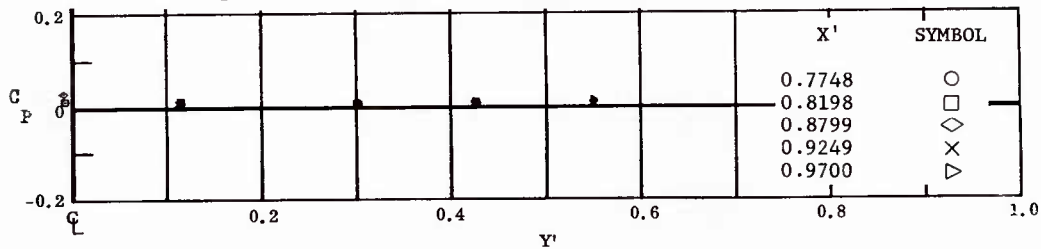


Fig. 28 Spanwise Distributions of Pressure Coefficients; Basic Configuration + Canards, No Flap Deflections,  $\alpha = -12^\circ$ ,  $\beta = 0^\circ$ ,  $Re_\infty / ft = 3,300,000$ .

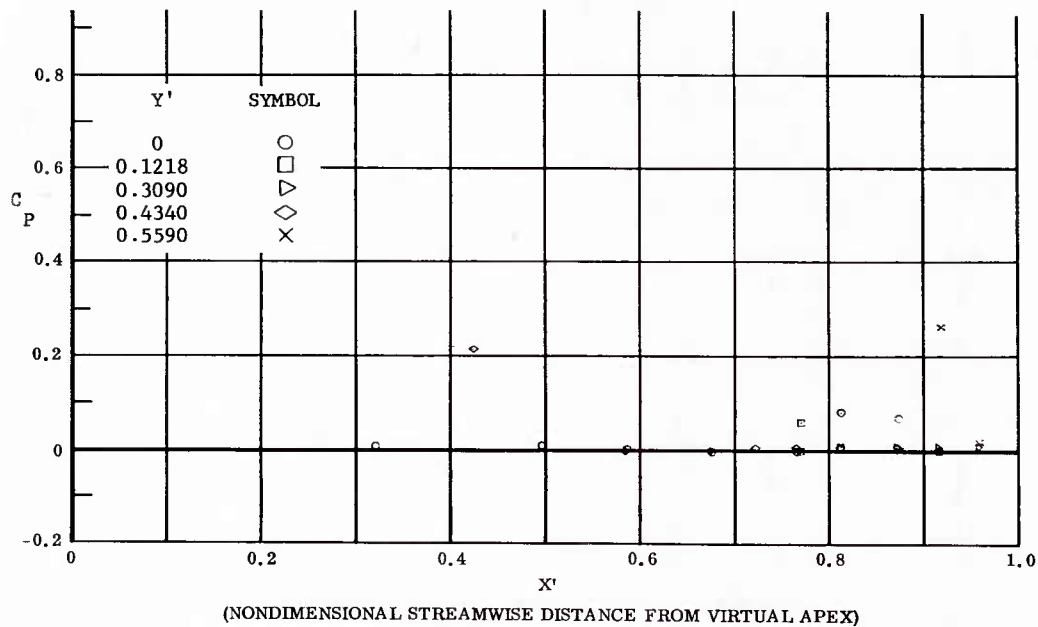


Fig. 29 Streamwise Distributions of Pressure Coefficients; Basic Configuration, Bottom Flaps Deflected  $+10^\circ$ ,  $\alpha = -12^\circ$ ,  $\beta = 0^\circ$ ,  $Re_\infty/ft = 3,300,000$ .

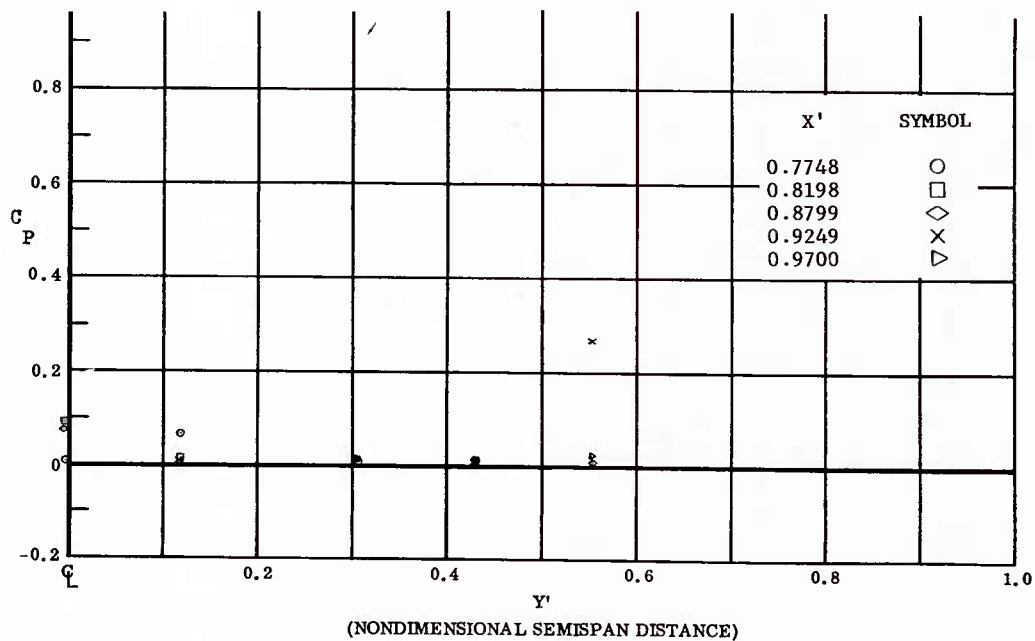


Fig. 29 Spanwise Distributions of Pressure Coefficients; Basic Configuration, Bottom Flaps Deflected  $+10^\circ$ ,  $\alpha = -12^\circ$ ,  $\beta = 0^\circ$ ,  $Re_\infty/ft = 3,300,000$ .

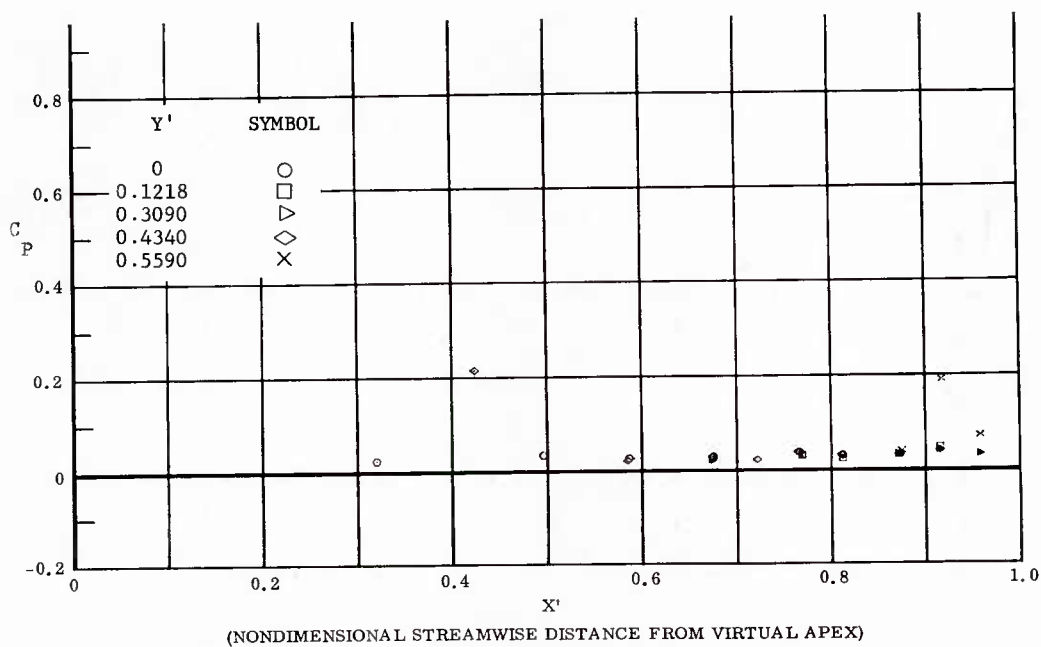


Fig. 30 Streamwise Distributions of Pressure Coefficients; Basic Configuration, Bottom Flaps Deflected  $+20^\circ$ ,  $\alpha = -12^\circ$ ,  $\beta = 0^\circ$ ,  $Re_\infty/ft = 1,100,000$ .

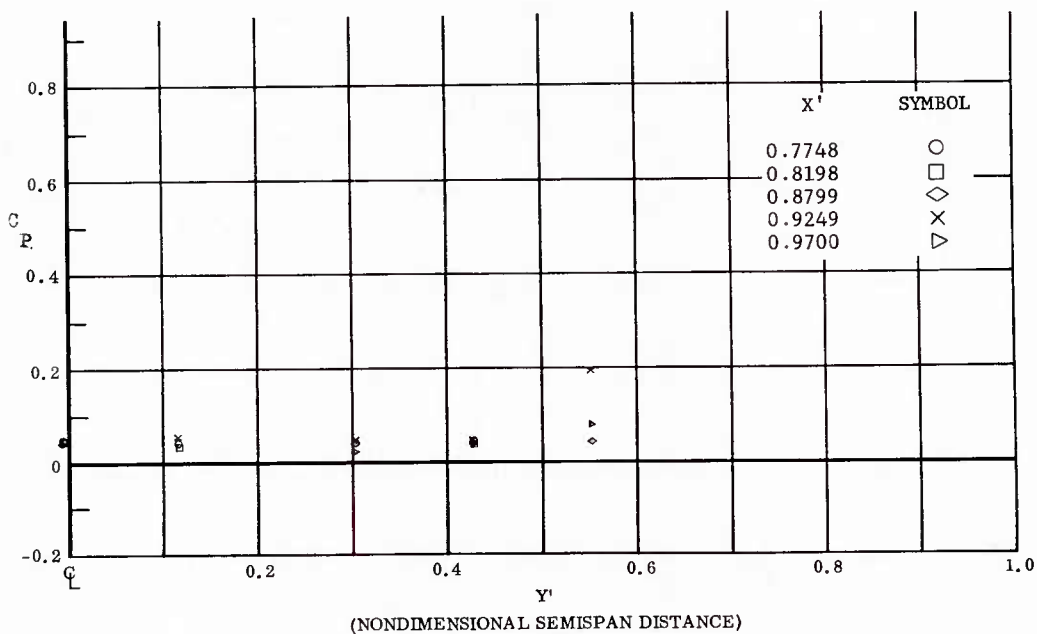


Fig. 30 Spanwise Distributions of Pressure Coefficients; Basic Configuration, Bottom Flaps Deflected  $+20^\circ$ ,  $\alpha = -12^\circ$ ,  $\beta = 0^\circ$ ,  $Re_\infty/ft = 1,100,000$ .

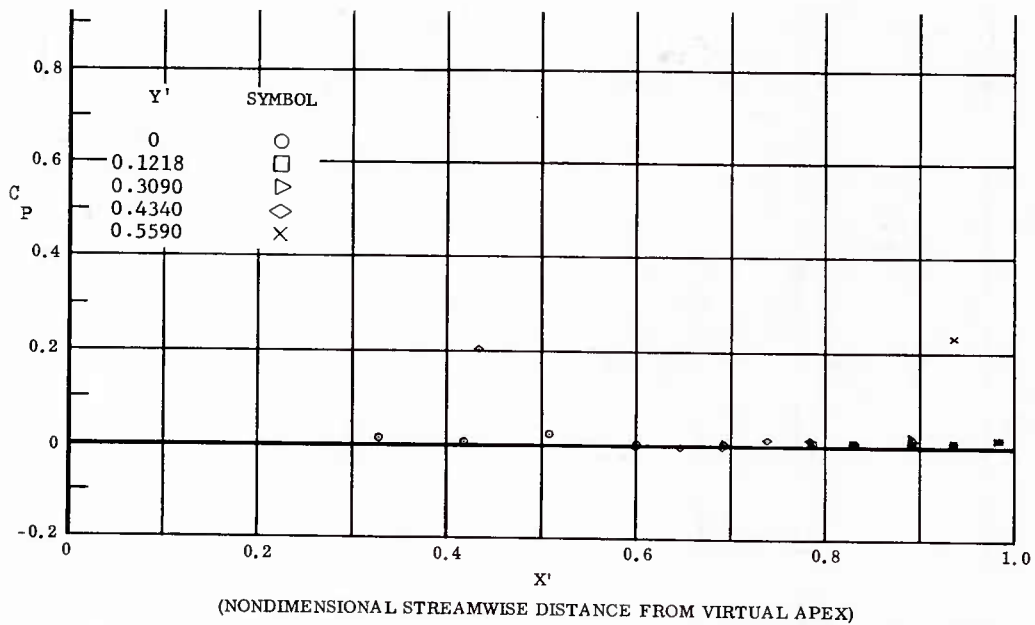


Fig. 31 Streamwise Distributions of Pressure Coefficients; Basic Configuration, Bottom Flaps Deflected +20°,  $\alpha = -12^\circ$ ,  $\beta = 0^\circ$ ,  $Re_\infty/ft = 3,300,000$ .

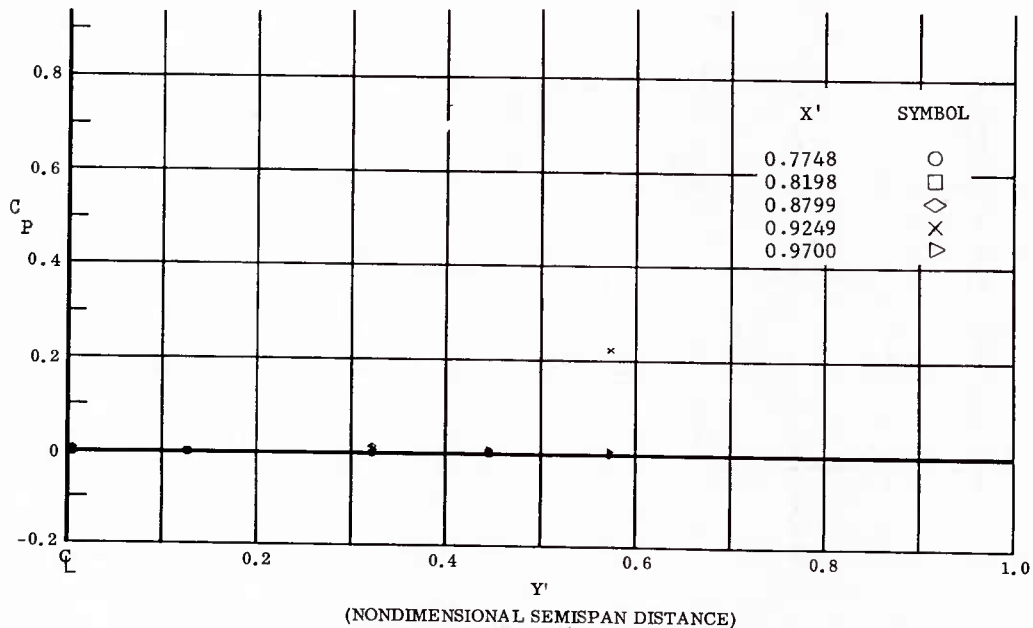


Fig. 31 Spanwise Distributions of Pressure Coefficients; Basic Configuration, Bottom Flaps Deflected +20°,  $\alpha = -12^\circ$ ,  $\beta = 0^\circ$ ,  $Re_\infty/ft = 3,300,000$ .

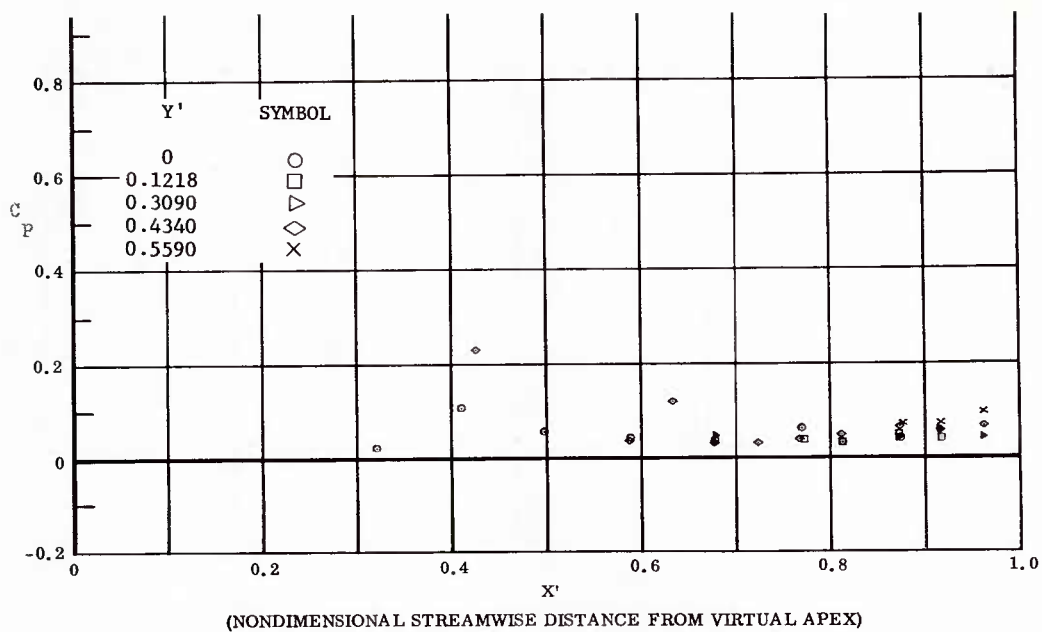


Fig. 32 Streamwise Distributions of Pressure Coefficients; Basic Configuration + Longer Chord Flaps, Bottom Flaps Deflected +20°,  $\alpha = -12^\circ$ ,  $\beta = 0^\circ$ ,  $Re_\infty / ft = 1,100,000$ .

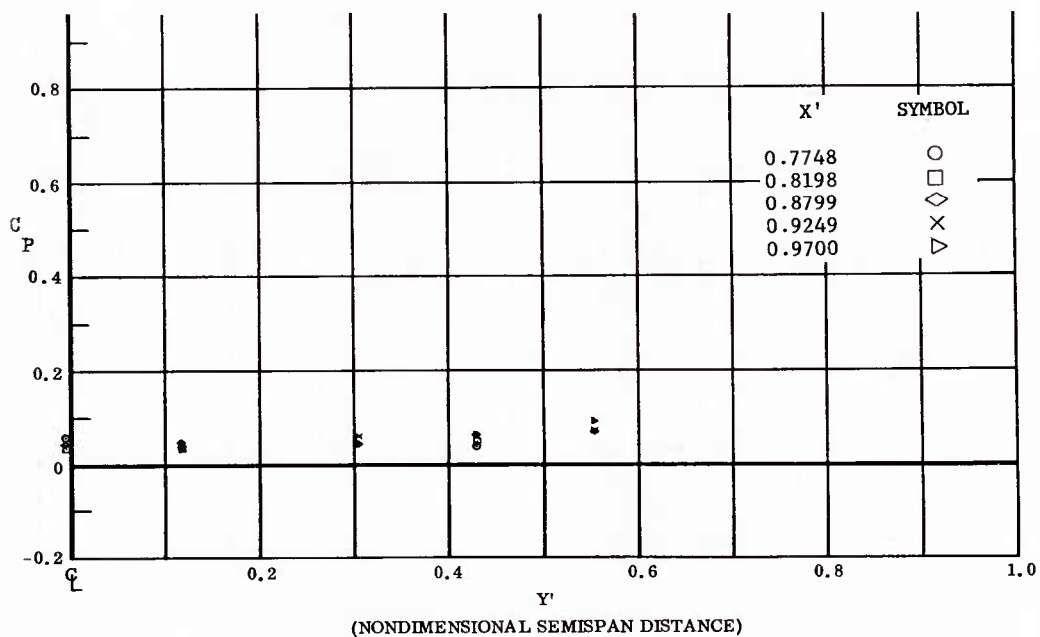


Fig. 32 Spanwise Distributions of Pressure Coefficients; Basic Configuration + Longer Chord Flaps, Bottom Flaps Deflected +20°,  $\alpha = -12^\circ$ ,  $\beta = 0^\circ$ ,  $Re_\infty / ft = 1,100,000$ .



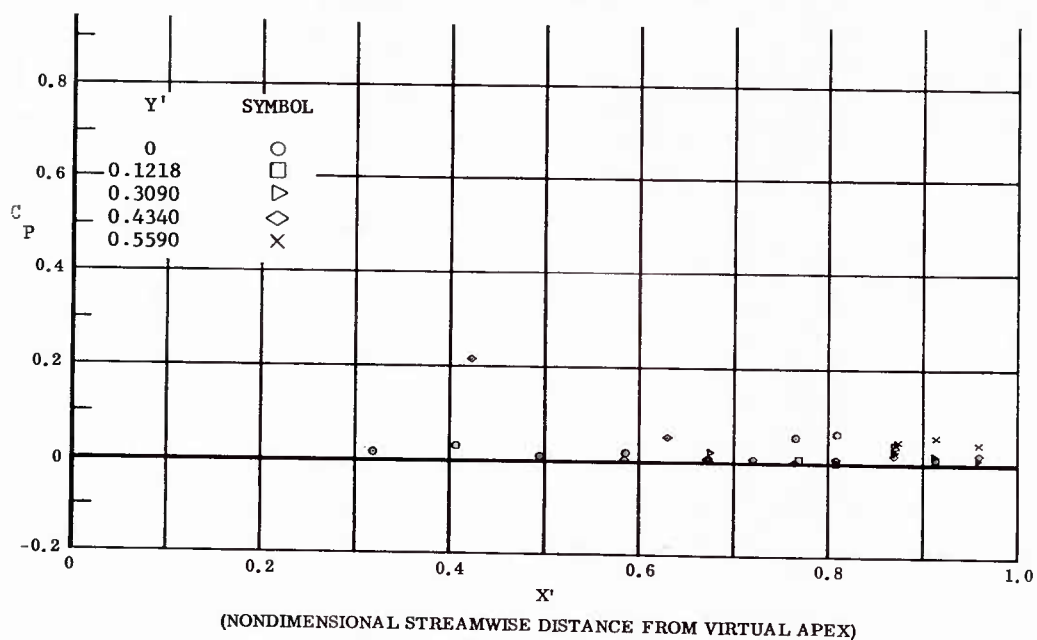


Fig. 33 Streamwise Distributions of Pressure Coefficients; Basic Configuration + Longer Chord Flaps, Bottom Flaps Deflected +20°,  $\alpha = -12^\circ$ ,  $\beta = 0^\circ$ ,  $Re_\infty/ft = 3,300,000$ .

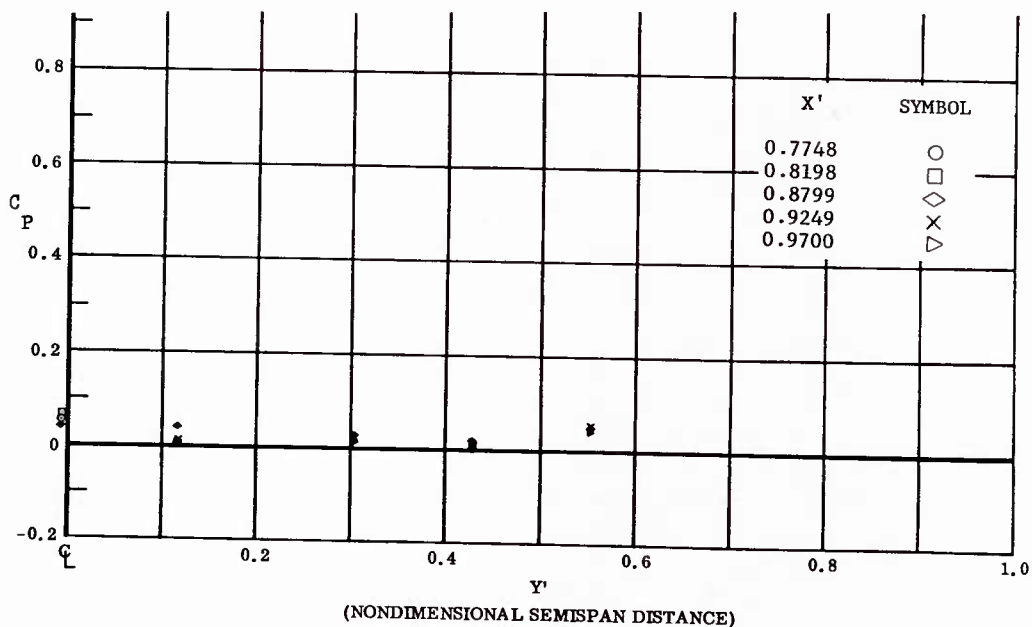


Fig. 33 Spanwise Distributions of Pressure Coefficients; Basic Configuration + Longer Chord Flaps, Bottom Flaps Deflected +20°,  $\alpha = -12^\circ$ ,  $\beta = 0^\circ$ ,  $Re_\infty/ft = 3,300,000$ .

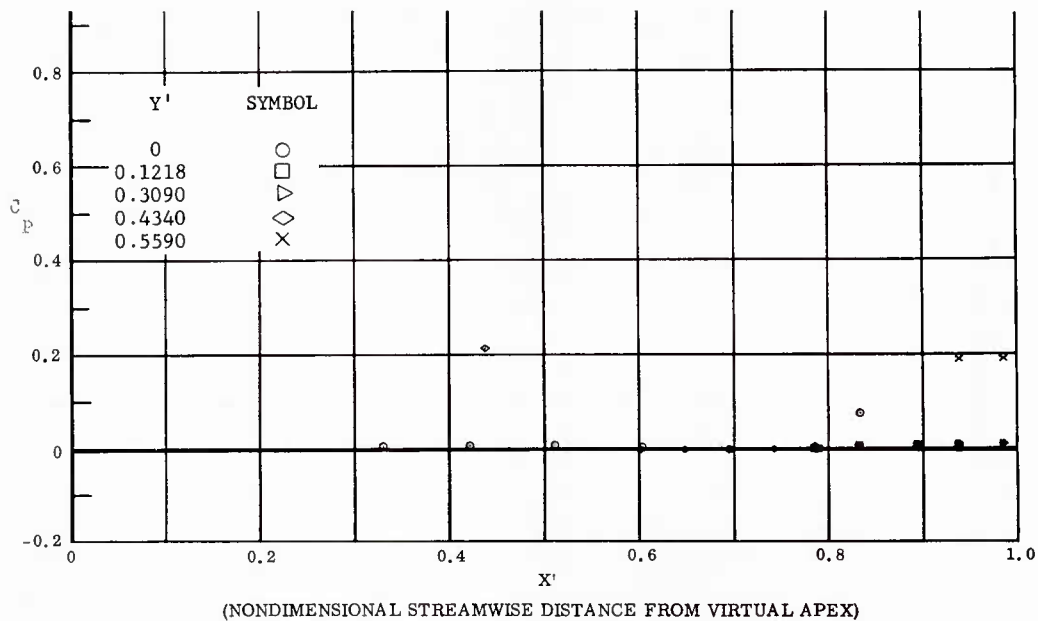


Fig. 34 Streamwise Distributions of Pressure Coefficients; Basic Configuration, Bottom Flaps Deflected  $+30^\circ$ ,  $\alpha = -12^\circ$ ,  $\beta = 0^\circ$ ,  $Re_\infty/ft = 3,300,000$ .

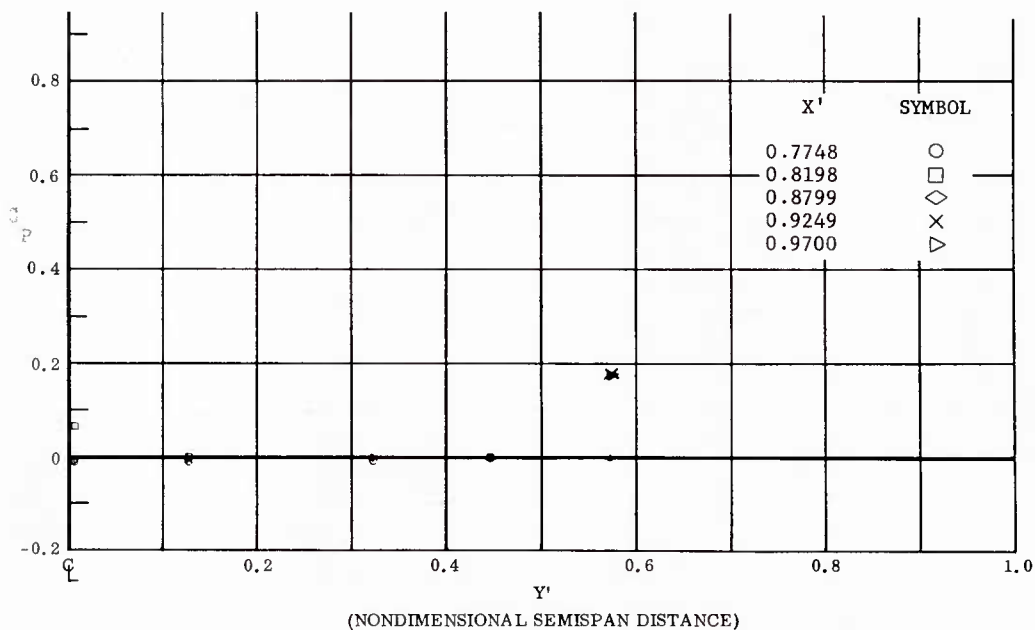


Fig. 34 Spanwise Distributions of Pressure Coefficients; Basic Configuration, Bottom Flaps Deflected  $+30^\circ$ ,  $\alpha = -12^\circ$ ,  $\beta = 0^\circ$ ,  $Re_\infty/ft = 3,300,000$ .

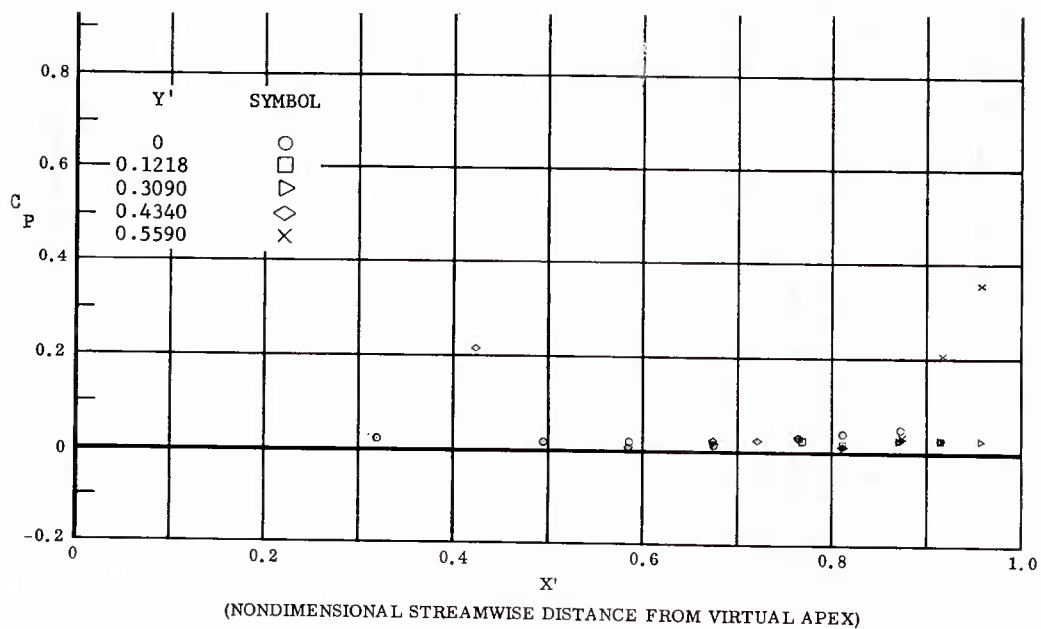


Fig. 35 Streamwise Distributions of Pressure Coefficients; Basic Configuration, Bottom Flaps Deflected  $+40^\circ$ ,  $\alpha = -12^\circ$ ,  $\beta = 0^\circ$ ,  $Re_\infty/ft = 1,100,000$ .

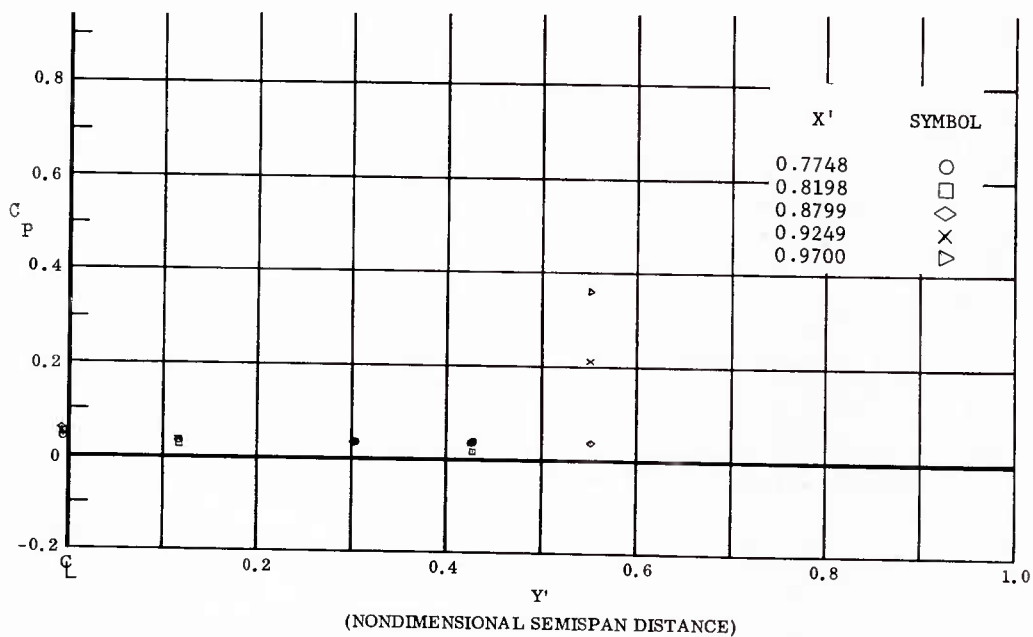


Fig. 35 Spanwise Distributions of Pressure Coefficients; Basic Configuration, Bottom Flaps Deflected  $+40^\circ$ ,  $\alpha = -12^\circ$ ,  $\beta = 0^\circ$ ,  $Re_\infty/ft = 1,100,000$ .

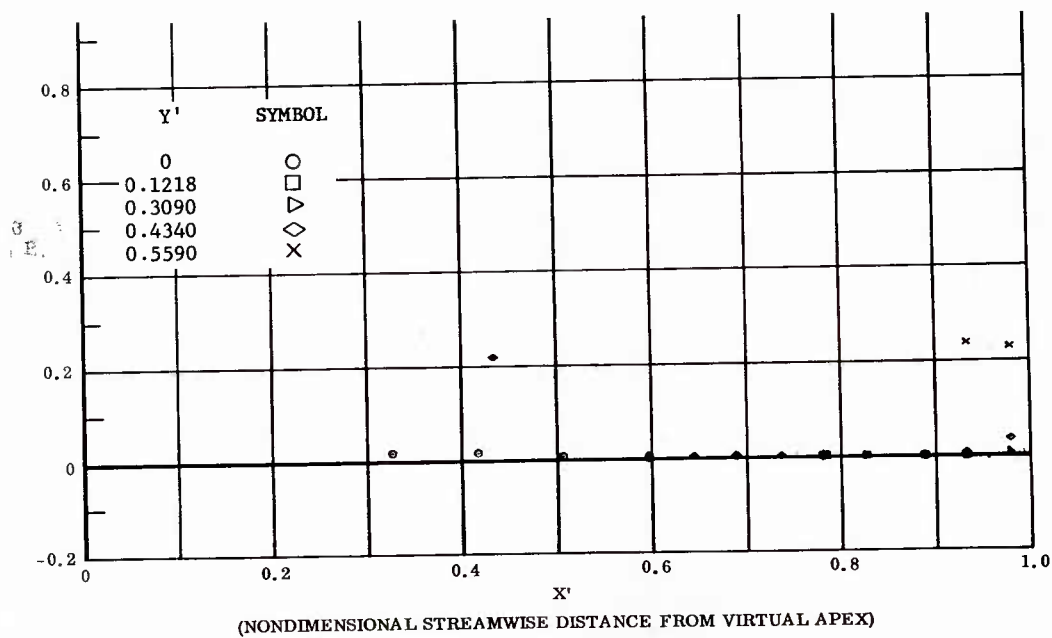


Fig. 36 Streamwise Distributions of Pressure Coefficients; Basic Configuration, Bottom Flaps Deflected  $+40^\circ$ ,  $\alpha = -12^\circ$ ,  $\beta = 0^\circ$ ,  $Re_\infty/ft = 3,300,000$ .

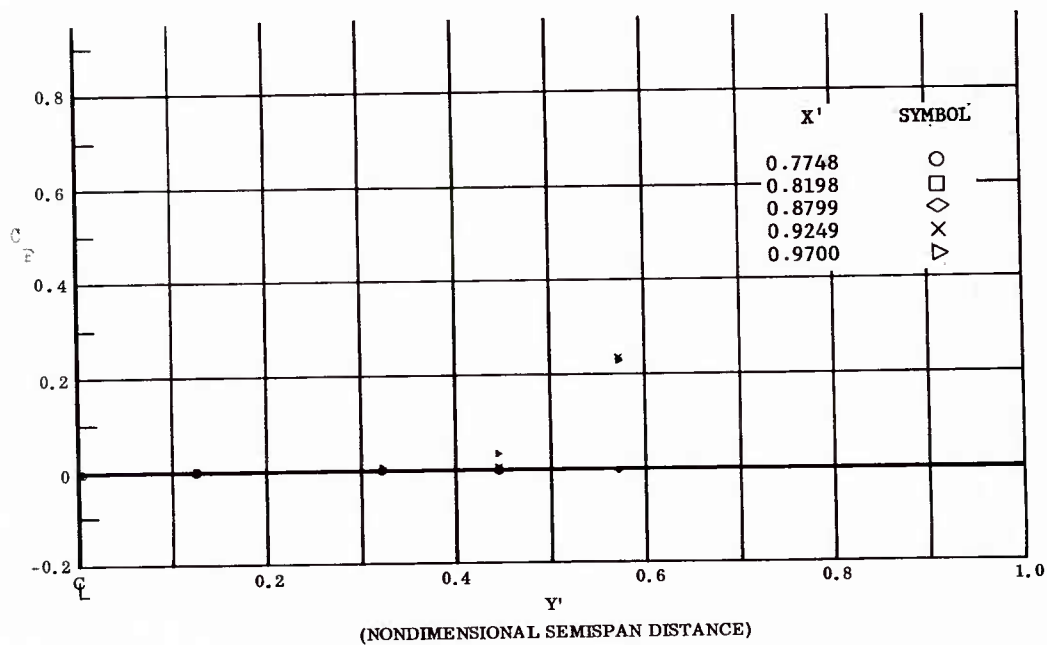


Fig. 36 Spanwise Distributions of Pressure Coefficients; Basic Configuration, Bottom Flaps Deflected  $+40^\circ$ ,  $\alpha = -12^\circ$ ,  $\beta = 0^\circ$ ,  $Re_\infty/ft = 3,300,000$ .

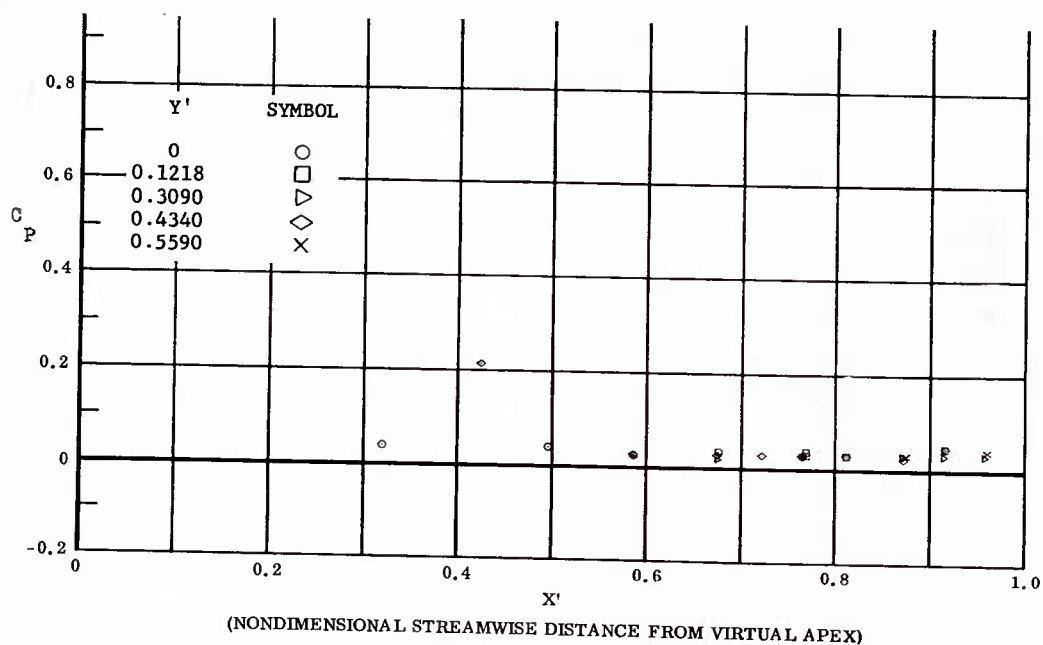


Fig. 37 Streamwise Distributions of Pressure Coefficients; Basic Configuration, Left and Right (Upper) Flaps Deflected  $-40^\circ$ ,  $\alpha = 0^\circ$ ,  $\beta = 0^\circ$ ,  $Re_\infty/ft = 1,100,000$ .

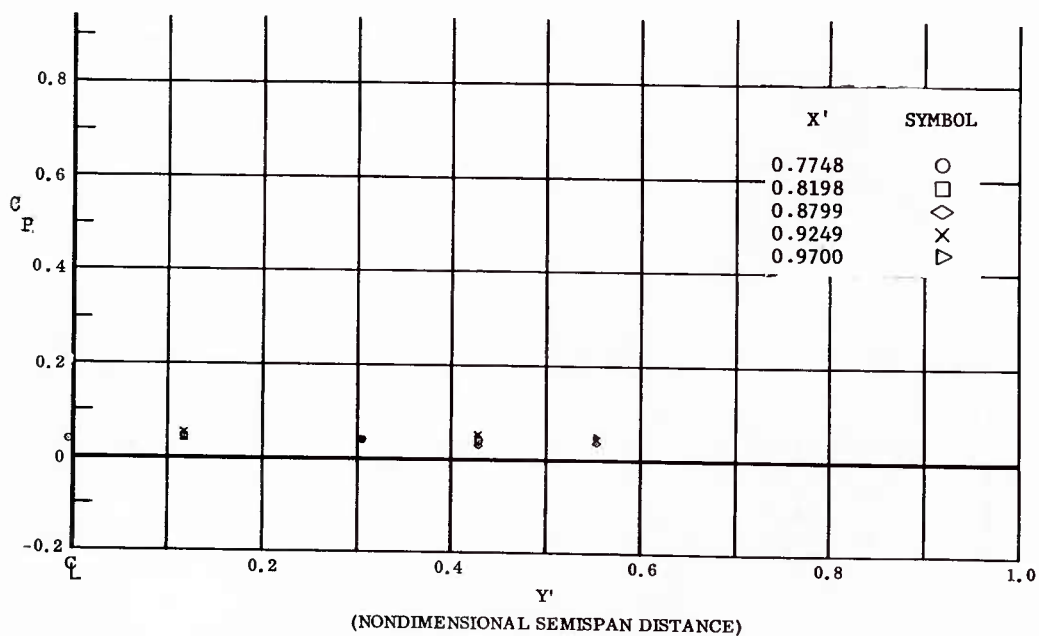


Fig. 37 Spanwise Distributions of Pressure Coefficients; Basic Configuration, Left and Right (Upper) Flaps Deflected  $-40^\circ$ ,  $\alpha = 0^\circ$ ,  $\beta = 0^\circ$ ,  $Re_\infty/ft = 1,100,000$ .

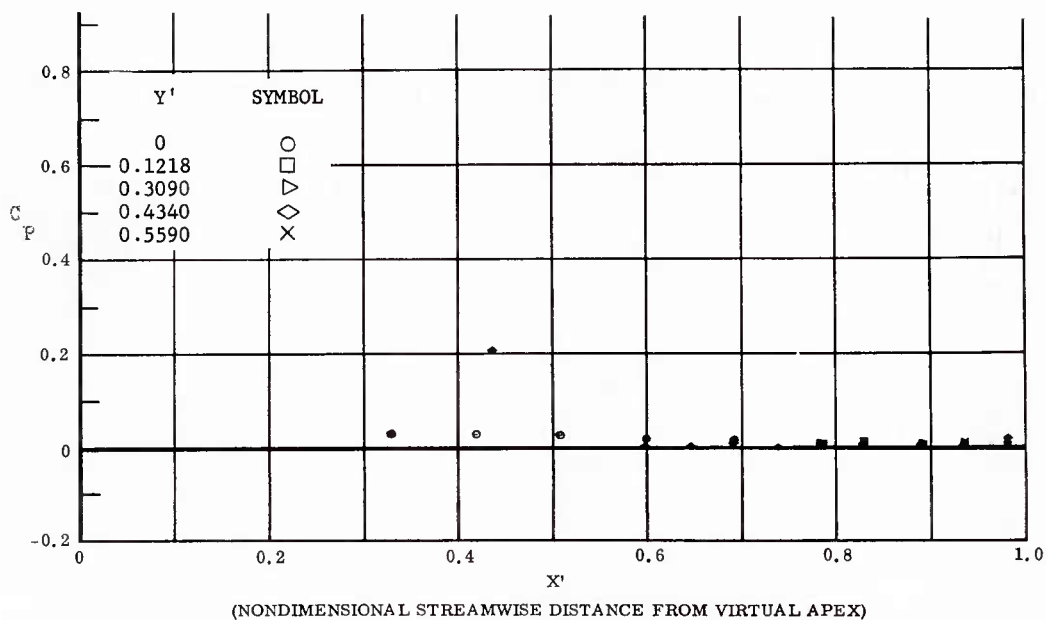


Fig. 38 Streamwise Distributions of Pressure Coefficients, Basic Configuration, Left and Right (Upper) Flaps Deflected  $-40^\circ$ ,  $\alpha = 0^\circ$ ,  $\beta = 0^\circ$ ,  $Re_\infty/ft = 3,300,000$ .

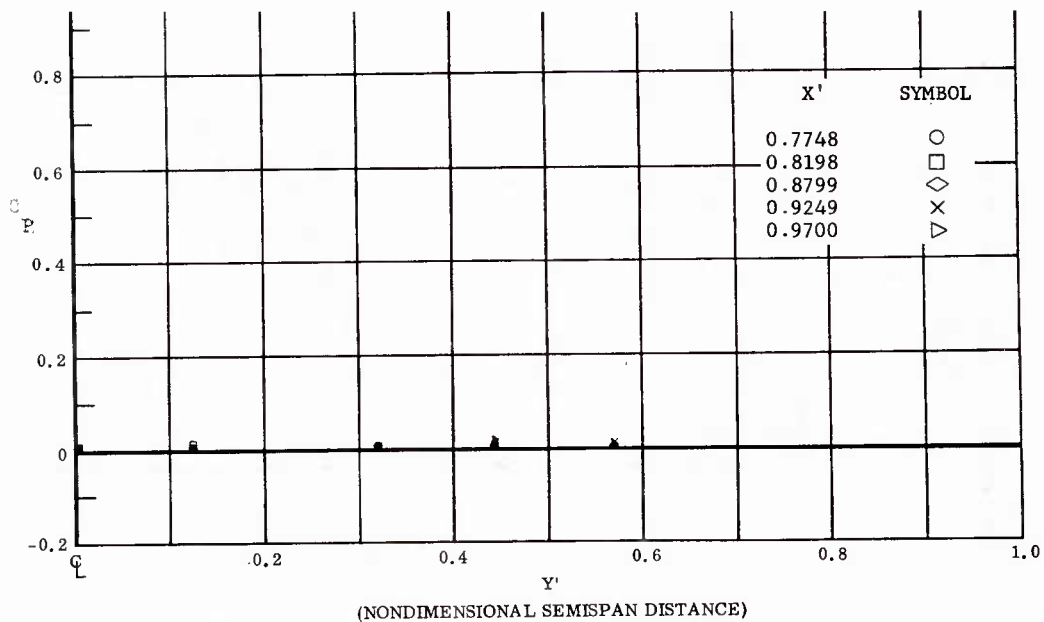


Fig. 38 Spanwise Distributions of Pressure Coefficients, Basic Configuration, Left and Right (Upper) Flaps Deflected  $-40^\circ$ ,  $\alpha = 0^\circ$ ,  $\beta = 0^\circ$ ,  $Re_\infty/ft = 3,300,000$ .



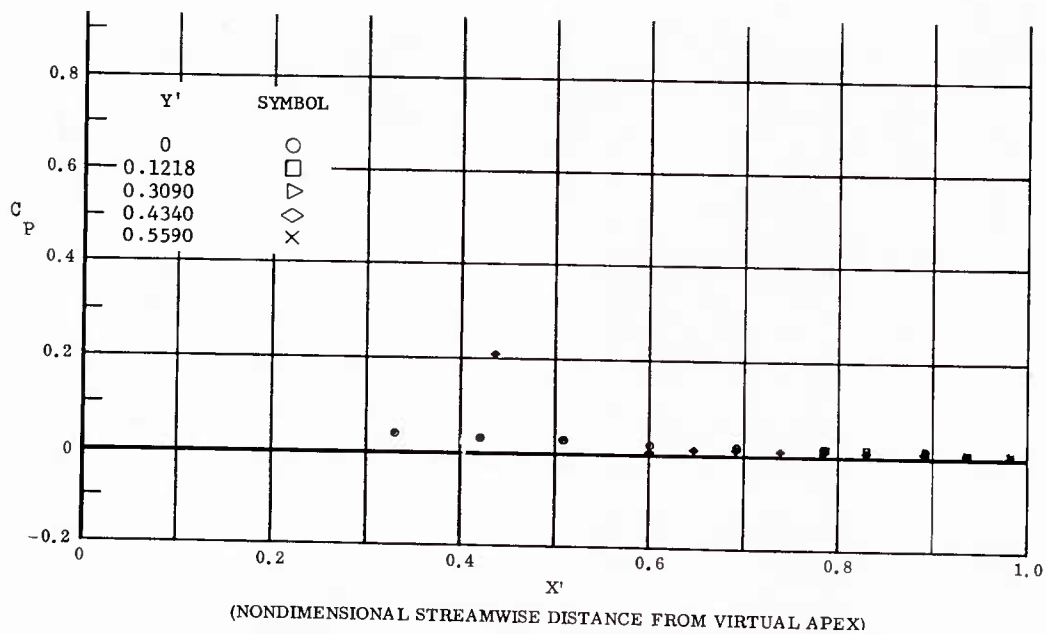


Fig. 39 Streamwise Distributions of Pressure Coefficients, Basic Configuration, Left (Upper) Flap Deflected -40°,  $\alpha = 0^\circ$ ,  $\beta = 0^\circ$ ,  $Re_\infty/ft = 3,300,000$ .

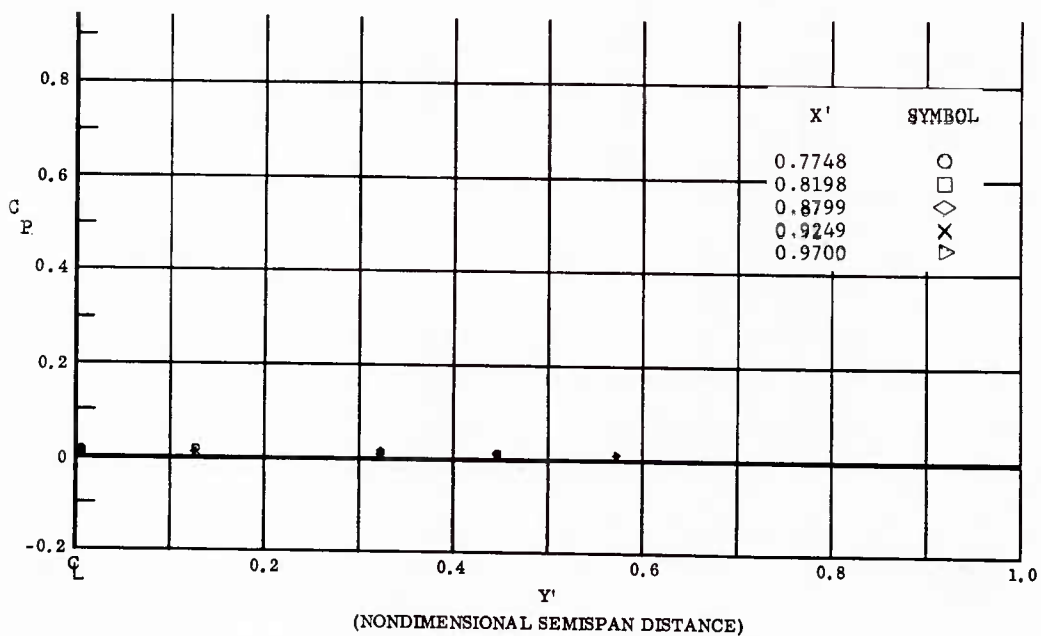


Fig. 39 Spanwise Distributions of Pressure Coefficients, Basic Configuration, Left (Upper) Flap Deflected -40°,  $\alpha = 0^\circ$ ,  $\beta = 0^\circ$ ,  $Re_\infty/ft = 3,300,000$ .

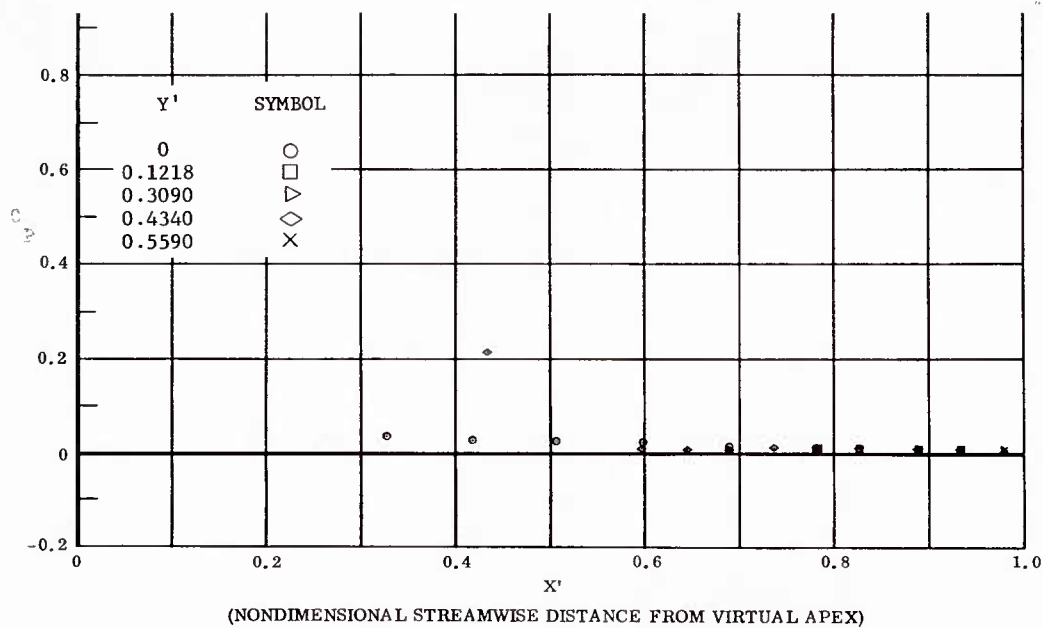


Fig. 40 Streamwise Distributions of Pressure Coefficients, Basic Configuration, Right (Upper) Flap Deflected  $-40^\circ$ ,  $\alpha = 0^\circ$ ,  $\beta = 0^\circ$ ,  $Re_\infty/ft = 3,300,000$ .

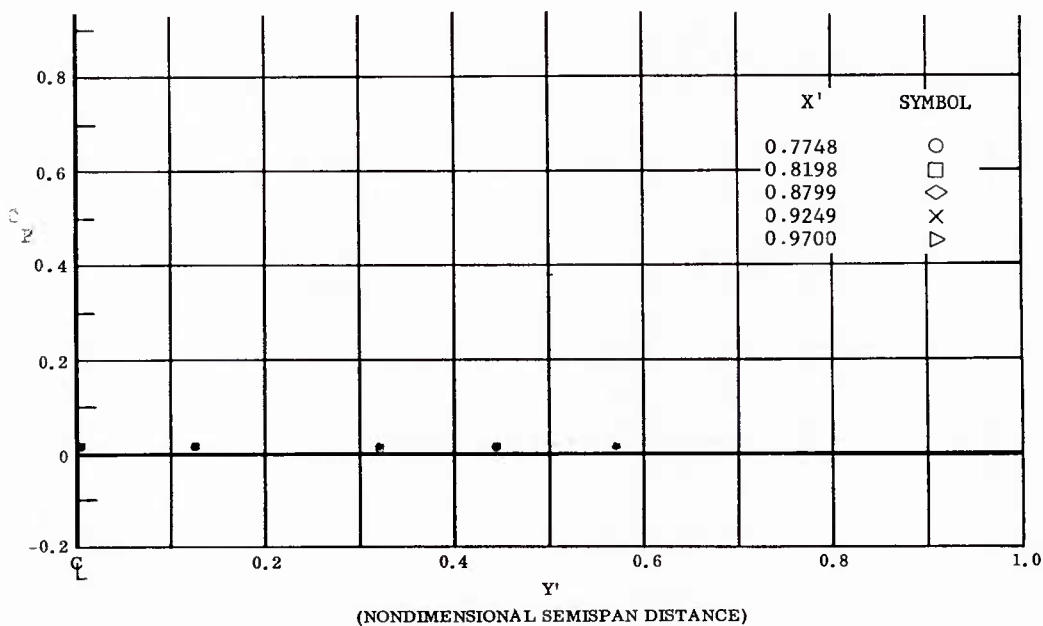


Fig. 40 Spanwise Distributions of Pressure Coefficients, Basic Configuration, Right (Upper) Flap Deflected  $-40^\circ$ ,  $\alpha = 0^\circ$ ,  $\beta = 0^\circ$ ,  $Re_\infty/ft = 3,300,000$ .

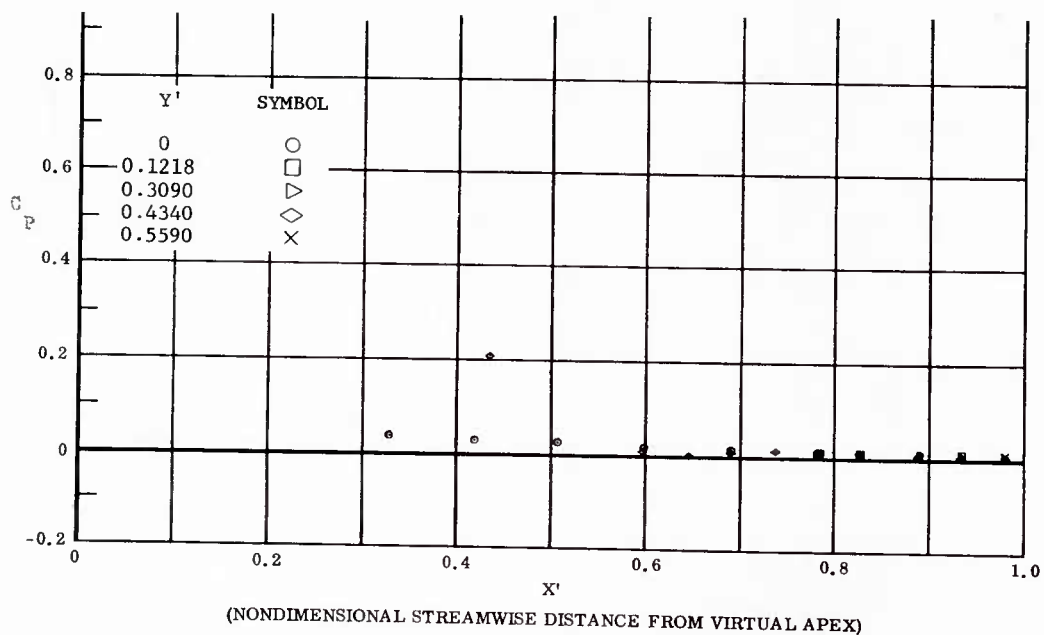


Fig. 41 Streamwise Distributions of Pressure Coefficients, Basic Configuration, Left and Right (Upper) Flaps Deflected  $-30^\circ$ ,  $\alpha = 0^\circ$ ,  $\beta = 0^\circ$ ,  $Re_\infty/ft = 3,300,000$ .

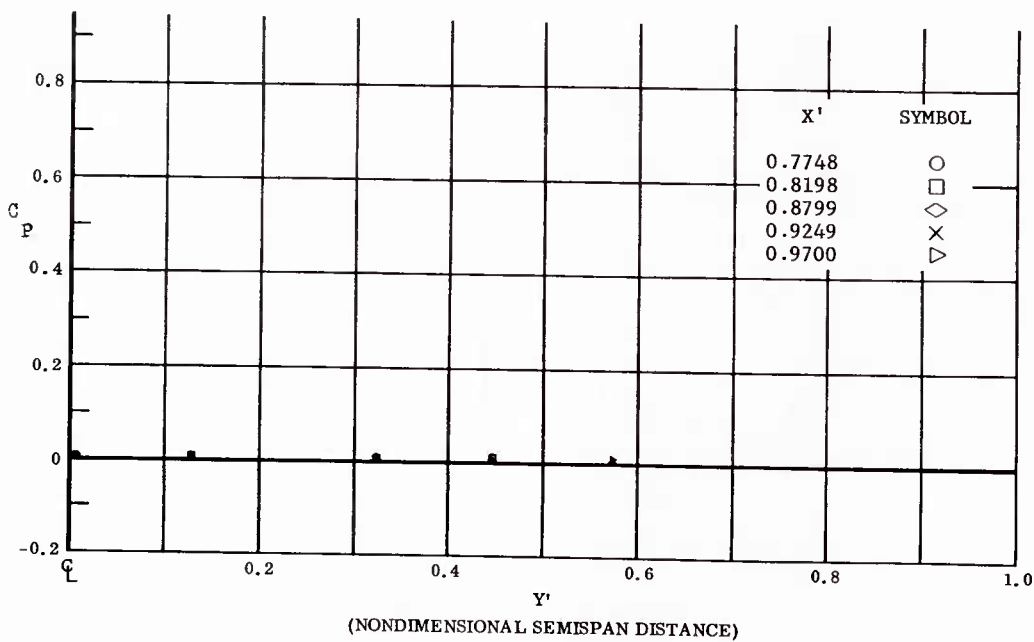


Fig. 41 Spanwise Distributions of Pressure Coefficients, Basic Configuration Left and Right (Upper) Flaps Deflected  $-30^\circ$ ,  $\alpha = 0^\circ$ ,  $\beta = 0^\circ$ ,  $Re_\infty/ft = 3,300,000$ .

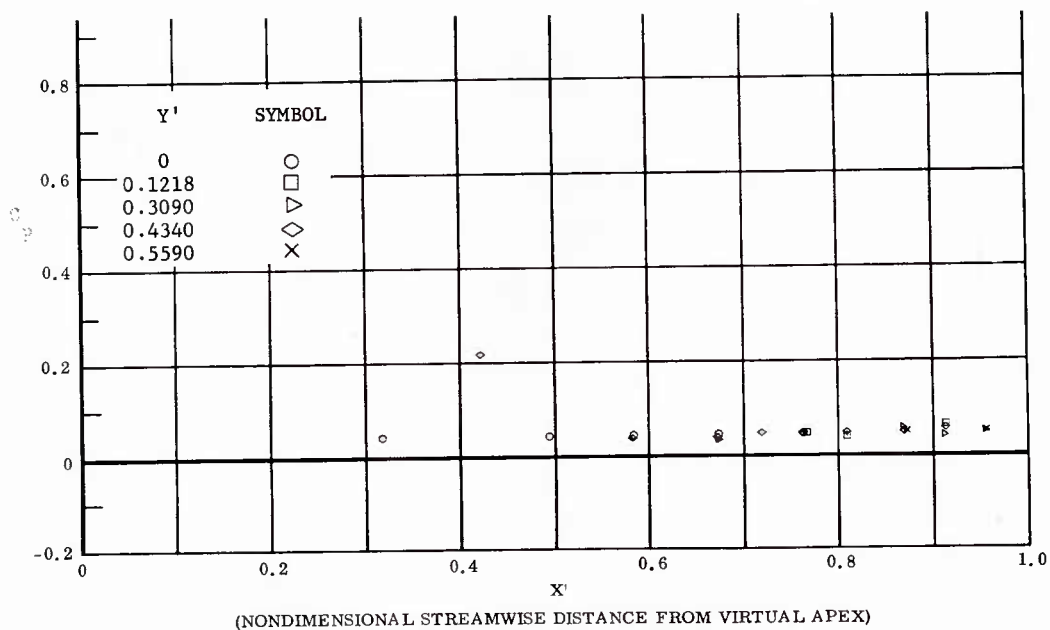


Fig. 42 Streamwise Distributions of Pressure Coefficients, Basic Configuration, Left and Right (Upper) Flaps Deflected  $-20^\circ$ ,  $\alpha = 0^\circ$ ,  $\beta = 0^\circ$ ,  $Re_\infty/ft = 1,100,000$ .

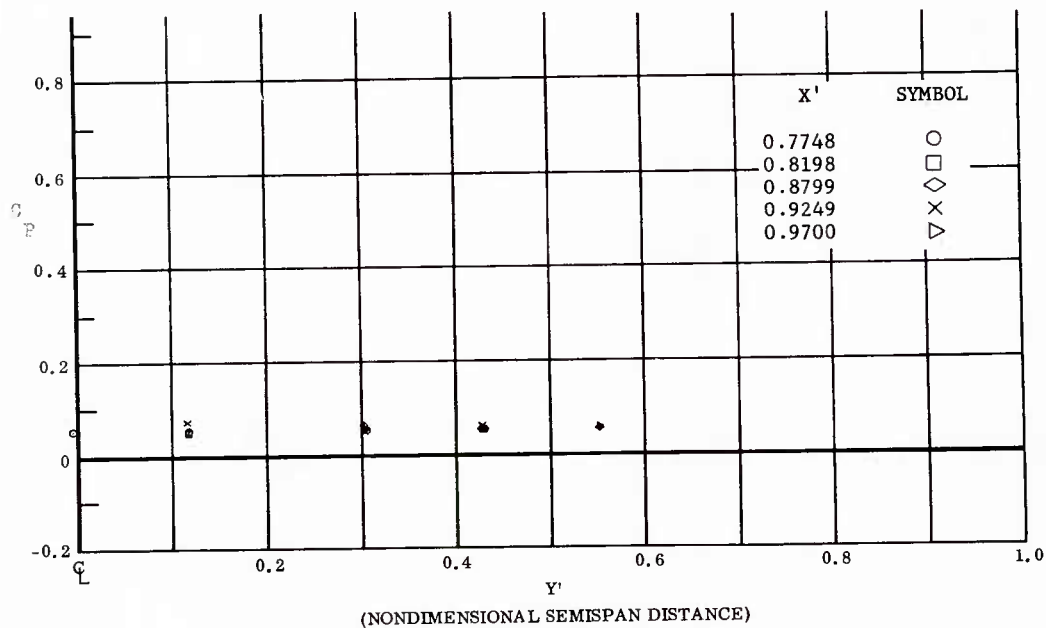


Fig. 42 Spanwise Distributions of Pressure Coefficients, Basic Configuration, Left and Right (Upper) Flaps Deflected  $-20^\circ$ ,  $\alpha = 0^\circ$ ,  $\beta = 0^\circ$ ,  $Re_\infty/ft = 1,100,000$ .

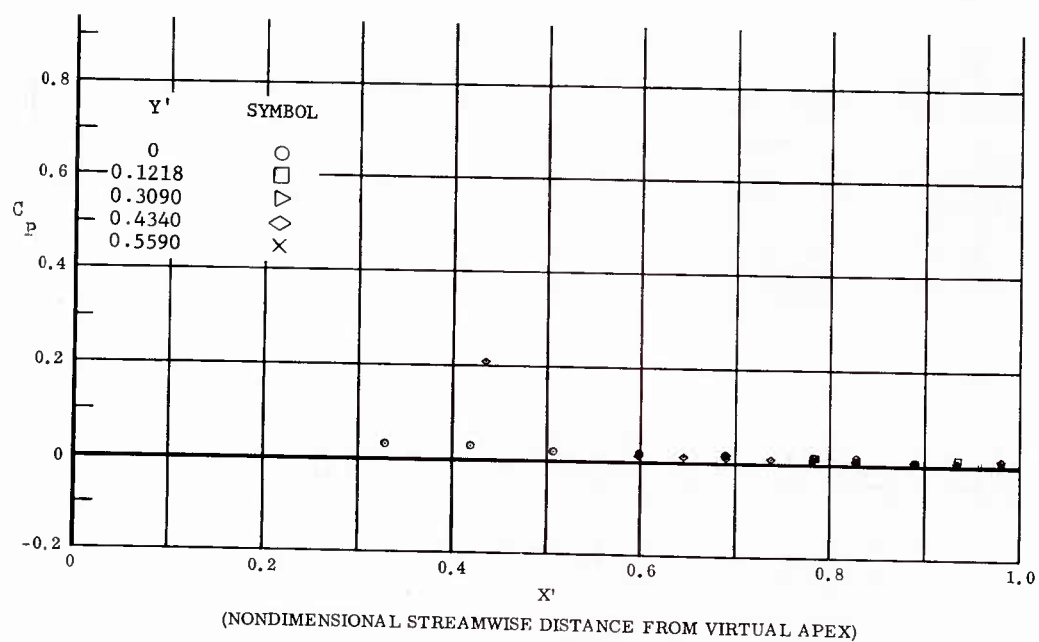


Fig. 43 Streamwise Distributions of Pressure Coefficients, Basic Configuration, Left and Right (Upper) Flaps Deflected  $-20^\circ$ ,  $\alpha = 0^\circ$ ,  $\beta = 0^\circ$ ,  $Re_\infty/ft = 3,300,000$ .

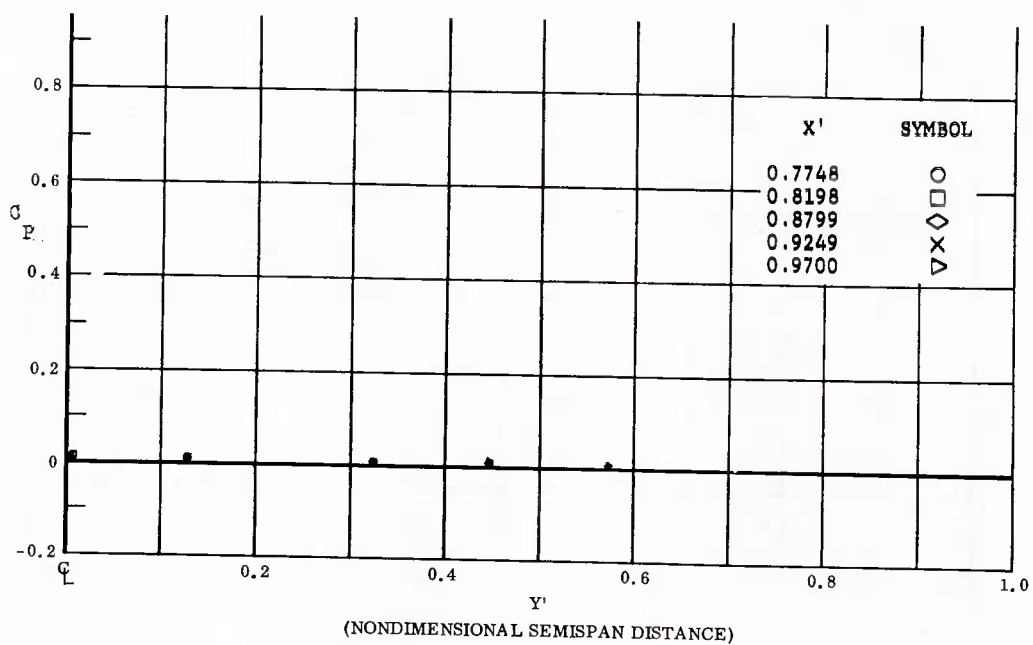


Fig. 43 Spanwise Distributions of Pressure Coefficients, Basic Configuration, Left and Right (Upper) Flaps Deflected  $-20^\circ$ ,  $\alpha = 0^\circ$ ,  $\beta = 0^\circ$ ,  $Re_\infty/ft = 3,300,000$ .

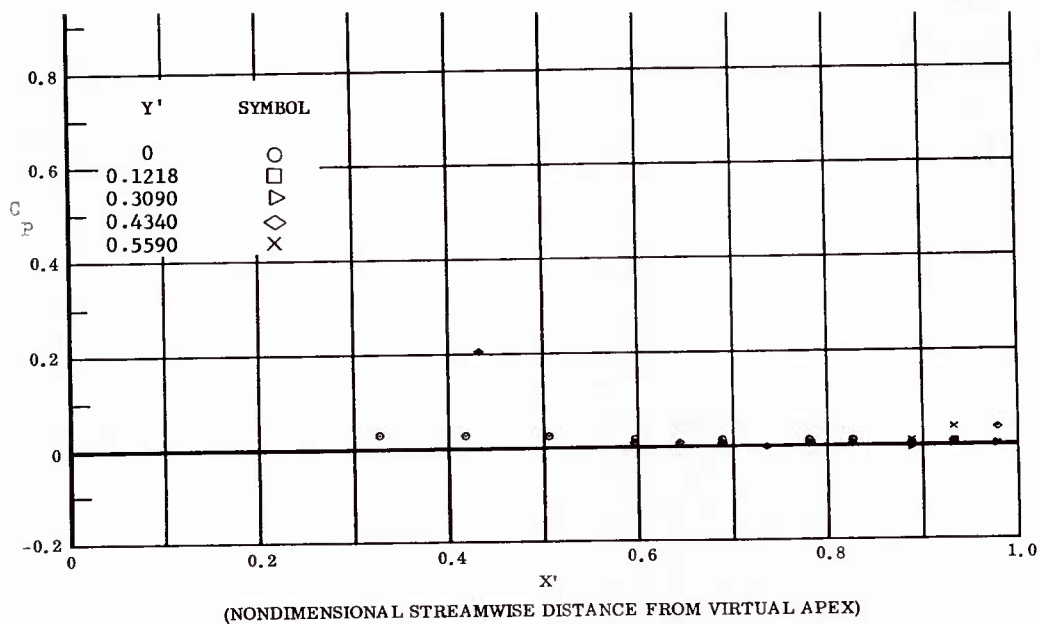


Fig. 44 Streamwise Distributions of Pressure Coefficients, Basic Configuration, Left (Upper) Flap Deflected  $-20^\circ$ ,  $\alpha = 0^\circ$ ,  $\beta = 0^\circ$ ,  $Re_\infty/ft = 3,300,000$ .

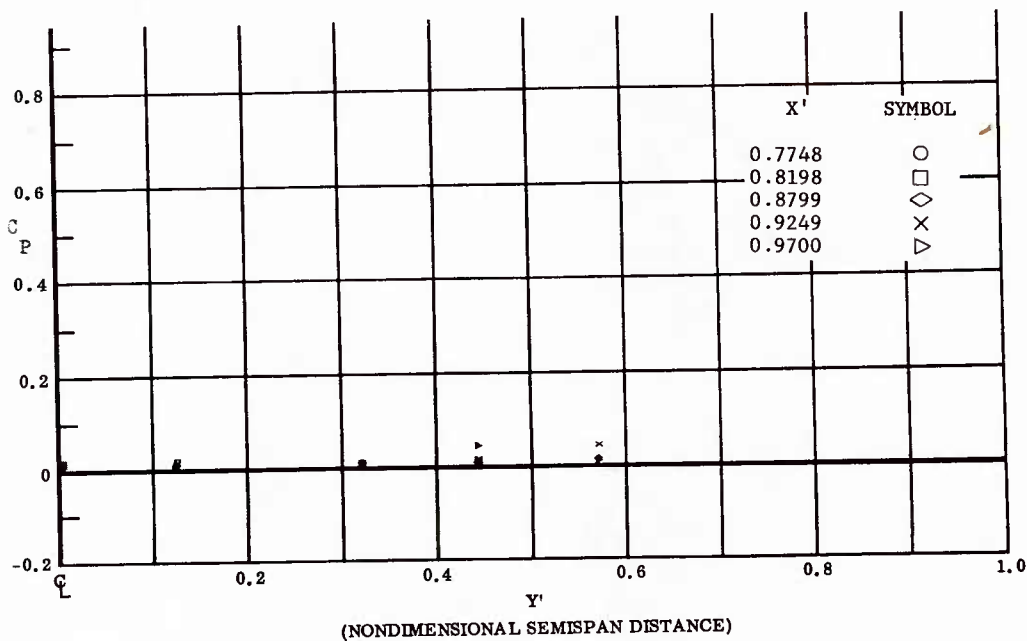


Fig. 44 Spanwise Distributions of Pressure Coefficients, Basic Configuration, Left (Upper) Flap Deflected  $-20^\circ$ ,  $\alpha = 0^\circ$ ,  $\beta = 0^\circ$ ,  $Re_\infty/ft = 3,300,000$ .



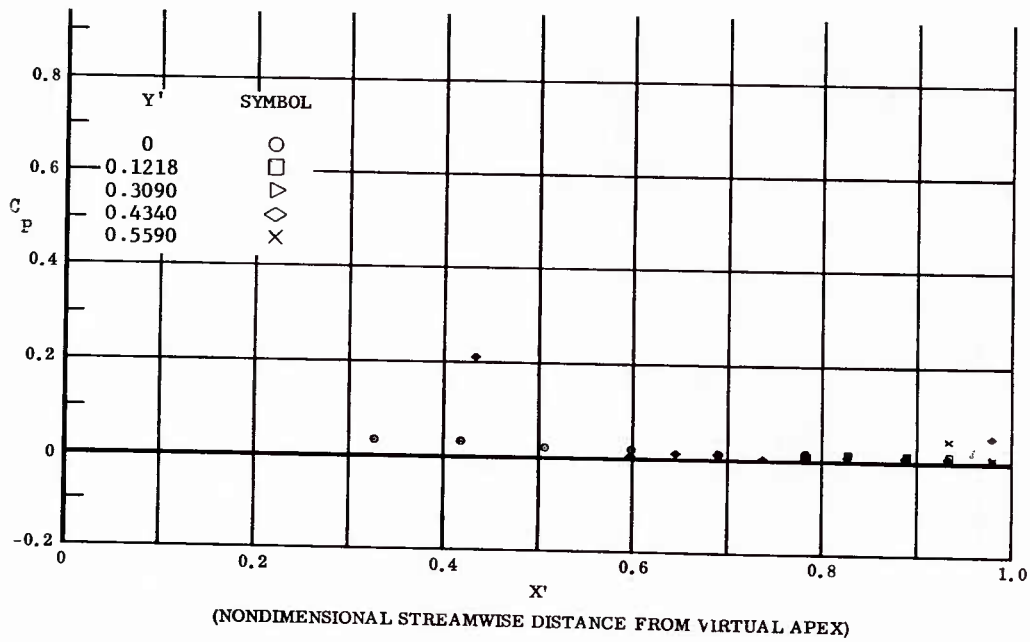


Fig. 45 Streamwise Distributions of Pressure Coefficients, Basic Configuration, Right (Upper) Flap Deflected  $-20^\circ$ ,  $\alpha = 0^\circ$ ,  $\beta = 0^\circ$ ,  $Re_\infty / ft = 3,300,000$ .

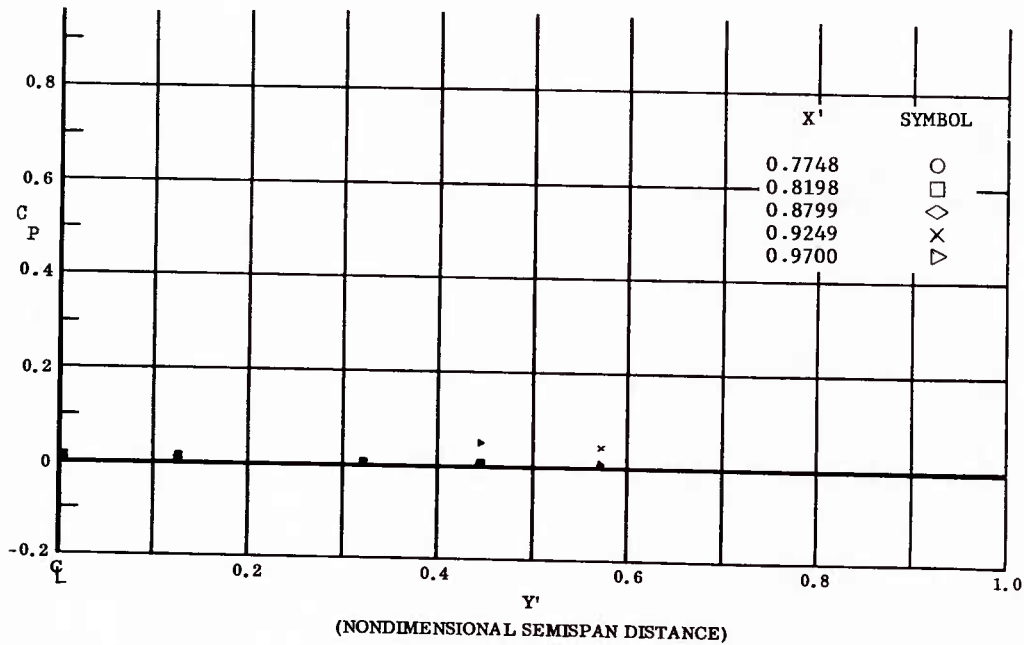


Fig. 45 Spanwise Distributions of Pressure Coefficients, Basic Configuration, Right (Upper) Flap Deflected  $-20^\circ$ ,  $\alpha = 0^\circ$ ,  $\beta = 0^\circ$ ,  $Re_\infty / ft = 3,300,000$ .

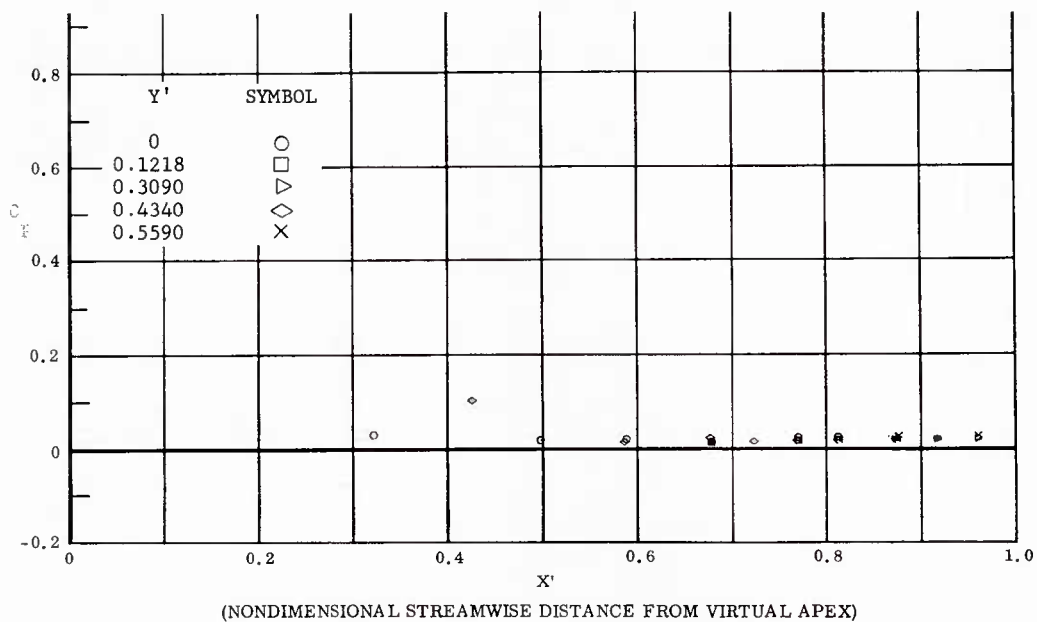


Fig. 46 Streamwise Distributions of Pressure Coefficients, Basic Configuration + Canards, Left and Right (Upper) Flaps Deflected  $-20^\circ$ ,  $\alpha = 0^\circ$ ,  $\beta = 0^\circ$ ,  $Re_\infty/ft = 3,300,000$ .

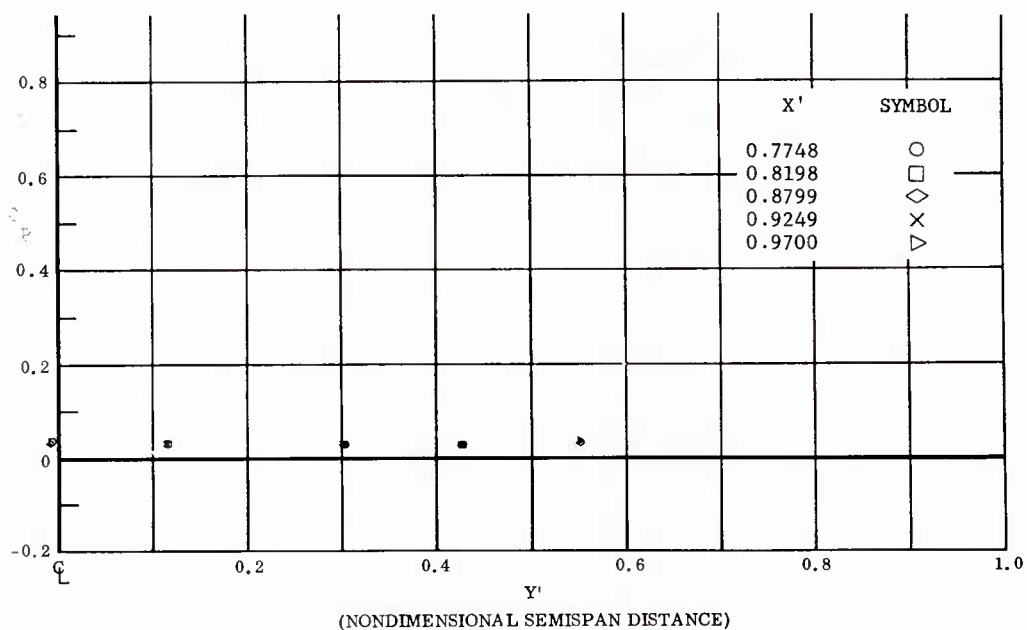


Fig. 46 Spanwise Distributions of Pressure Coefficients, Basic Configuration + Canards, Left and Right (Upper) Flaps Deflected  $-20^\circ$ ,  $\alpha = 0^\circ$ ,  $\beta = 0^\circ$ ,  $Re_\infty/ft = 3,300,000$ .

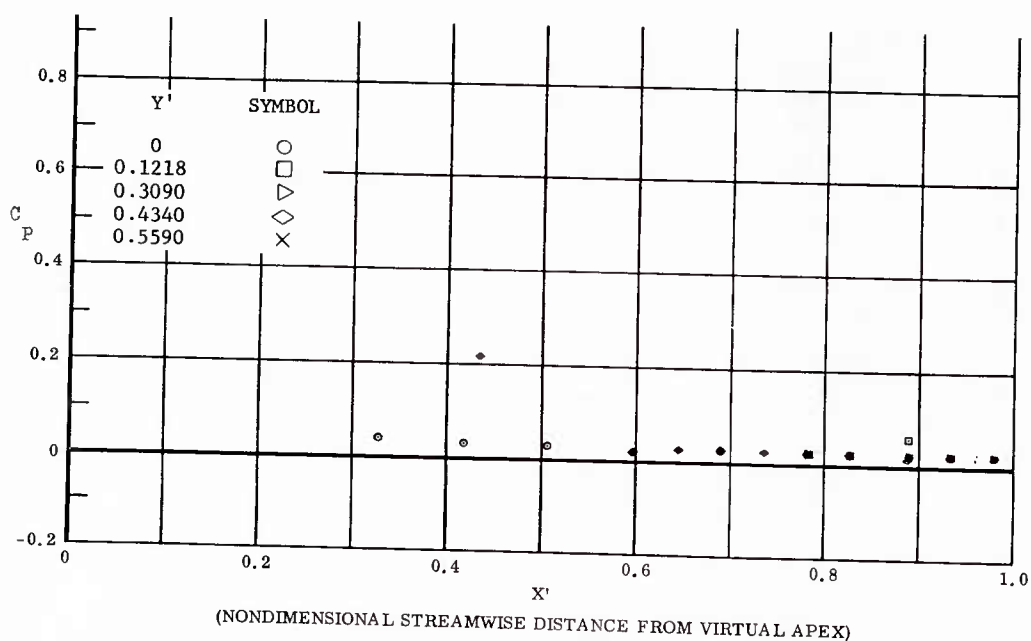


Fig. 47 Streamwise Distributions of Pressure Coefficients, Basic Configuration, Left and Right (Upper) Flaps Deflected  $-10^\circ$ ,  $\alpha = 0^\circ$ ,  $\beta = 0^\circ$ ,  $Re_\infty / ft = 3,300,000$ .

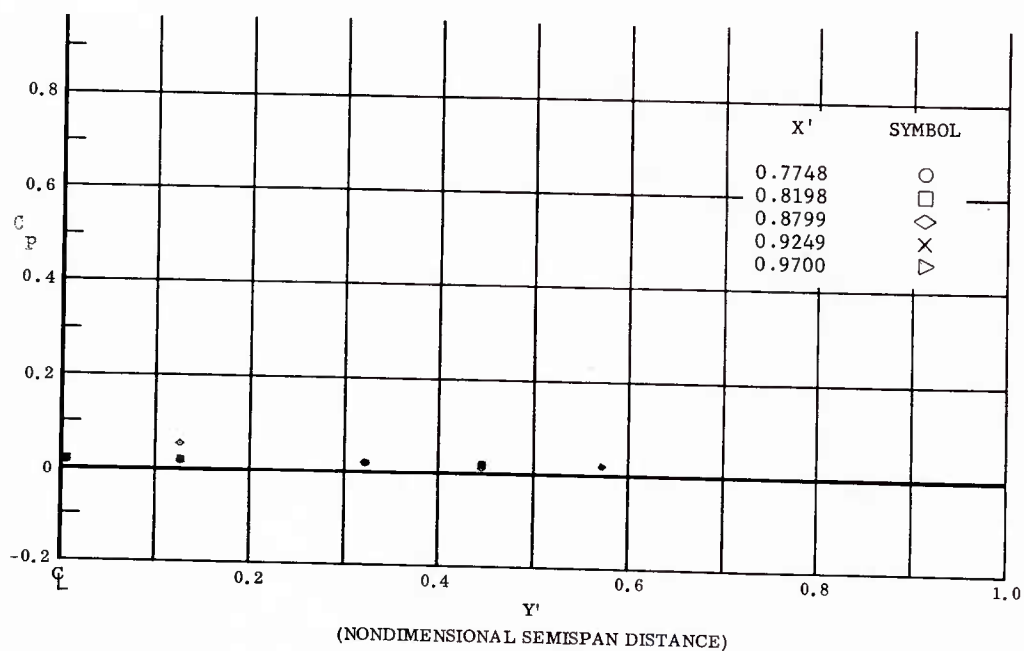


Fig. 47 Spanwise Distributions of Pressure Coefficients; Basic Configuration, Left and Right (Upper) Flaps Deflected  $-10^\circ$ ,  $\alpha = 0^\circ$ ,  $\beta = 0^\circ$ ,  $Re_\infty / ft = 3,300,000$ .

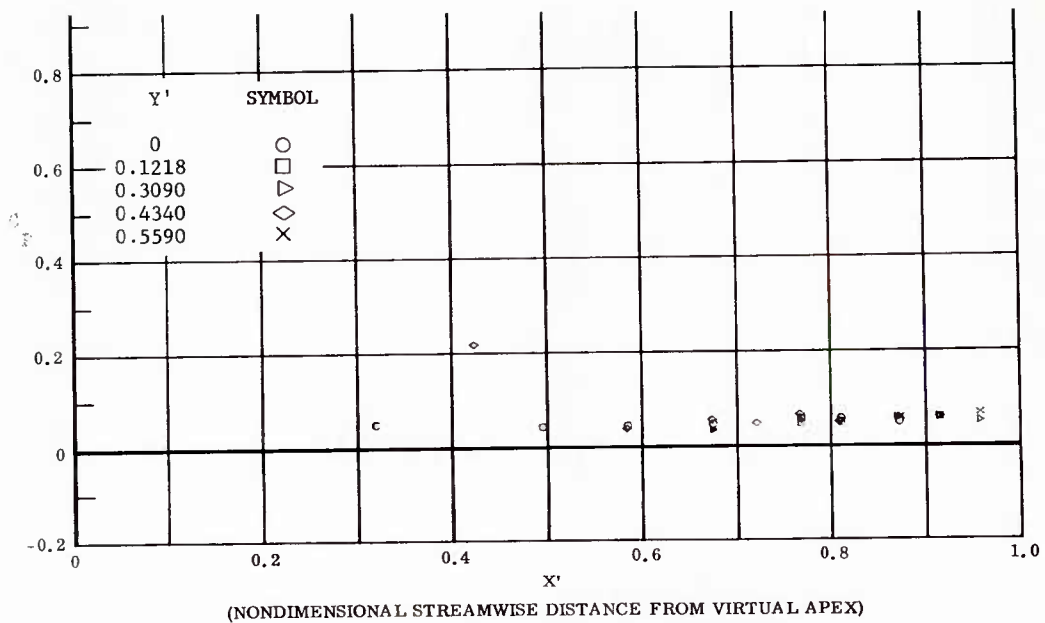


Fig. 48 Streamwise Distributions of Pressure Coefficients; Basic Configuration, No Flap Deflections,  $\alpha = 0^\circ$ ,  $\beta = 0^\circ$ ,  $Re_\infty/ft = 1,100,000$ .

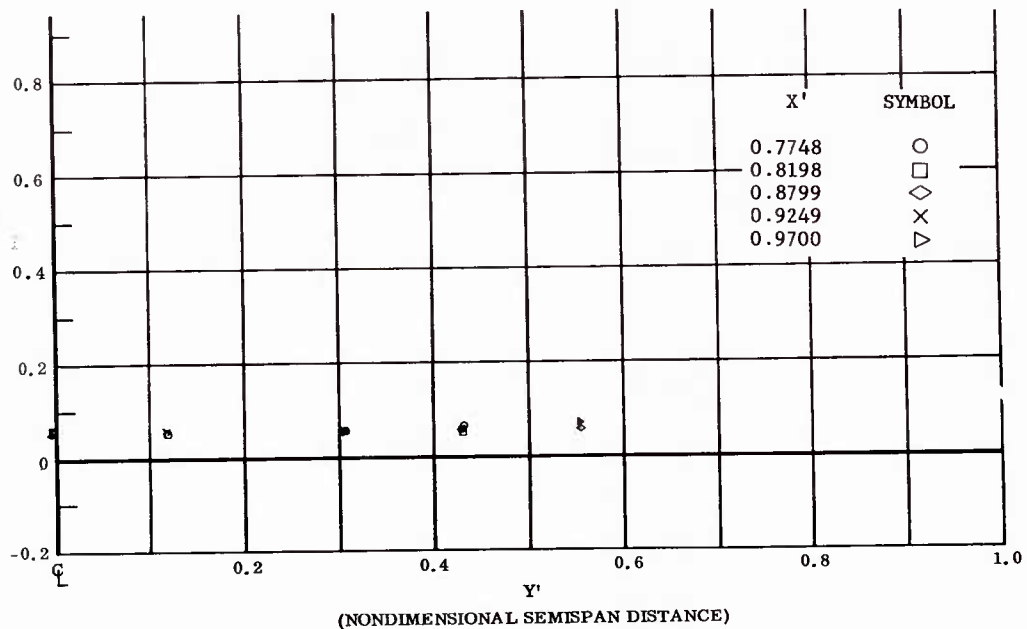


Fig. 48 Spanwise Distributions of Pressure Coefficients; Basic Configuration, No Flap Deflections,  $\alpha = 0^\circ$ ,  $\beta = 0^\circ$ ,  $Re_\infty/ft = 1,100,000$ .

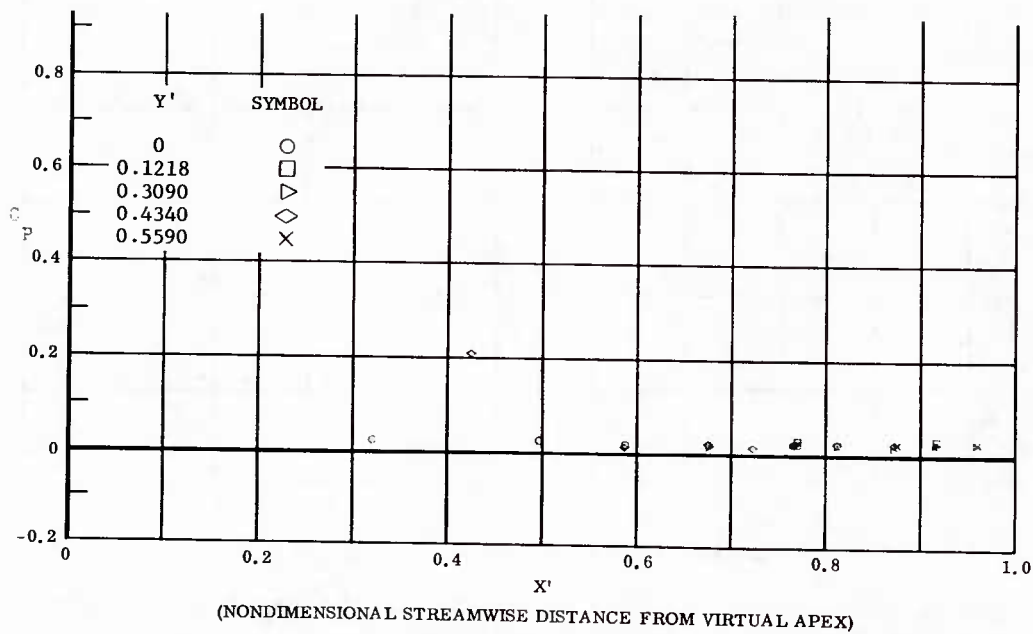


Fig. 49 Streamwise Distributions of Pressure Coefficients; Basic Configuration, No Flap Deflections,  $\alpha = 0^\circ$ ,  $\beta = 0^\circ$ ,  $Re_\infty / ft = 3,300,000$ .

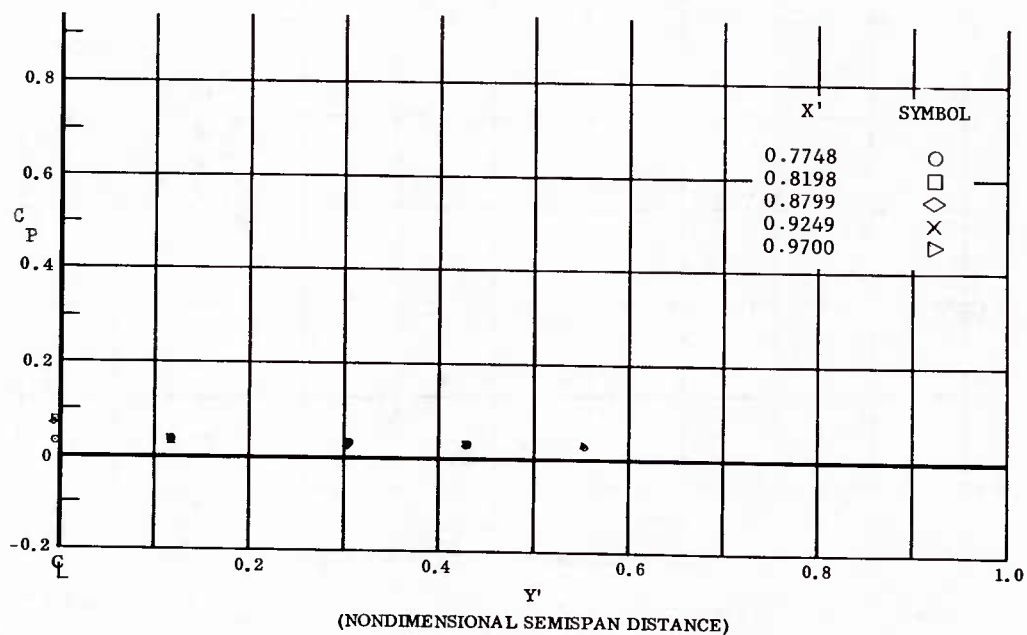


Fig. 49 Spanwise Distributions of Pressure Coefficients; Basic Configuration, No Flap Deflections,  $\alpha = 0^\circ$ ,  $\beta = 0^\circ$ ,  $Re_\infty / ft = 3,300,000$ .

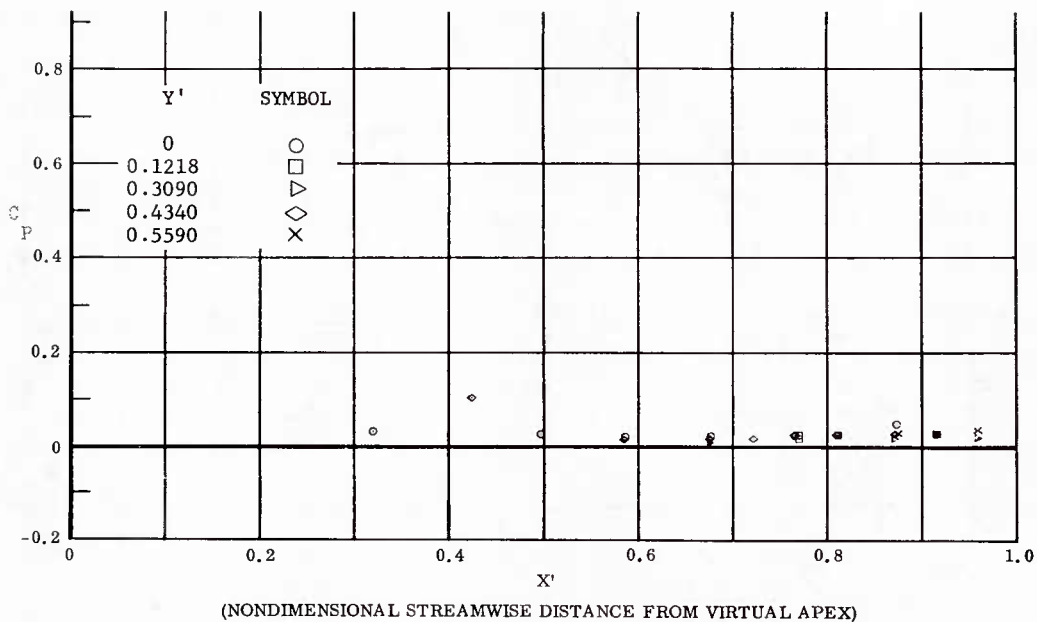


Fig. 50 Streamwise Distributions of Pressure Coefficients; Basic Configuration + Canards, No Flap Deflections,  $\alpha = 0^\circ$ ,  $\beta = 0^\circ$ ,  $Re_\infty/ft = 3,300,000$ .

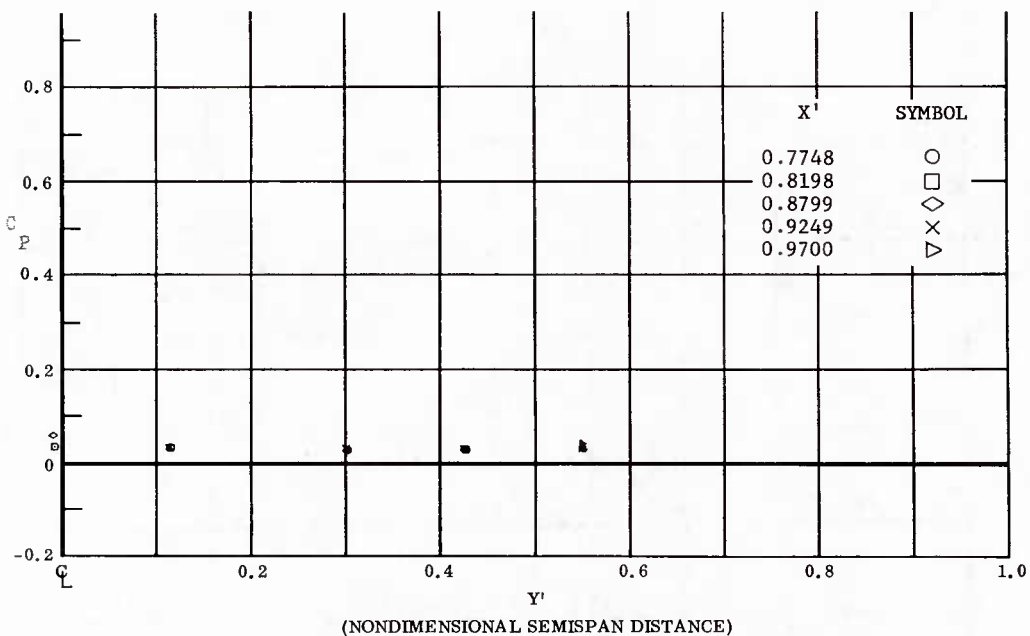


Fig. 50 Spanwise Distributions of Pressure Coefficients; Basic Configuration + Canards, No Flap Deflections,  $\alpha = 0^\circ$ ,  $\beta = 0^\circ$ ,  $Re_\infty/ft = 3,300,000$ .

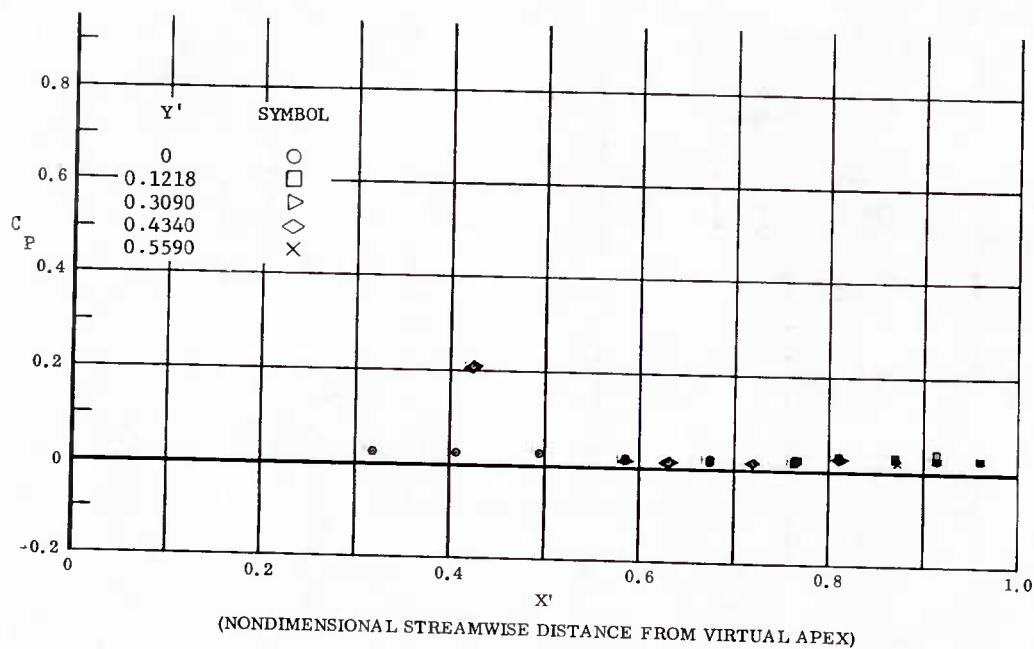


Fig. 51 Streamwise Distributions of Pressure Coefficients; Basic Configuration + Fin ( $\delta = 0$ ), No Flap Deflections,  $\alpha = 0^\circ$ ,  $\beta = 0^\circ$ ,  $Re_\infty/ft = 3,300,000$ .

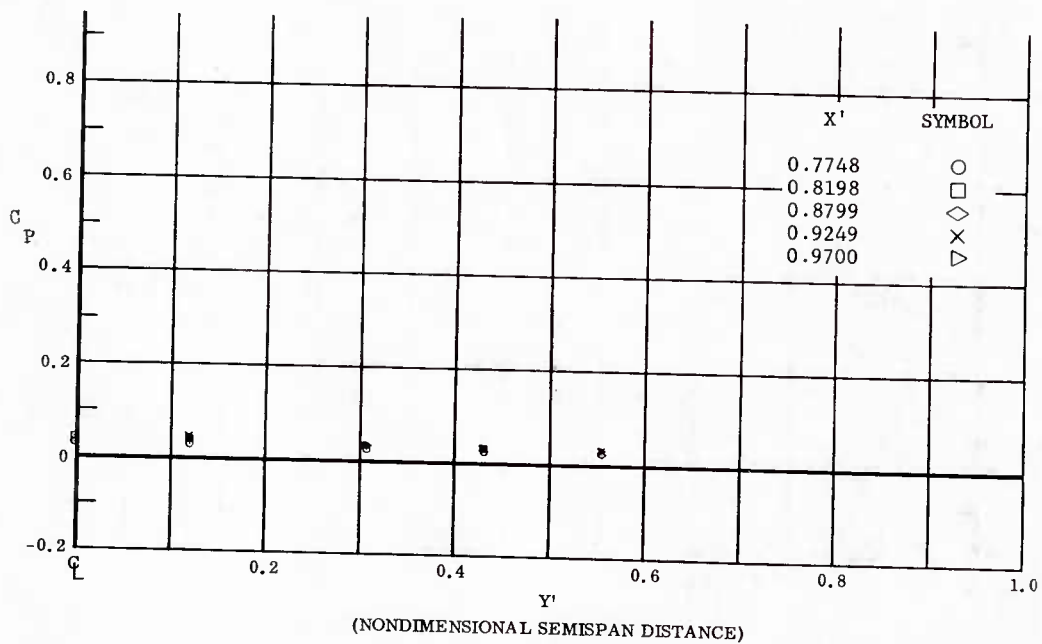


Fig. 51 Spanwise Distributions of Pressure Coefficients; Basic Configuration + Fin ( $\delta = 0$ ), No Flap Deflections,  $\alpha = 0^\circ$ ,  $\beta = 0^\circ$ ,  $Re_\infty/ft = 3,300,000$ .

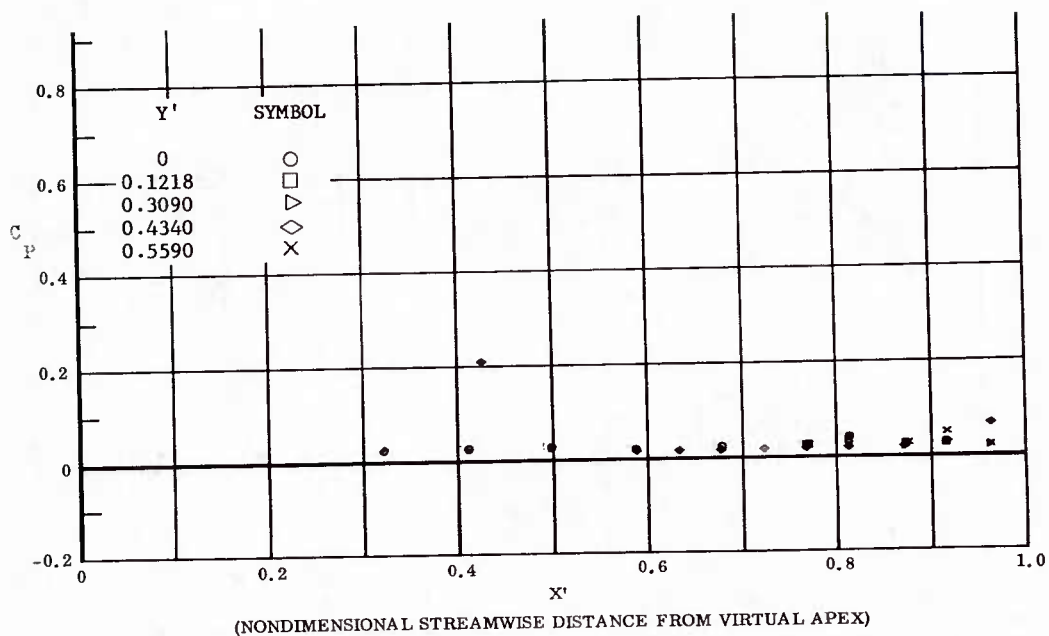


Fig. 52 Streamwise Distributions of Pressure Coefficients; Basic Configuration + Fin ( $\delta = 15^\circ$ ), No Flap Deflections,  $\alpha = 0^\circ$ ,  $\beta = 0^\circ$ ,  $Re_\infty/ft = 3,300,000$

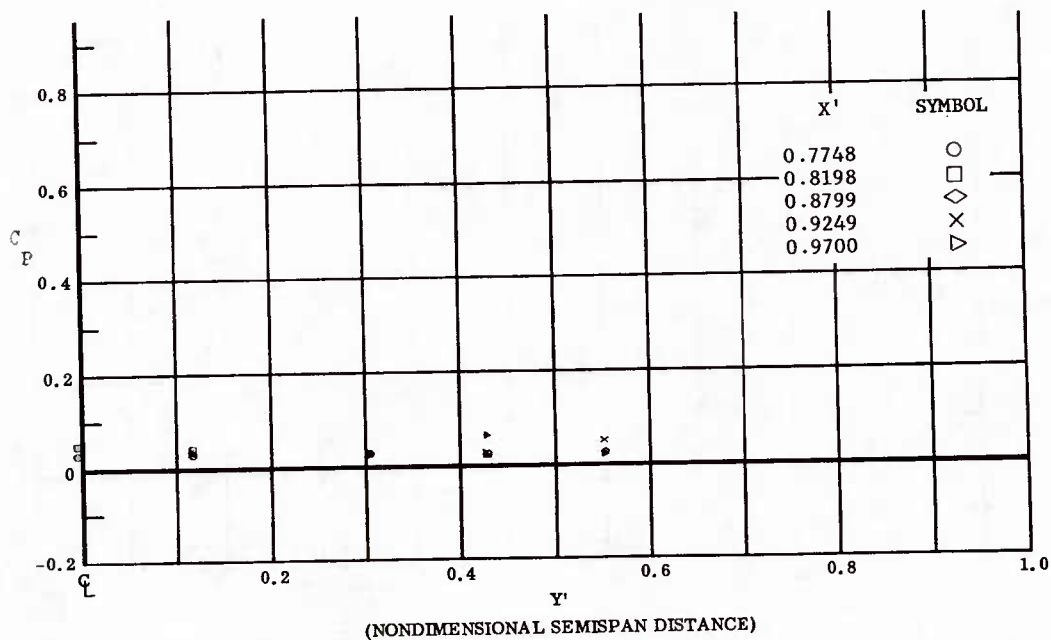


Fig. 52 Spanwise Distributions of Pressure Coefficients; Basic Configuration + Fin ( $\delta = 15^\circ$ ), No Flap Deflections,  $\alpha = 0^\circ$ ,  $\beta = 0^\circ$ ,  $Re_\infty/ft = 3,300,000$



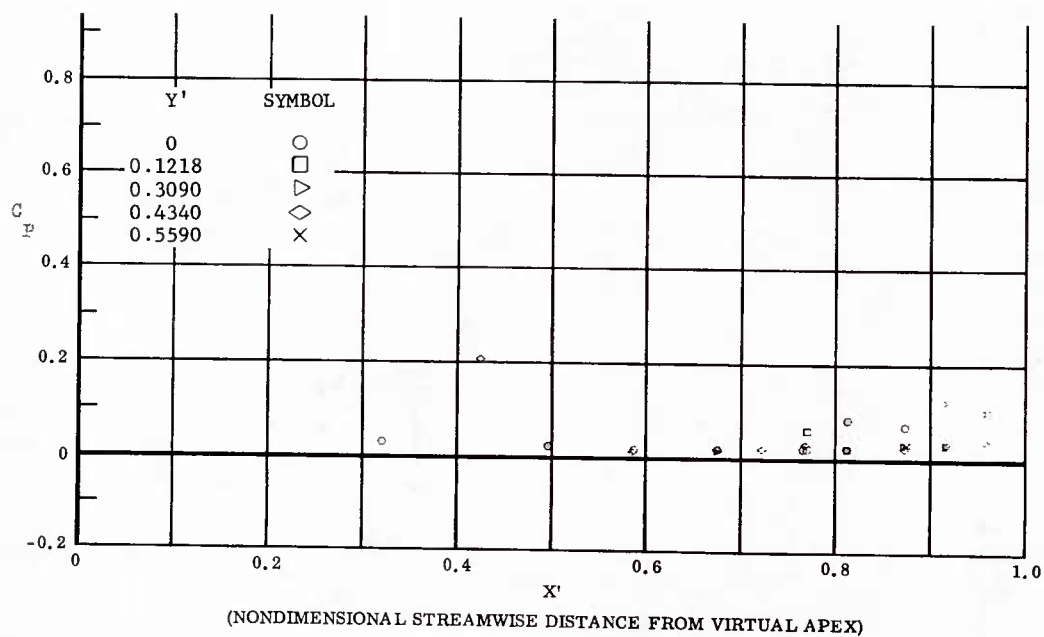


Fig. 53 Streamwise Distributions of Pressure Coefficients; Basic Configuration, Bottom Flaps Deflected  $+10^\circ$ ,  $\alpha = 0^\circ$ ,  $\beta = 0^\circ$ ,  $Re_\infty/ft = 3,300,000$ .

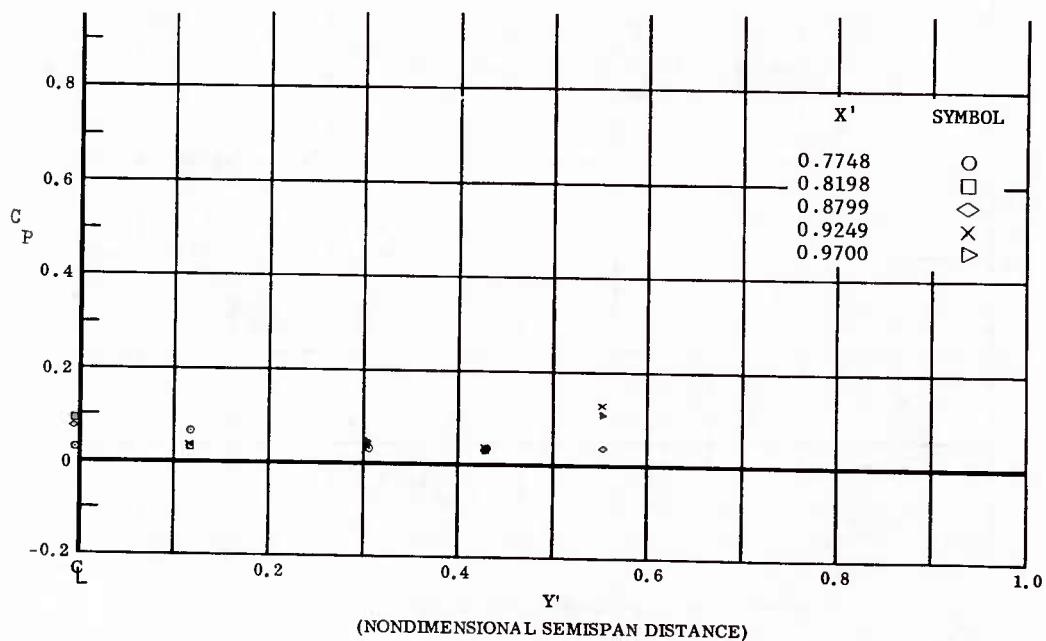


Fig. 53 Spanwise Distributions of Pressure Coefficients; Basic Configuration, Bottom Flaps Deflected  $+10^\circ$ ,  $\alpha = 0^\circ$ ,  $\beta = 0^\circ$ ,  $Re_\infty/ft = 3,300,000$ .

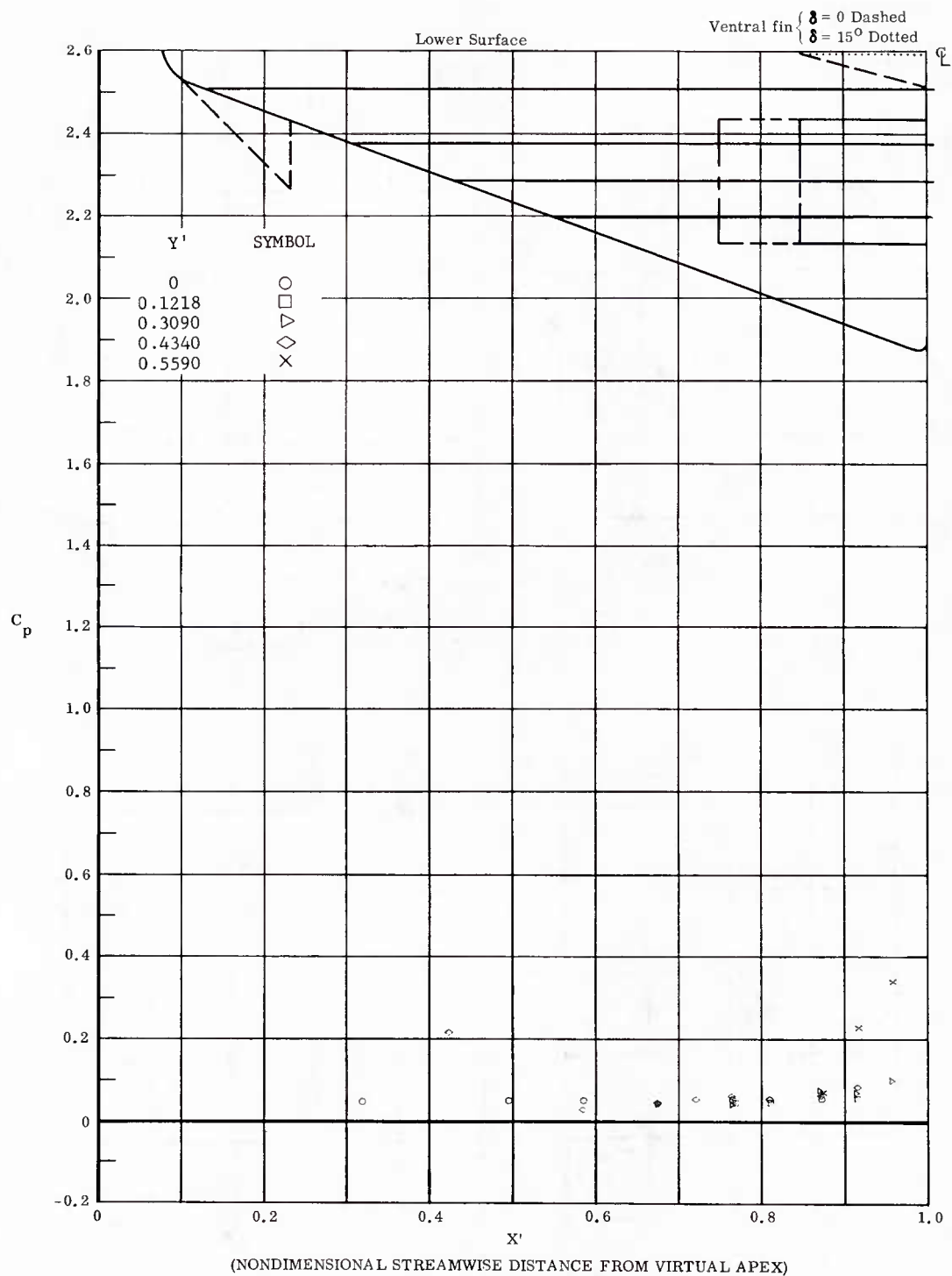


Fig. 54 Streamwise Distributions of Pressure Coefficients; Basic Configuration, Bottom Flaps Deflected  $+20^\circ$ ,  $\alpha = 0^\circ$ ,  $\beta = 0^\circ$ ,  $Re_\infty/ft = 1,100,000$ .

216

Graph Dp-3

	OFF	
Ventral Fin	ON $\delta = 0$	
	ON $\delta = 15$	

Canard	OFF	
	ON	
Bottom Flap Chord	Short	
	Long	

$\delta_1 =$        $M_\infty =$        $\alpha =$        $\beta =$   
 $\delta_2 =$        $Re_\infty / 10^6 \text{ ft} =$   
 $\delta_3 =$

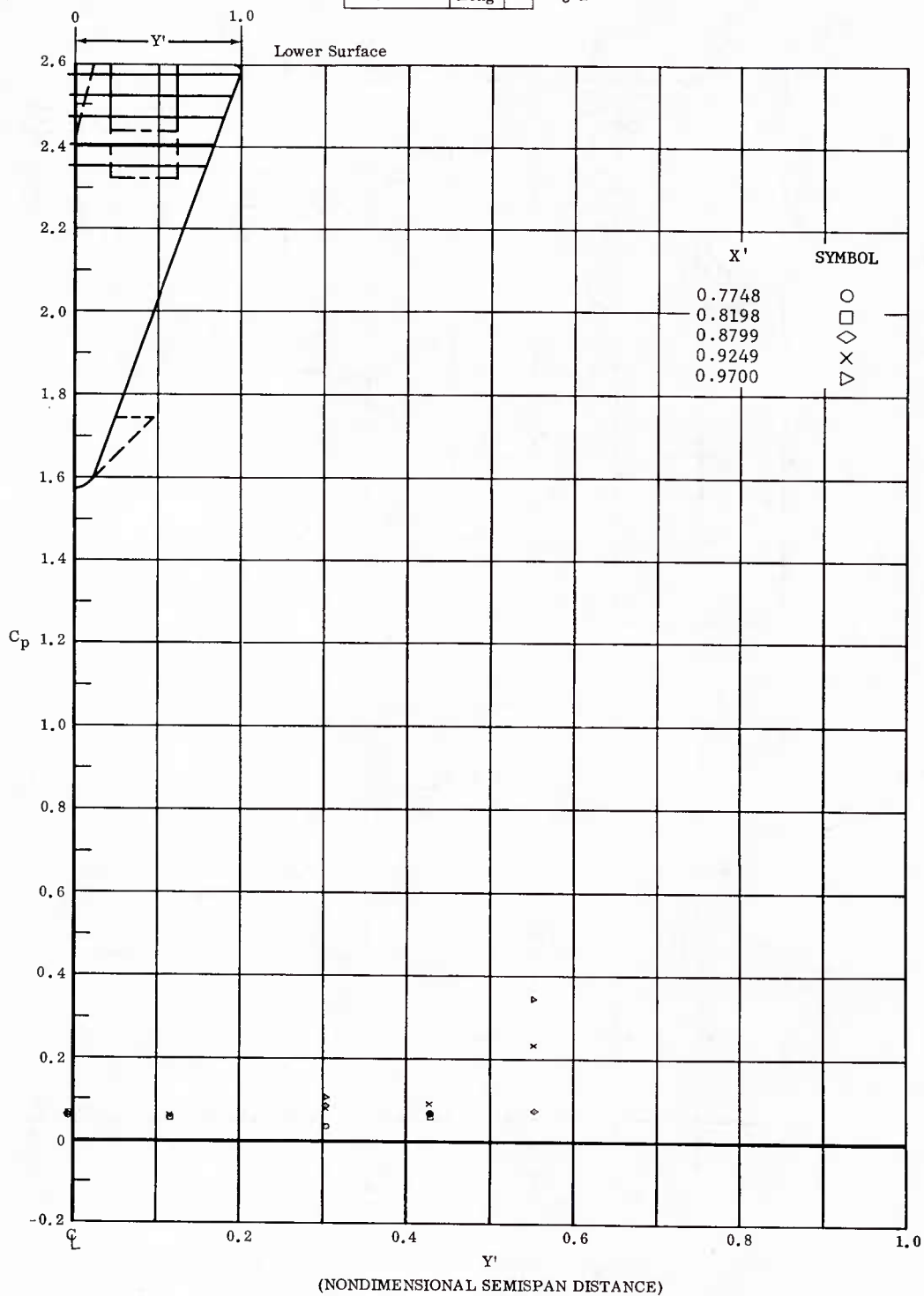


Fig. 54 Spanwise Distributions of Pressure Coefficients; Basic Configuration, Bottom Flaps Deflected  $+20^\circ$ ,  $\alpha = 0^\circ$ ,  $\beta = 0^\circ$ ,  $Re_\infty / \text{ft} = 1,100,000$ .

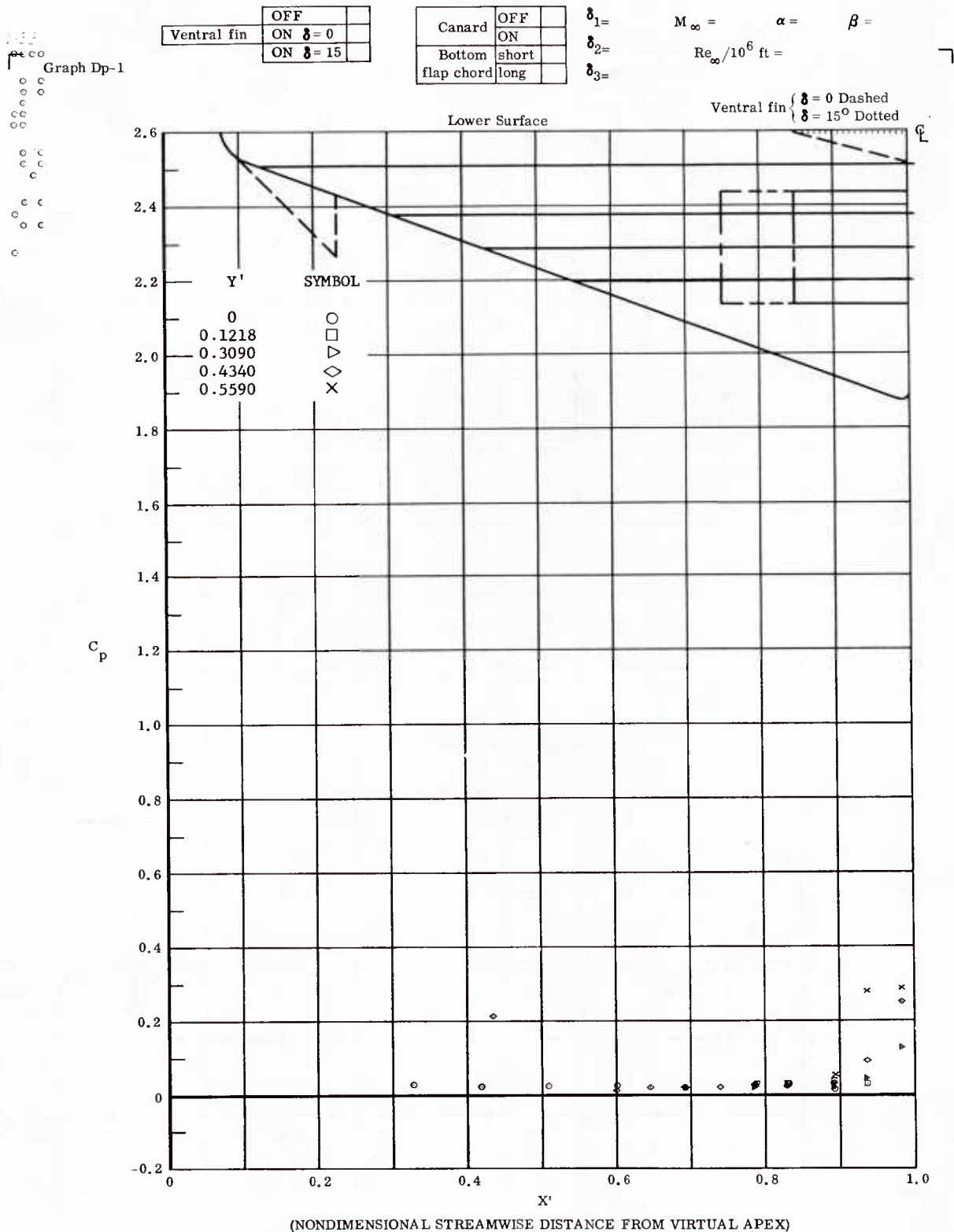


Fig. 55 Streamwise Distributions of Pressure Coefficients; Basic Configuration, Bottom Flaps Deflected  $+20^\circ$ ,  $\alpha = 0^\circ$ ,  $\beta = 0^\circ$ ,  $Re_\infty / \text{ft} = 3,300,000$ .

233

Graph Dp-3

Graph Dp-3

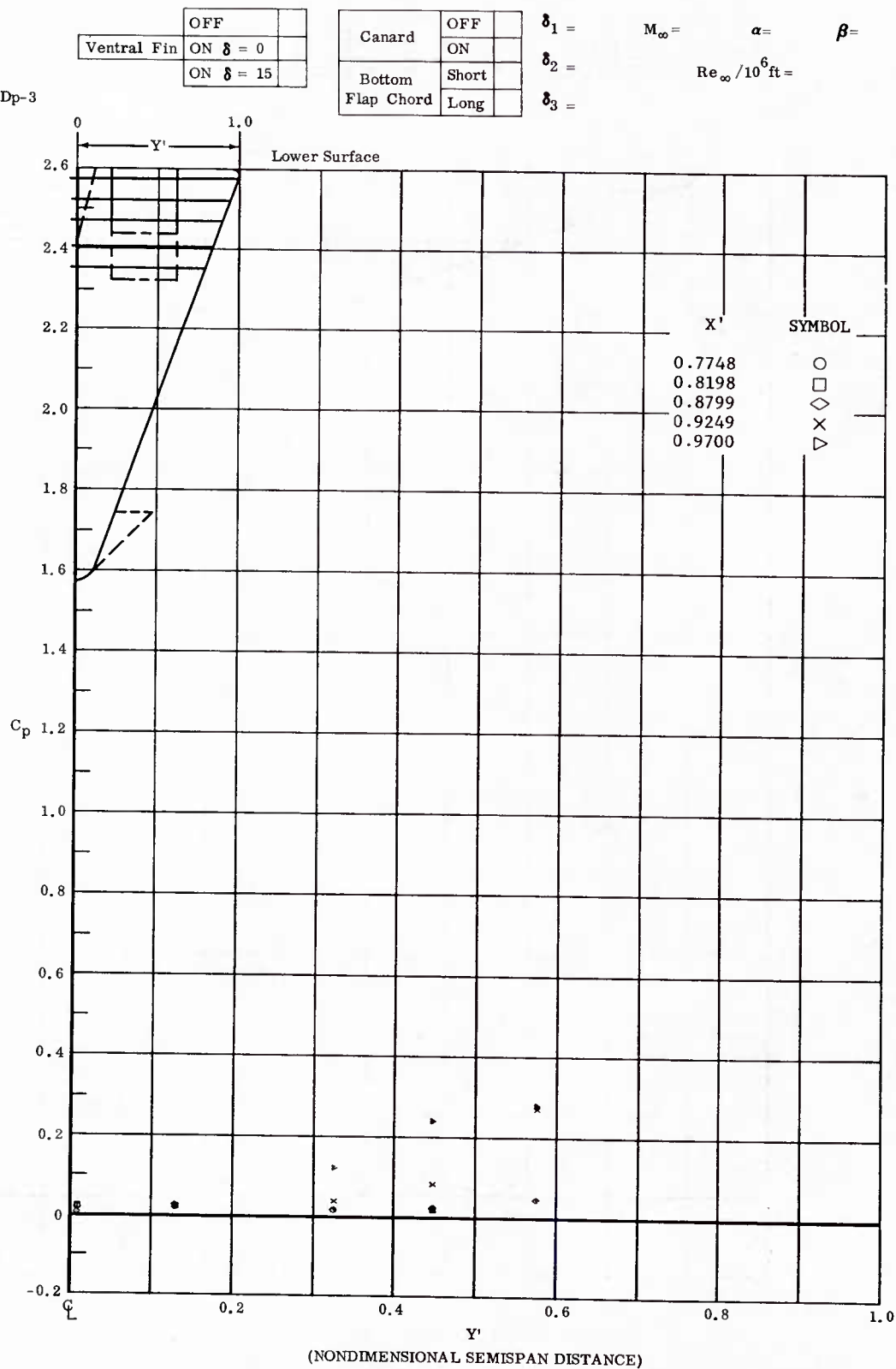


Fig. 55 Spanwise Distributions of Pressure Coefficients; Basic Configuration, Bottom Flaps Deflected +20°,  $\alpha = 0^\circ$ ,  $\beta = 0^\circ$ ,  $Re_\infty / \text{ft} = 3,300,000$ .

269  
Graph Dp-1

	OFF	
Ventral fin	ON $\delta = 0$	
	ON $\delta = 15$	

Canard	OFF	
	ON	
Bottom flap chord	short	
	long	

$\delta_1 =$   $M_\infty =$   $\alpha =$   $\beta =$   
 $\delta_2 =$   $Re_\infty / 10^6 \text{ ft} =$   
 $\delta_3 =$

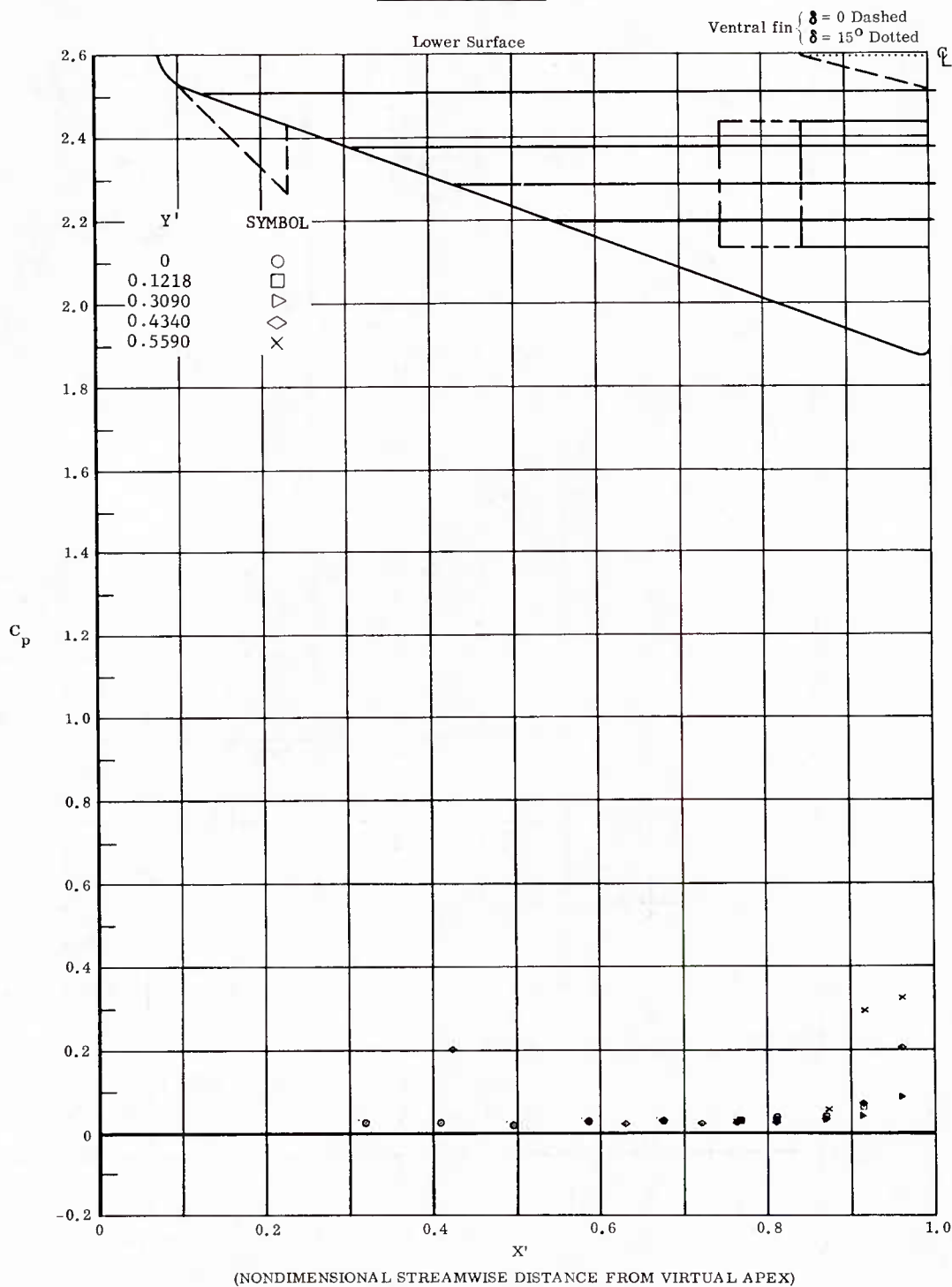


Fig. 56 Streamwise Distributions of Pressure Coefficients; Basic Configuration + Fin ( $\delta = 0$ ), Bottom Flaps Deflected  $+20^\circ$ ,  $\alpha = 0^\circ$ ,  $\beta = 0^\circ$ ,  $Re_\infty / \text{ft} = 3,300,000$ .

	OFF	
Ventral Fin	ON $\delta = 0$	
	ON $\delta = 15$	

Canard	OFF	
	ON	
Bottom Flap Chord	Short	
	Long	

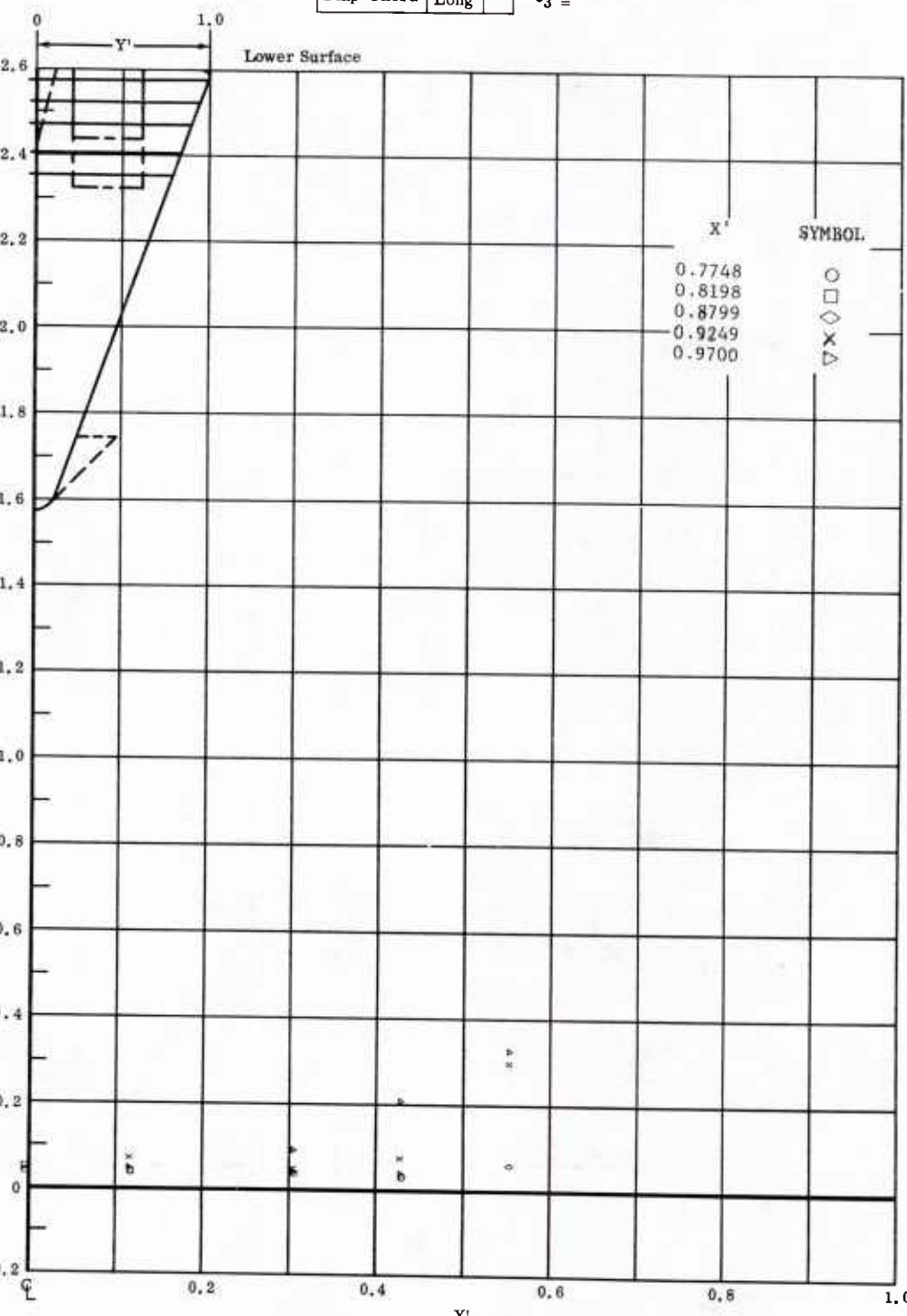
$$\begin{array}{ccccccc} \delta_1 = & & M_\infty = & & \alpha = & & \beta = \\ \delta_2 = & & & & & & \text{Re}_\infty / 10^6 \text{ ft} = \\ \delta_3 = & & & & & & \end{array}$$


Fig. 56 Spanwise Distributions of Pressure Coefficients; Basic Configuration + Fin ( $\delta = 0$ ), Bottom Flaps Deflected +20,  $\alpha = 0^\circ$ ,  $\beta = 0^\circ$ ,  $Re_\infty/ft = 3,300,000$ .

204  
Graph Dp-1

Ventral fin	OFF	
	ON $\delta = 0$	
	ON $\delta = 15$	

Canard	OFF	
	ON	
Bottom flap chord	short	
	long	

$\delta_1 =$   
 $\delta_2 =$   
 $\delta_3 =$

$M_\infty =$

$\alpha =$

$\beta =$

$Re_\infty / 10^6 \text{ ft} =$

Ventral fin {  $\delta = 0$  Dashed  
 $\delta = 15^\circ$  Dotted

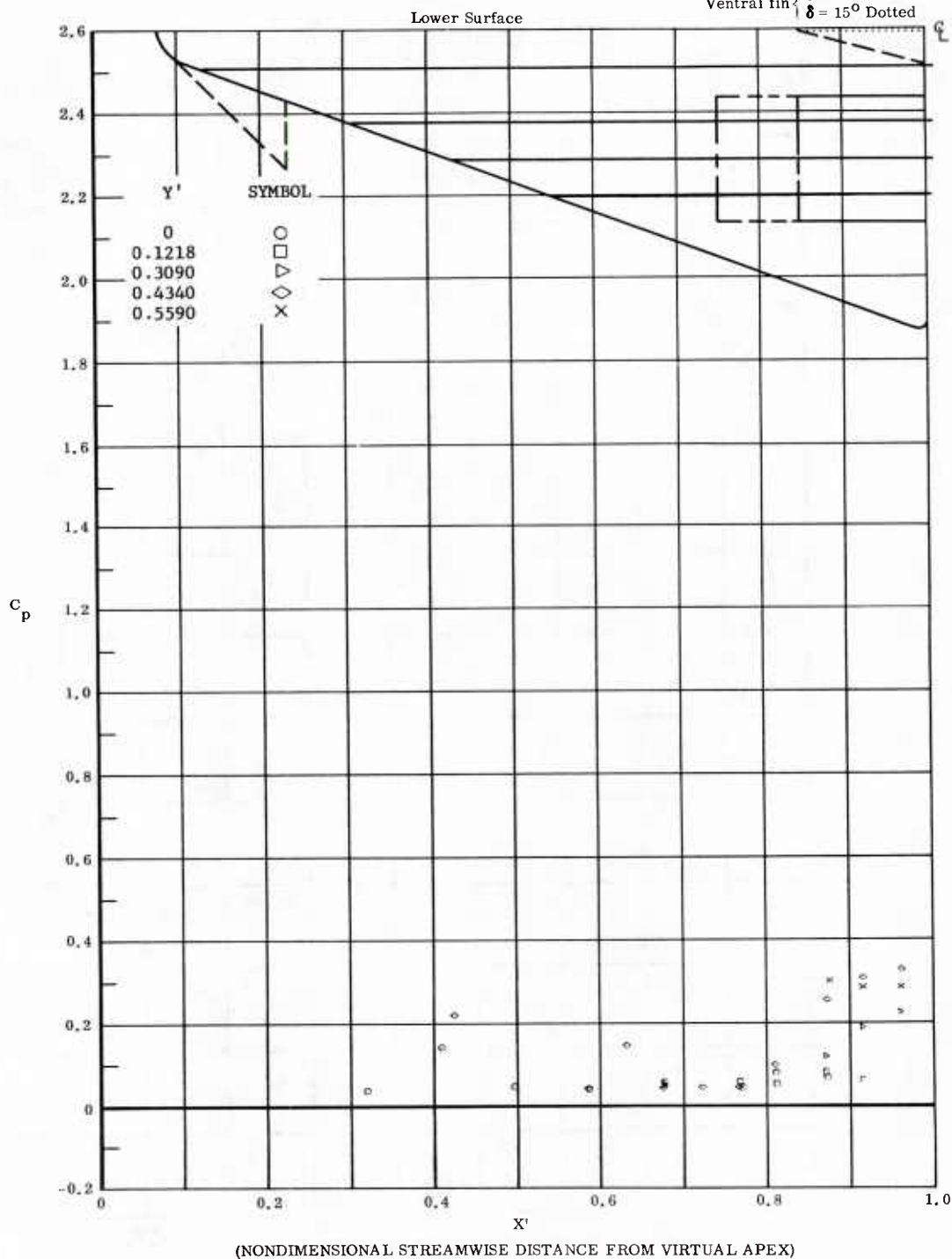


Fig. 57 Streamwise Distributions of Pressure Coefficients; Basic Configuration + Longer Chord Flaps, Bottom Flaps Deflected  $+20^\circ$ ,  $\alpha = 0^\circ$ ,  $\beta = 0^\circ$ ,  $Re_\infty / \text{ft} = 1,100,000$ .



204

Graph Dp-3

	OFF	
Ventral Fin	ON $\delta = 0$	
	ON $\delta = 15$	

Canard	OFF	
	ON	
Bottom	Short	
Flap Chord	Long	

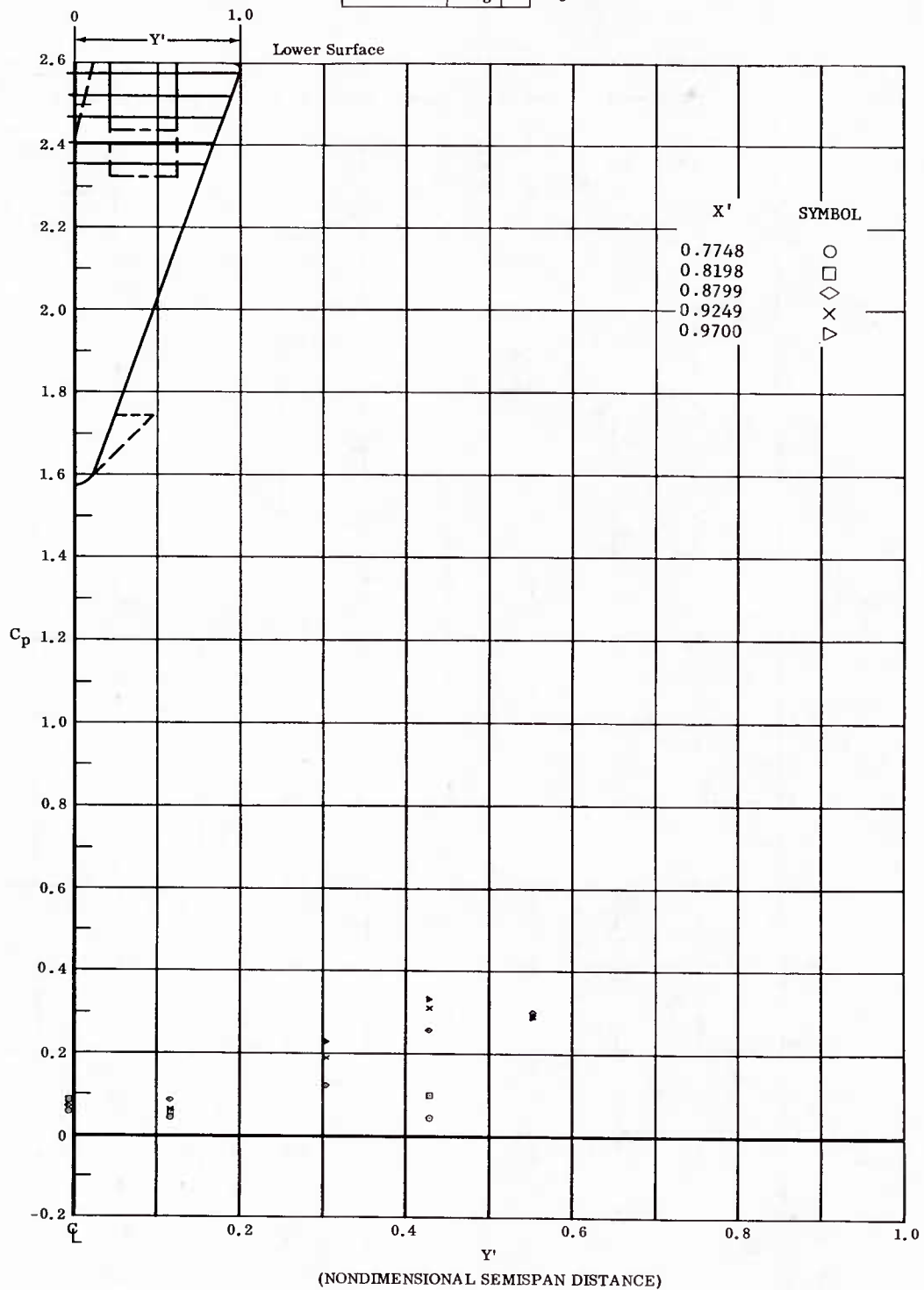
 $\delta_1 =$  $M_\infty =$  $\alpha =$  $\beta =$  $\delta_2 =$  $Re_\infty / 10^6 \text{ ft} =$  $\delta_3 =$ 

Fig. 57 Spanwise Distributions of Pressure Coefficients; Basic Configuration + Longer Chord Flaps, Bottom Flaps Deflected  $+20^\circ$ ,  $\alpha = 0^\circ$ ,  $\beta = 0^\circ$ ,  $Re_\infty / \text{ft} = 1,100,000$ .

201  
Graph Dp-1

	OFF	
Ventral fin	ON $\delta = 0$	
	ON $\delta = 15$	

Canard	OFF	
	ON	
Bottom flap chord	short	
	long	

$\delta_1 =$   $M_\infty =$   $\alpha =$   $\beta =$   
 $\delta_2 =$   $Re_\infty / 10^6 \text{ ft} =$   
 $\delta_3 =$

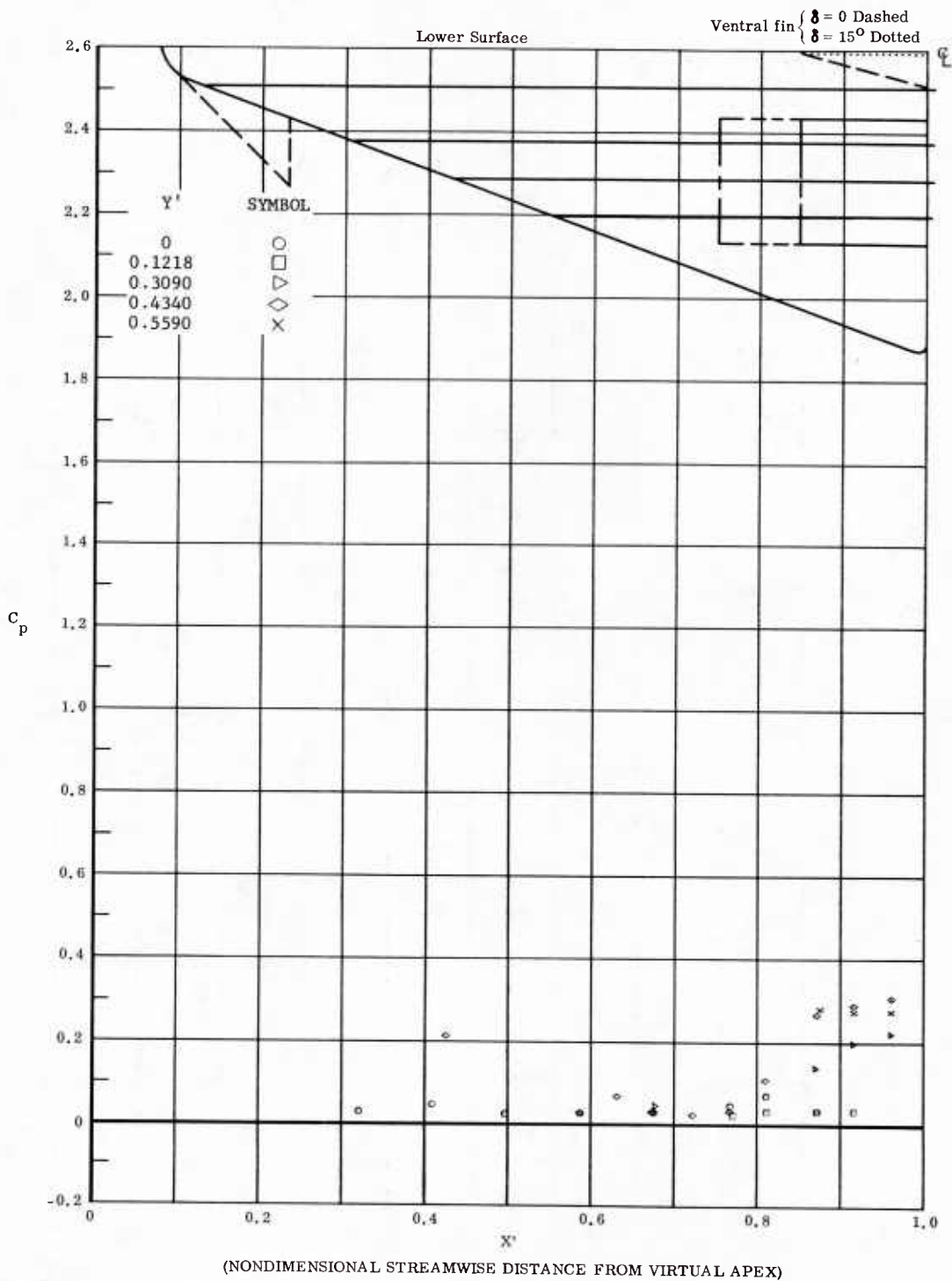


Fig. 53 Streamwise Distributions of Pressure Coefficients; Basic Configuration + Longer Chord Flaps, Bottom Flaps Deflected  $+20^\circ$ ,  $\alpha = 0^\circ$ ,  $\beta = 0^\circ$ ,  $Re_\infty / \text{ft} = 3,300,000$ .

201

Graph Dp-3

	OFF	
Ventral Fin	ON $\delta = 0$	
	ON $\delta = 15$	

Canard	OFF	
	ON	
Bottom	Short	
Flap Chord	Long	

$\delta_1 =$        $M_\infty =$        $\alpha =$        $\beta =$   
 $\delta_2 =$        $Re_\infty / 10^6 \text{ ft} =$   
 $\delta_3 =$

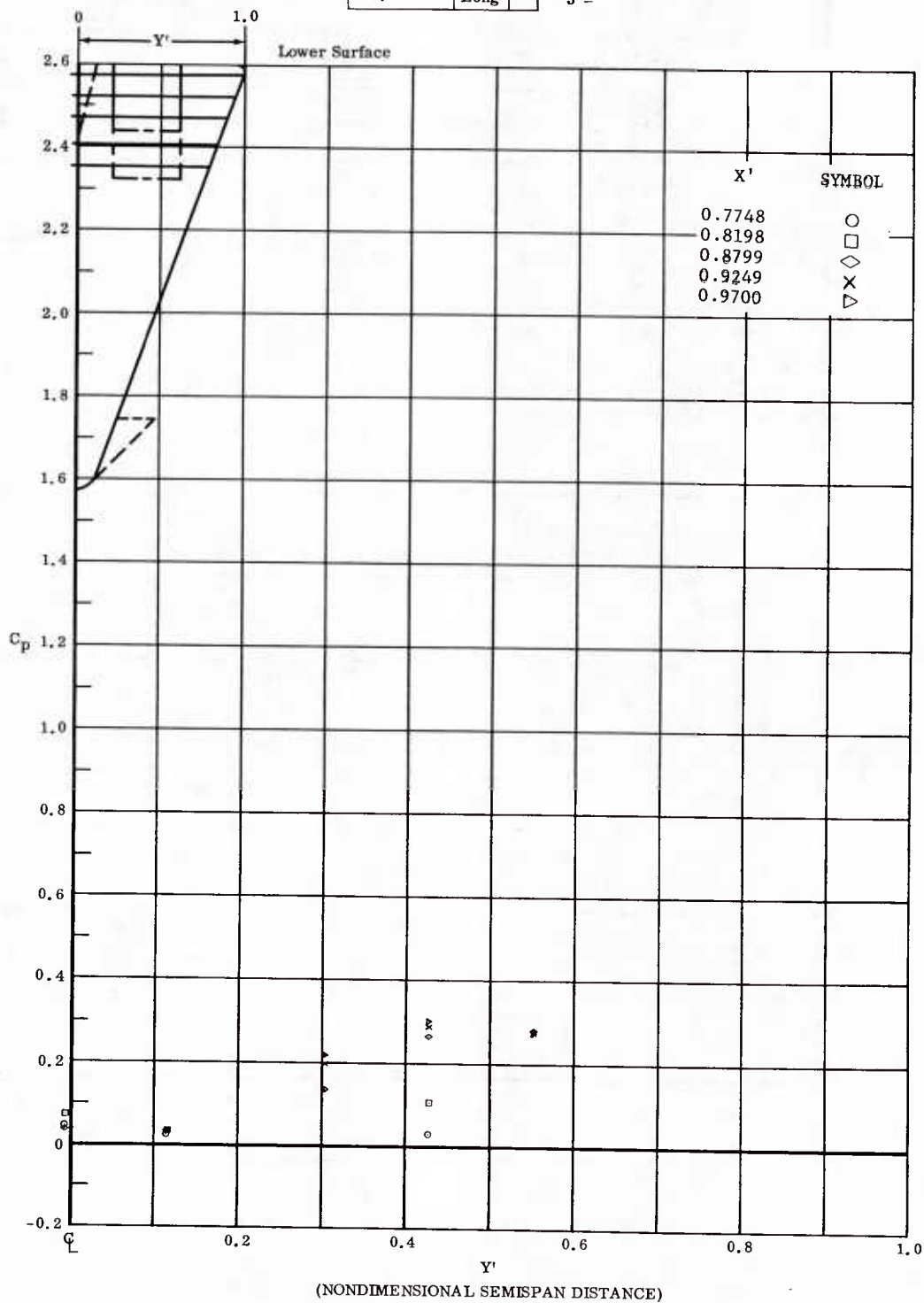


Fig. 58 Spanwise Distributions of Pressure Coefficients; Basic Configuration + Longer Chord Flaps, Bottom Flaps Deflected +20°,  $\alpha = 0^\circ$ ,  $\beta = 0^\circ$ ,  $Re_\infty / \text{ft} = 3,300,000$ .

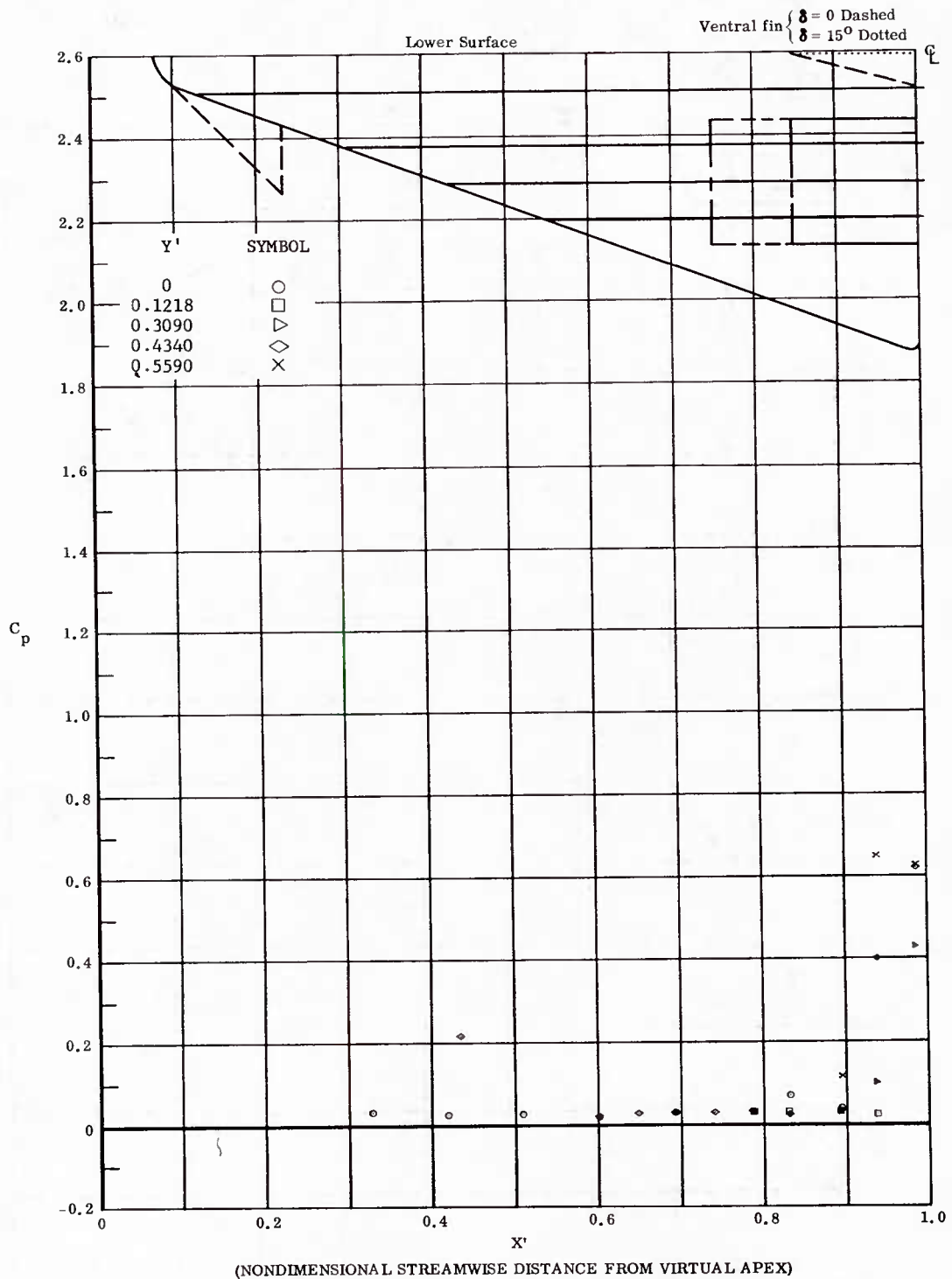


Fig. 59 Streamwise Distributions of Pressure Coefficients; Basic Configuration, Bottom Flaps Deflected  $+30^\circ$ ,  $\alpha = 0^\circ$ ,  $\beta = 0^\circ$ ,  $Re_\infty / ft = 3,300,000$ .

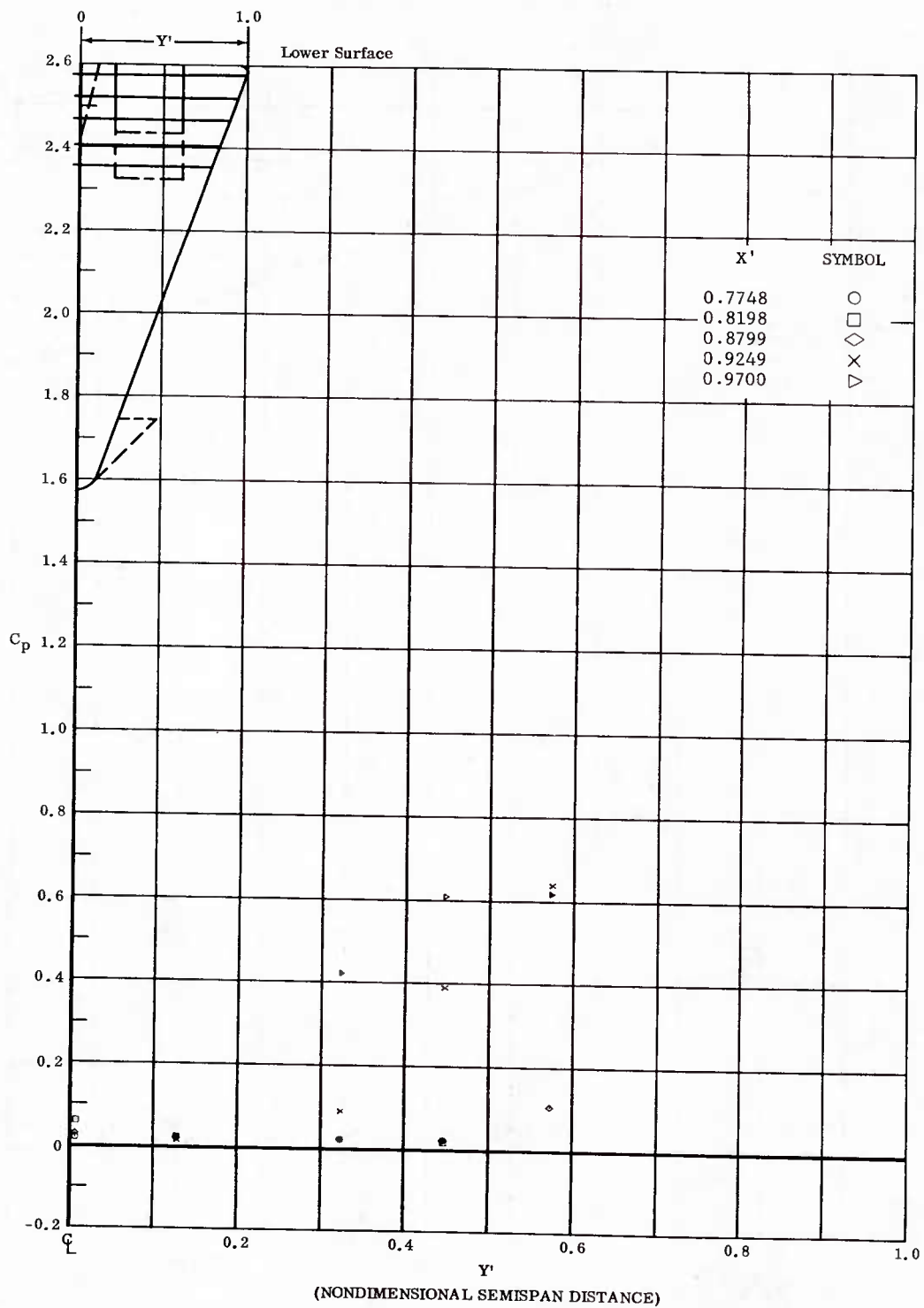


Fig. 59 Spanwise Distributions of Pressure Coefficients; Basic Configuration, Bottom Flaps Deflected +30°,  $\alpha = 0^\circ$ ,  $\beta = 0^\circ$ ,  $Re_\infty / ft = 3,300,000$ .

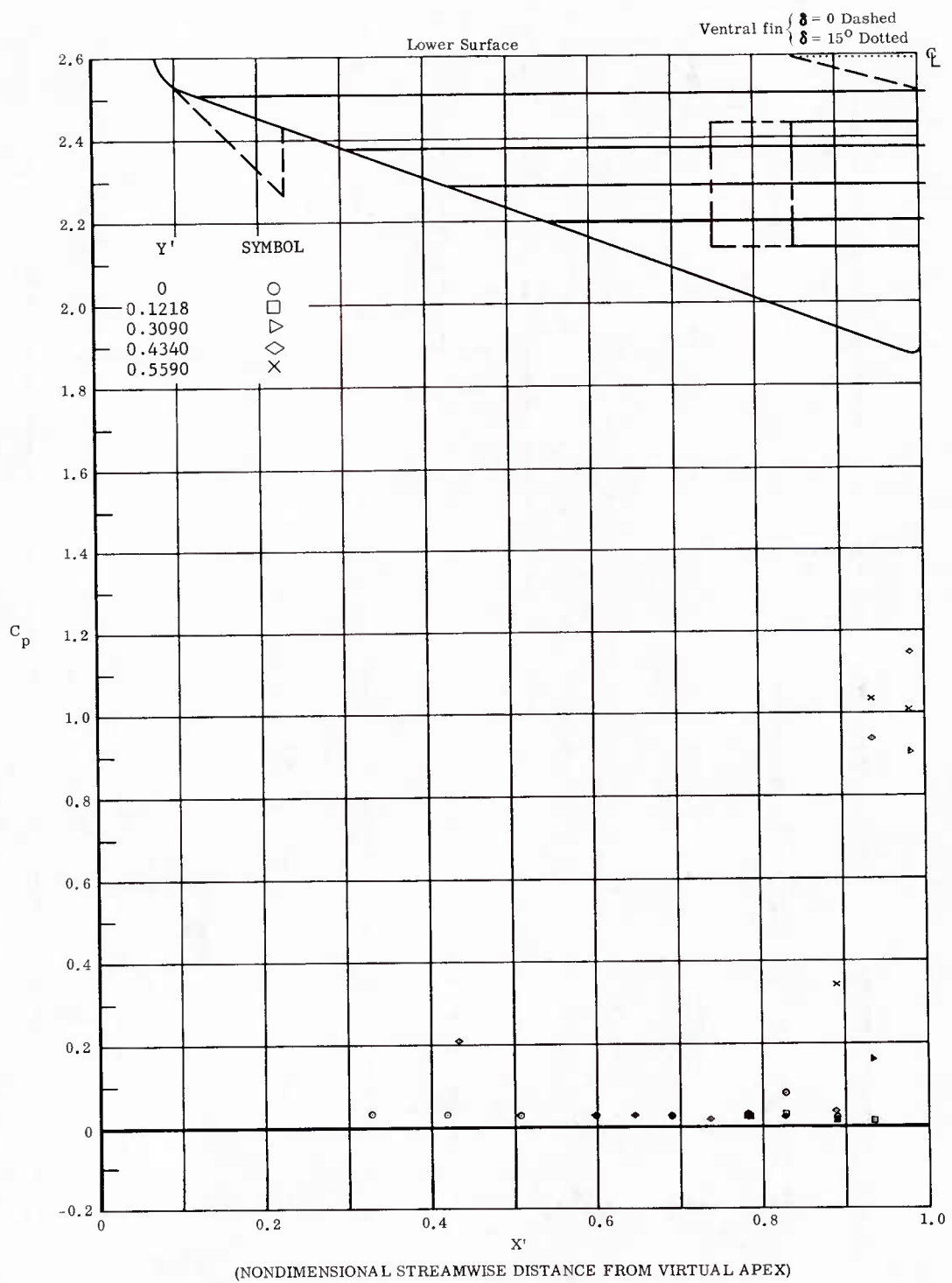


Fig. 60 Streamwise Distributions of Pressure Coefficients; Basic Configuration, Bottom Flaps Deflected  $+40^\circ$ ,  $\alpha = 0^\circ$ ,  $\beta = 0^\circ$ ,  $Re_\infty / ft = 3,300,000$ .

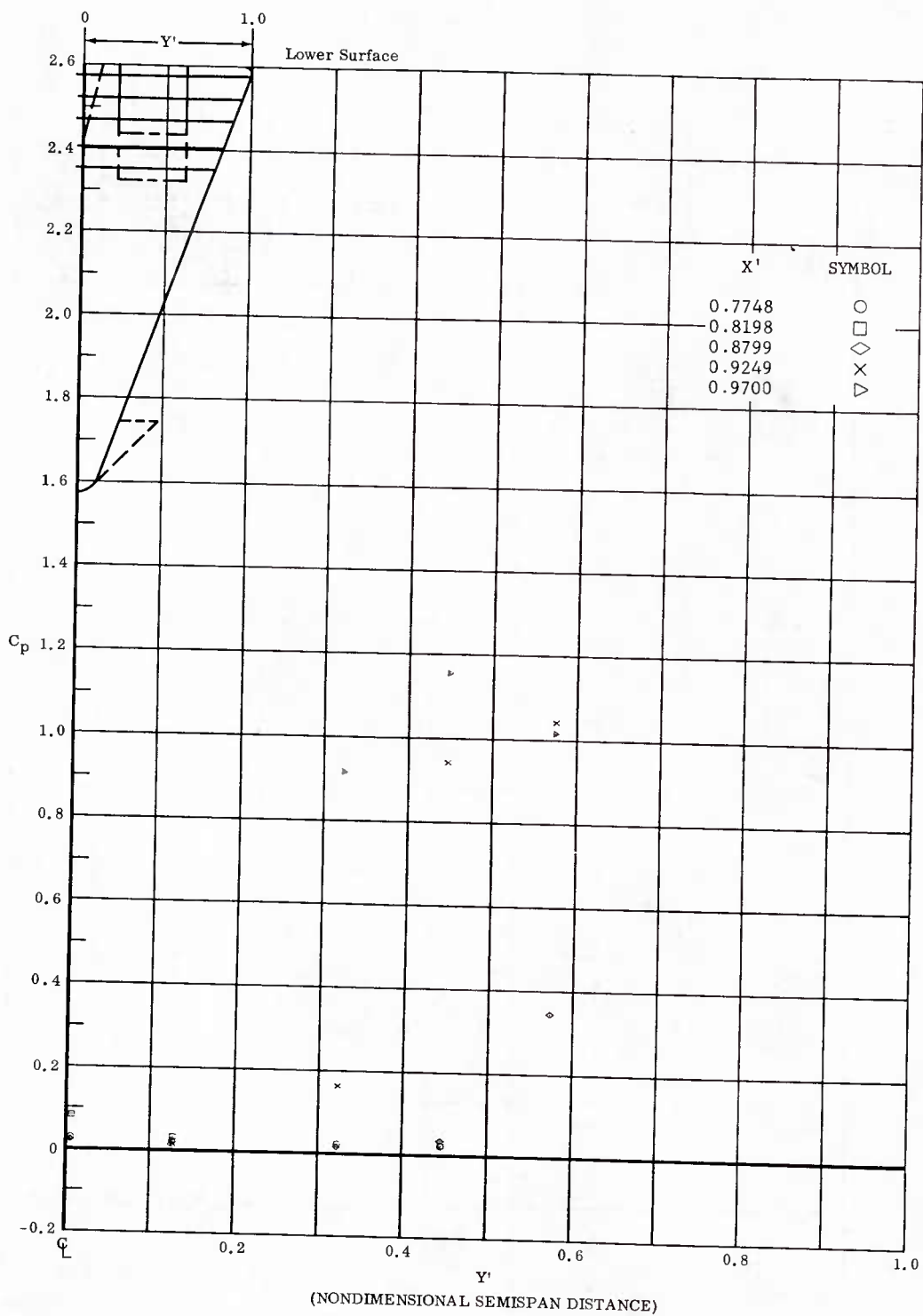


Fig. 60 Spanwise Distributions of Pressure Coefficients; Basic Configuration, Bottom Flaps Deflected  $+40^\circ$ ,  $\alpha = 0^\circ$ ,  $\beta = 0^\circ$ ,  $Re_\infty / ft = 3,300,000$ .

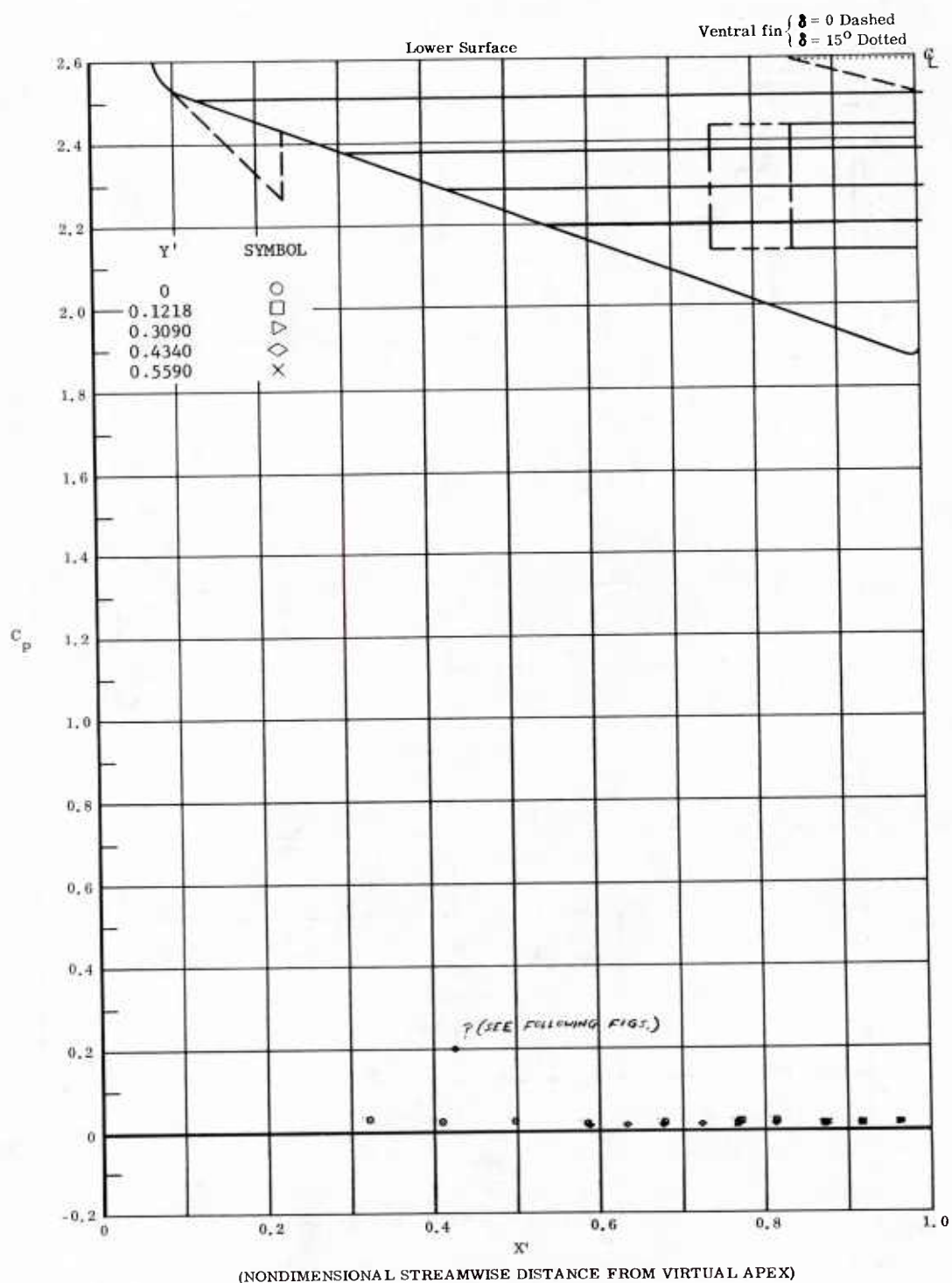


Fig. 61 Streamwise Distributions of Pressure Coefficients; Basic Configuration, Left (Upper) Flaps Deflected  $-20^\circ$ ,  $\alpha = 0^\circ$ ,  $\beta = +12^\circ$ ,  $Re_\infty / ft = 3,300,000$ .



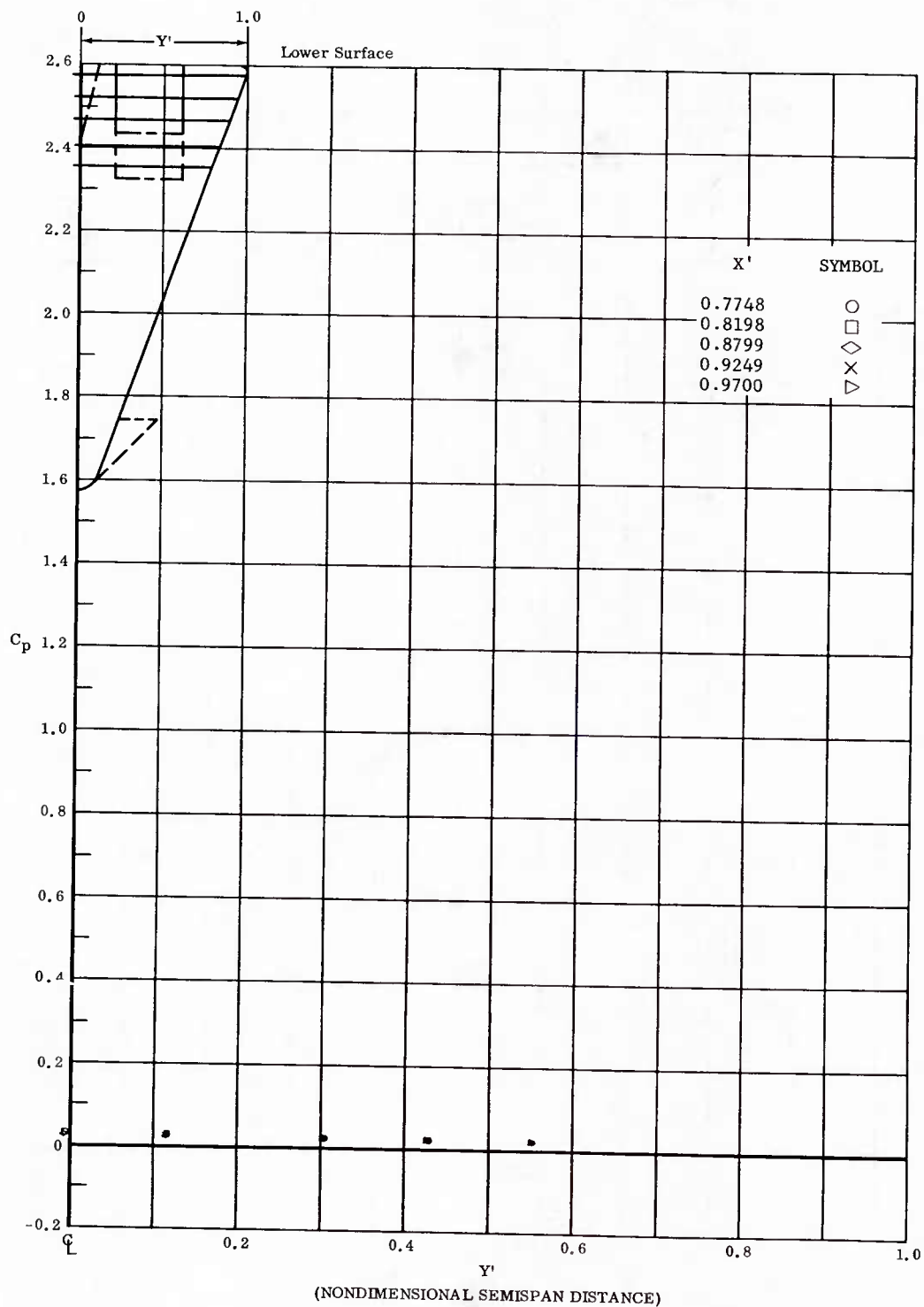


Fig. 61 Spanwise Distributions of Pressure Coefficients; Basic Configuration, Left (Upper) Flaps Deflected  $-20^\circ$ ,  $\alpha = 0^\circ$ ,  $\beta = +12^\circ$ ,  $Re_\infty / ft = 3,300,000$ .

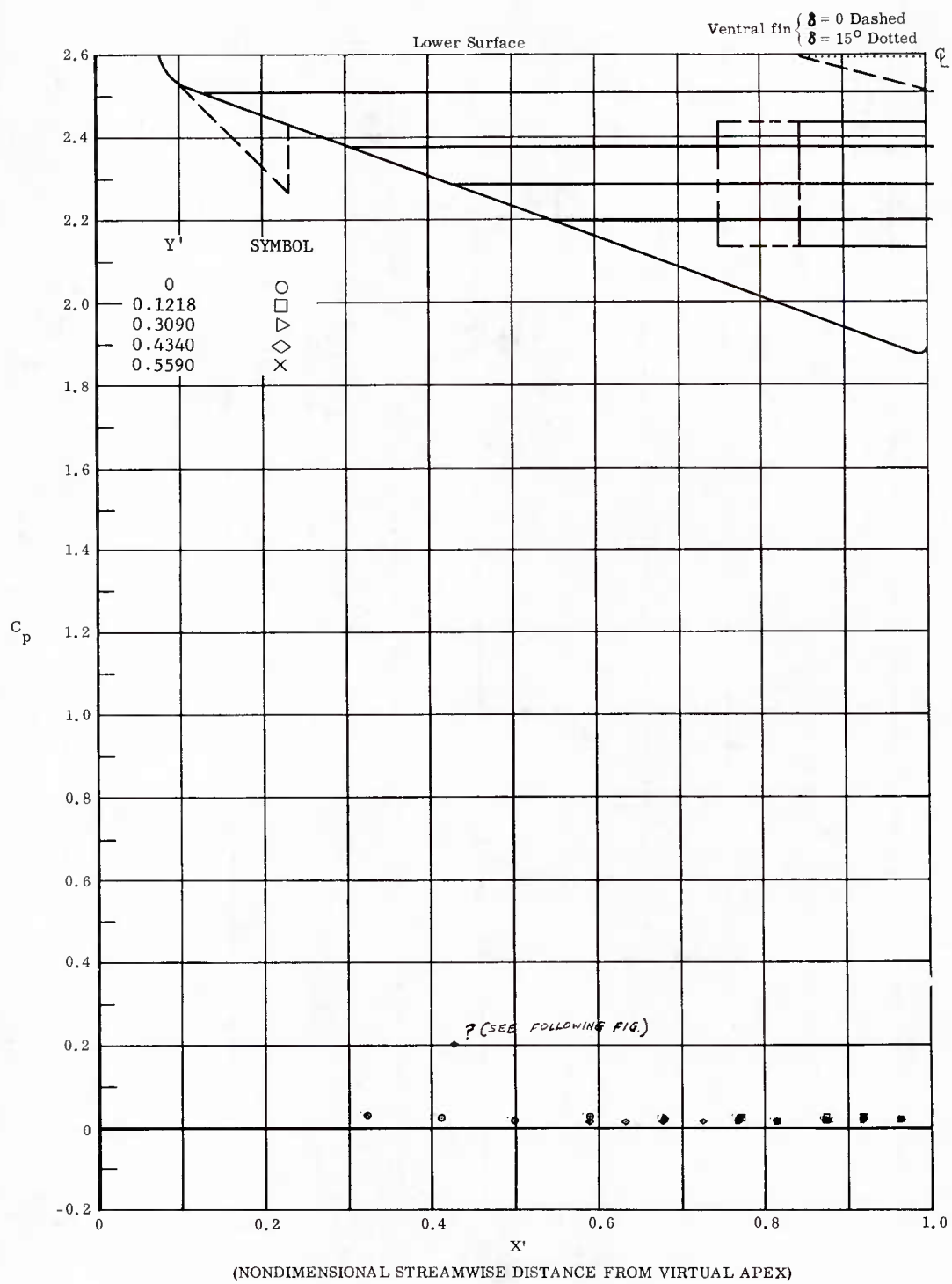


Fig. 62 Streamwise Distributions of Pressure Coefficients; Basic Configuration, No Flap Deflections,  $\alpha = 0^\circ$ ,  $\beta = +12^\circ$ ,  $Re_\infty/ft = 3,300,000$ .

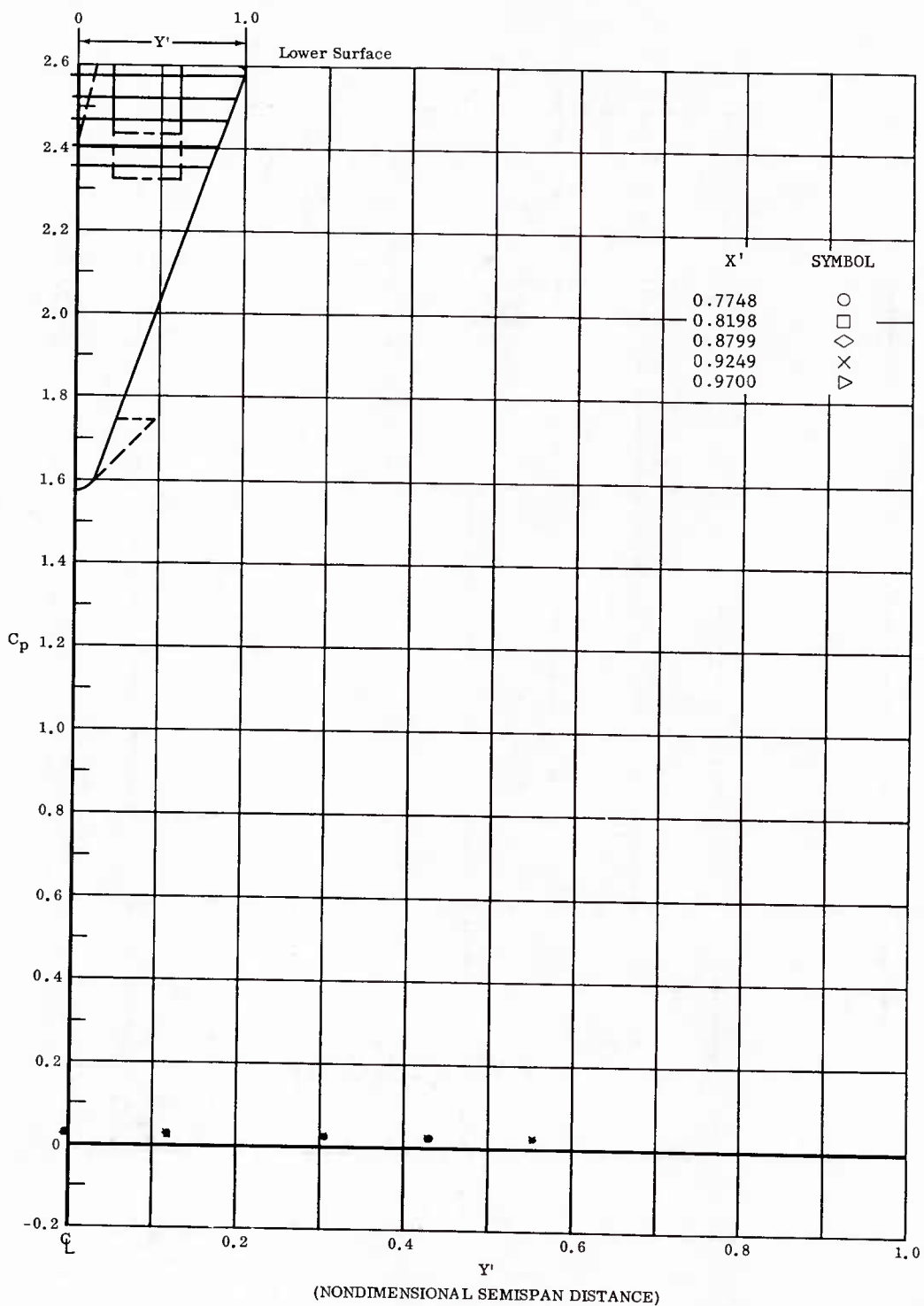


Fig. 62 Spanwise Distributions of Pressure Coefficients; Basic Configuration, No Flap Deflections,  $\alpha = 0^\circ$ ,  $\beta = +12^\circ$ ,  $Re_\infty / ft = 3,300,000$ .

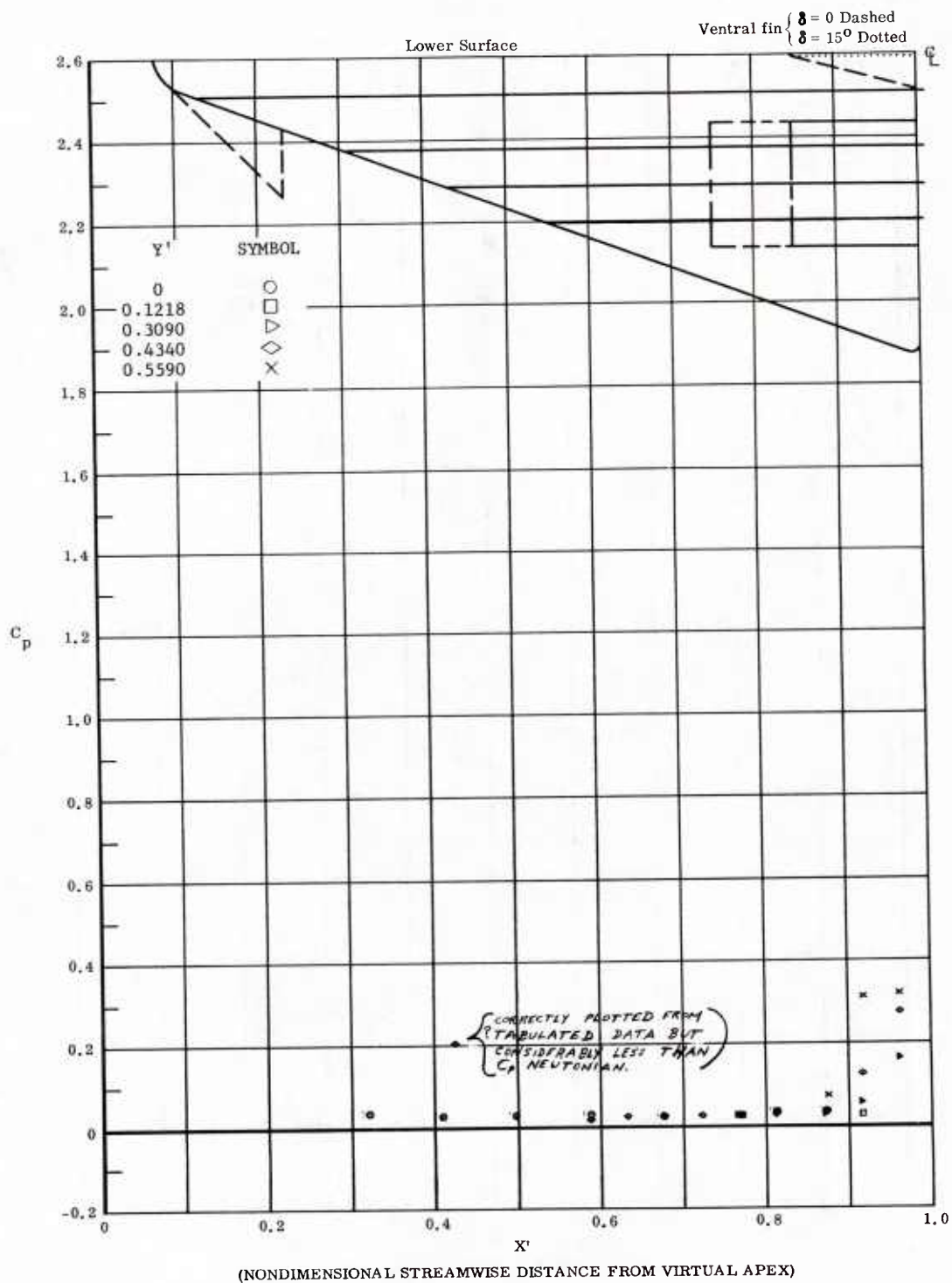


Fig. 63 Streamwise Distributions of Pressure Coefficients; Basic Configuration, Bottom Flaps Deflected  $+20^\circ$ ,  $\alpha = 0^\circ$ ,  $\beta = +12^\circ$ ,  $Re_\infty/ft = 3,300,000$ .

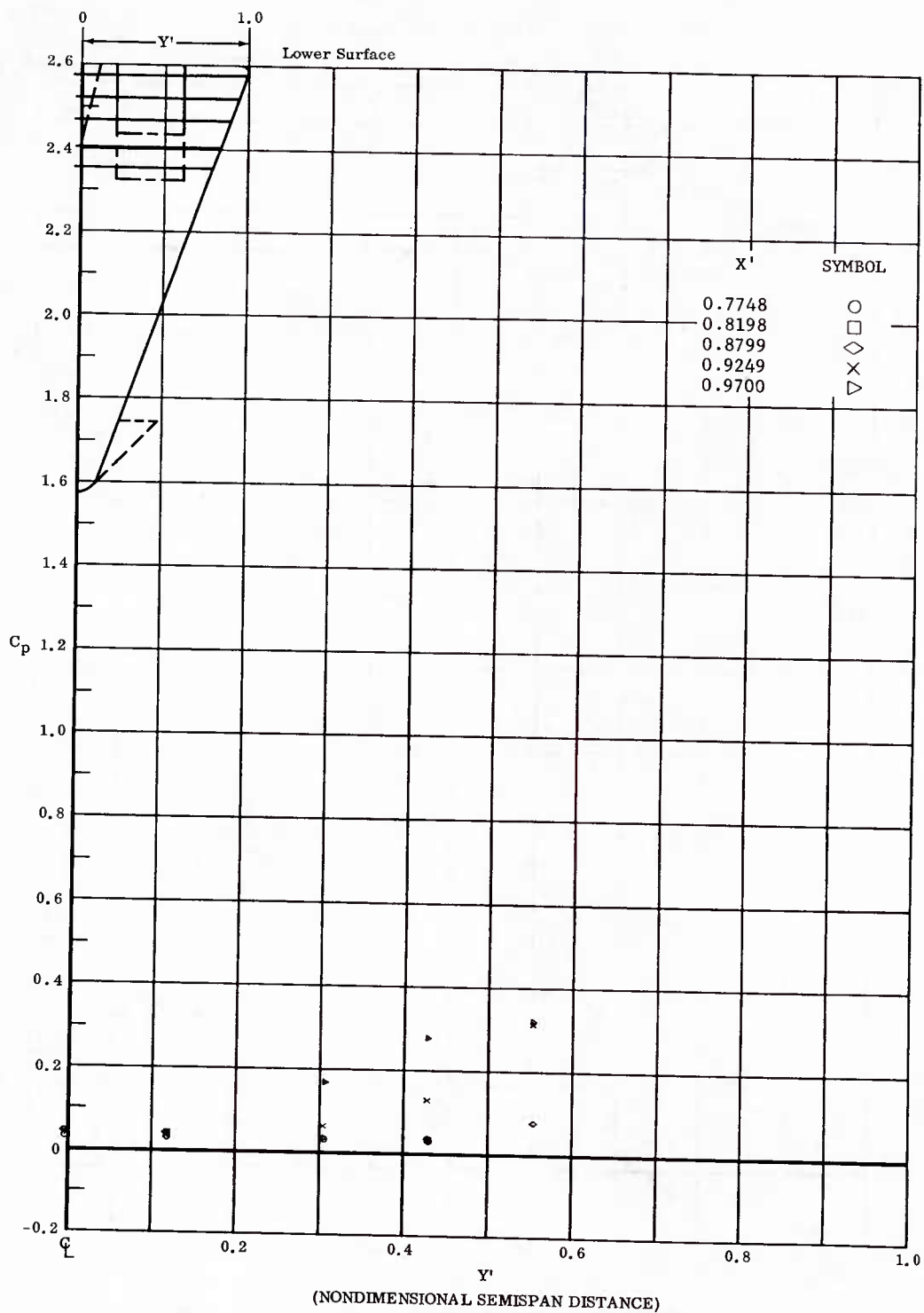


Fig. 63 Spanwise Distributions of Pressure Coefficients; Basic Configuration, Bottom Flaps Deflected  $+20^\circ$ ,  $\alpha = 0^\circ$ ,  $\beta = +12^\circ$ ,  $Re_\infty/ft = 3,300,000$ .

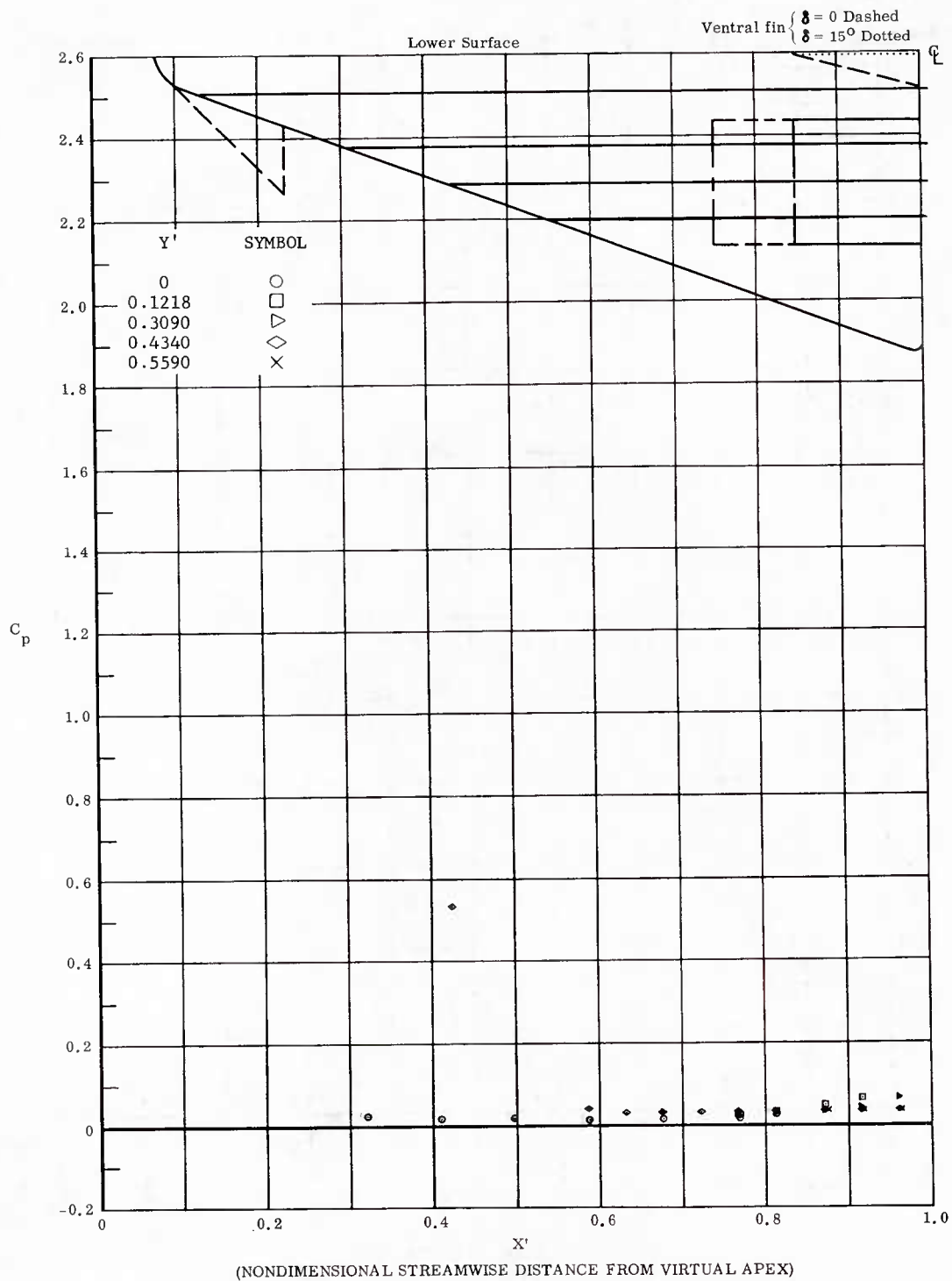


Fig. 64 Streamwise Distributions of Pressure Coefficients; Basic Configuration + Fin ( $\delta = 0$ ), No Flap Deflections,  $\alpha = 0^\circ$ ,  $\beta = +12^\circ$ ,  $Re_\infty/ft = 3,300,000$ .

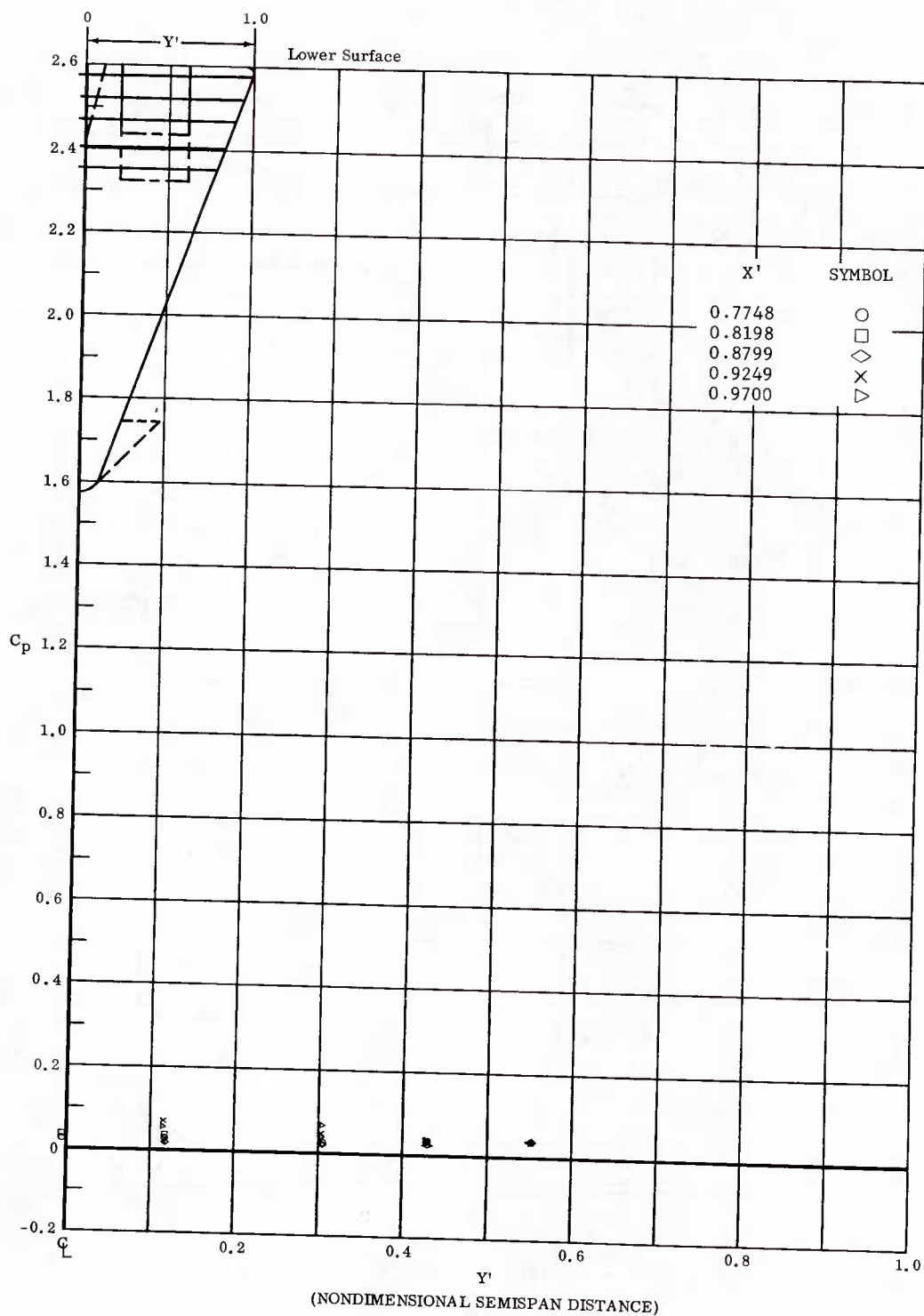


Fig. 64 Spanwise Distributions of Pressure Coefficients; Basic Configuration + Fin ( $\delta = 0$ ), No Flap Deflections,  $\alpha = 0^\circ$ ,  $\beta = +12^\circ$ ,  $Re_\infty/ft = 3,300,000$ .

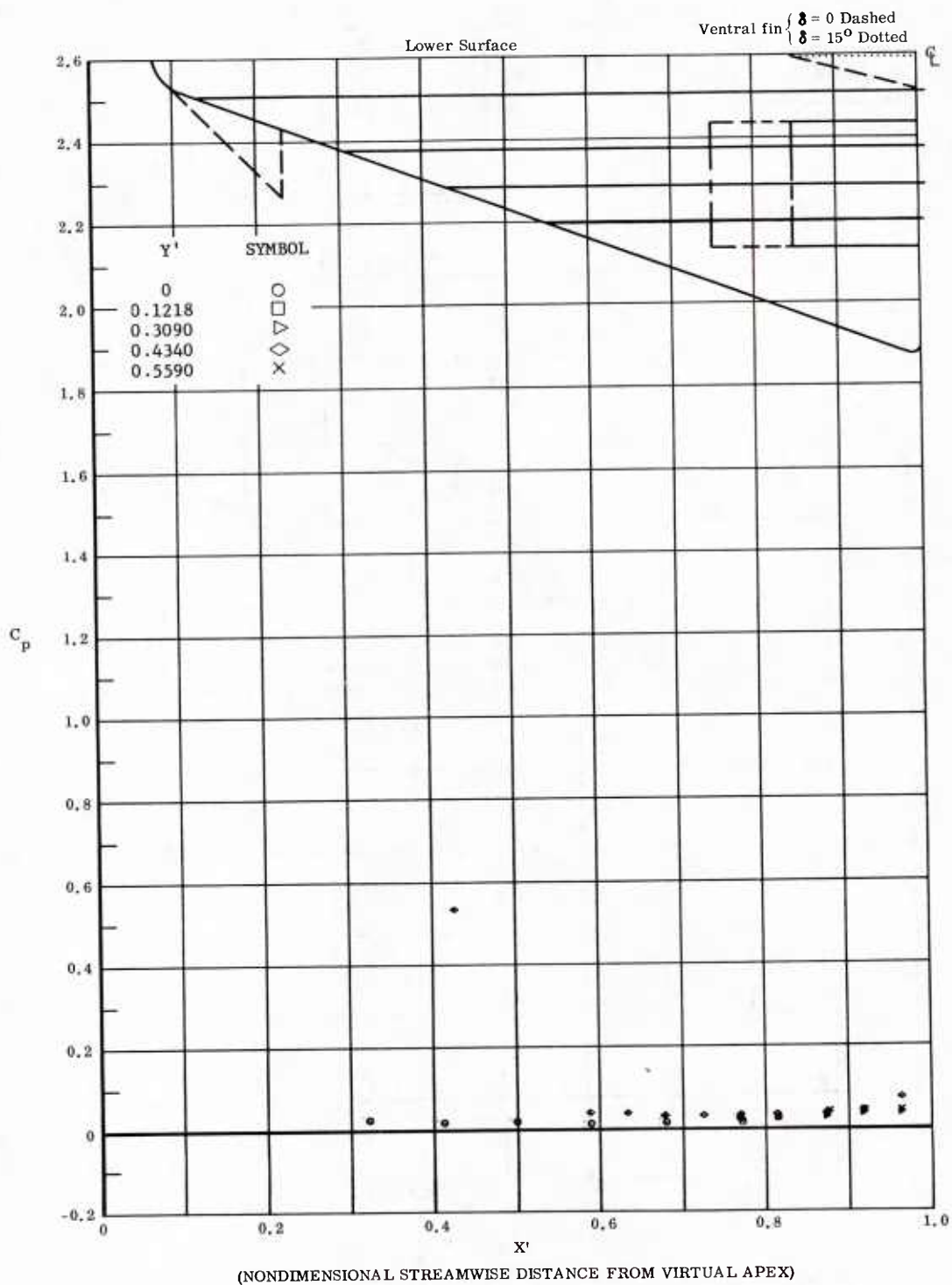


Fig. 65 Streamwise Distributions of Pressure Coefficients; Basic Configuration + Fin ( $\delta = 15^\circ$ ), No Flap Deflections,  $\alpha = 0^\circ$ ,  $\beta = +12^\circ$ ,  $Re_\infty / ft = 3,300,000$ .



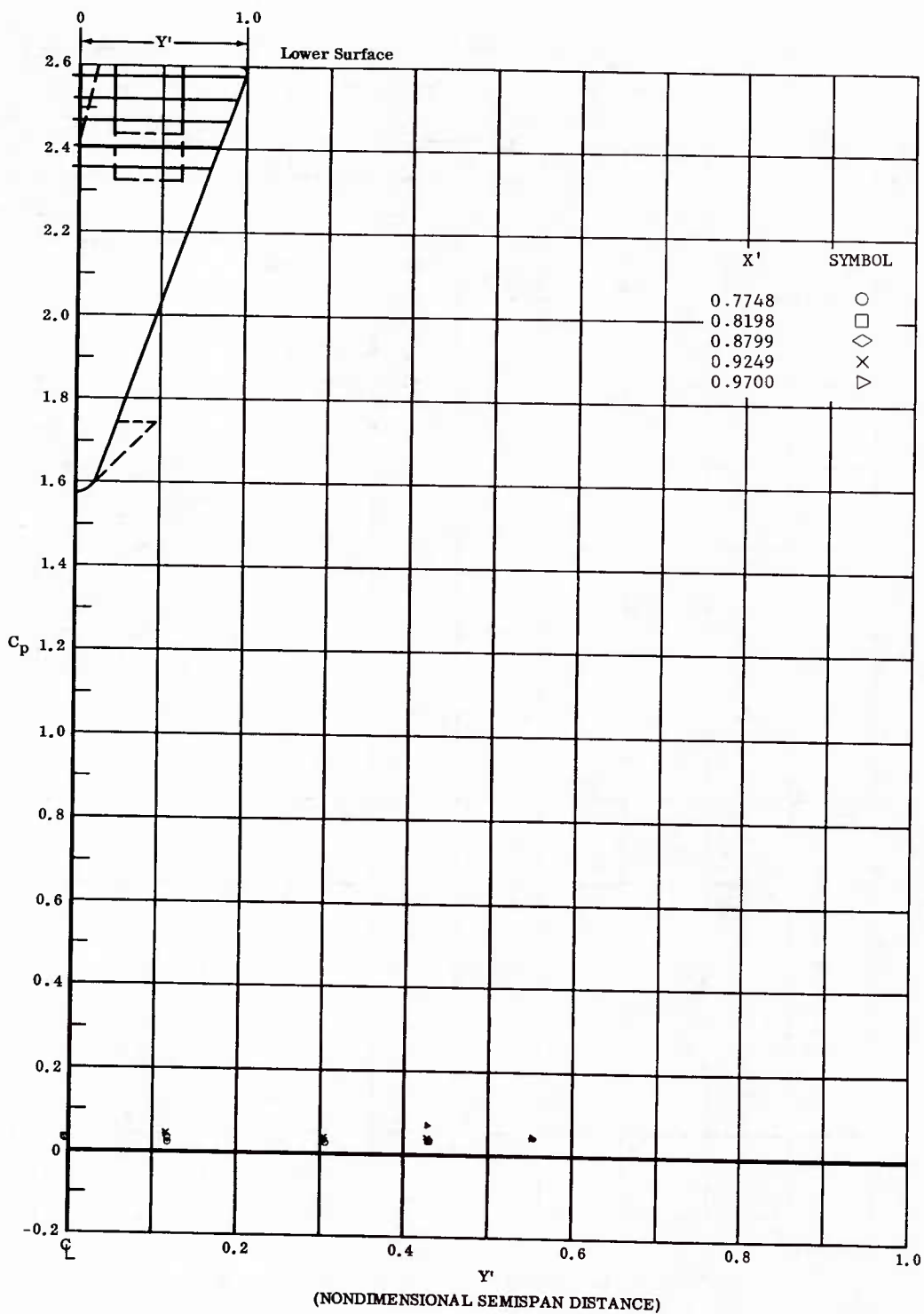


Fig. 65 Spanwise Distributions of Pressure Coefficients; Basic Configuration + Fin ( $\delta = 15^\circ$ ), No Flap Deflections,  $\alpha = 0^\circ$ ,  $\beta = +12^\circ$ ,  $Re_\infty / ft = 3,300,000$ .

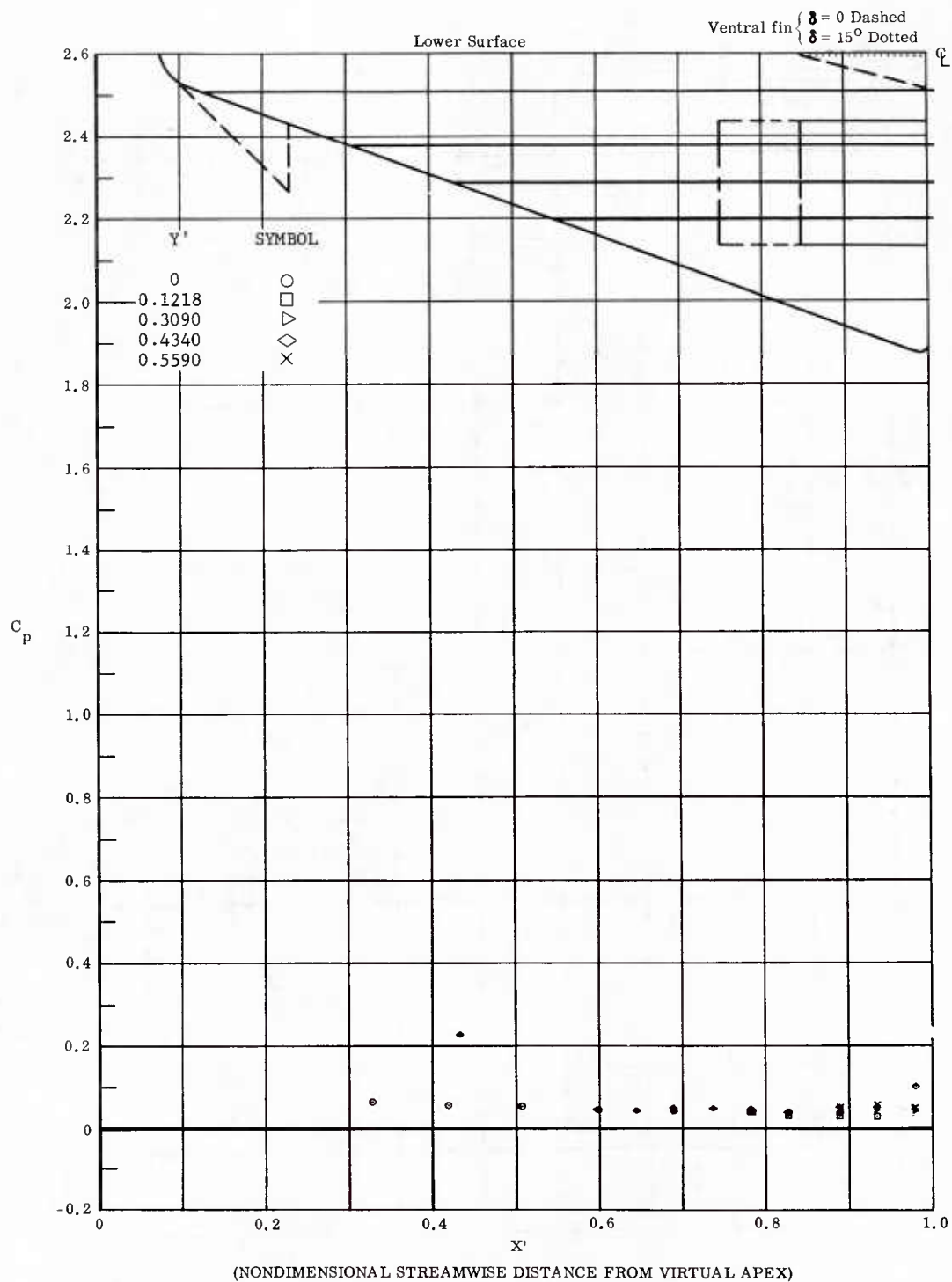


Fig. 66 Streamwise Distributions of Pressure Coefficients; Basic Configuration, Left and Right (Upper) Flaps Deflected  $-40^\circ$ ,  $\alpha = +7^\circ$ ,  $\beta = 0^\circ$ ,  $Re_\infty / ft = 3,300,000$ .

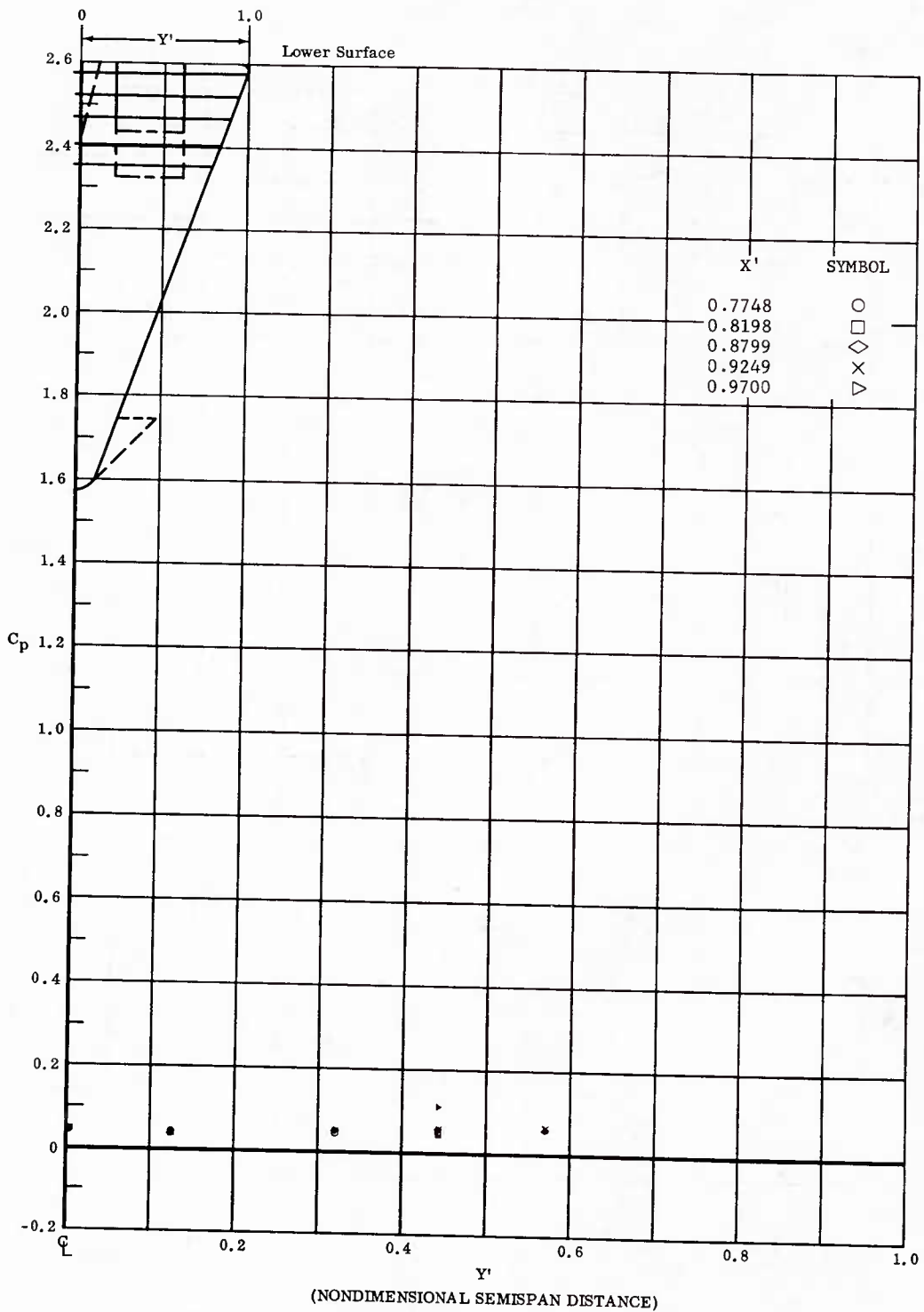


Fig. 66 Spanwise Distributions of Pressure Coefficients; Basic Configuration, Left and Right (Upper) Flaps Deflected  $-40^\circ$ ,  $\alpha = +7^\circ$ ,  $\beta = 0^\circ$ ,  $Re_\infty/ft = 3,300,000$ .

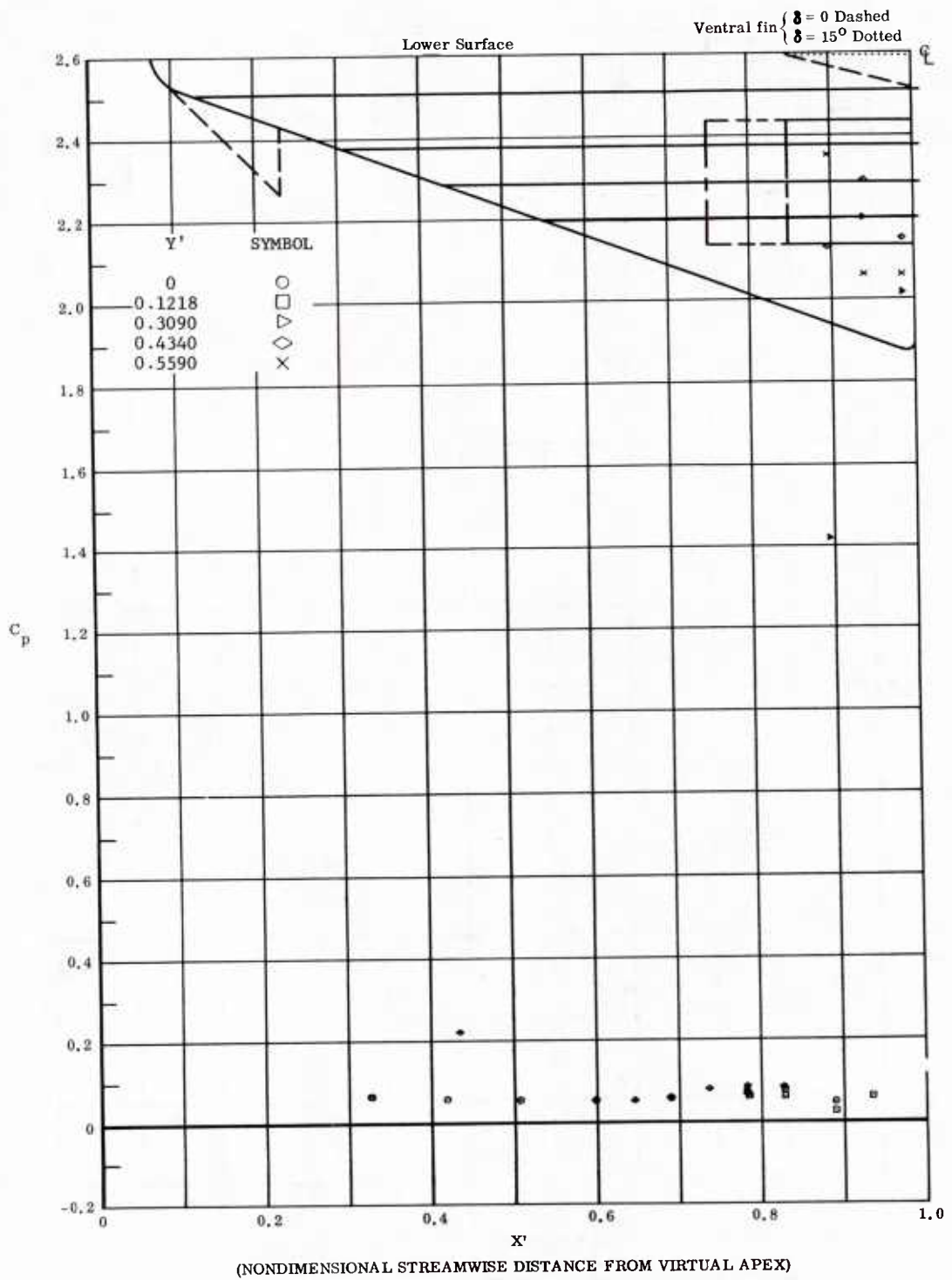


Fig. 67 Streamwise Distributions of Pressure Coefficients; Basic Configuration, Bottom Flaps Deflected  $+40^\circ$ ,  $\alpha = +7^\circ$ ,  $\beta = 0^\circ$ ,  $Re_\infty/ft = 3,300,000$ .

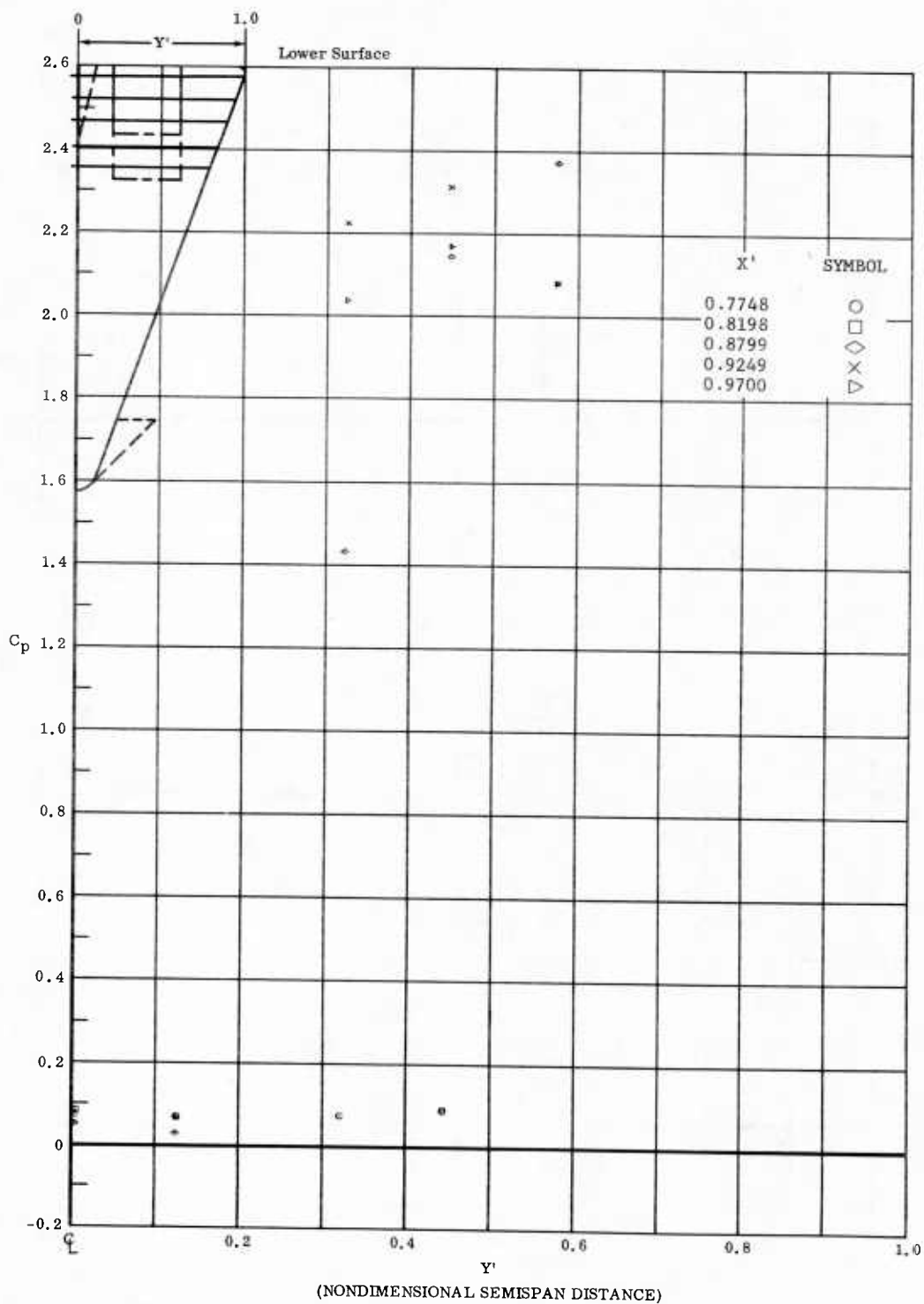


Fig. 67 Spanwise Distributions of Pressure Coefficients; Basic Configuration, Bottom Flaps Deflected  $+40^\circ$ ,  $\alpha = +7^\circ$ ,  $\beta = 0^\circ$ ,  $Re_\infty/ft = 3,300,000$ .

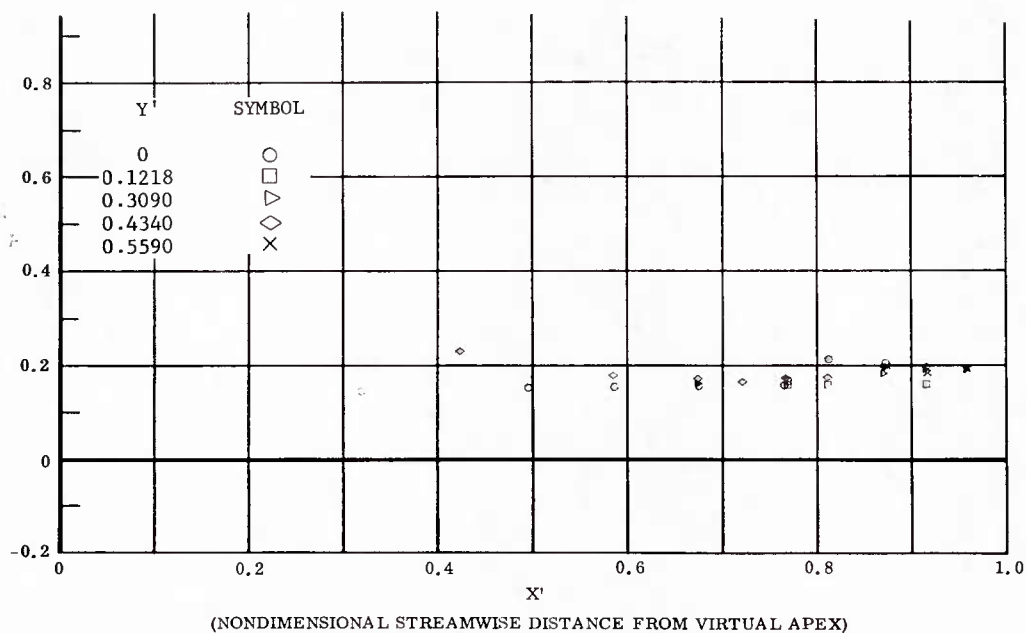


Fig. 68 Streamwise Distributions of Pressure Coefficients; Basic Configuration, Left and Right (Upper) Flaps Deflected  $-40^\circ$ ,  $\alpha = +14.3^\circ$ ,  $\beta = 0^\circ$ ,  $Re_\infty/ft = 1,100,000$ .

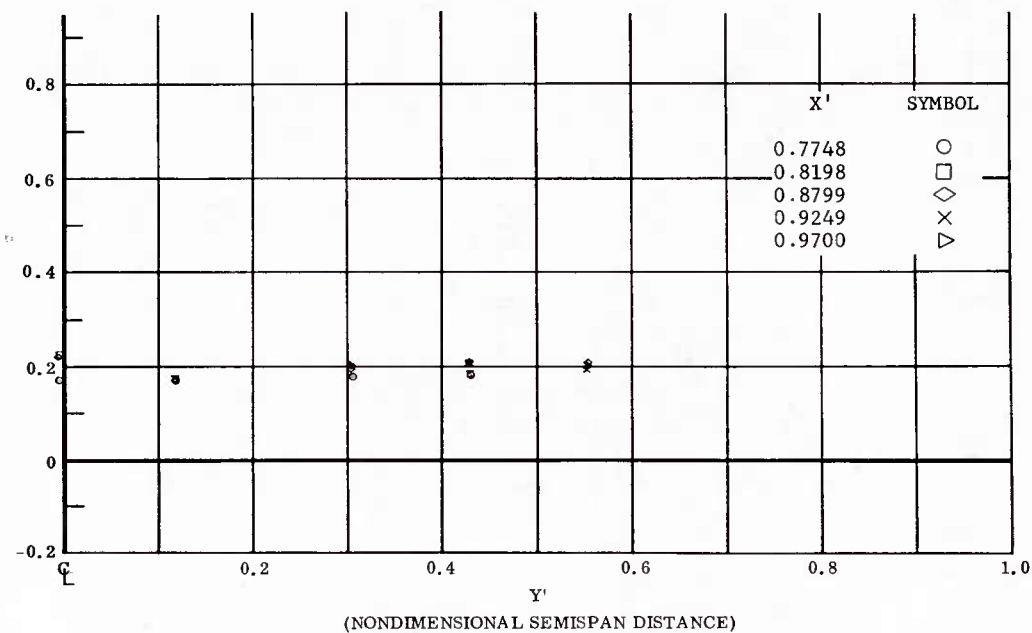


Fig. 68 Spanwise Distributions of Pressure Coefficients; Basic Configuration, Left and Right (Upper) Flaps Deflected  $-40^\circ$ ,  $\alpha = +14.3^\circ$ ,  $\beta = 0^\circ$ ,  $Re_\infty/ft = 1,100,000$ .

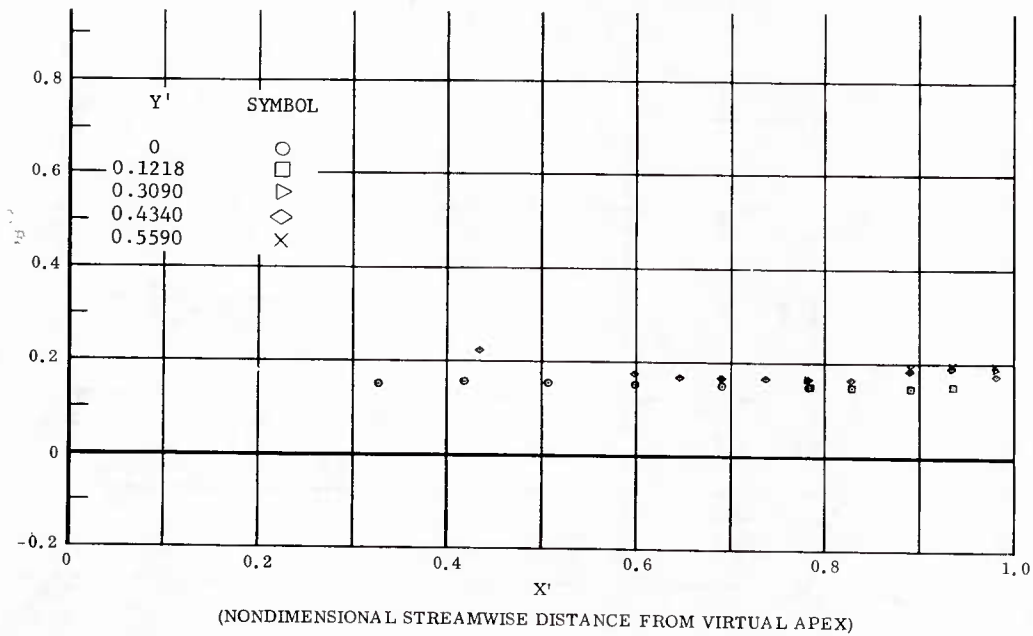


Fig. 69 Streamwise Distributions of Pressure Coefficients; Basic Configuration, Left and Right (Upper) Flaps Deflected  $-40^\circ$ ,  $\alpha = +14.3^\circ$ ,  $\beta = 0^\circ$ ,  $Re_\infty/ft = 3,300,000$ .

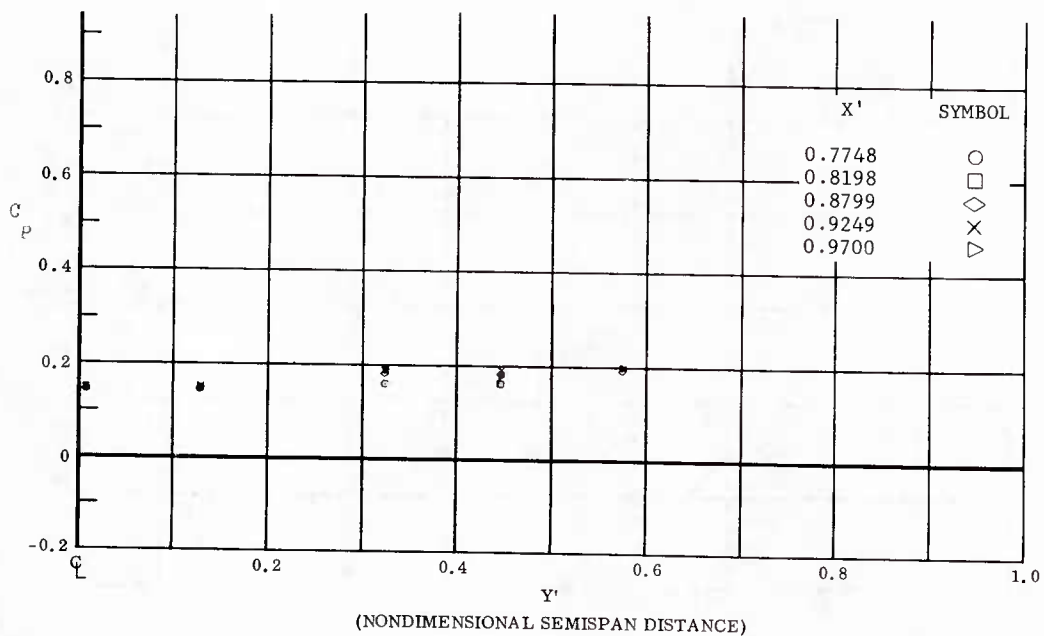


Fig. 69 Spanwise Distributions of Pressure Coefficients; Basic Configuration, Left and Right (Upper) Flaps Deflected  $-40^\circ$ ,  $\alpha = +14.3^\circ$ ,  $\beta = 0^\circ$ ,  $Re_\infty/ft = 3,300,000$ .

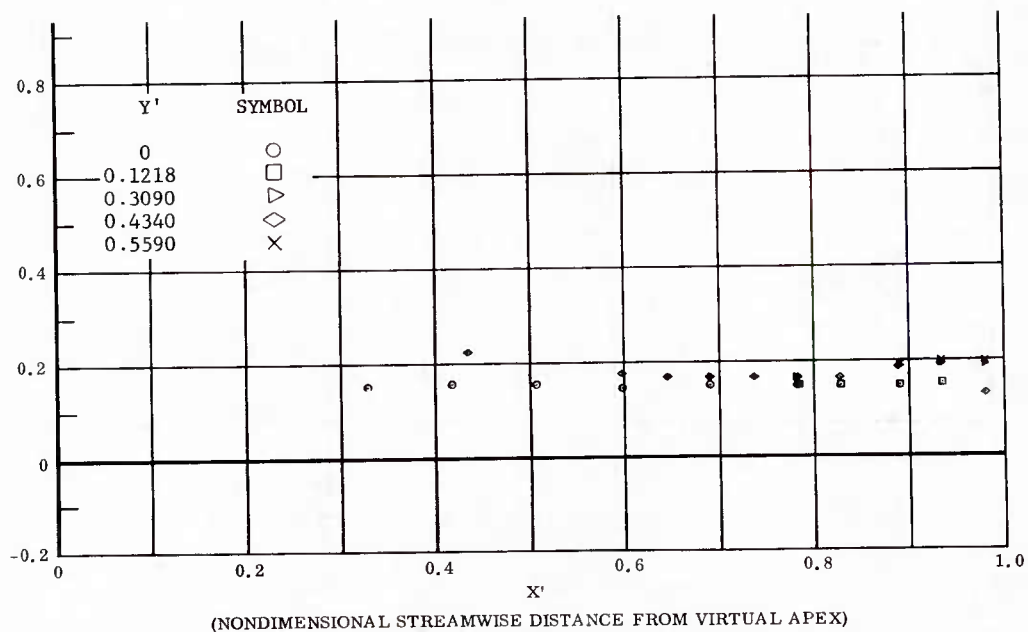


Fig. 70 Streamwise Distributions of Pressure Coefficients; Basic Configuration, Left (Upper) Flaps Deflected  $-40^\circ$ ,  $\alpha = +14.3^\circ$ ,  $\beta = 0^\circ$ ,  $Re_\infty/ft = 3,300,000$ .

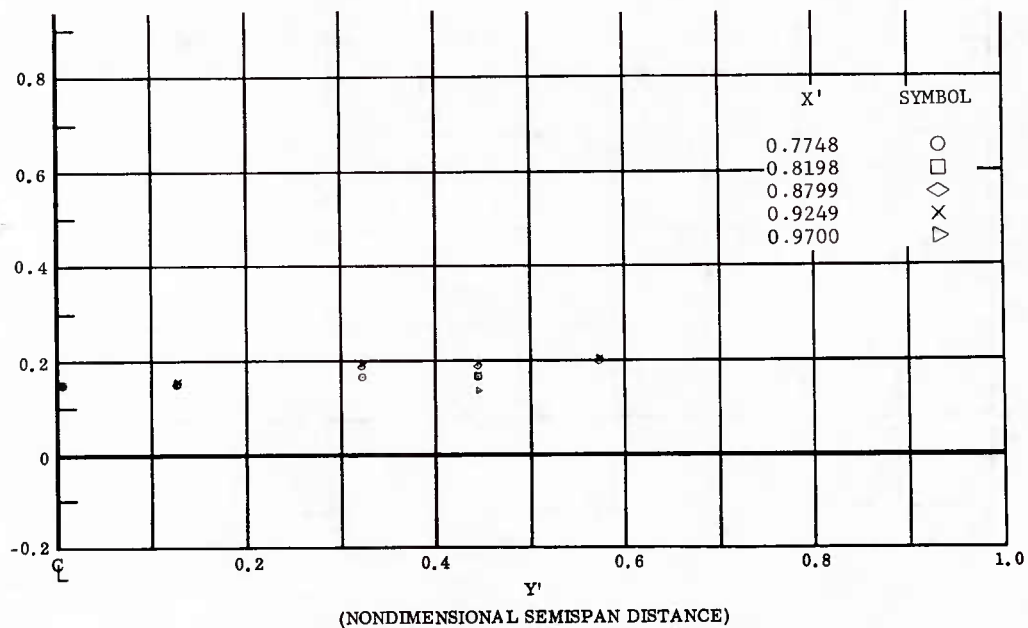


Fig. 70 Spanwise Distributions of Pressure Coefficients; Basic Configuration, Left (Upper) Flaps Deflected  $-40^\circ$ ,  $\alpha = +14.3^\circ$ ,  $\beta = 0^\circ$ ,  $Re_\infty/ft = 3,300,000$ .



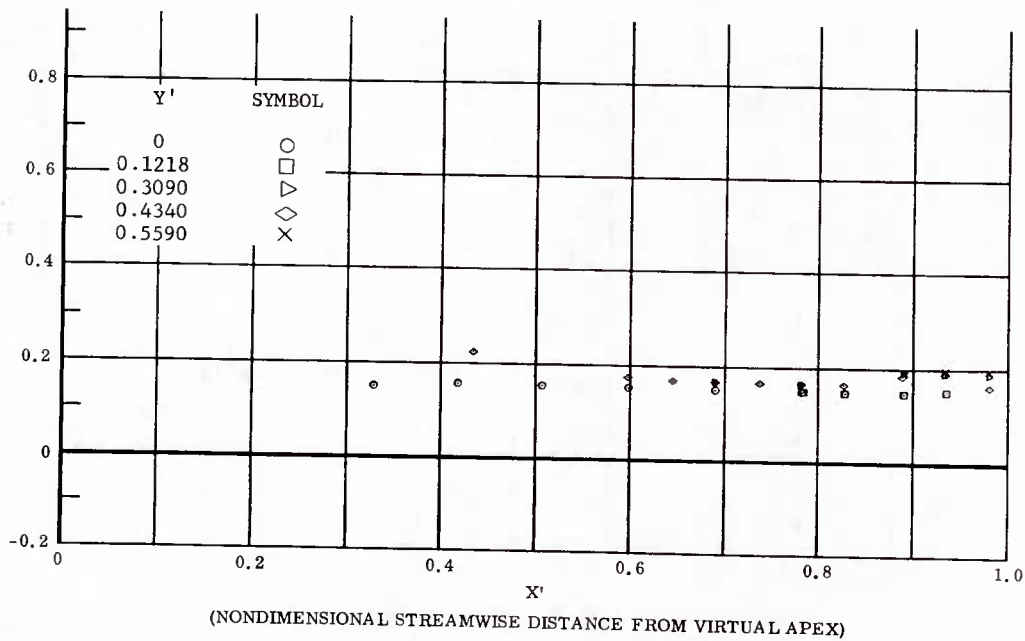


Fig. 71 Streamwise Distributions of Pressure Coefficients; Basic Configuration, Right (Upper) Flaps Deflected  $-40^\circ$ ,  $\alpha = +14.3^\circ$ ,  $\beta = 0^\circ$ ,  $Re_\infty / ft = 3,300,000$ .

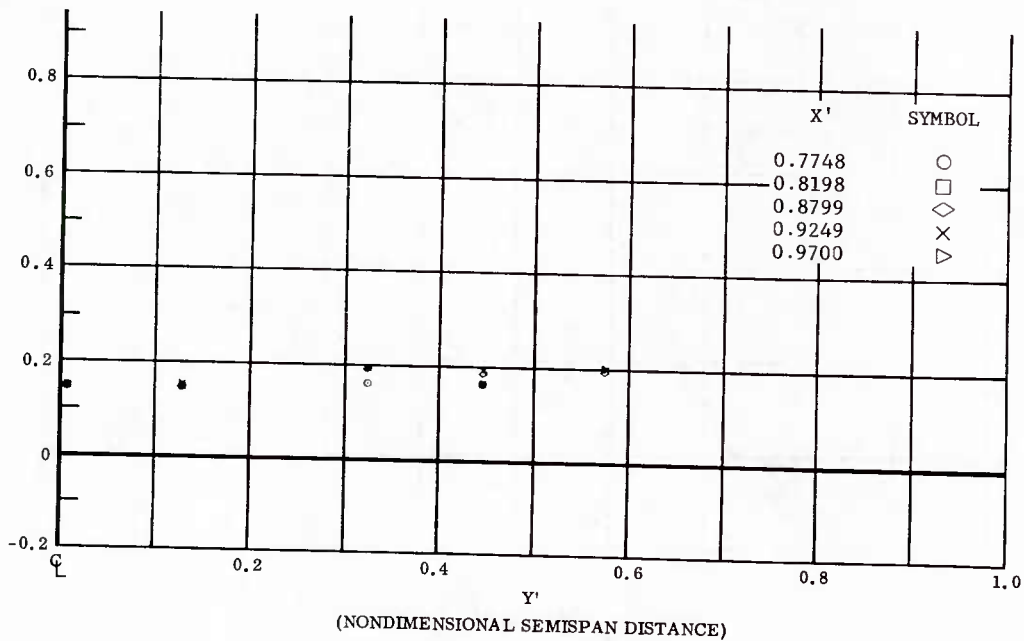


Fig. 71 Spanwise Distributions of Pressure Coefficients; Basic Configuration, Right (Upper) Flaps Deflected  $-40^\circ$ ,  $\alpha = +14.3^\circ$ ,  $\beta = 0^\circ$ ,  $Re_\infty / ft = 3,300,000$ .

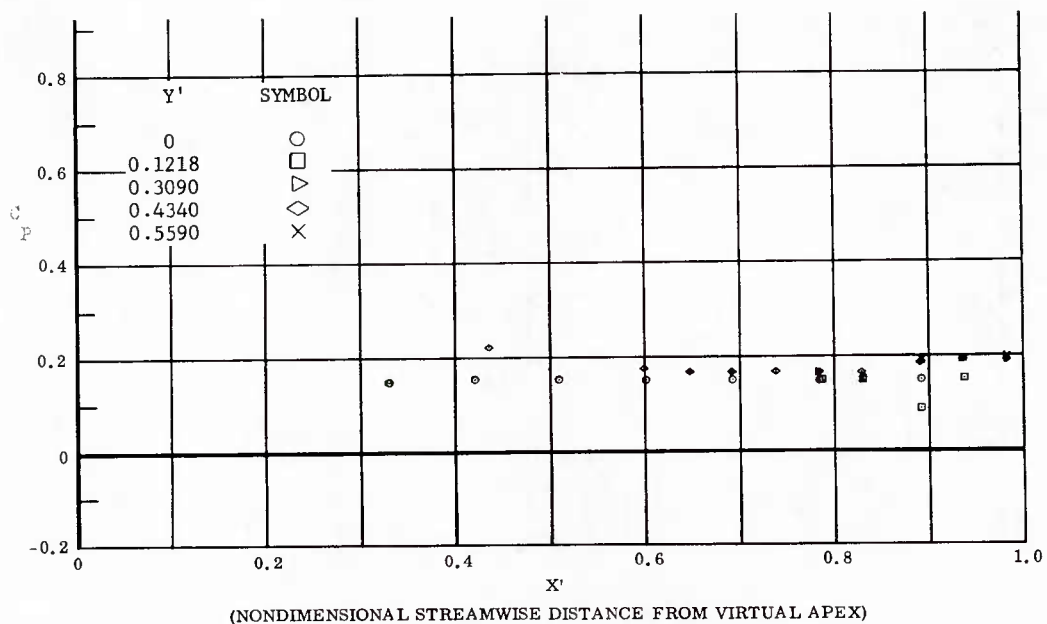


Fig. 72 Streamwise Distributions of Pressure Coefficients; Basic Configuration, Left and Right (Upper) Flaps Deflected  $-30^\circ$ ,  $\alpha = +14.3^\circ$ ,  $\beta = 0^\circ$ ,  $Re_\infty/ft = 3,300,000$ .

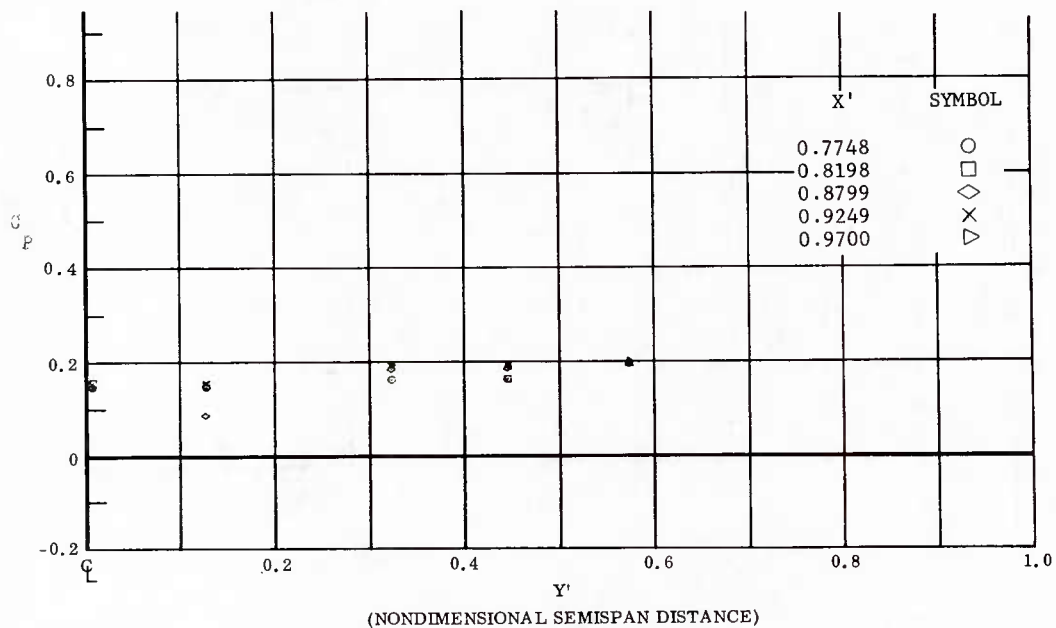


Fig. 72 Spanwise Distributions of Pressure Coefficients; Basic Configuration, Left and Right (Upper) Flaps Deflected  $-30^\circ$ ,  $\alpha = +14.3^\circ$ ,  $\beta = 0^\circ$ ,  $Re_\infty/ft = 3,300,000$ .

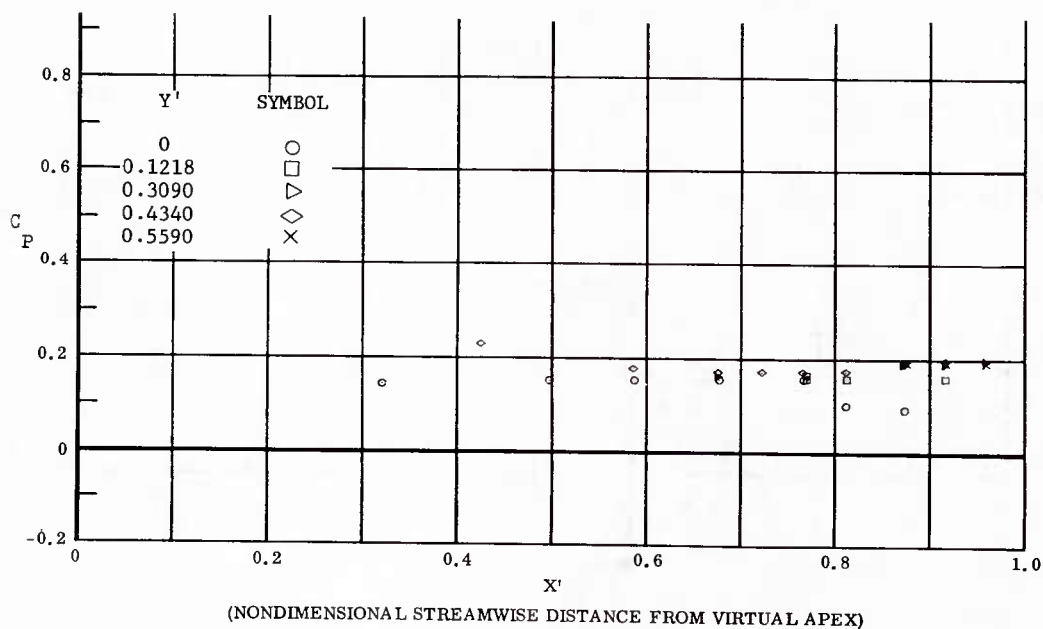


Fig. 73 Streamwise Distributions of Pressure Coefficients; Basic Configuration, Left and Right (Upper) Flaps Deflected  $-20^\circ$ ,  $\alpha = +14.3^\circ$ ,  $\beta = 0^\circ$ ,  $Re_\infty / ft = 1,100,000$ .

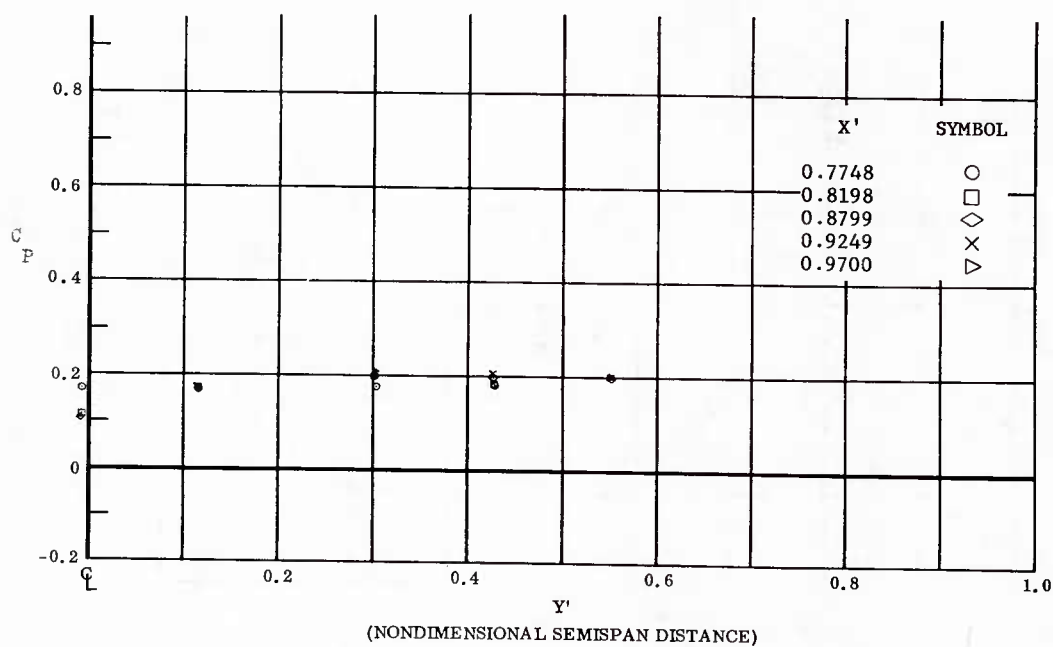


Fig. 73 Spanwise Distributions of Pressure Coefficients; Basic Configuration, Left and Right (Upper) Flaps Deflected  $-20^\circ$ ,  $\alpha = +14.3^\circ$ ,  $\beta = 0^\circ$ ,  $Re_\infty / ft = 1,100,000$ .

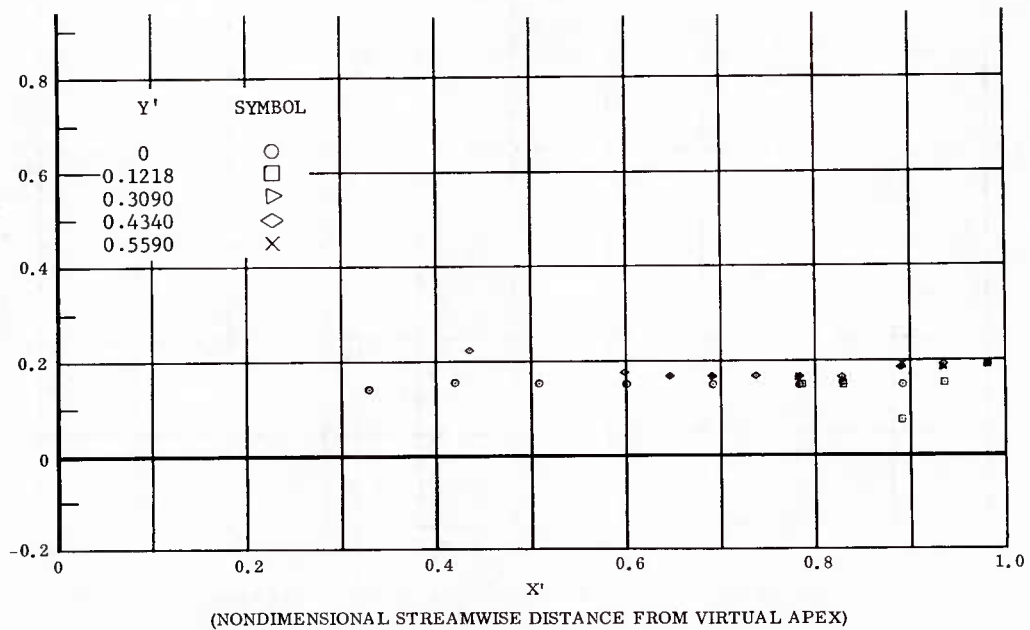


Fig. 74 Streamwise Distributions of Pressure Coefficients; Basic Configuration, Left and Right (Upper) Flaps Deflected  $-20^\circ$ ,  $\alpha = +14.3^\circ$ ,  $\beta = 0^\circ$ ,  $Re_\infty / ft = 3,300,000$ .

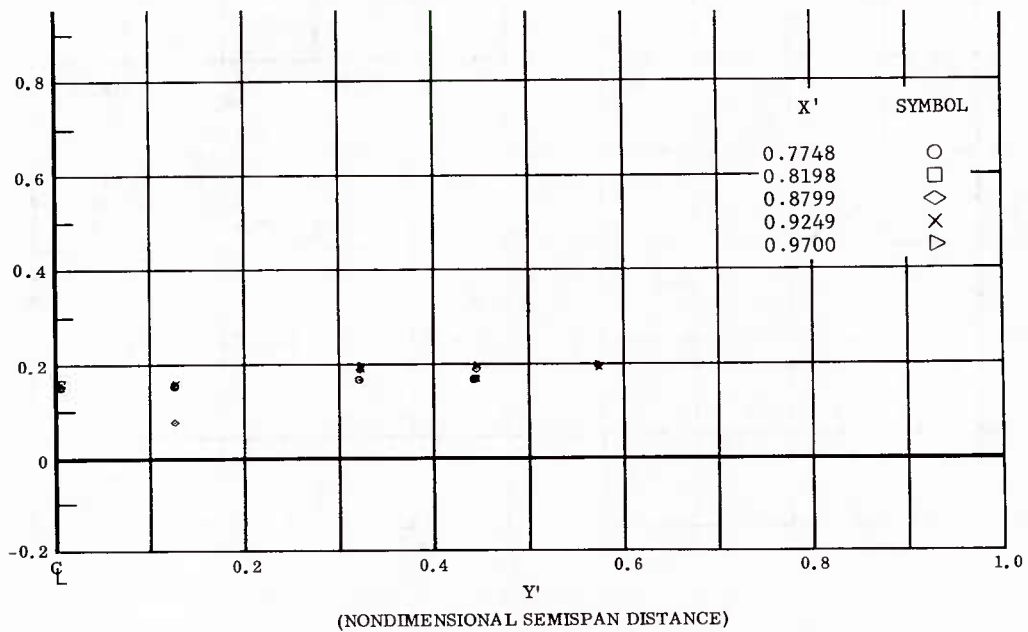


Fig. 74 Spanwise Distributions of Pressure Coefficients; Basic Configuration, Left and Right (Upper) Flaps Deflected  $-20^\circ$ ,  $\alpha = +14.3^\circ$ ,  $\beta = 0^\circ$ ,  $Re_\infty / ft = 3,300,000$ .

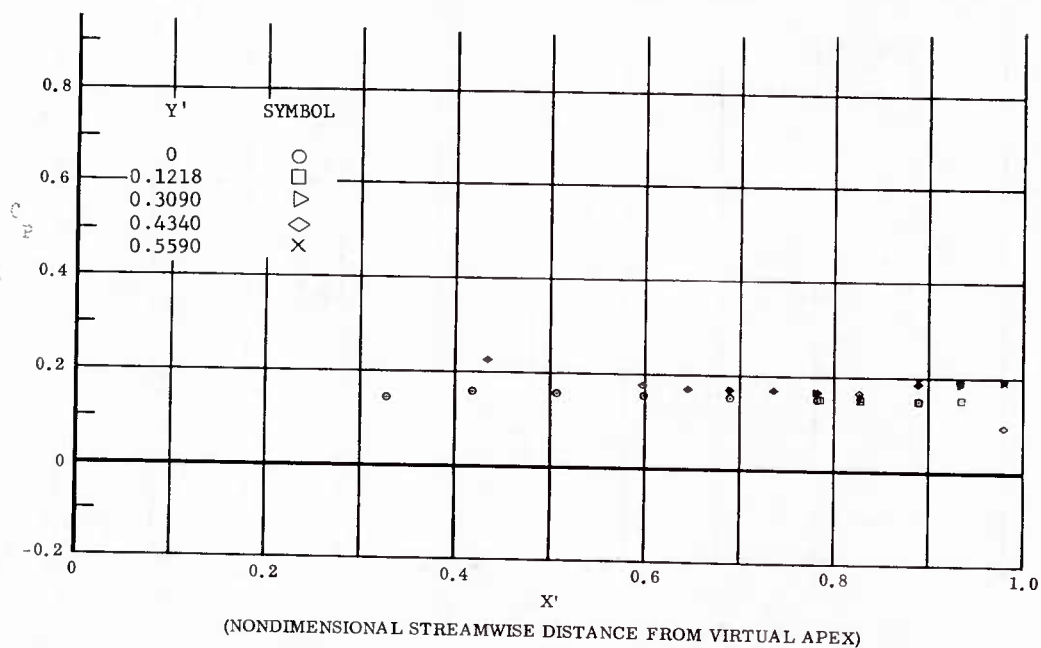


Fig. 75 Streamwise Distributions of Pressure Coefficients; Basic Configuration Left (Upper) Flaps Deflected  $-20^\circ$ ,  $\alpha = +14.3^\circ$ ,  $\beta = 0^\circ$ ,  $Re_{\infty}/ft = 3,300,000$ .

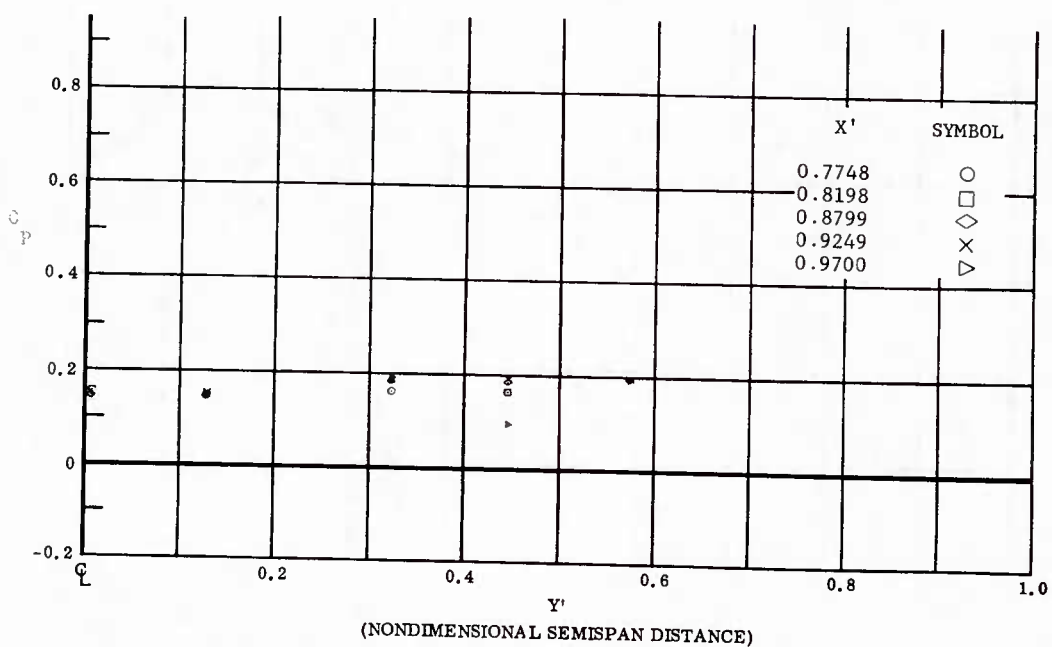


Fig. 75 Spanwise Distributions of Pressure Coefficients; Basic Configuration, Left (Upper) Flaps Deflected  $-20^\circ$ ,  $\alpha = +14.3^\circ$ ,  $\beta = 0^\circ$ ,  $Re_{\infty}/ft = 3,300,000$ .

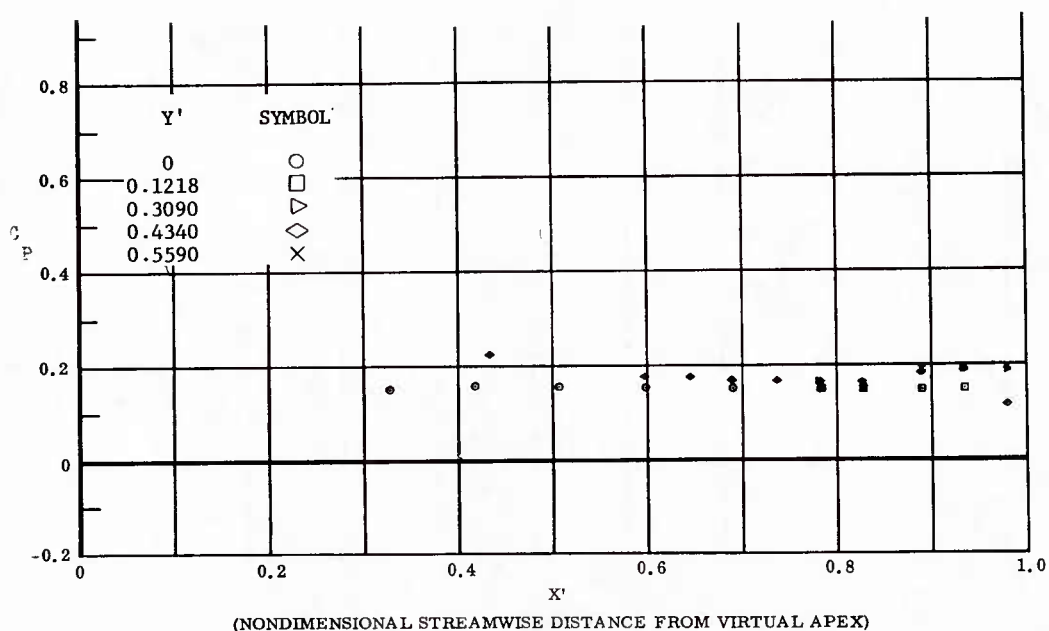


Fig. 76 Streamwise Distributions of Pressure Coefficients; Basic Configuration, Right (Upper) Flaps Deflected  $-20^\circ$ ,  $\alpha = +14.3^\circ$ ,  $\beta = 0^\circ$ ,  $Re_\infty/ft = 3,300,000$ .

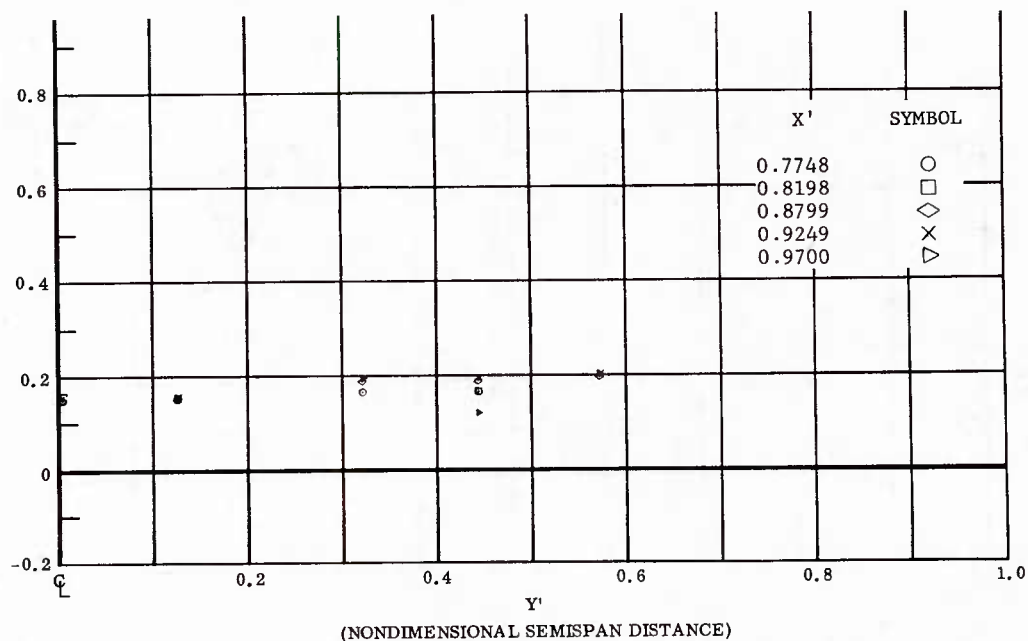


Fig. 76 Spanwise Distributions of Pressure Coefficients; Basic Configuration, Right (Upper) Flaps Deflected  $-20^\circ$ ,  $\alpha = +14.3^\circ$ ,  $\beta = 0^\circ$ ,  $Re_\infty/ft = 3,300,000$ .

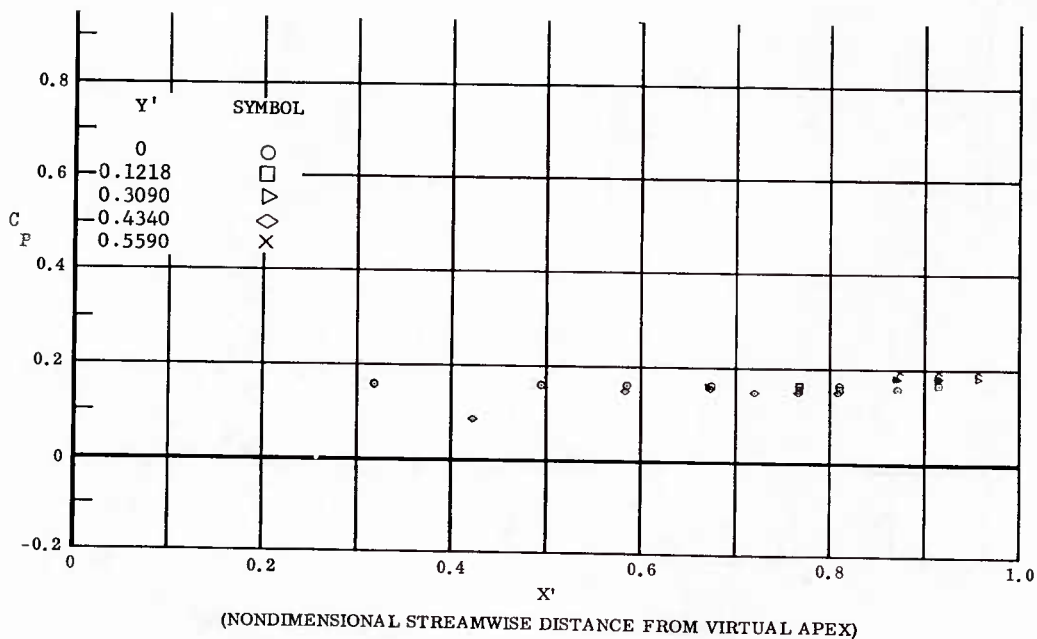


Fig. 77 Streamwise Distributions of Pressure Coefficients; Basic Configuration + Canards, Left and Right (Upper) Flaps Deflected  $-20^\circ$ ,  $\alpha = +14.3^\circ$ ,  $\beta = 0^\circ$ ,  $Re_\infty/ft = 3,300,000$ .

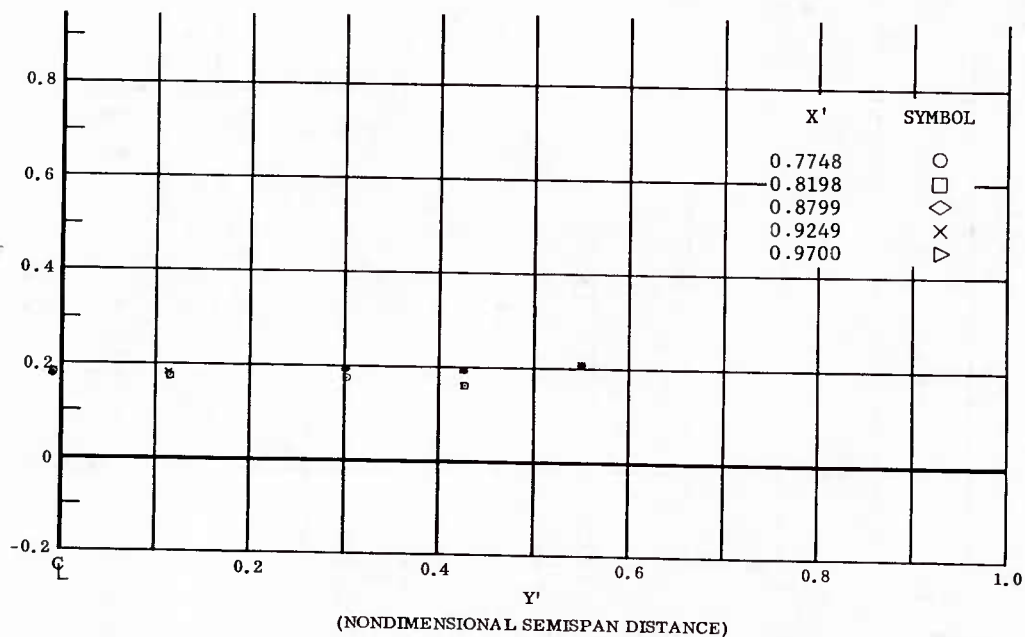


Fig. 77 Spanwise Distributions of Pressure Coefficients; Basic Configuration + Canards, Left and Right (Upper) Flaps Deflected  $-20^\circ$ ,  $\alpha = +14.3^\circ$ ,  $\beta = 0^\circ$ ,  $Re_\infty/ft = 3,300,000$ .

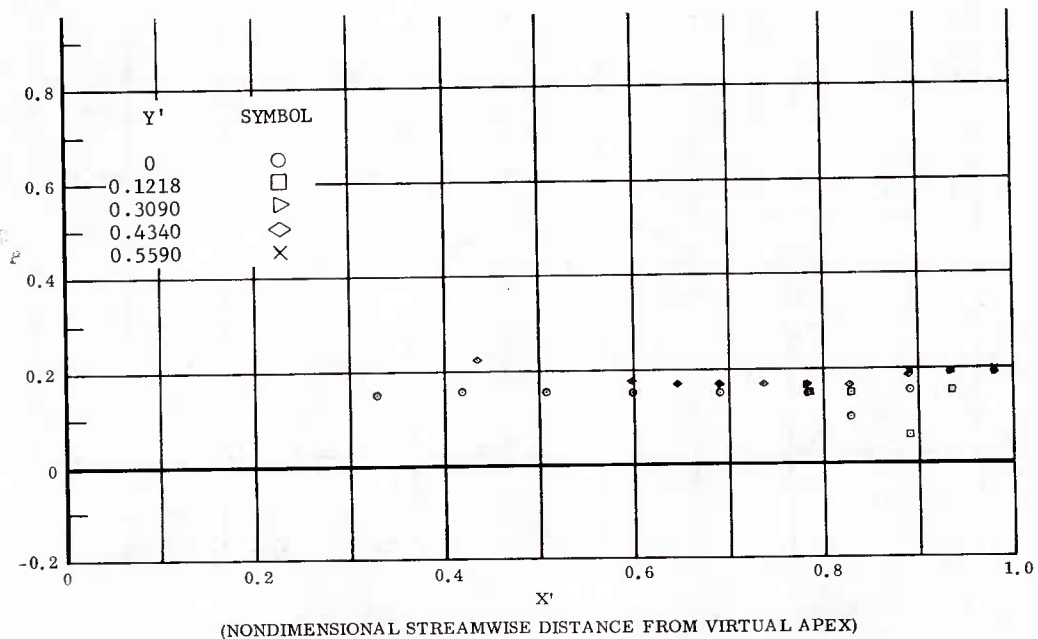


Fig. 78 Streamwise Distributions of Pressure Coefficients; Basic Configuration, Left and Right (Upper) Flaps Deflected  $-10^\circ$ ,  $\alpha = +14.3^\circ$ ,  $\beta = 0^\circ$ ,  $Re_\infty/ft = 3,300,000$ .

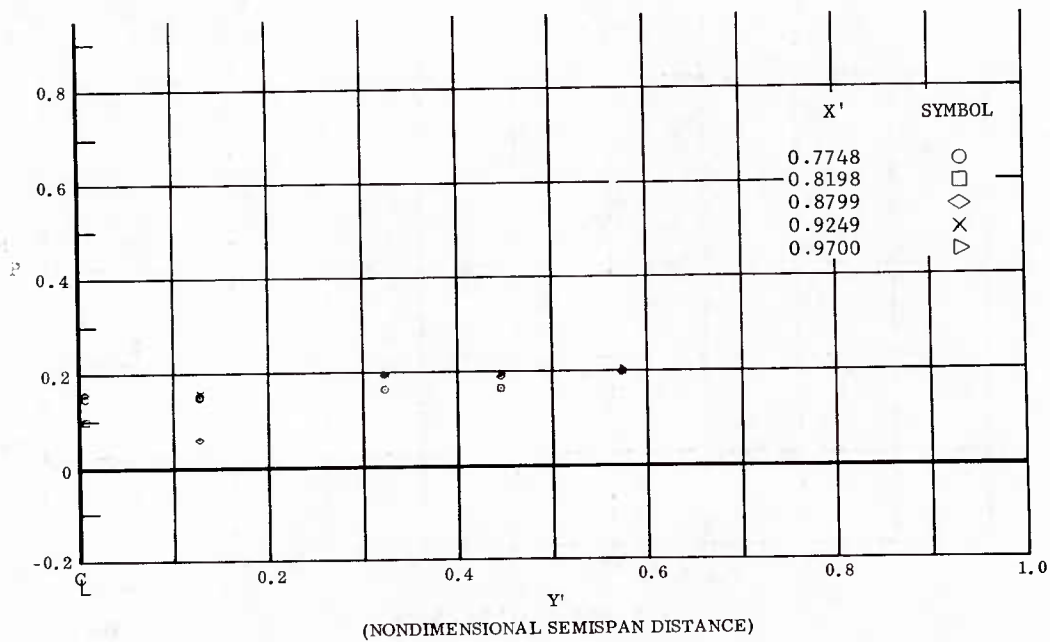


Fig. 78 Spanwise Distributions of Pressure Coefficients; Basic Configuration, Left and Right (Upper) Flaps Deflected  $-10^\circ$ ,  $\alpha = +14.3^\circ$ ,  $\beta = 0^\circ$ ,  $Re_\infty/ft = 3,300,000$ .



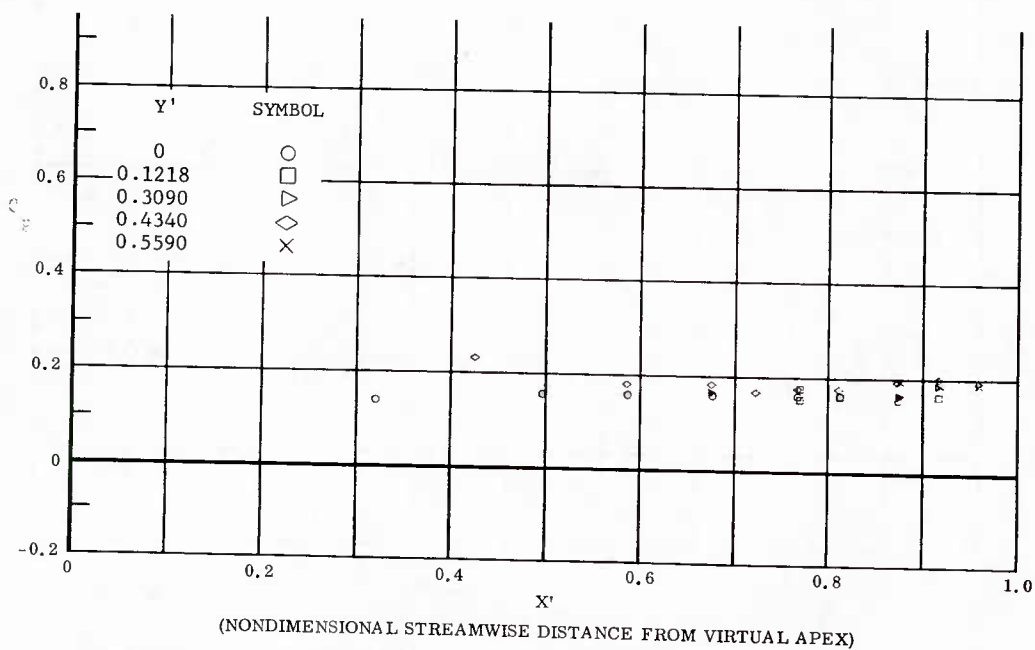


Fig. 79 Streamwise Distributions of Pressure Coefficients; Basic Configuration, No Flap Deflections,  $\alpha = +14.3^\circ$ ,  $\beta = 0^\circ$ ,  $Re_\infty/ft = 1,100,000$ .

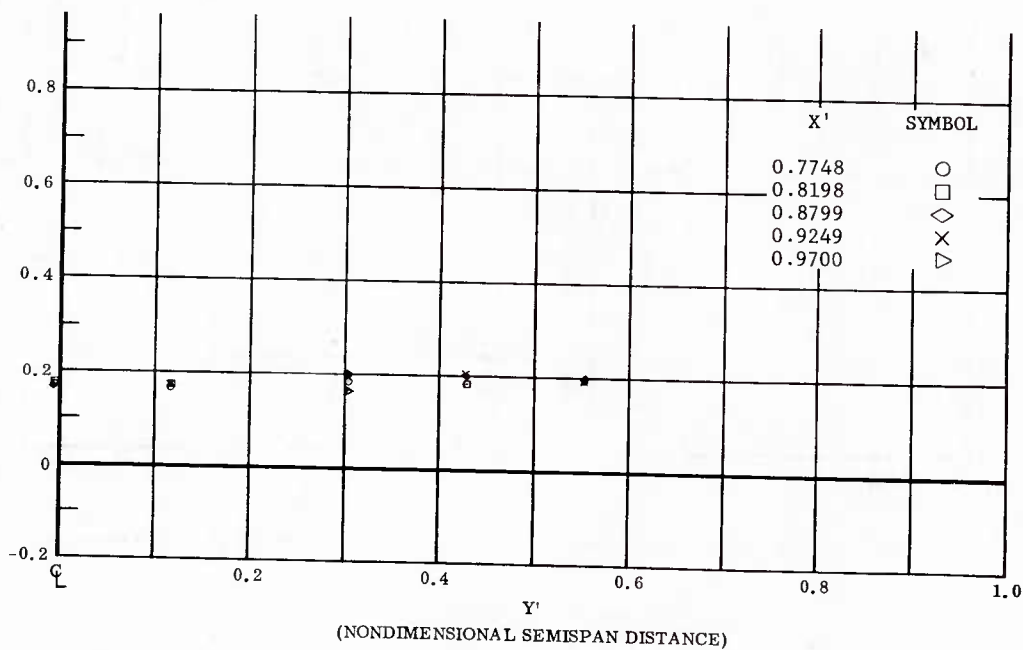


Fig. 79 Spanwise Distributions of Pressure Coefficients; Basic Configuration, No Flap Deflections,  $\alpha = +14.3^\circ$ ,  $\beta = 0^\circ$ ,  $Re_\infty/ft = 1,100,000$ .

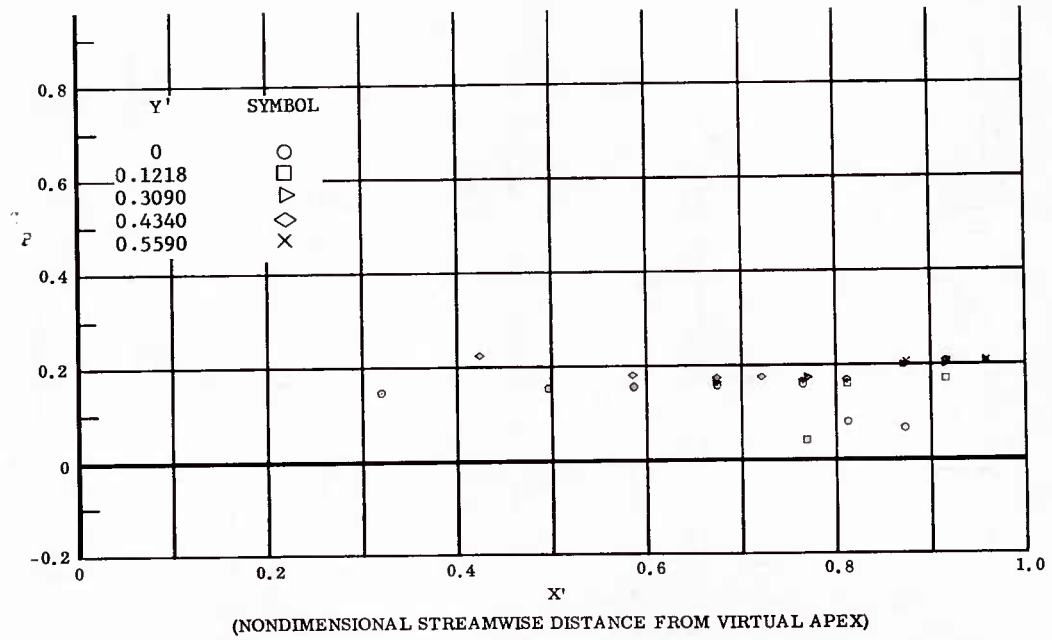


Fig. 30 Streamwise Distributions of Pressure Coefficients; Basic Configuration, No Flap Deflections,  $\alpha = +14.3^\circ$ ,  $\beta = 0^\circ$ ,  $Re_\infty/ft = 3,300,000$ .

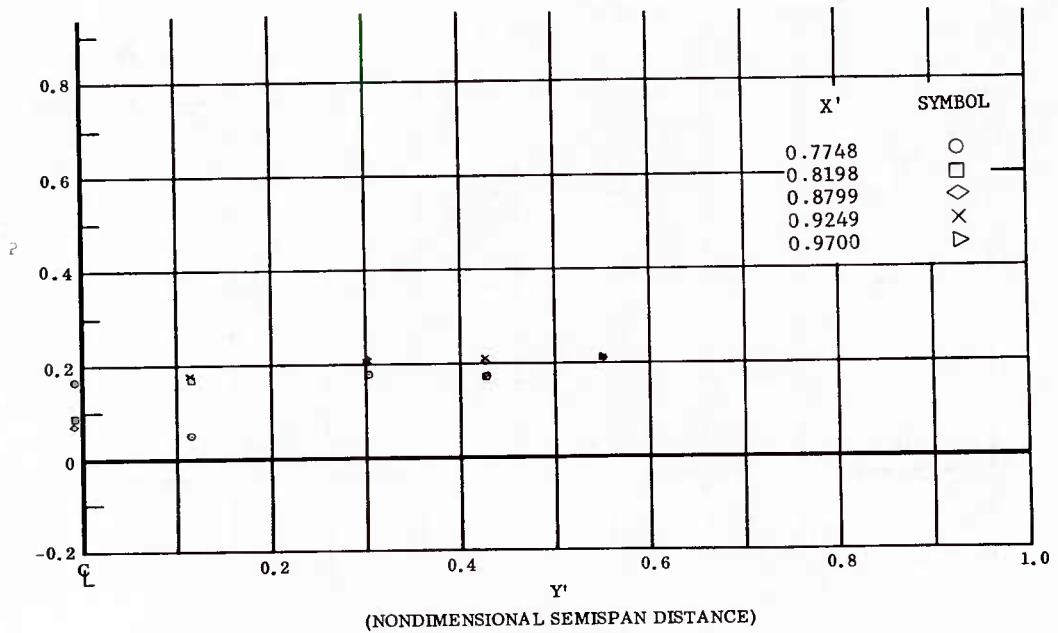


Fig. 30 Spanwise Distributions of Pressure Coefficients; Basic Configuration, No Flap Deflections,  $\alpha = +14.3^\circ$ ,  $\beta = 0^\circ$ ,  $Re_\infty/ft = 3,300,000$ .

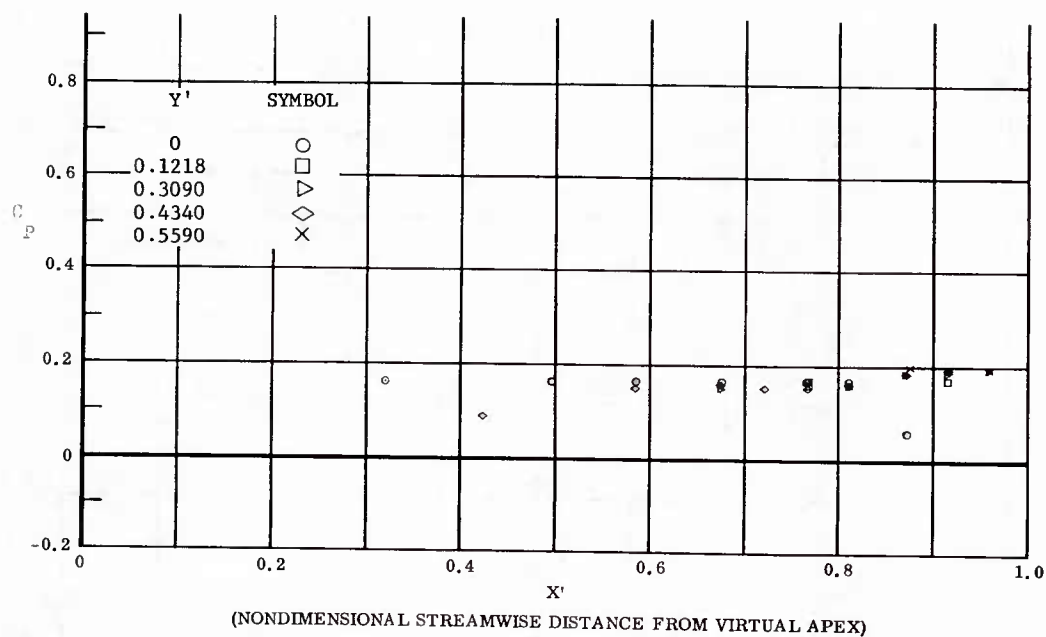


Fig. 81 Streamwise Distributions of Pressure Coefficients; Basic Configuration + Canards, No Flap Deflections,  $\alpha = +14.3^\circ$ ,  $\beta = 0^\circ$ ,  $Re_\infty/ft = 3,300,000$ .

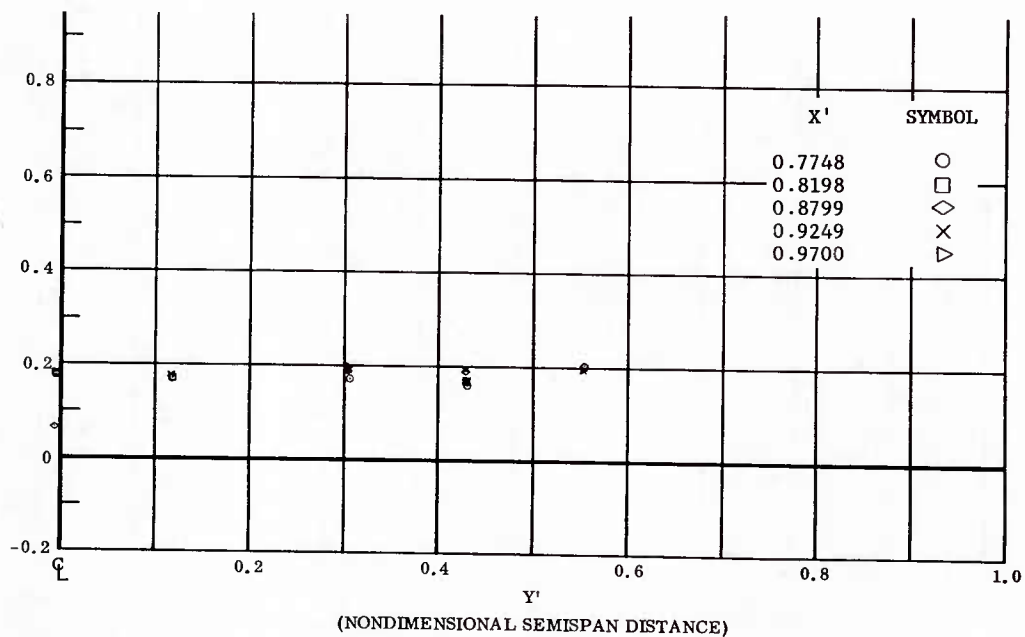


Fig. 81 Spanwise Distributions of Pressure Coefficients; Basic Configuration + Canards, No Flap Deflections,  $\alpha = +14.3^\circ$ ,  $\beta = 0^\circ$ ,  $Re_\infty/ft = 3,300,000$ .

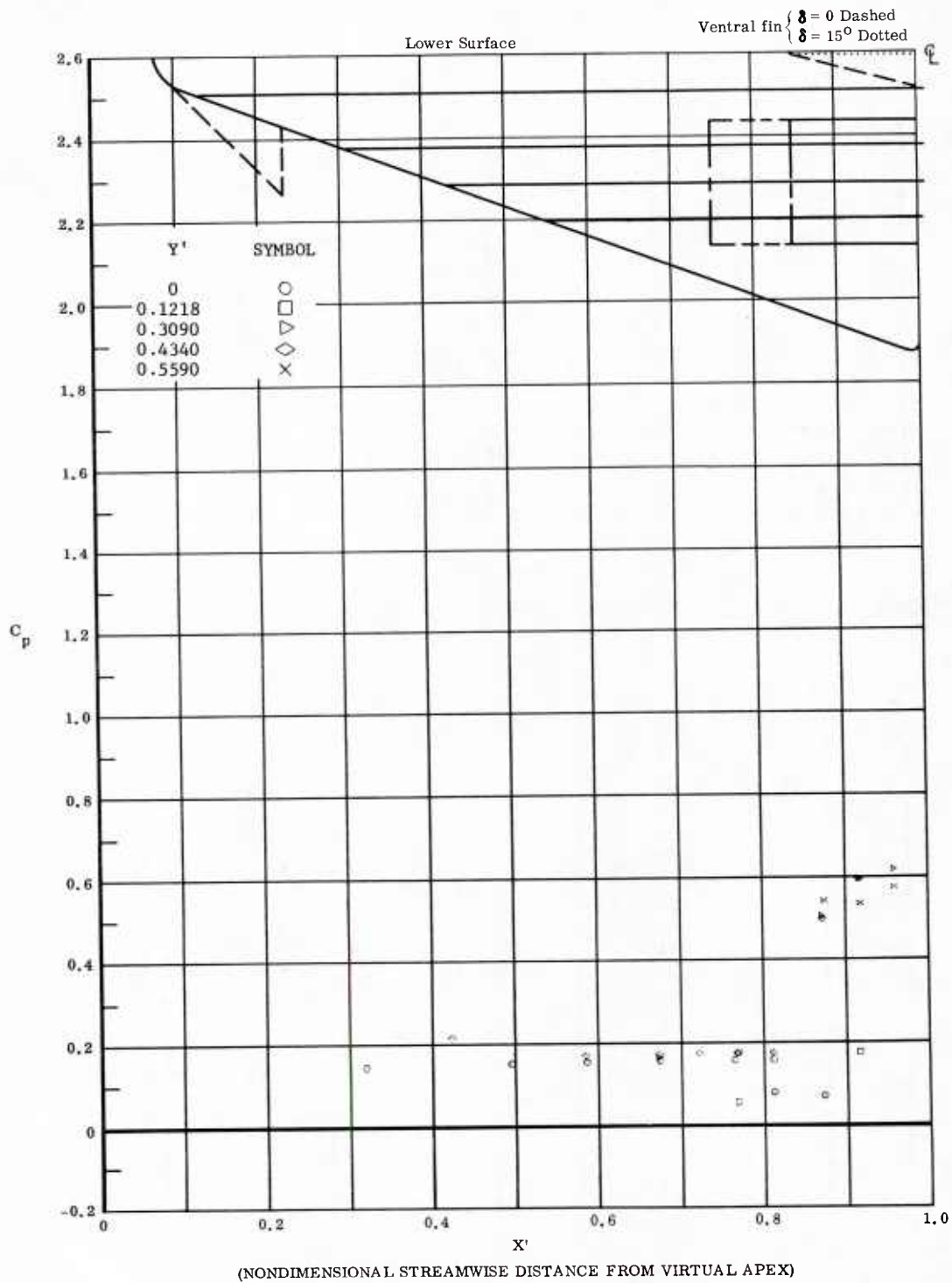


Fig. 32 Streamwise Distributions of Pressure Coefficients; Basic Configuration, Bottom Flaps Deflected  $+10^\circ$ ,  $\alpha = +14.3^\circ$ ,  $\beta = 0^\circ$ ,  $Re_\infty/ft = 3,300,000$ .

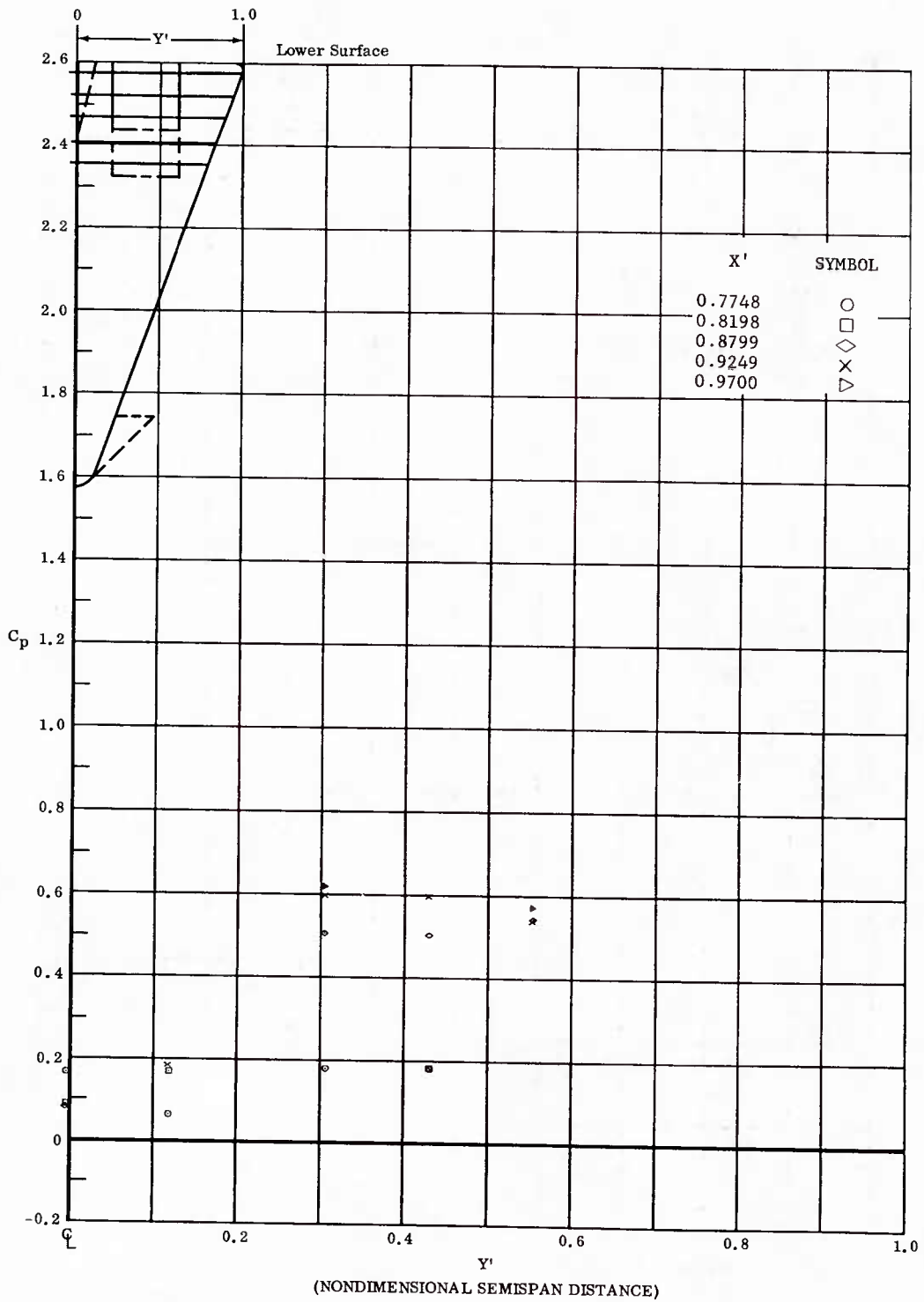


Fig. 82 Spanwise Distributions of Pressure Coefficients; Basic Configuration, Bottom Flaps Deflected  $+10^\circ$ ,  $\alpha = +14.3^\circ$ ,  $\beta = 0^\circ$ ,  $Re_\infty/ft = 3,300,000$ .

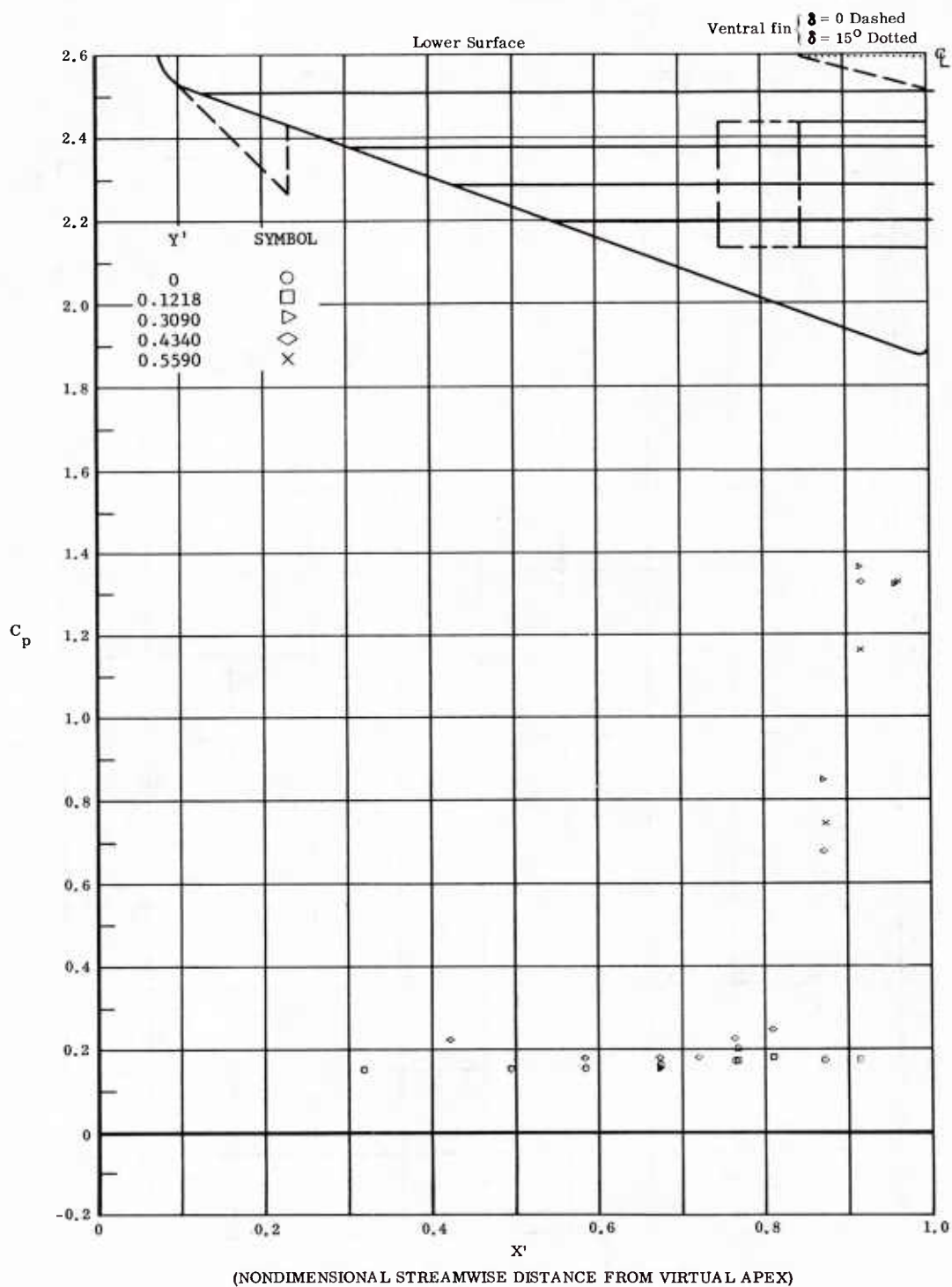


Fig. 33 Streamwise Distributions of Pressure Coefficients; Basic Configuration, Bottom Flaps Deflected  $+20^\circ$ ,  $\alpha = +14.3^\circ$ ,  $\beta = 0^\circ$ ,  $Re_\infty/ft = 1,100,000$ .

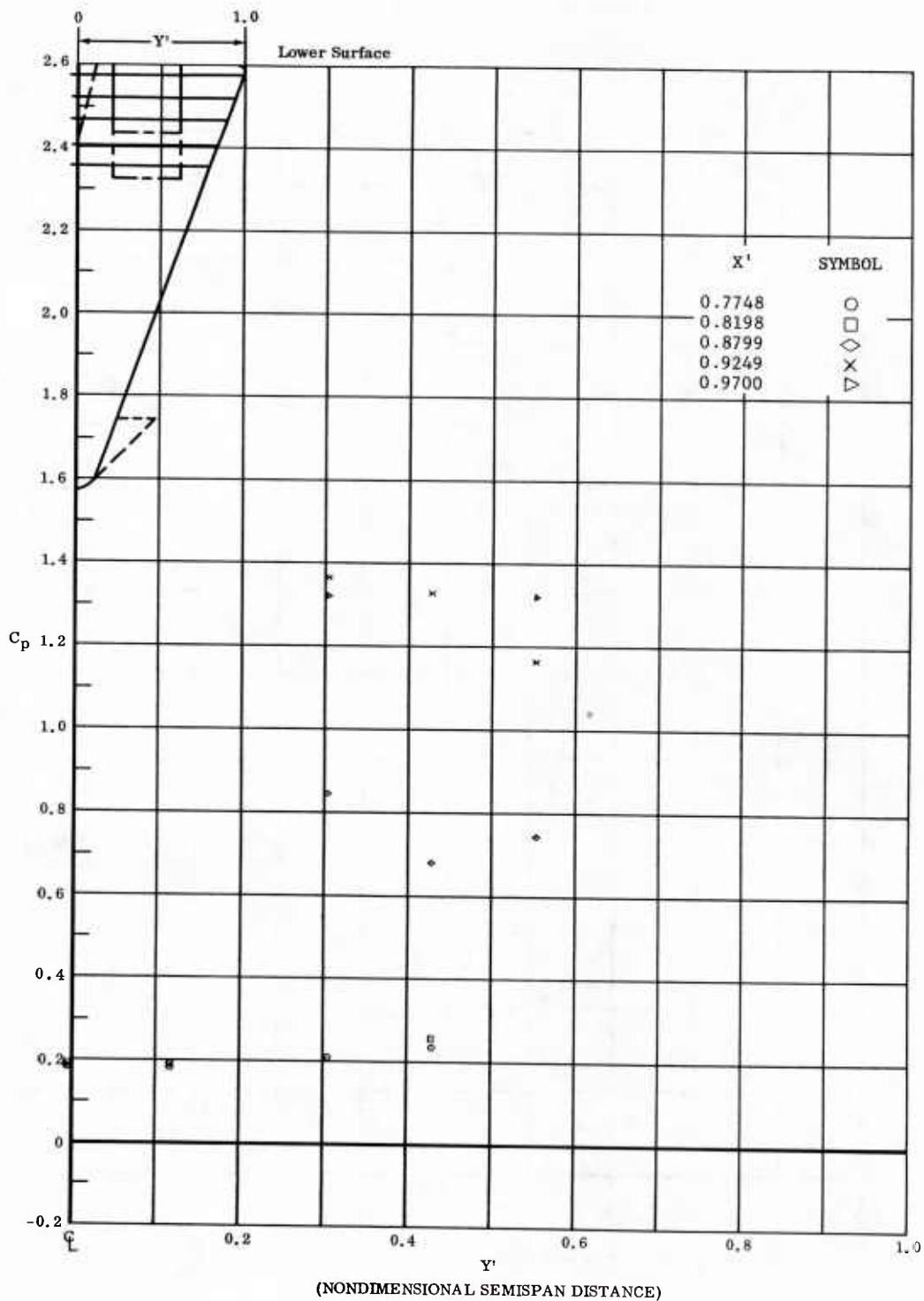


Fig. 83 Spanwise Distributions of Pressure Coefficients; Basic Configuration, Bottom Flaps Deflected  $+20^\circ$ ,  $\alpha = +14.3^\circ$ ,  $\beta = 0^\circ$ ,  $Re_\infty/ft = 1,100,000$ .

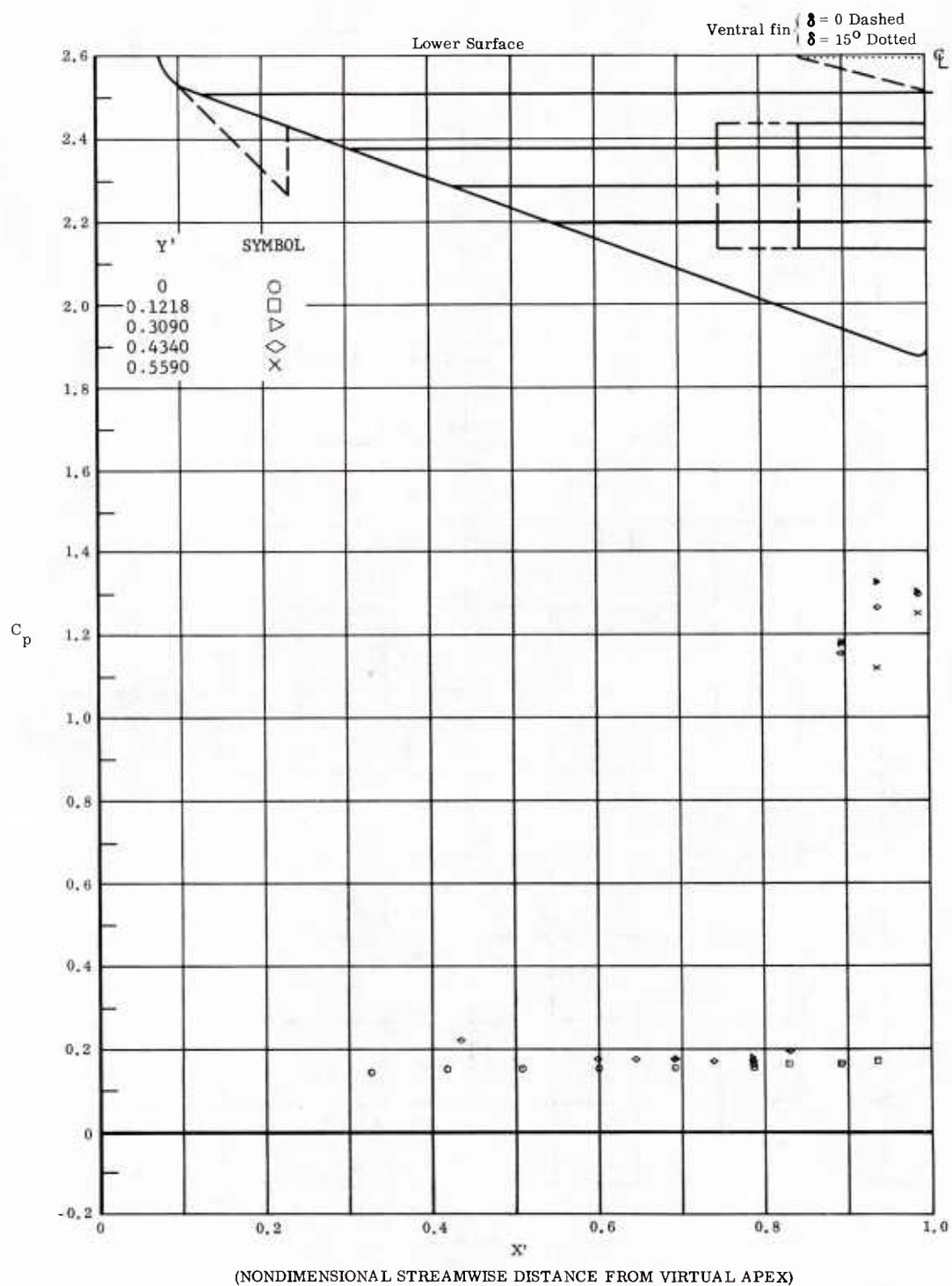


Fig. 34 Streamwise Distributions of Pressure Coefficients; Basic Configuration, Bottom Flaps Deflected  $+20^\circ$ ,  $\alpha = +14.3^\circ$ ,  $\beta = 0^\circ$ ,  $Re_\infty / ft = 3,300,000$ .



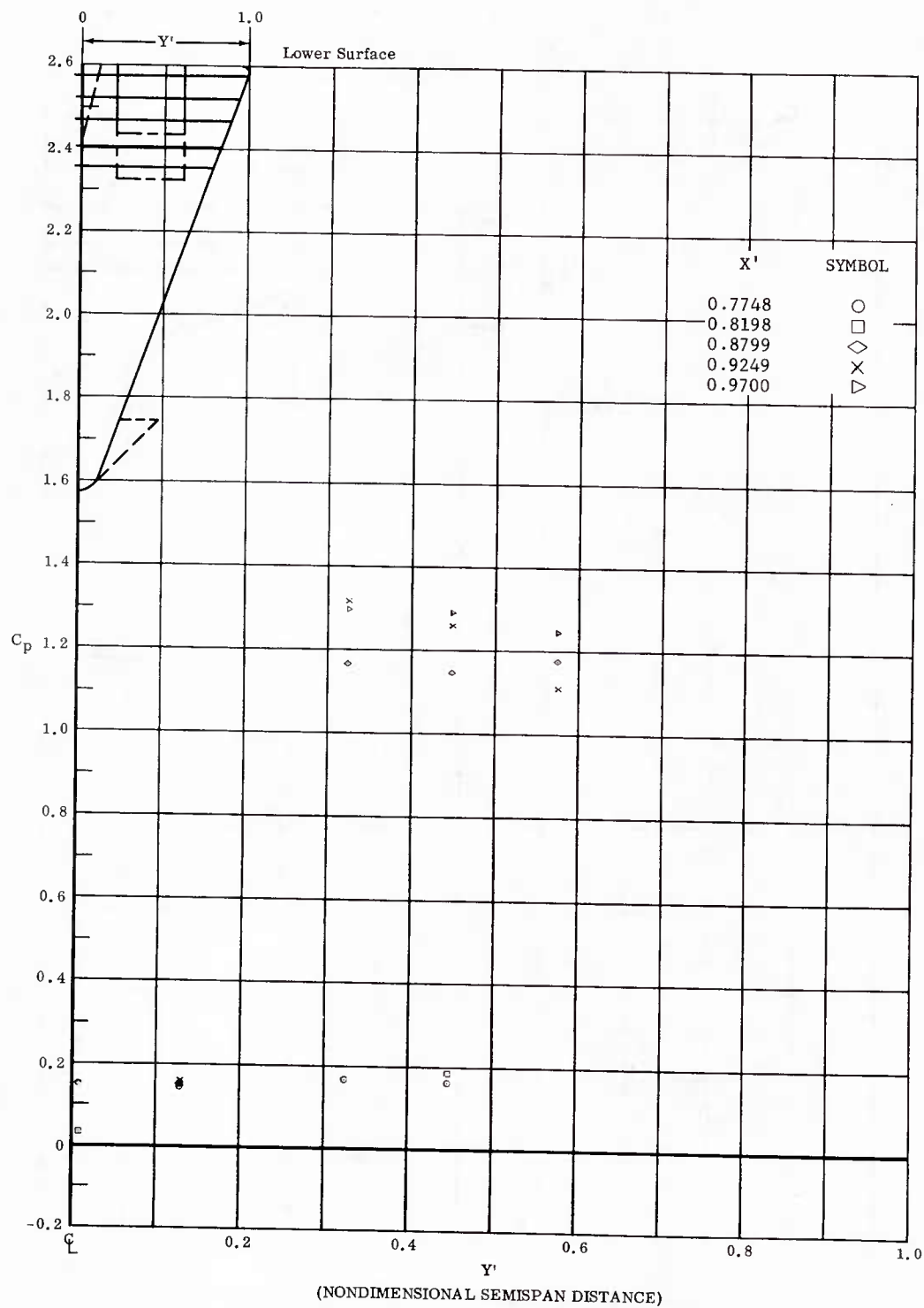


Fig. 84 Spanwise Distributions of Pressure Coefficients; Basic Configuration, Bottom Flaps Deflected  $+20^\circ$ ,  $\alpha = +14.3^\circ$ ,  $\beta = 0^\circ$ ,  $Re_\infty/ft = 3,300,000$ .

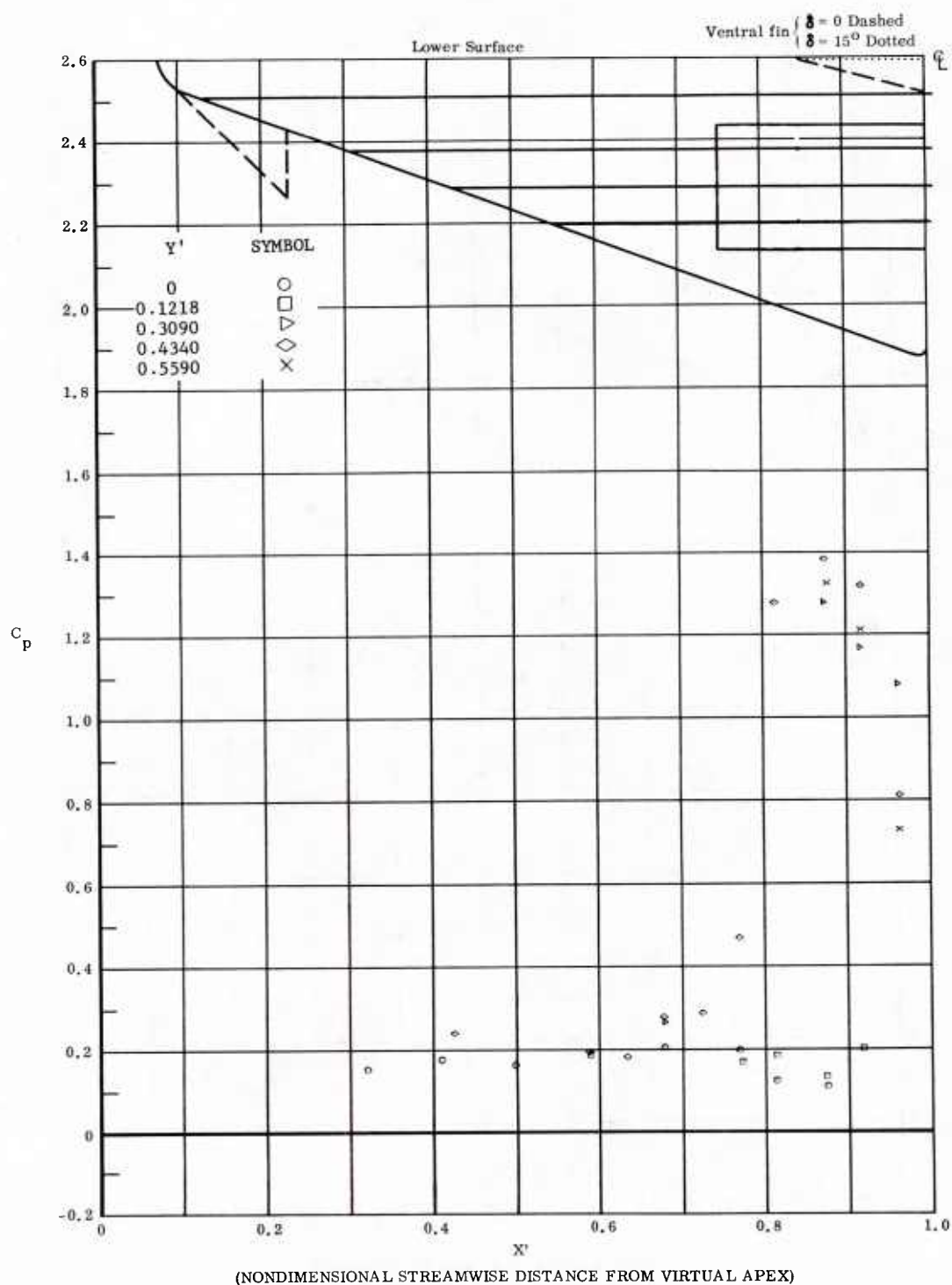


Fig. 85 Streamwise Distributions of Pressure Coefficients; Basic Configuration + Longer Chord Flaps, Bottom Flaps Deflected  $+20^\circ$ ,  $\alpha = +14.3^\circ$ ,  $\beta = 0^\circ$ ,  $Re_\infty/ft = 1,100,000$ .

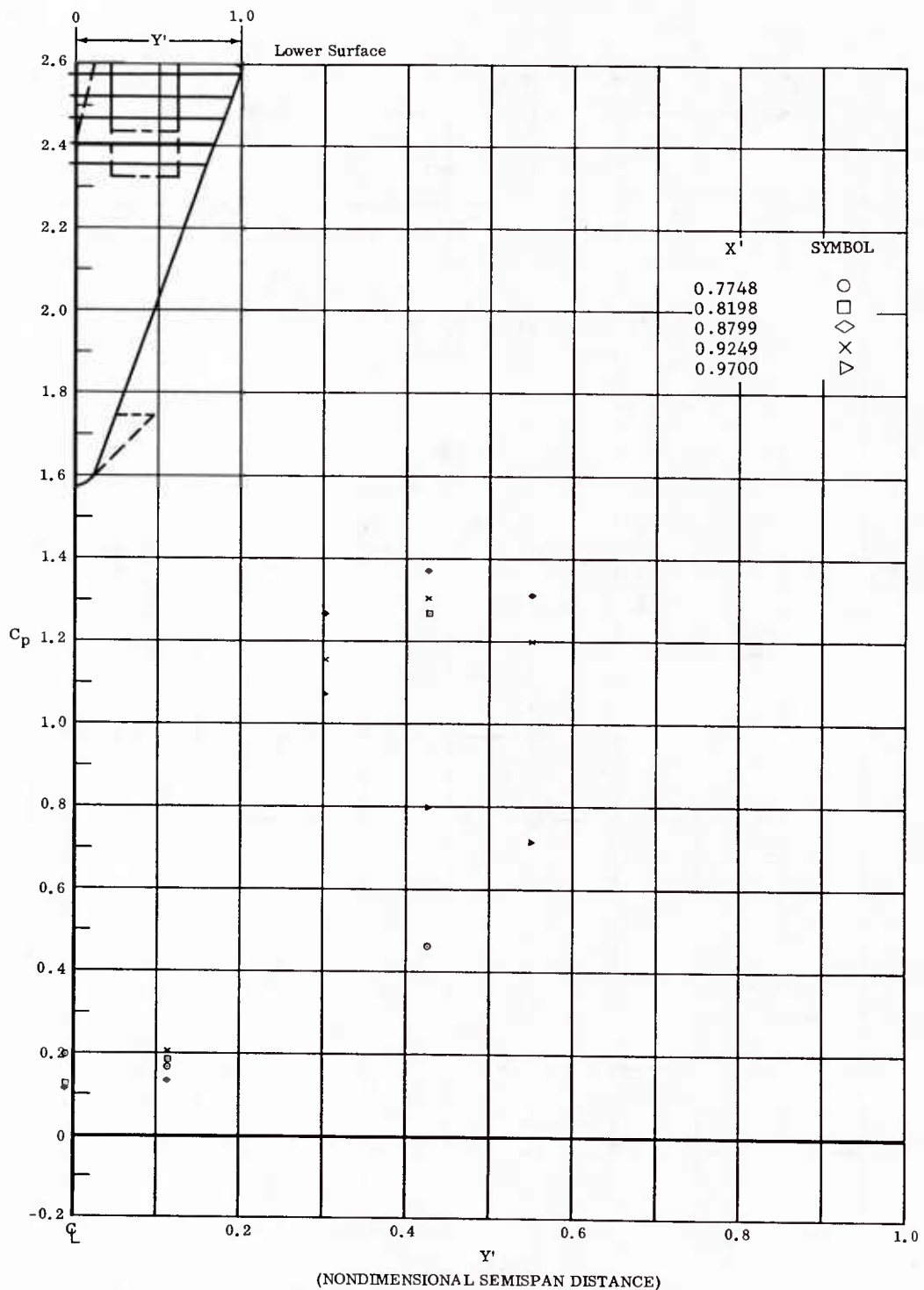


Fig. 85 Spanwise Distributions of Pressure Coefficients; Basic Configuration + Longer Chord Flaps, Bottom Flaps Deflected  $+20^\circ$ ,  $\alpha = +14.3^\circ$ ,  $\beta = 0^\circ$ ,  $Re_\infty / ft = 1,100,000$ .

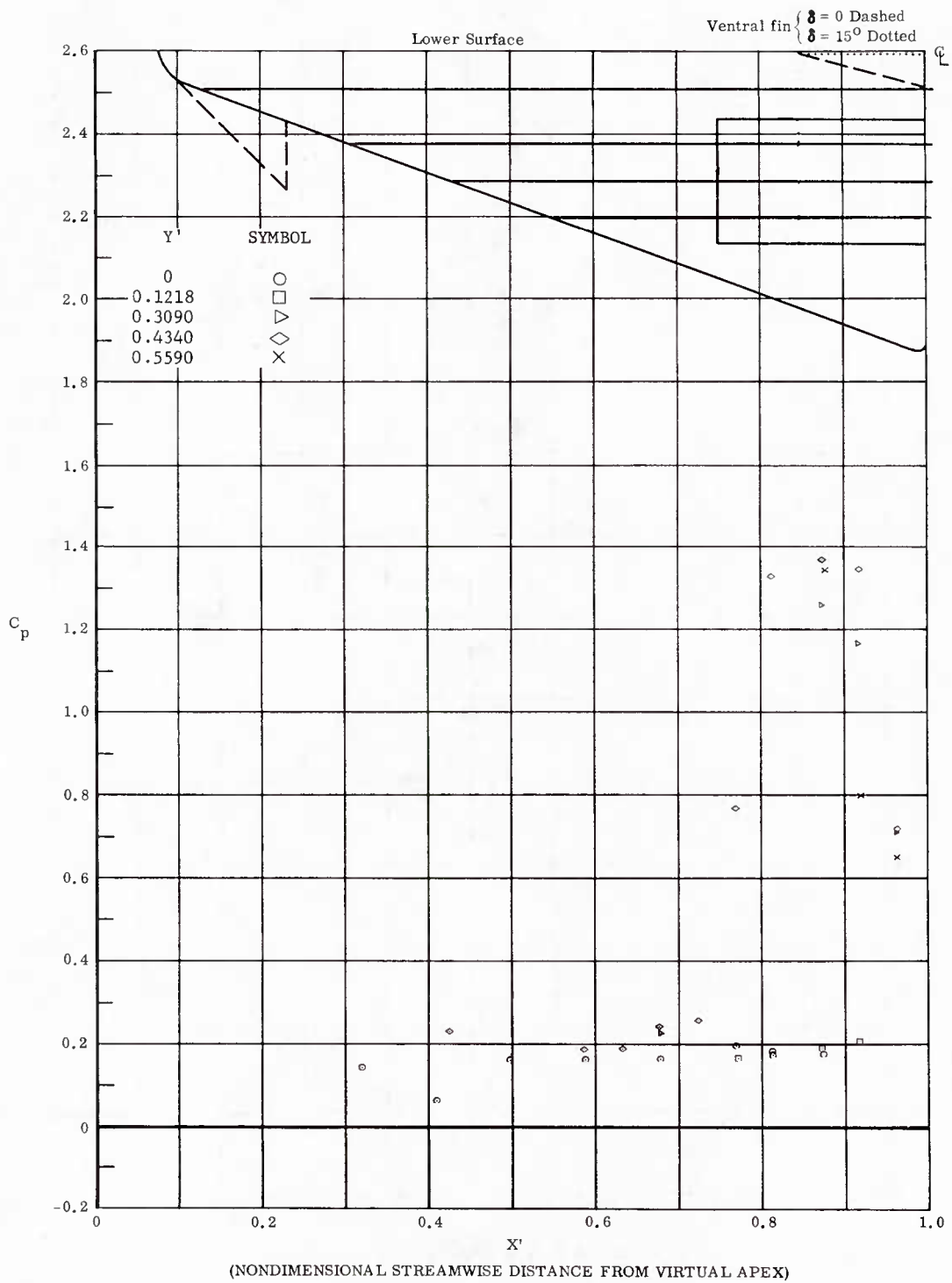


Fig. 86 Streamwise Distributions of Pressure Coefficients; Basic Configuration + Longer Chord Flaps, Bottom Flaps Deflected  $+20^\circ$ ,  $\alpha = +14.3^\circ$ ,  $\beta = 0^\circ$ ,  $Re_\infty / ft = 3,300,000$ .

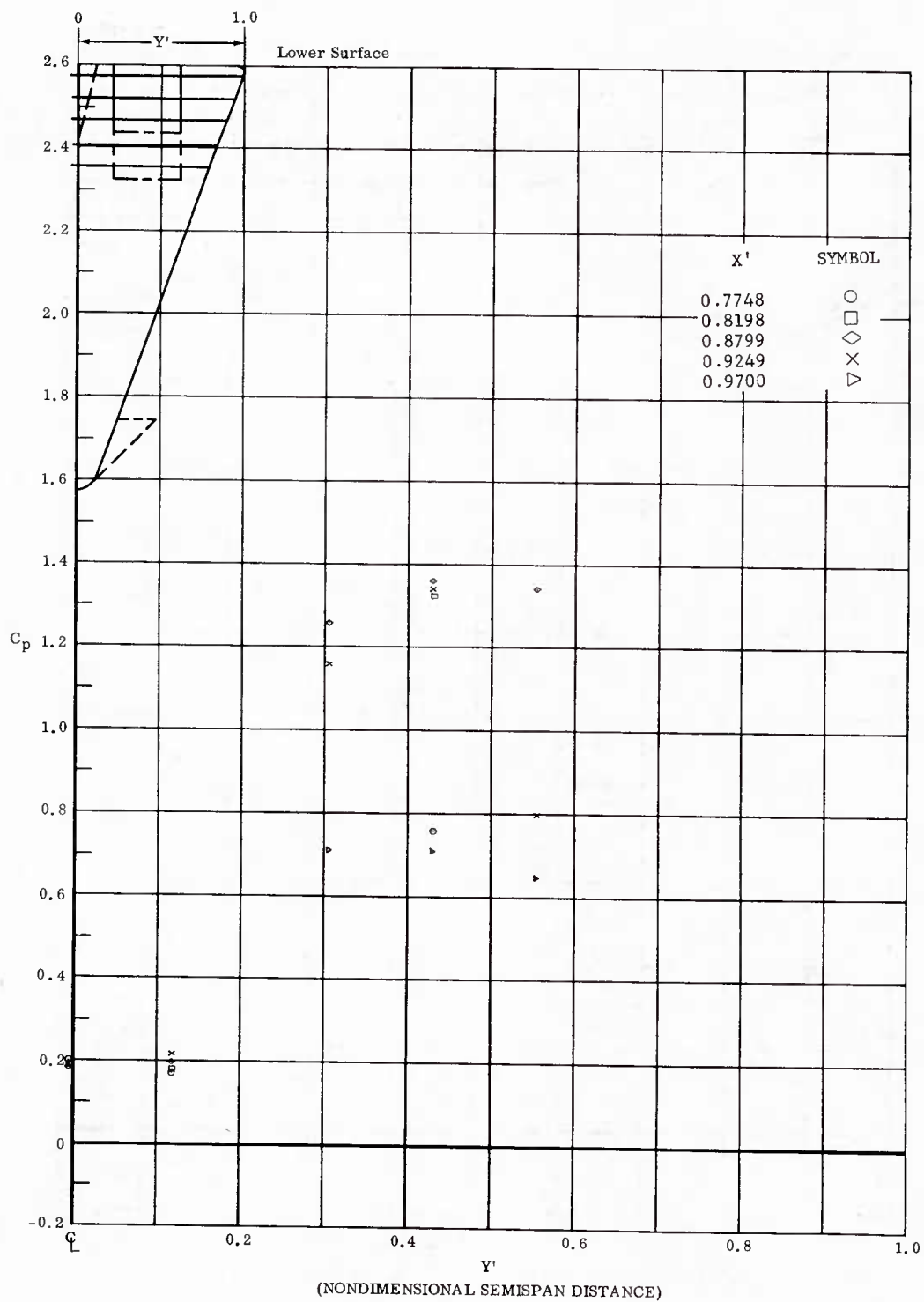


Fig. 86 Spanwise Distributions of Pressure Coefficients; Basic Configuration + Longer Chord Flaps, Bottom Flaps Deflected  $+20^\circ$ ,  $\alpha = +14.3^\circ$ ,  $\beta = 0^\circ$ ,  $Re_\infty / ft = 3,300,000$ .

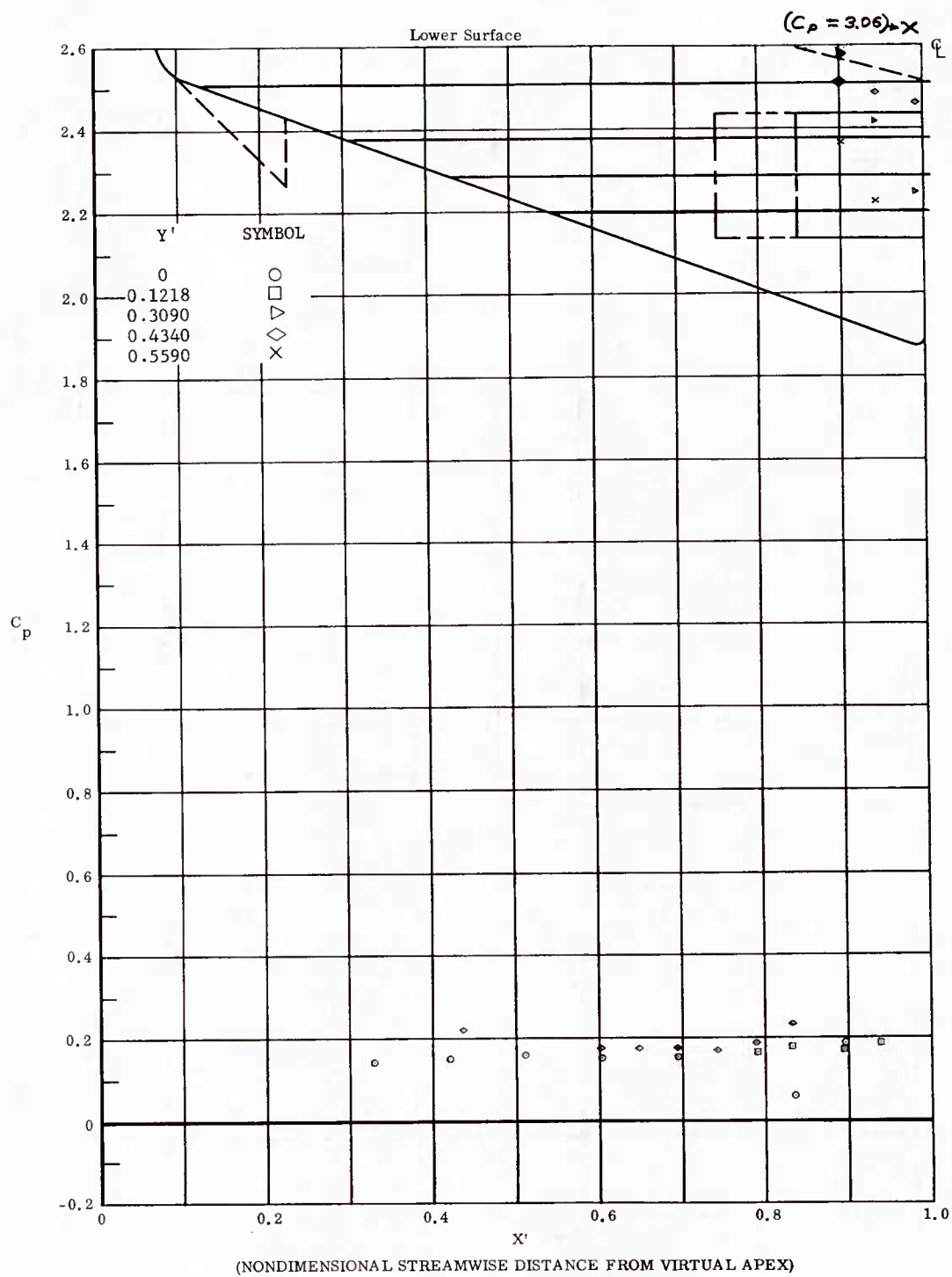


Fig. 87 Streamwise Distributions of Pressure Coefficients; Basic Configuration, Bottom Flaps Deflected  $+30^\circ$ ,  $\alpha = +14.3^\circ$ ,  $\beta = 0^\circ$ ,  $Re_\infty/ft = 3,300,000$ .

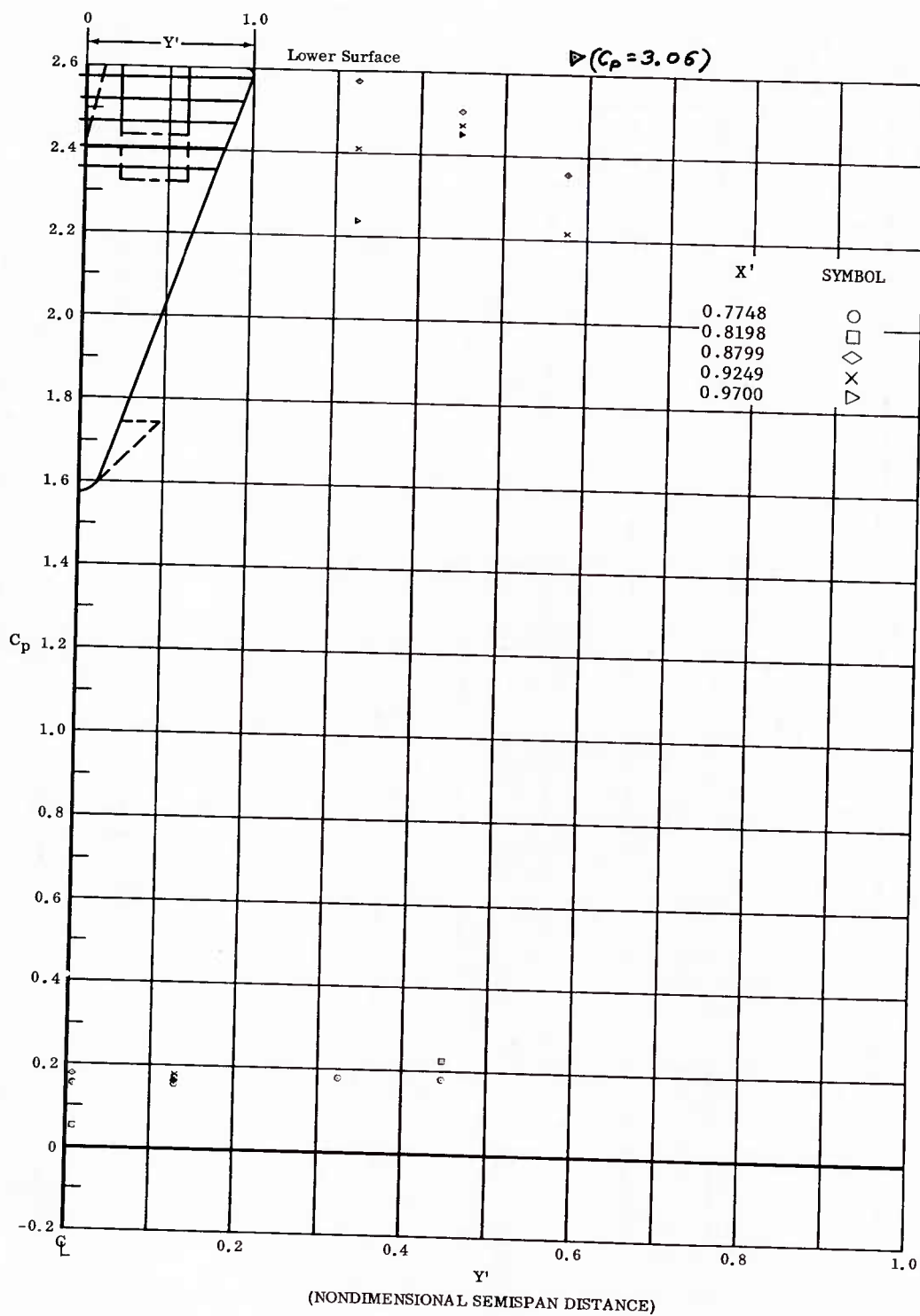


Fig. 87 Spanwise Distributions of Pressure Coefficients; Basic Configuration, Bottom Flaps Deflected  $+30^\circ$ ,  $\alpha = +14.3^\circ$ ,  $\beta = 0^\circ$ ,  $Re_\infty/ft = 3,300,000$ .

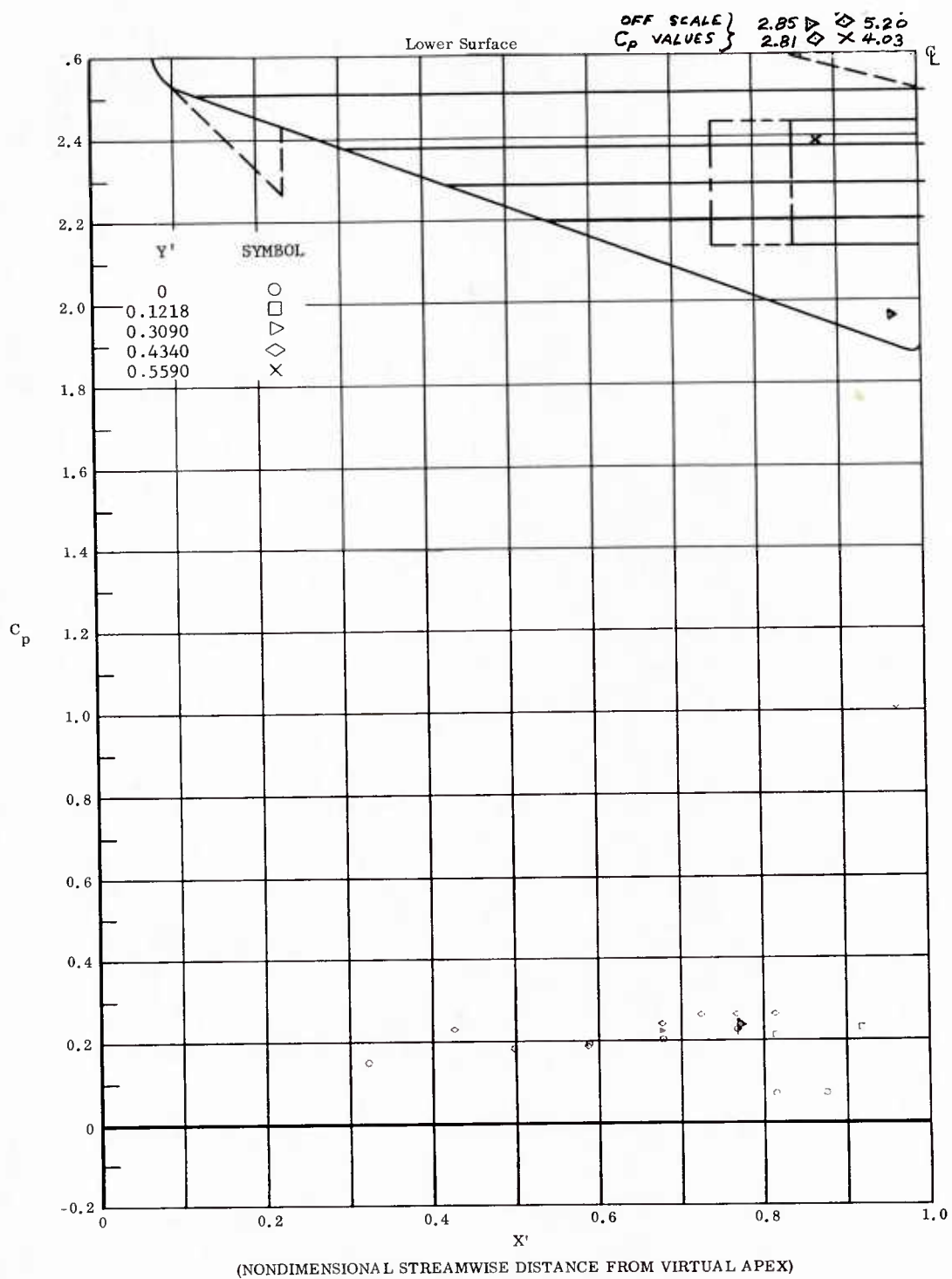


Fig. 38 Streamwise Distributions of Pressure Coefficients; Basic Configuration, Bottom Flaps Deflected +40°,  $\alpha = +14.3^\circ$ ,  $\beta = 0^\circ$ ,  $Re_\infty / ft = 1,100,000$ .



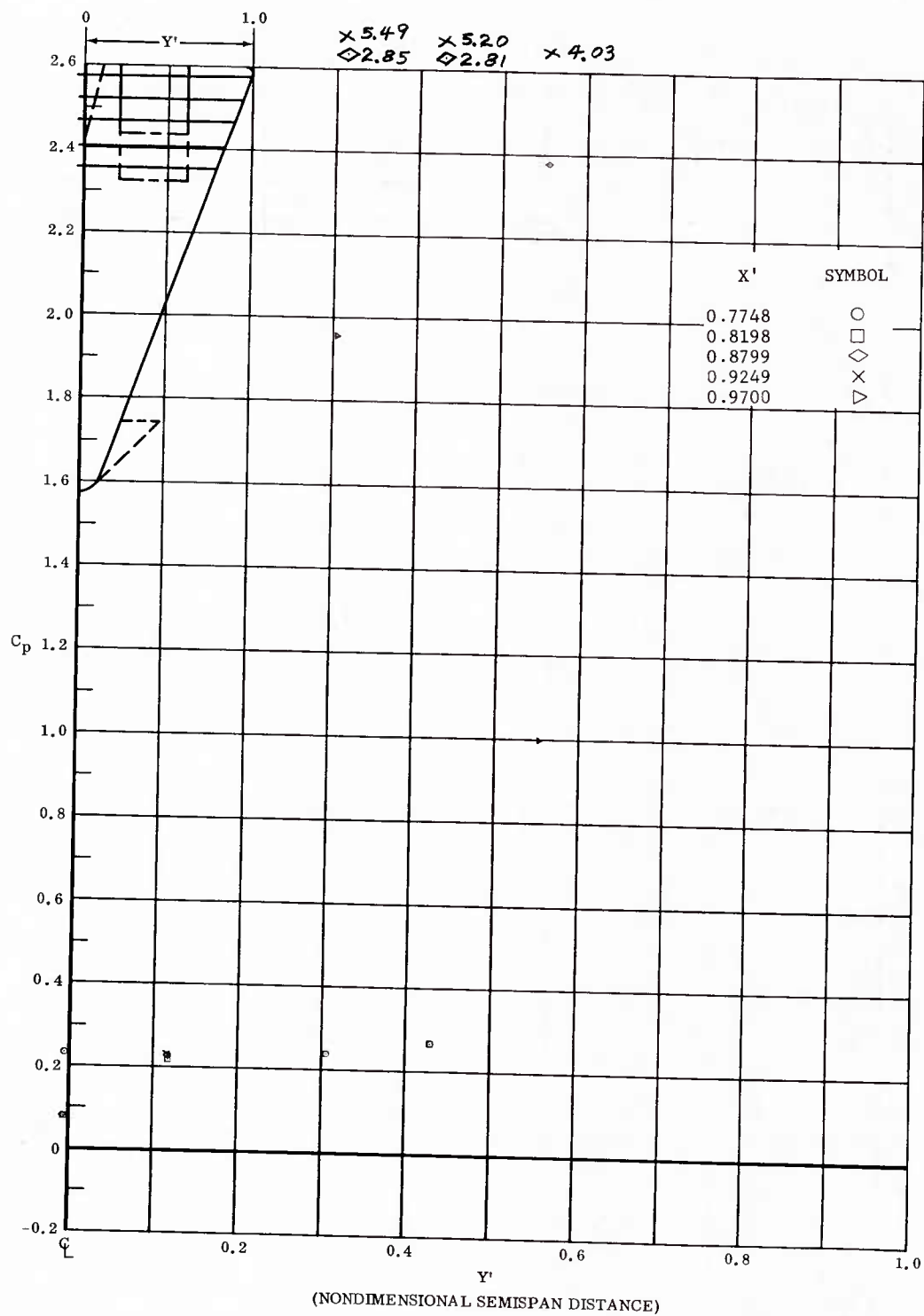


Fig. 88 Spanwise Distributions of Pressure Coefficients; Basic Configuration, Bottom Flaps Deflected  $+40^\circ$ ,  $\alpha = +14.3^\circ$ ,  $\beta = 0^\circ$ ,  $Re_\infty / ft = 1,100,000$ .

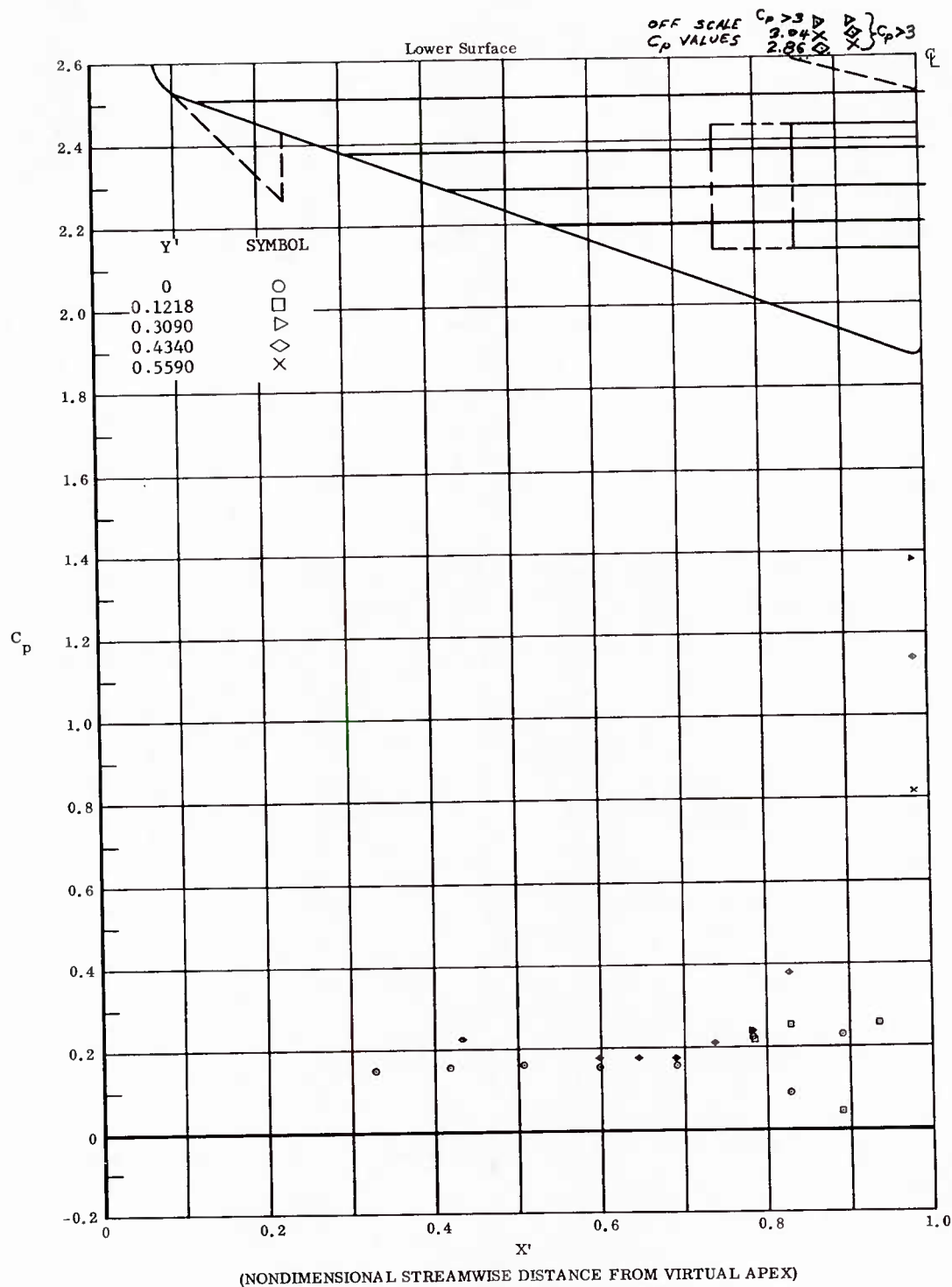


Fig. 89 Streamwise Distributions of Pressure Coefficients; Basic Configuration, Bottom Flaps Deflected  $+40^\circ$ ,  $\alpha = +14.3^\circ$ ,  $\beta = 0^\circ$ ,  $Re_\infty / ft = 3,300,000$ .

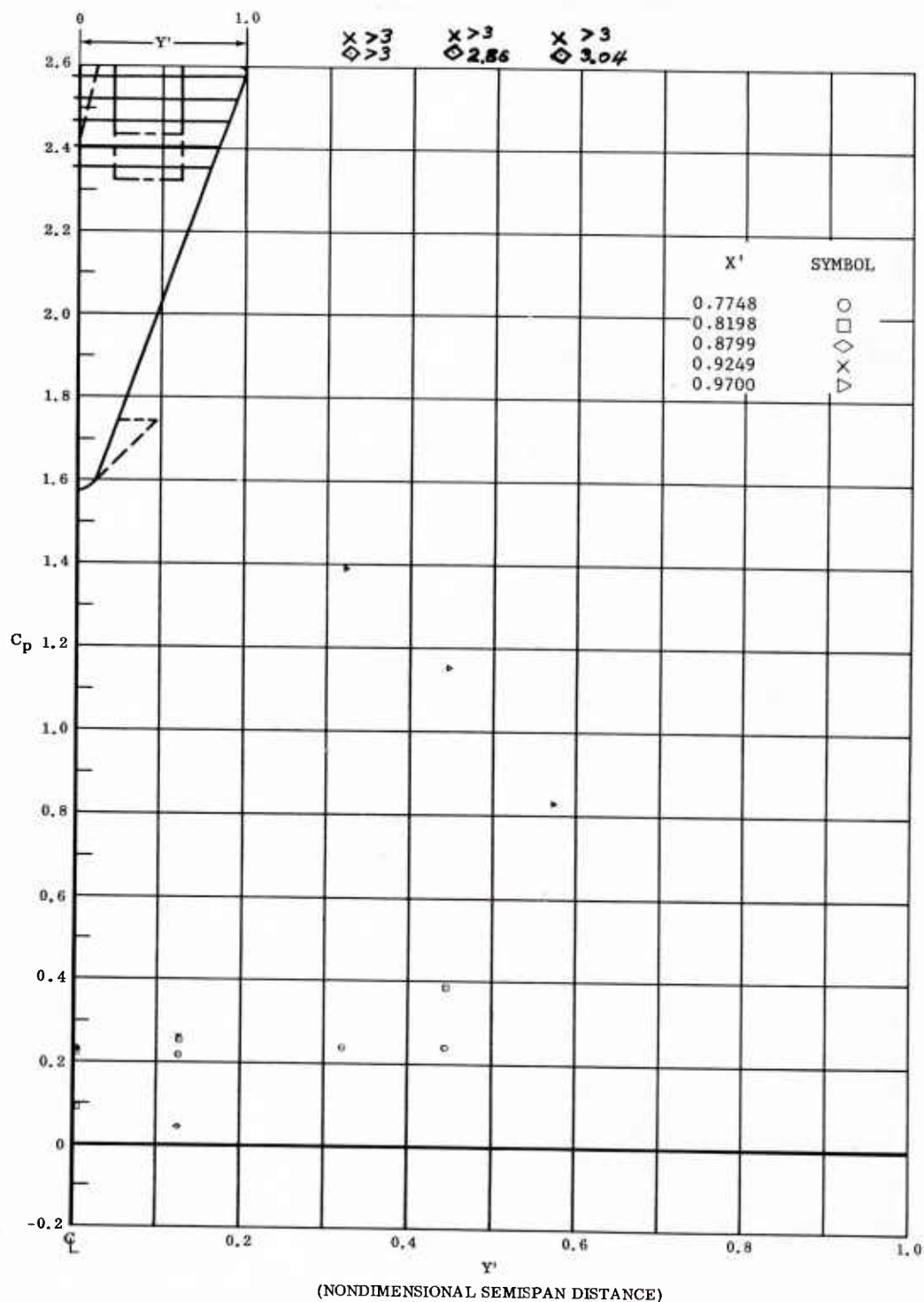


Fig. 39 Spanwise Distributions of Pressure Coefficients; Basic Configuration, Bottom Flaps Deflected  $+40^\circ$ ,  $\alpha = +14.3^\circ$ ,  $\beta = 0^\circ$ ,  $Re_\infty/ft = 3,300,000$ .

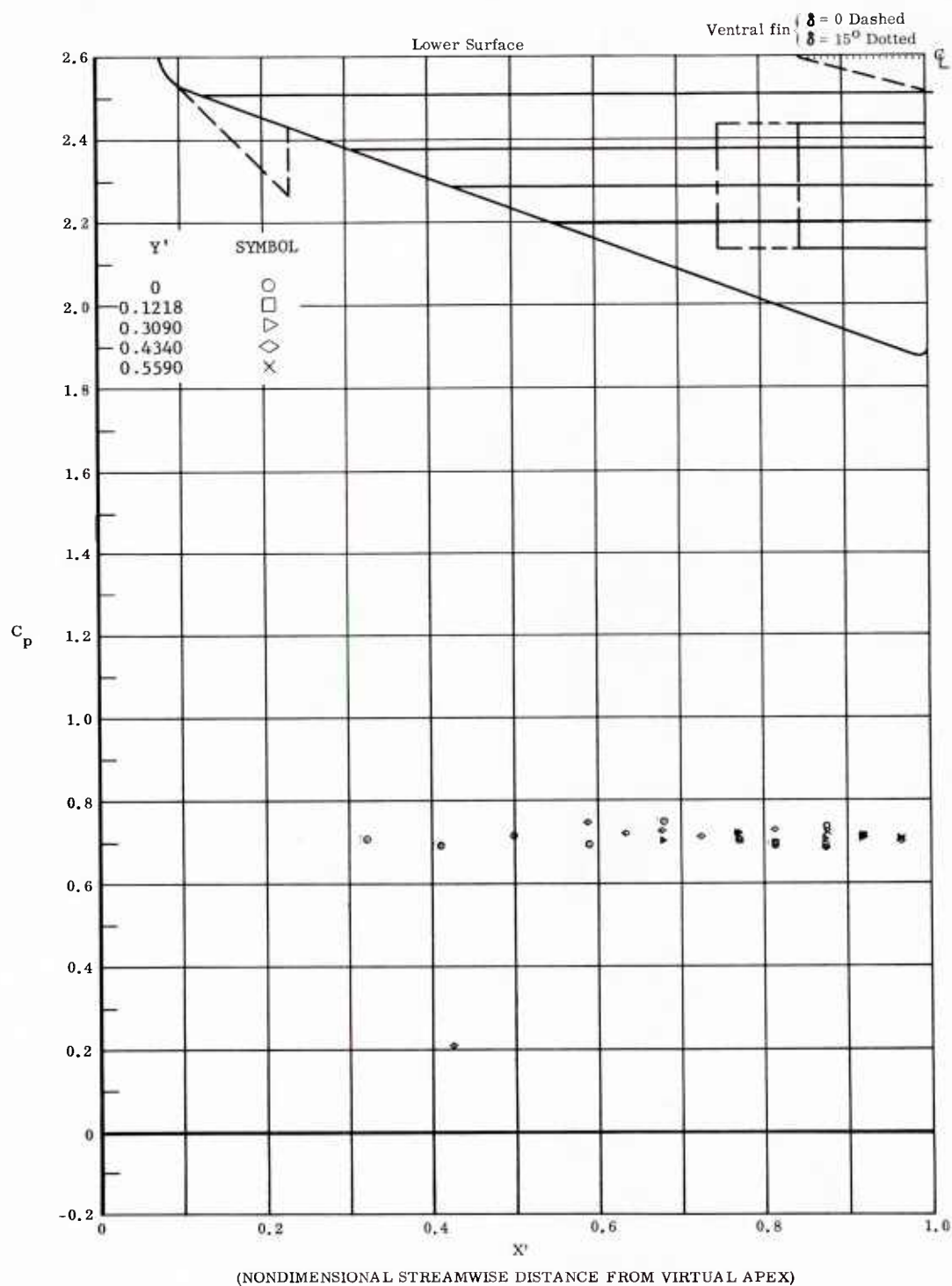


Fig. 90 Streamwise Distributions of Pressure Coefficients; Basic Configuration, Left and Right (Upper) Flaps Deflected  $-40^\circ$ ,  $\alpha = +33^\circ$ ,  $\beta = 0^\circ$ ,  $Re_{\infty}/ft = 3,300,000$ .

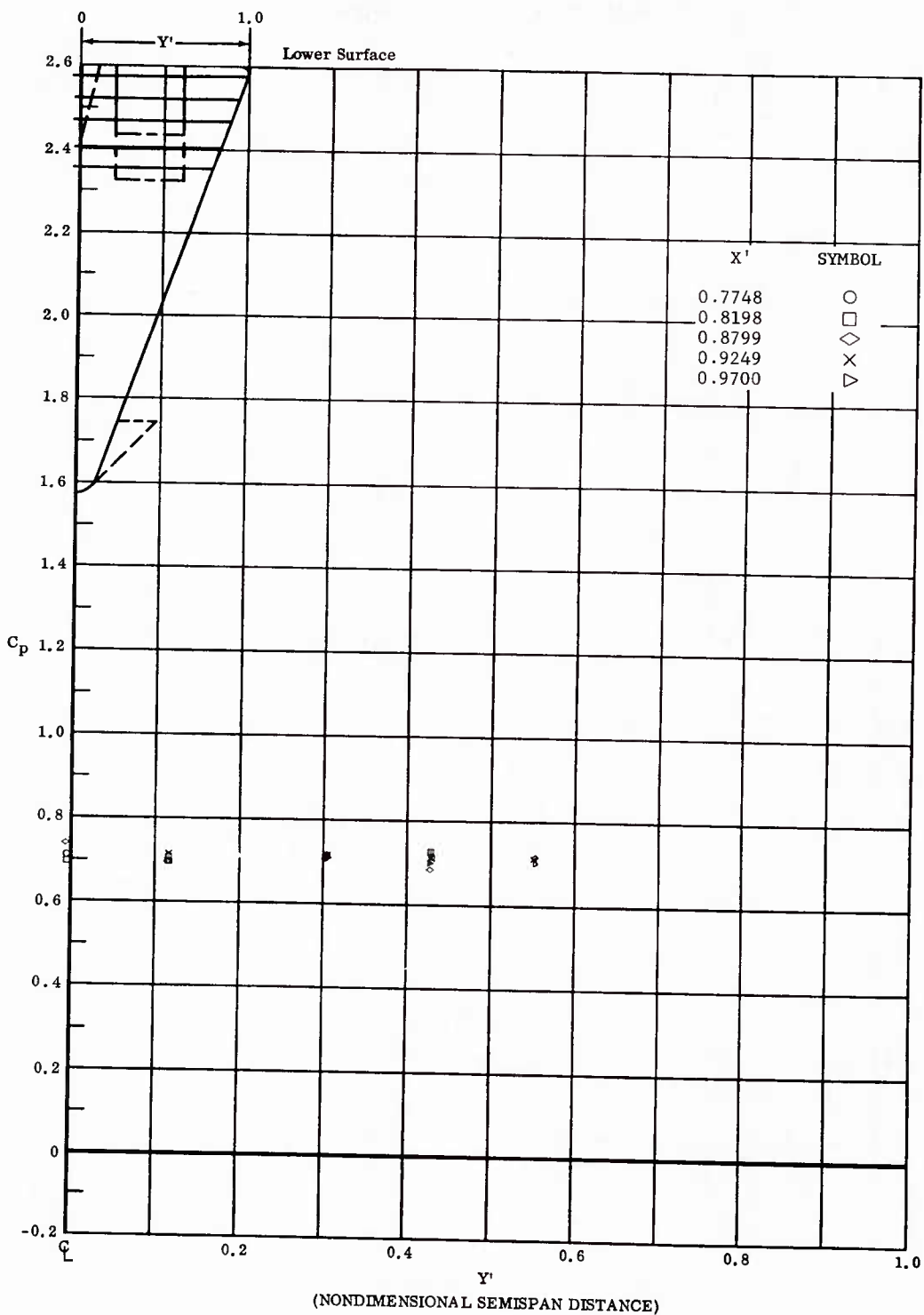


Fig. 90 Spanwise Distributions of Pressure Coefficients; Basic Configuration, Left and Right (Upper) Flaps Deflected  $-40^\circ$ ,  $\alpha = +33^\circ$ ,  $\beta = 0^\circ$ ,  $Re_\infty/ft = 3,300,000$ .

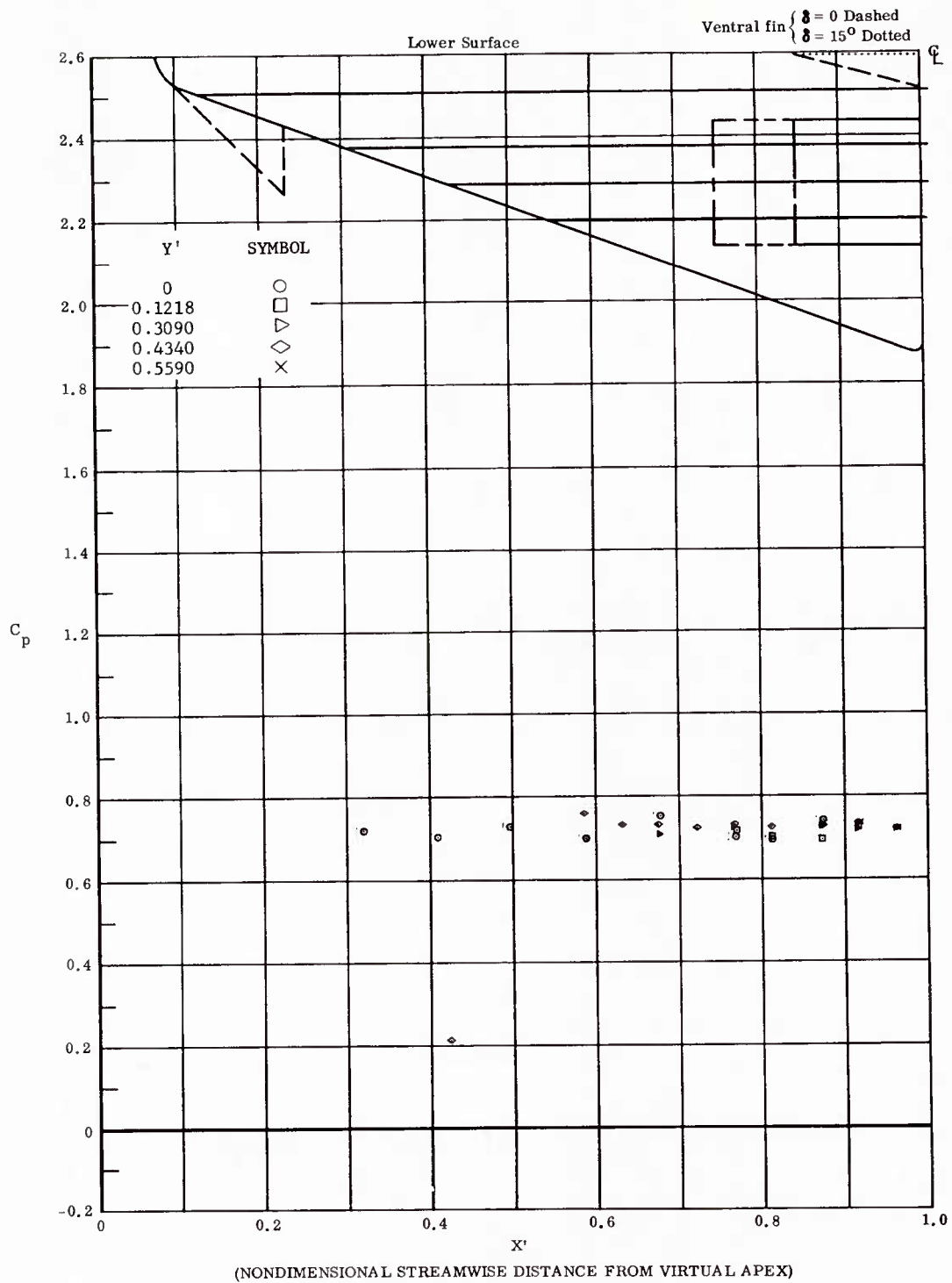


Fig. 91 Streamwise Distributions of Pressure Coefficients; Basic Configuration, No Flap Deflections,  $\alpha = +33^\circ$ ,  $\beta = 0^\circ$ ,  $Re_\infty/ft = 3,300,000$ .

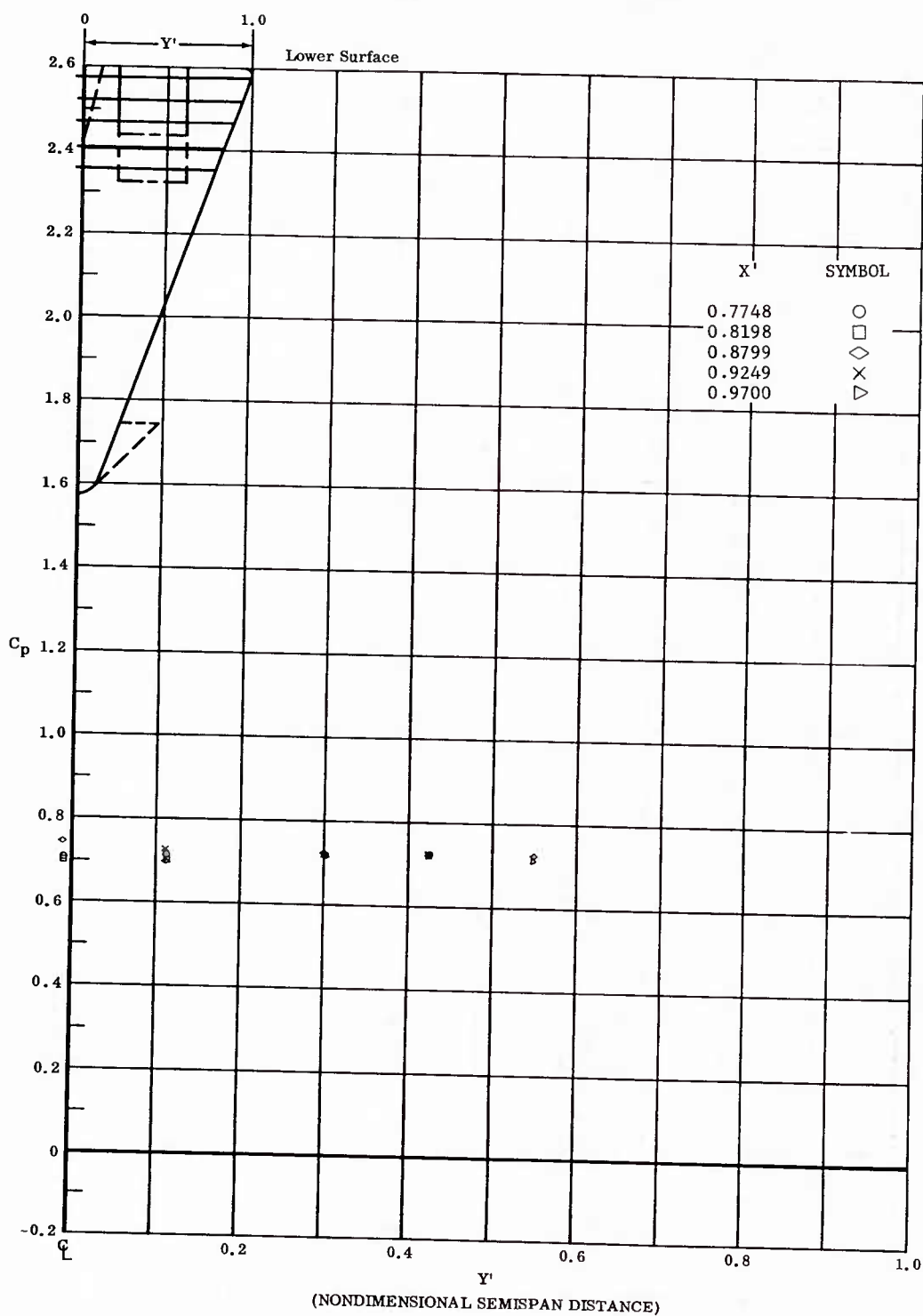


Fig. 91 Spanwise Distributions of Pressure Coefficients; Basic Configuration, No Flap Deflections,  $\alpha = +33^\circ$ ,  $\beta = 0^\circ$ ,  $Re_\infty/ft = 3,300,000$ .

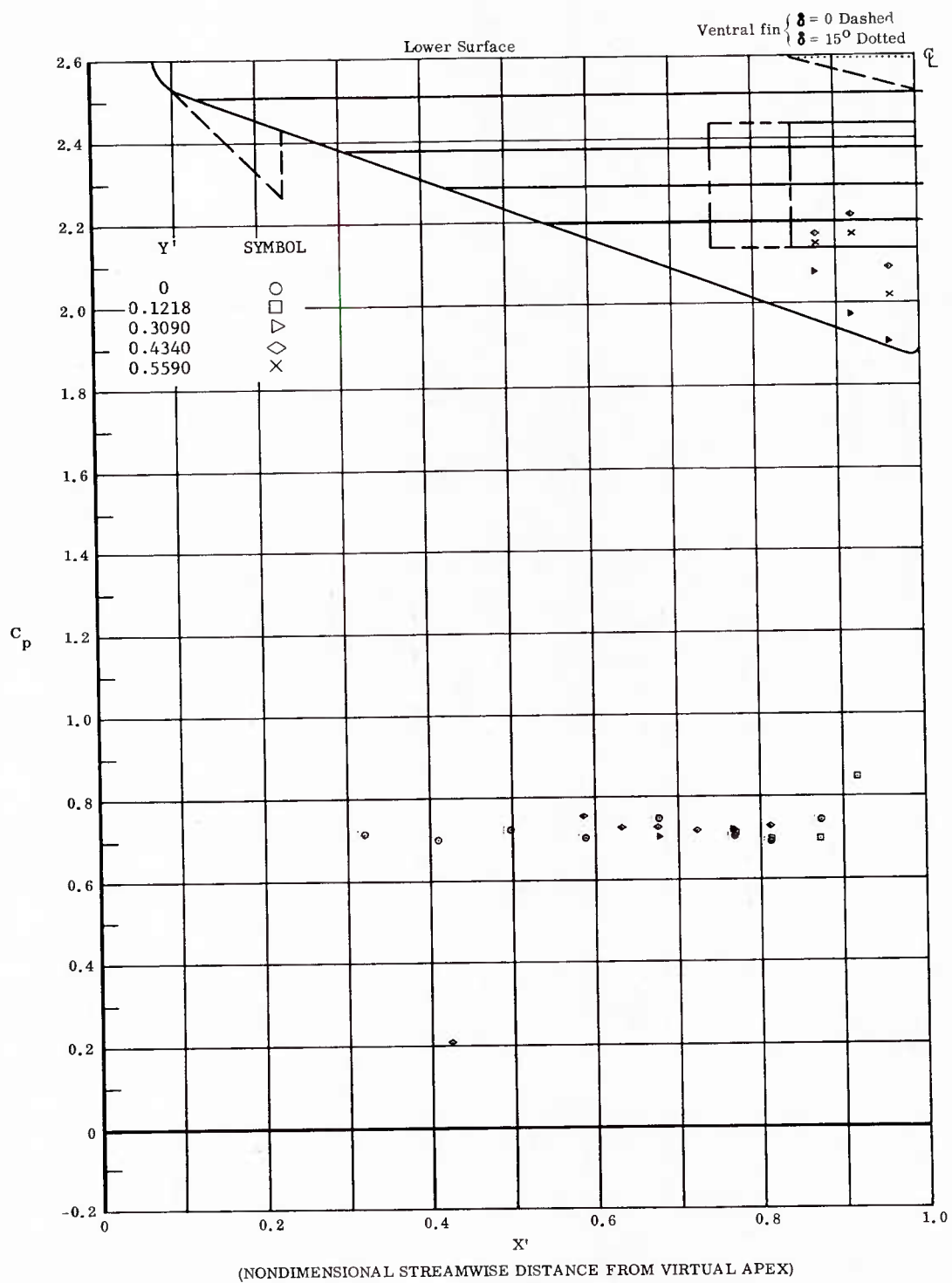


Fig. 92 Streamwise Distributions of Pressure Coefficients; Basic Configuration, Bottom Flaps Deflected  $+20^\circ$ ,  $\alpha = +33^\circ$ ,  $\beta = 0^\circ$ ,  $Re_\infty/ft = 3,300,000$ .



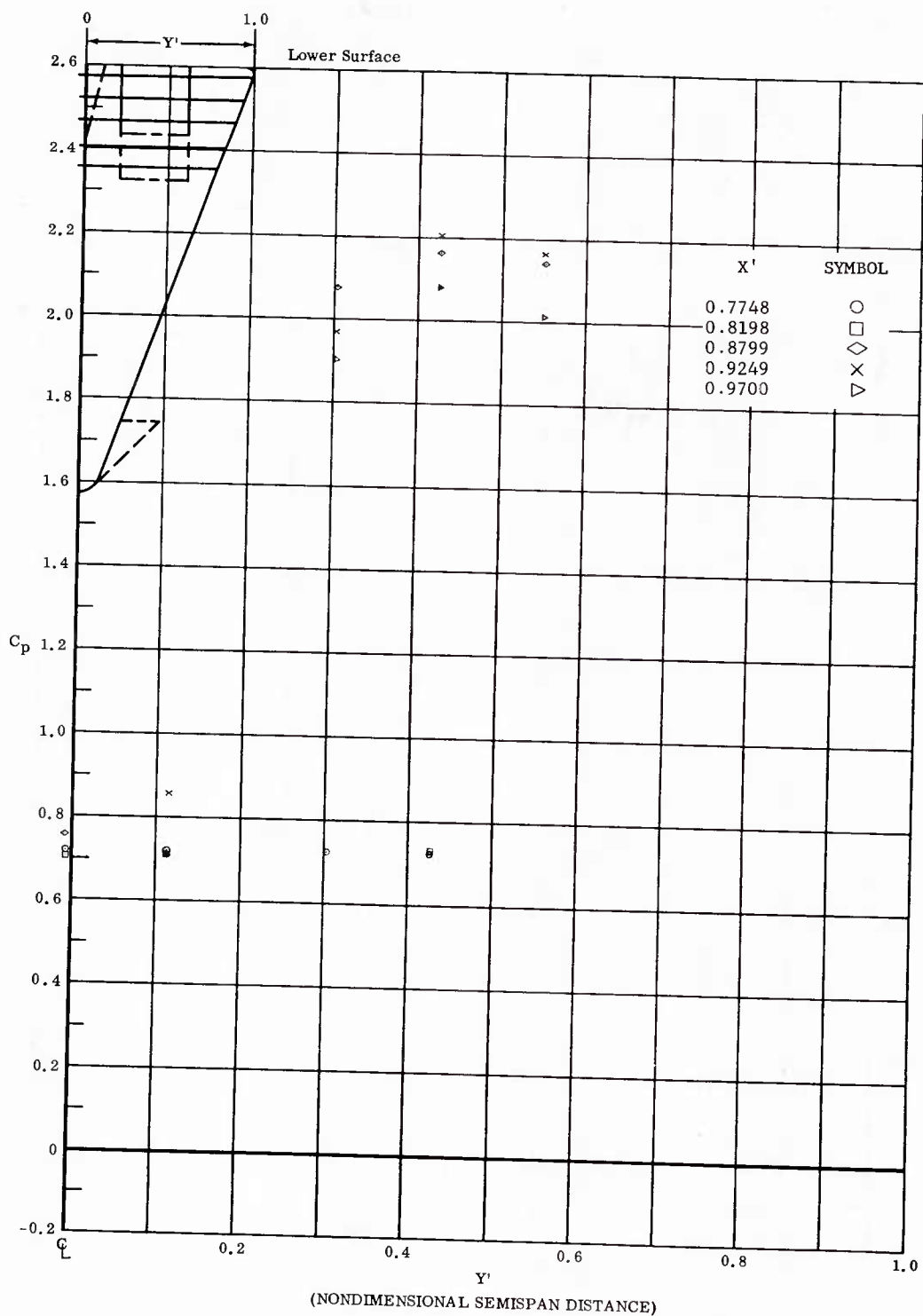


Fig. 92 Spanwise Distributions of Pressure Coefficients; Basic Configuration  
Bottom Flaps Deflected  $+20^\circ$ ,  $\alpha = +33^\circ$ ,  $\beta = 0^\circ$ ,  $Re_\infty/ft = 3,300,000$ .

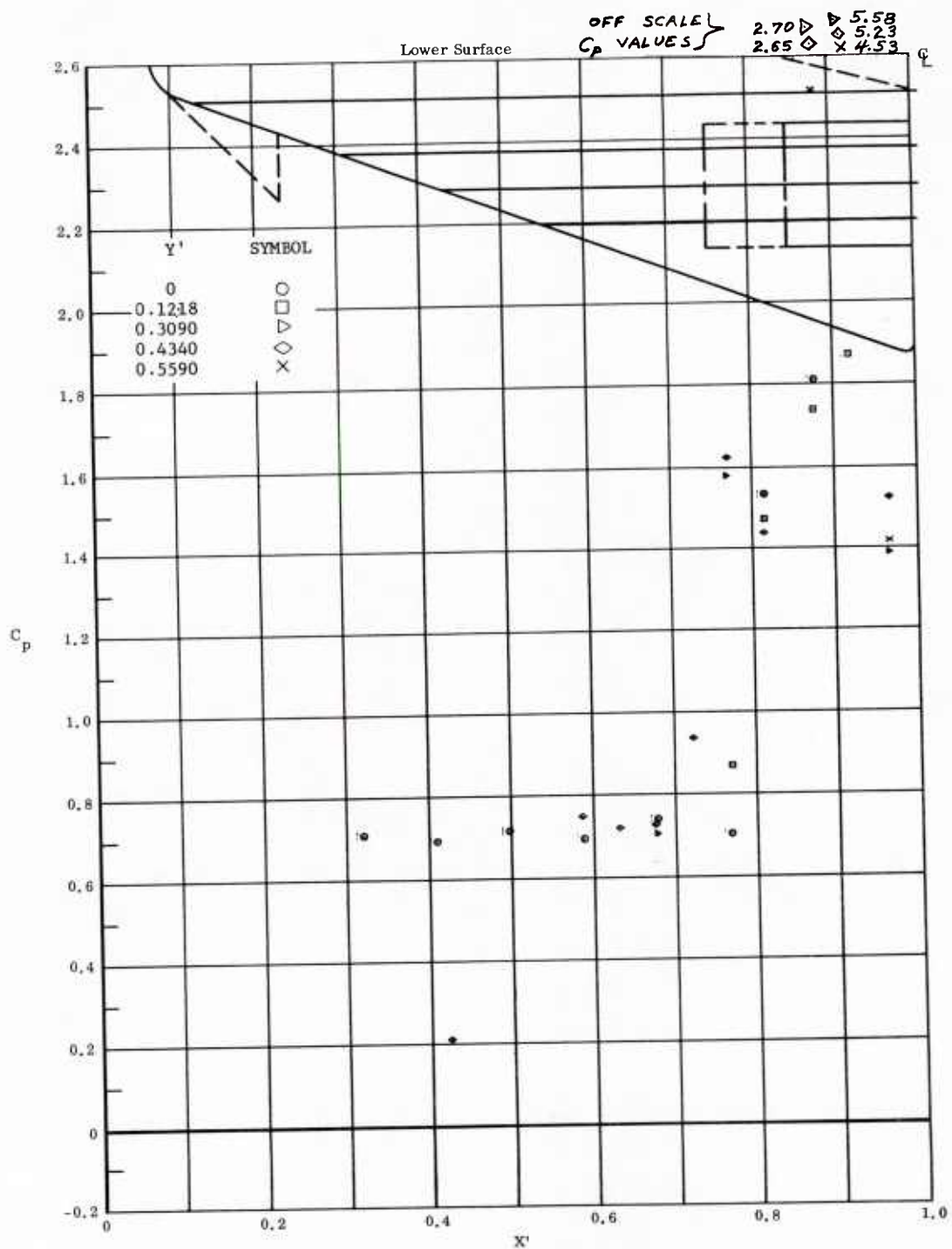


Fig. 93 Streamwise Distributions of Pressure Coefficients; Basic Configuration, Bottom Flaps Deflected +40°,  $\alpha = +33^\circ$ ,  $\beta = 0^\circ$ ,  $Re_\infty/ft = 3,300,000$ .

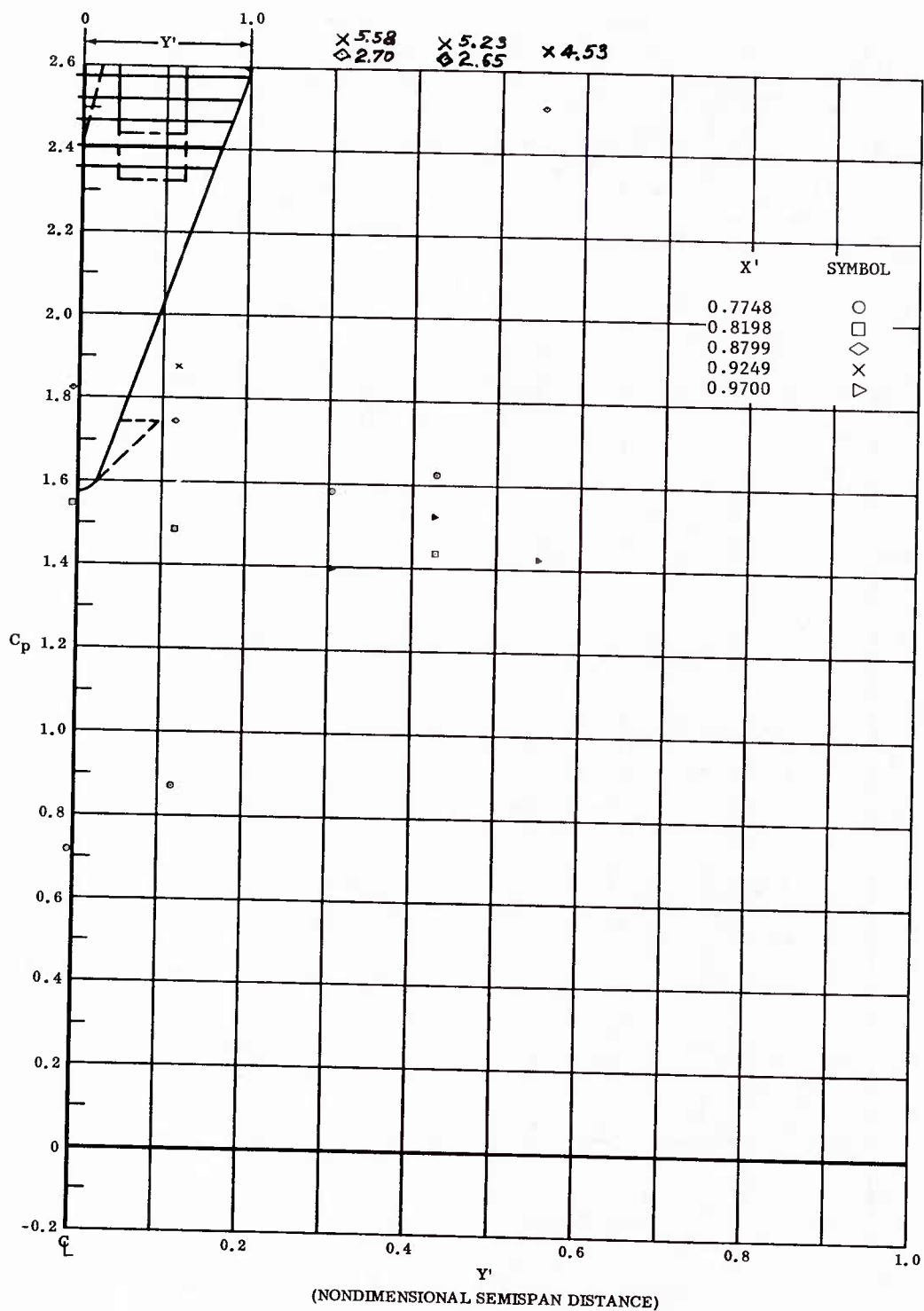


Fig. 93 Spanwise Distributions of Pressure Coefficients; Basic Configuration, Bottom Flaps Deflected +40°,  $\alpha = +33^\circ$ ,  $\beta = 0^\circ$ ,  $Re_\infty/ft = 3,300,000$ .

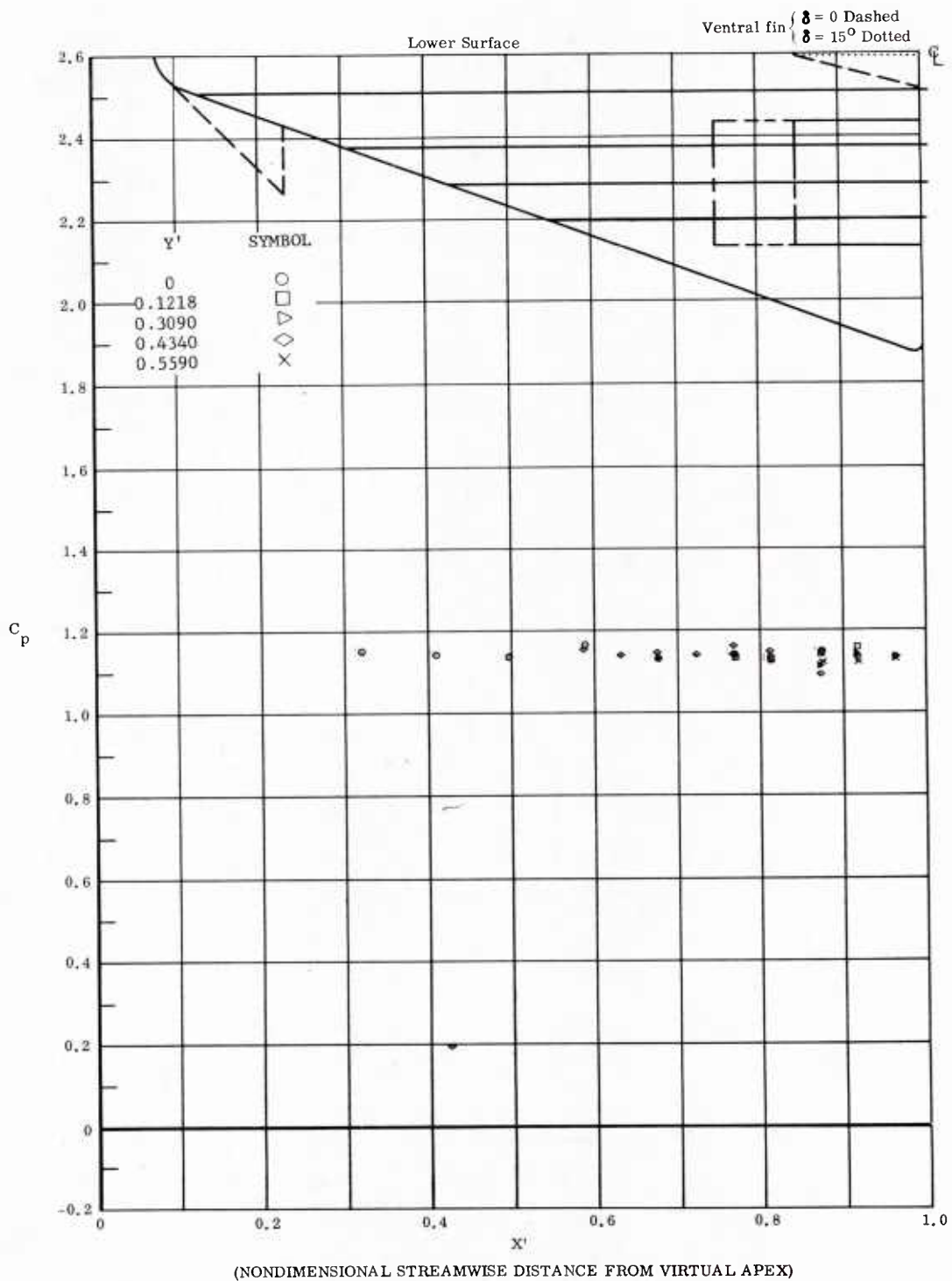


Fig. 94 Streamwise Distributions of Pressure Coefficients; Basic Configuration, Left and Right (Upper) Flaps Deflected  $-40^\circ$ ,  $\alpha = +45^\circ$ ,  $\beta = 0^\circ$ ,  $Re_\infty/ft = 3,300,000$ .

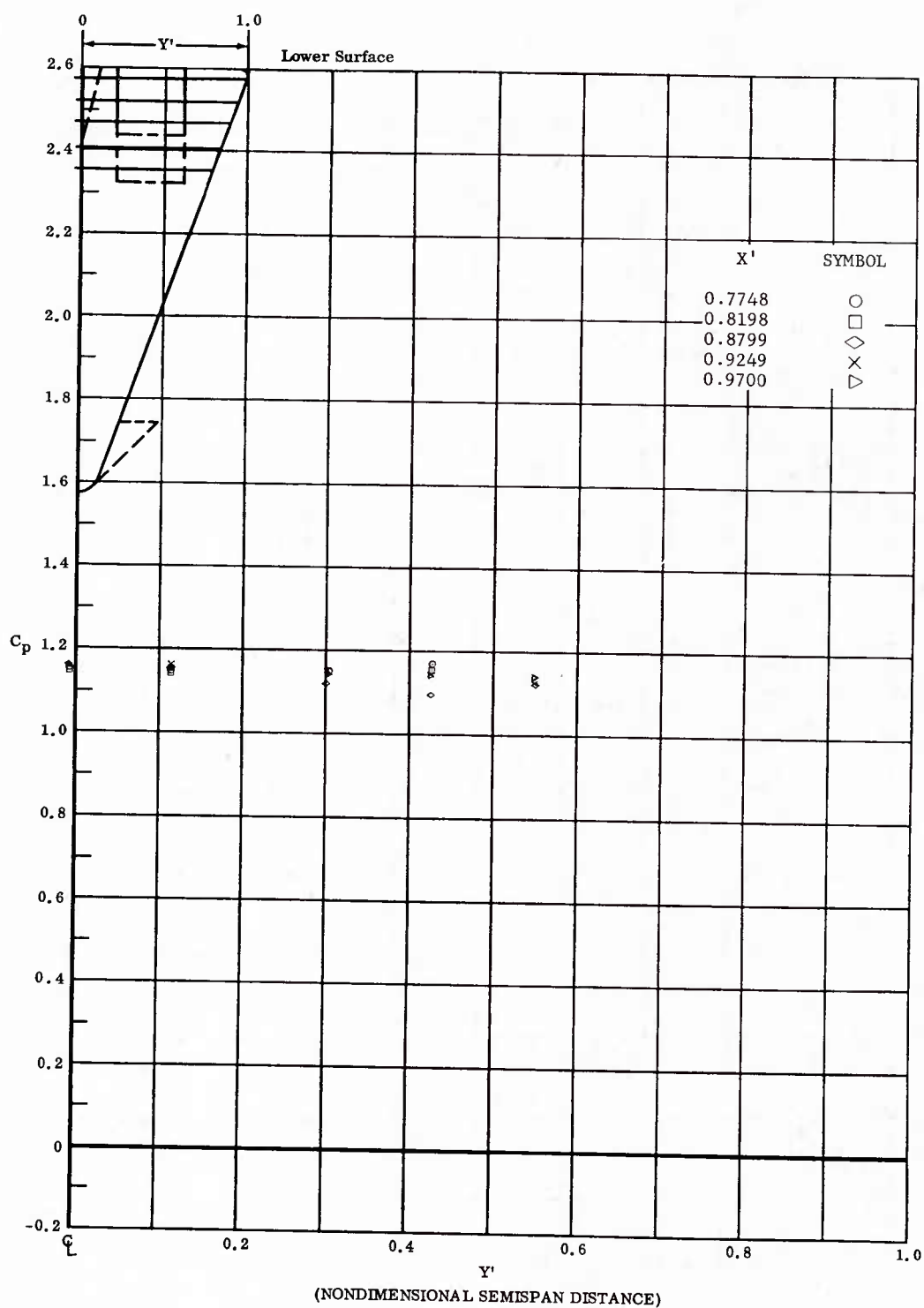


Fig. 94 Spanwise Distributions of Pressure Coefficients; Basic Configuration, Left and Right (Upper) Flaps Deflected  $-40^\circ$ ,  $\alpha = +45^\circ$ ,  $\beta = 0^\circ$ ,  $Re_\infty/ft = 3,300,000$ .

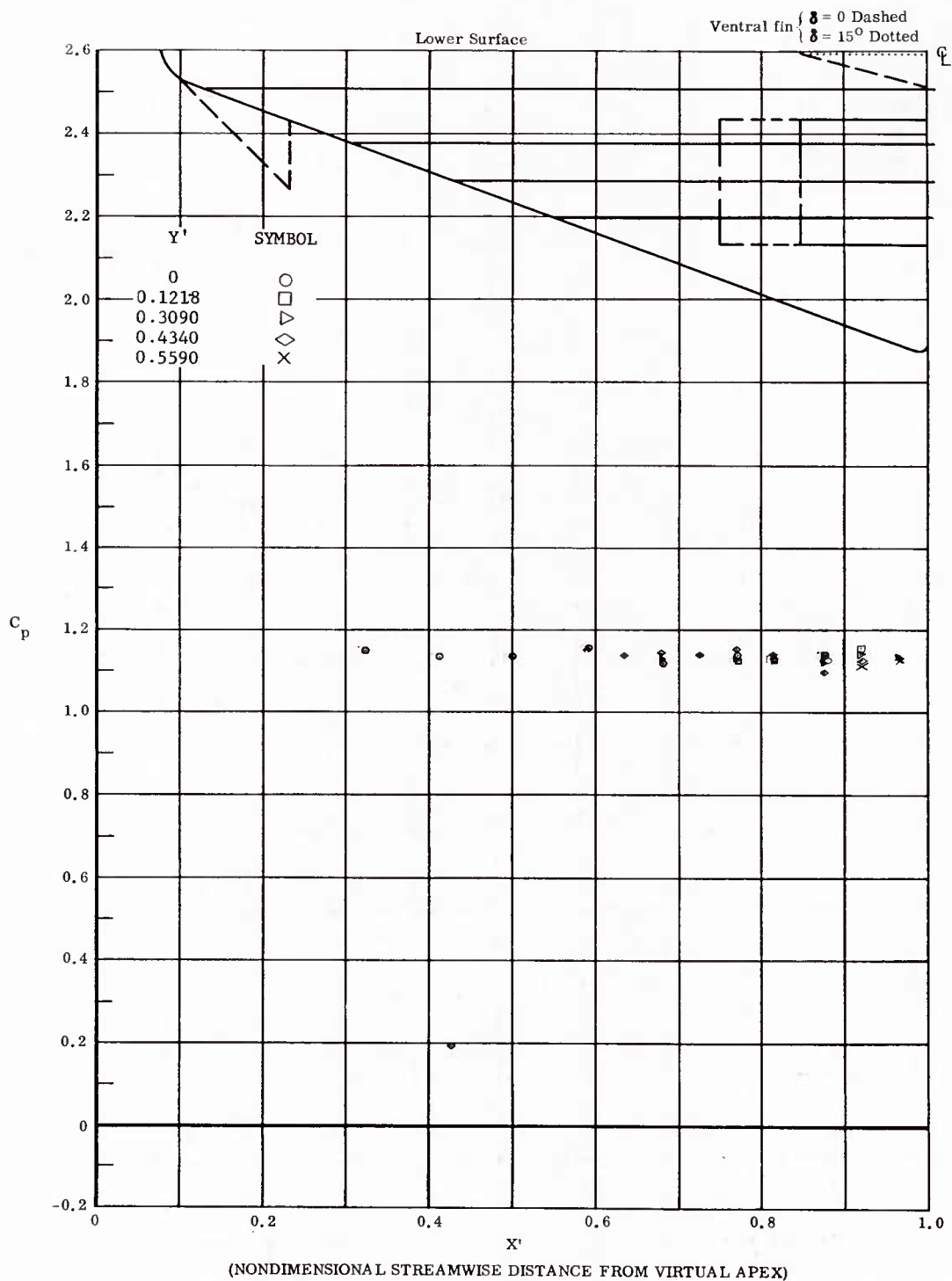


Fig. 95 Streamwise Distributions of Pressure Coefficients; Basic Configuration, Left and Right (Upper) Flaps Deflected  $-20^\circ$ ,  $\alpha = +45^\circ$ ,  $\beta = 0^\circ$ ,  $Re_\infty / ft = 3,300,000$ .

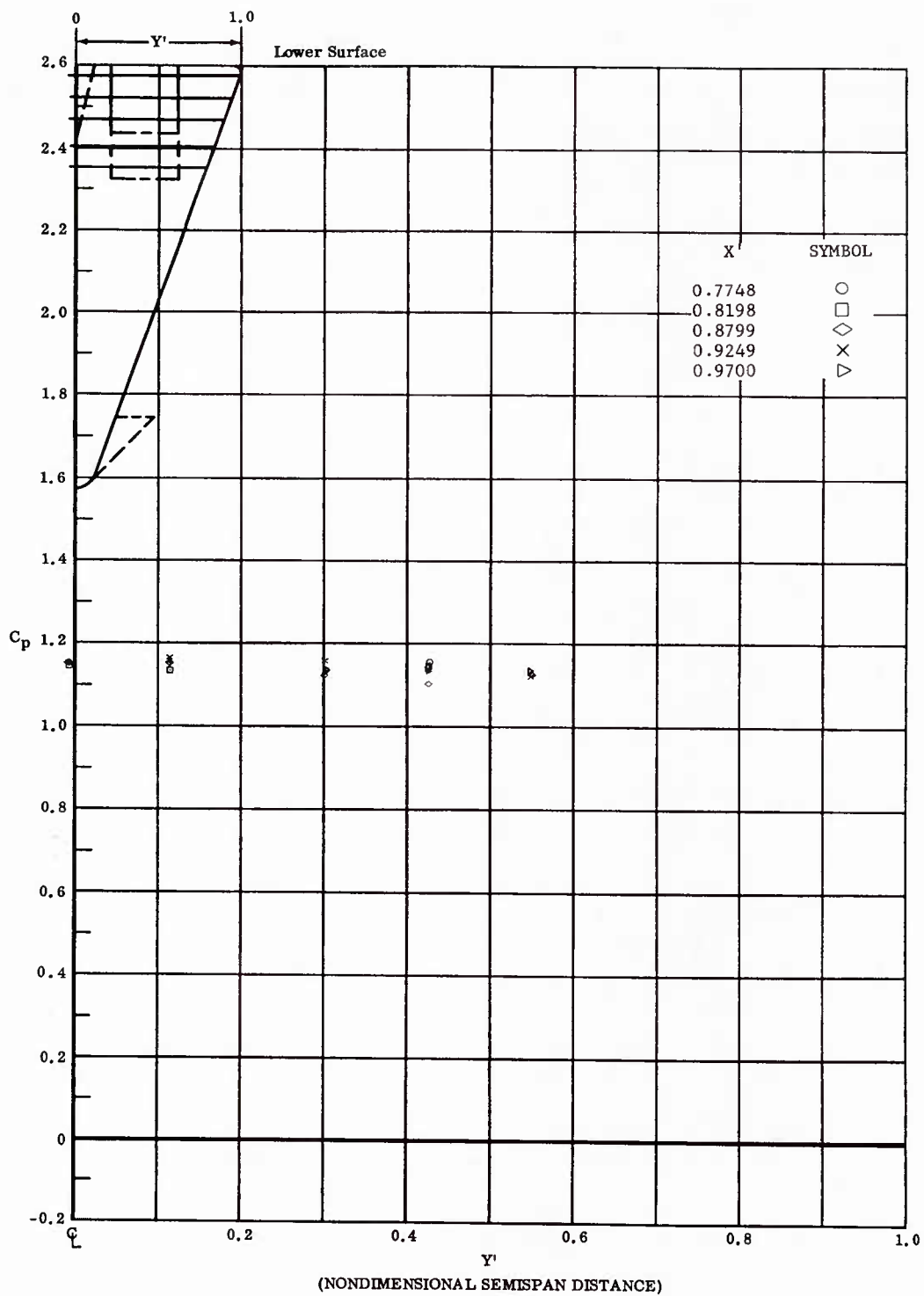


Fig. 95 Spanwise Distributions of Pressure Coefficients; Basic Configuration, Left and Right (Upper) Flaps Deflected  $-20^\circ$ ,  $\alpha = +45^\circ$ ,  $\beta = 0^\circ$ ,  $Re_\infty/ft = 3,300,000$ .

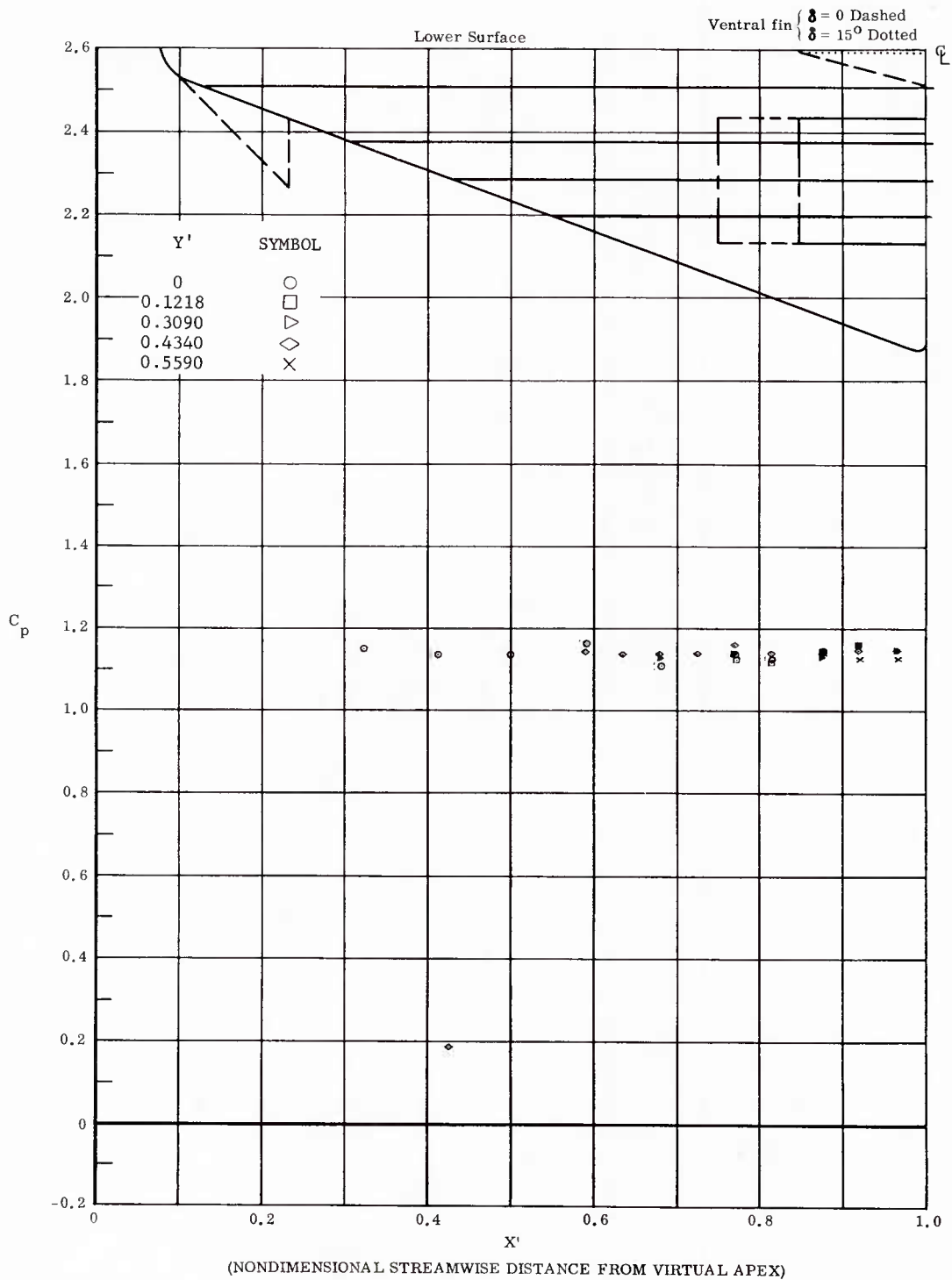


Fig. 96 Streamwise Distributions of Pressure Coefficients; Basic Configuration, No Flap Deflections,  $\alpha = +45^\circ$ ,  $\beta = 0^\circ$ ,  $Re_\infty/ft = 3,300,000$ .



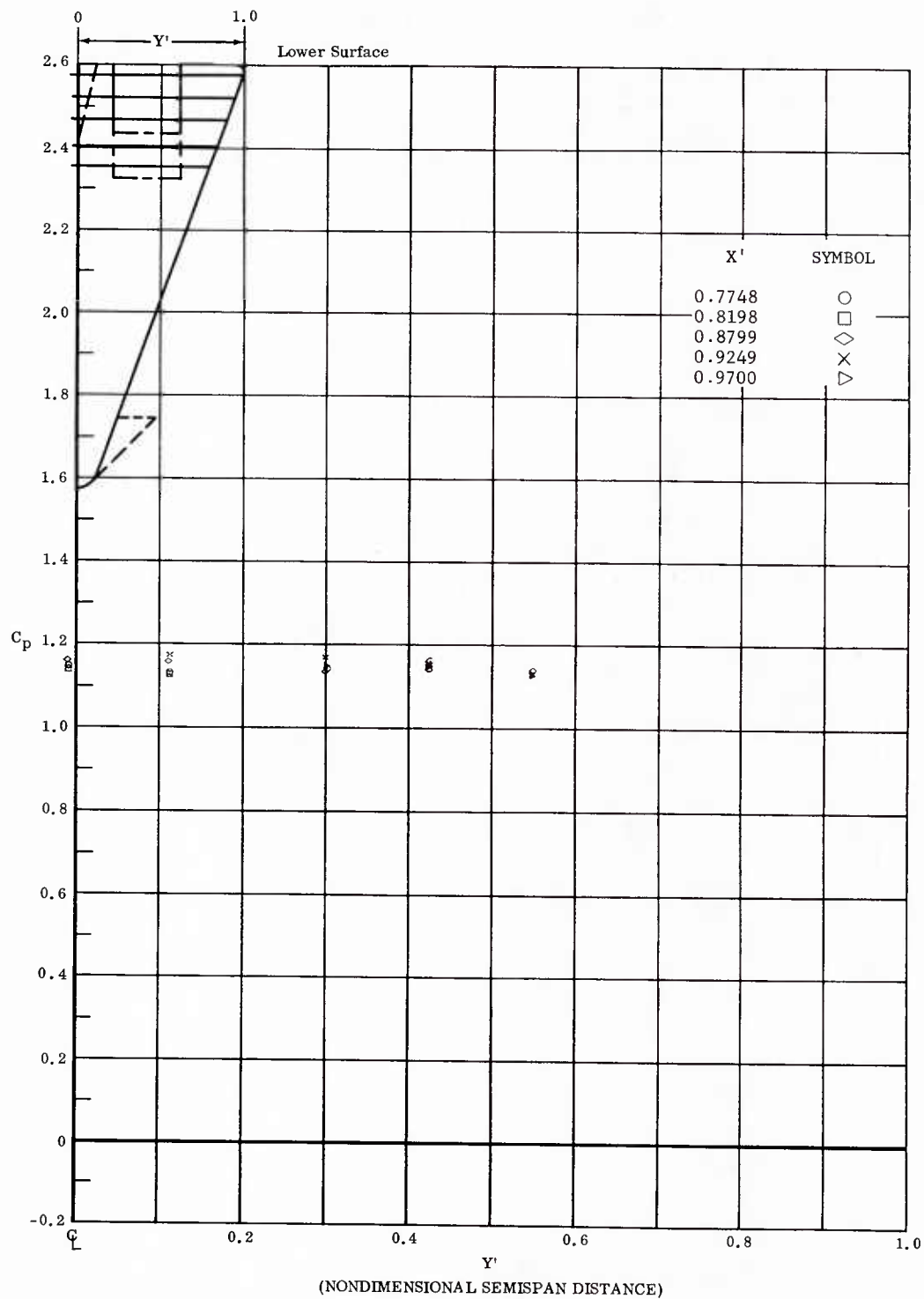


Fig. 96 Spanwise Distributions of Pressure Coefficients; Basic Configuration, No Flap Deflections,  $\alpha = +45^\circ$ ,  $\beta = 0^\circ$ ,  $Re_\infty/ft = 3,300,000$ .

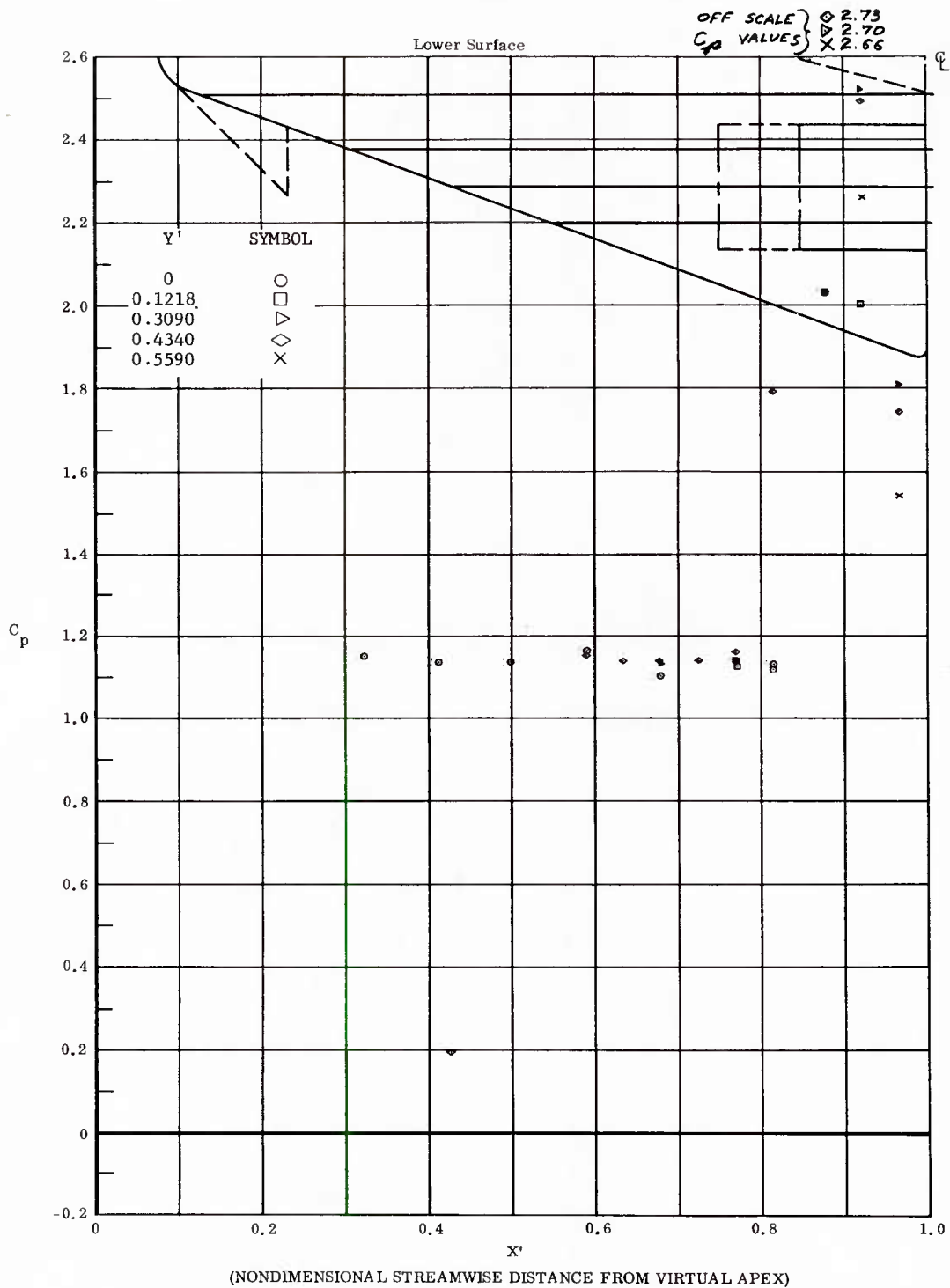


Fig. 97 Streamwise Distributions of Pressure Coefficients; Basic Configuration, Bottom Flaps Deflected  $+20^\circ$ ,  $\alpha = +45^\circ$ ,  $\beta = 0^\circ$ ,  $Re_\infty/\text{ft} = 3,300,000$ .

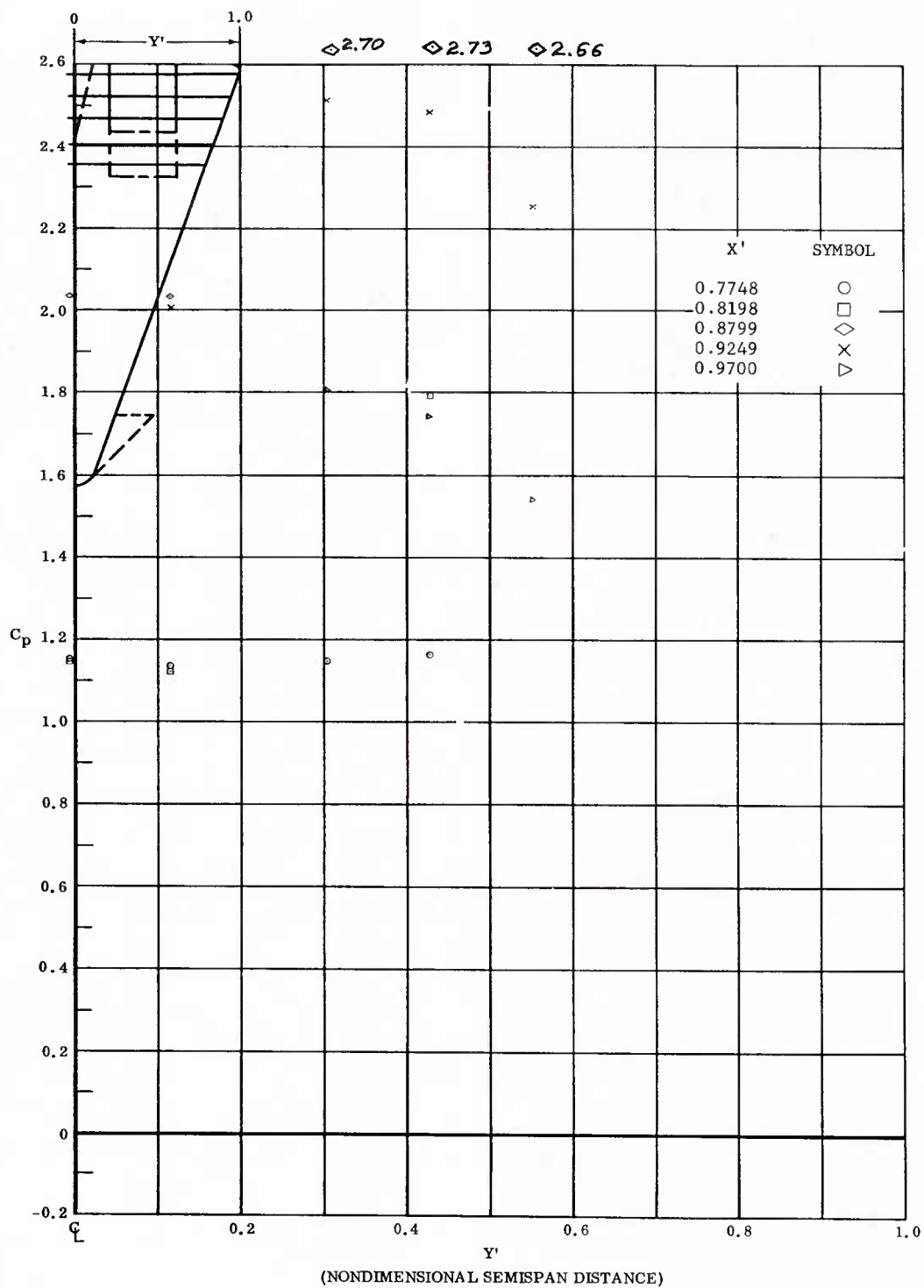


Fig. 97 Spanwise Distributions of Pressure Coefficients; Basic Configuration, Bottom Flaps Deflected  $+20^\circ$ ,  $\alpha = +45^\circ$ ,  $\beta = 0^\circ$ ,  $Re_\infty / ft = 3,300,000$ .

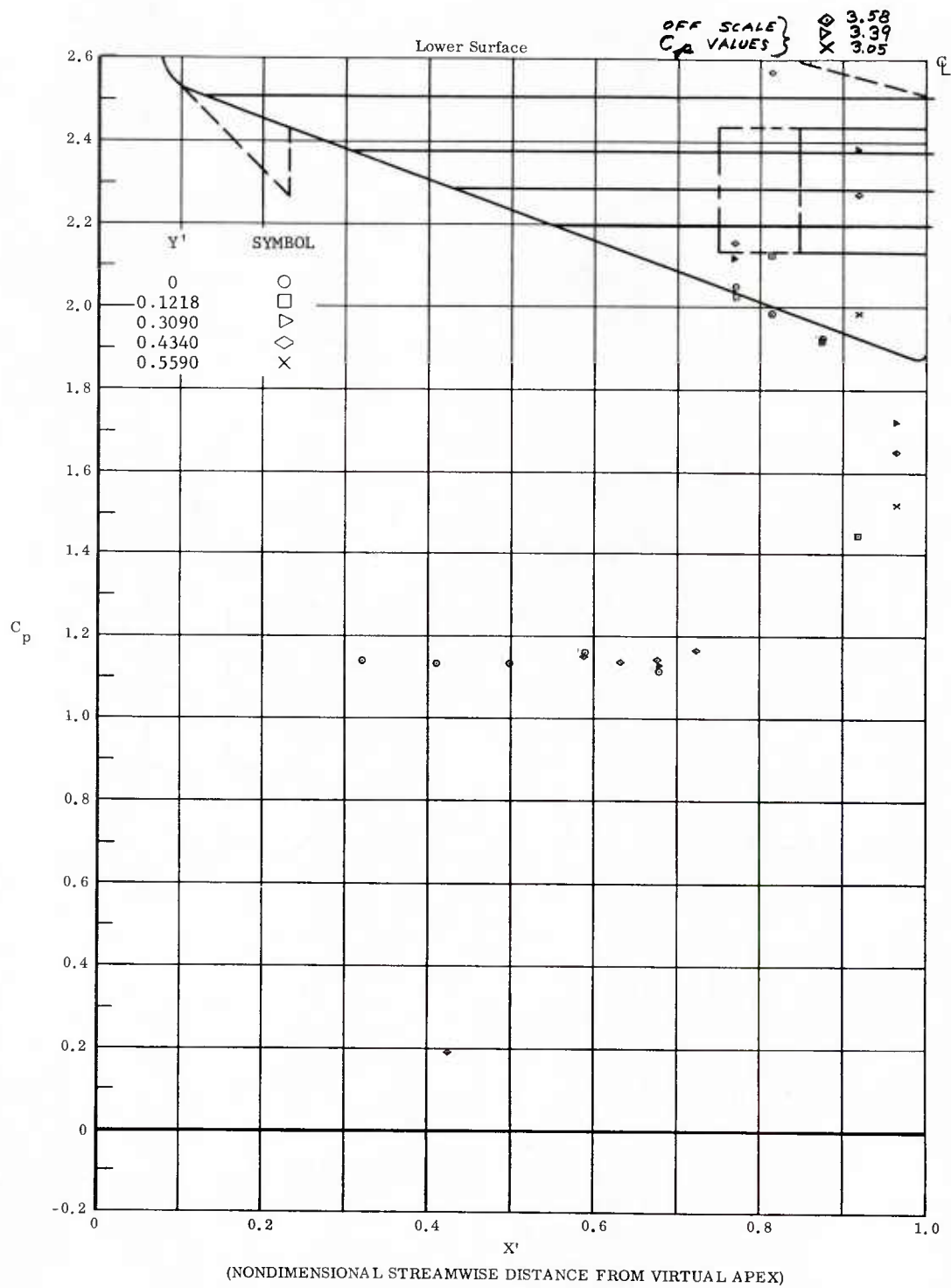


Fig. 93 Streamwise Distributions of Pressure Coefficients; Basic Configuration, Bottom Flaps Deflected  $+40^\circ$ ,  $\alpha = +45^\circ$ ,  $\beta = 0^\circ$ ,  $Re_\infty/ft = 3,300,000$ .

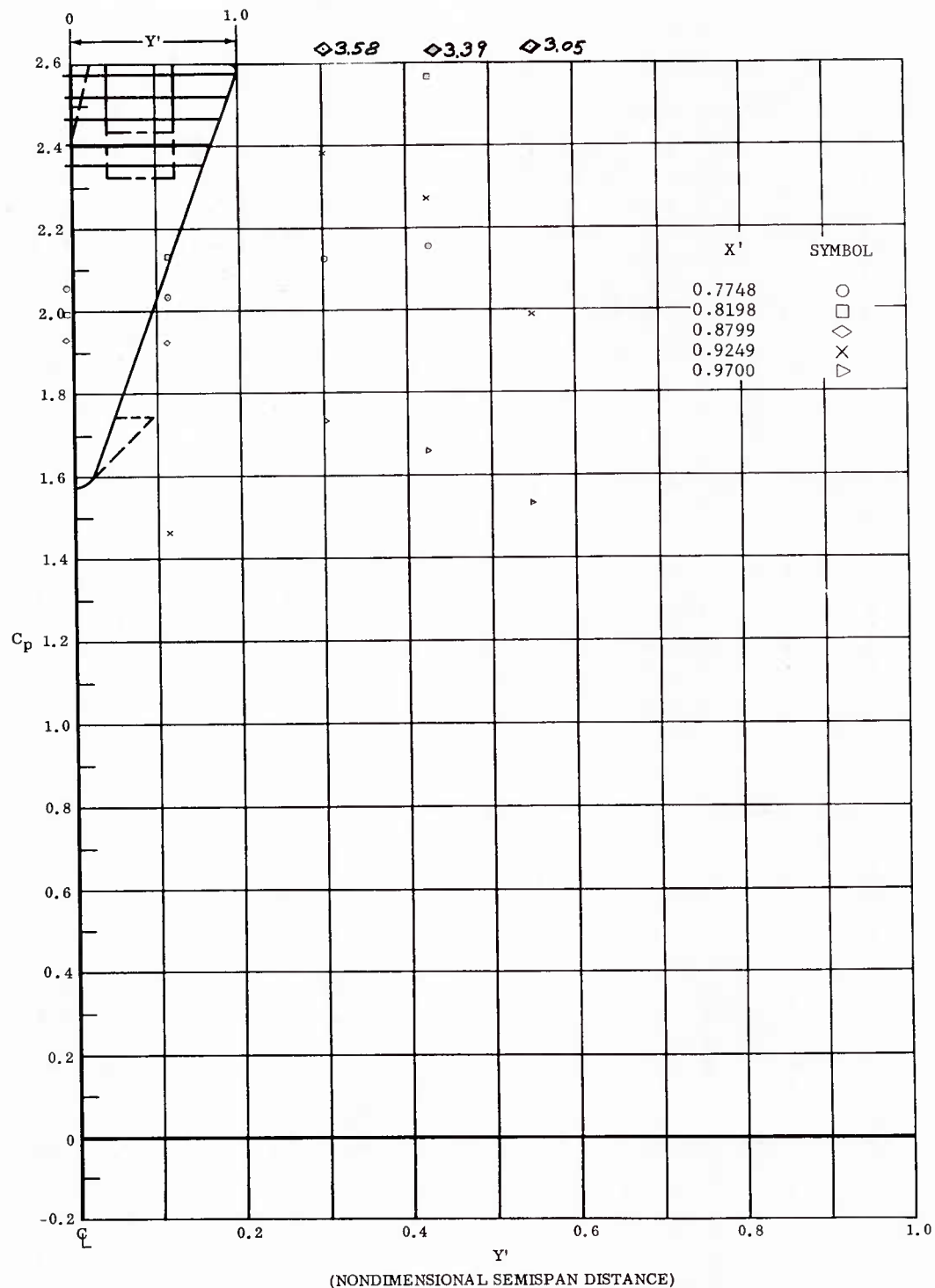


Fig. 98 Spanwise Distributions of Pressure Coefficients; Basic Configuration, Bottom Flaps Deflected  $+40^\circ$ ,  $\alpha = +45^\circ$ ,  $\beta = 0^\circ$ ,  $Re_\infty/ft = 3,300,000$ .

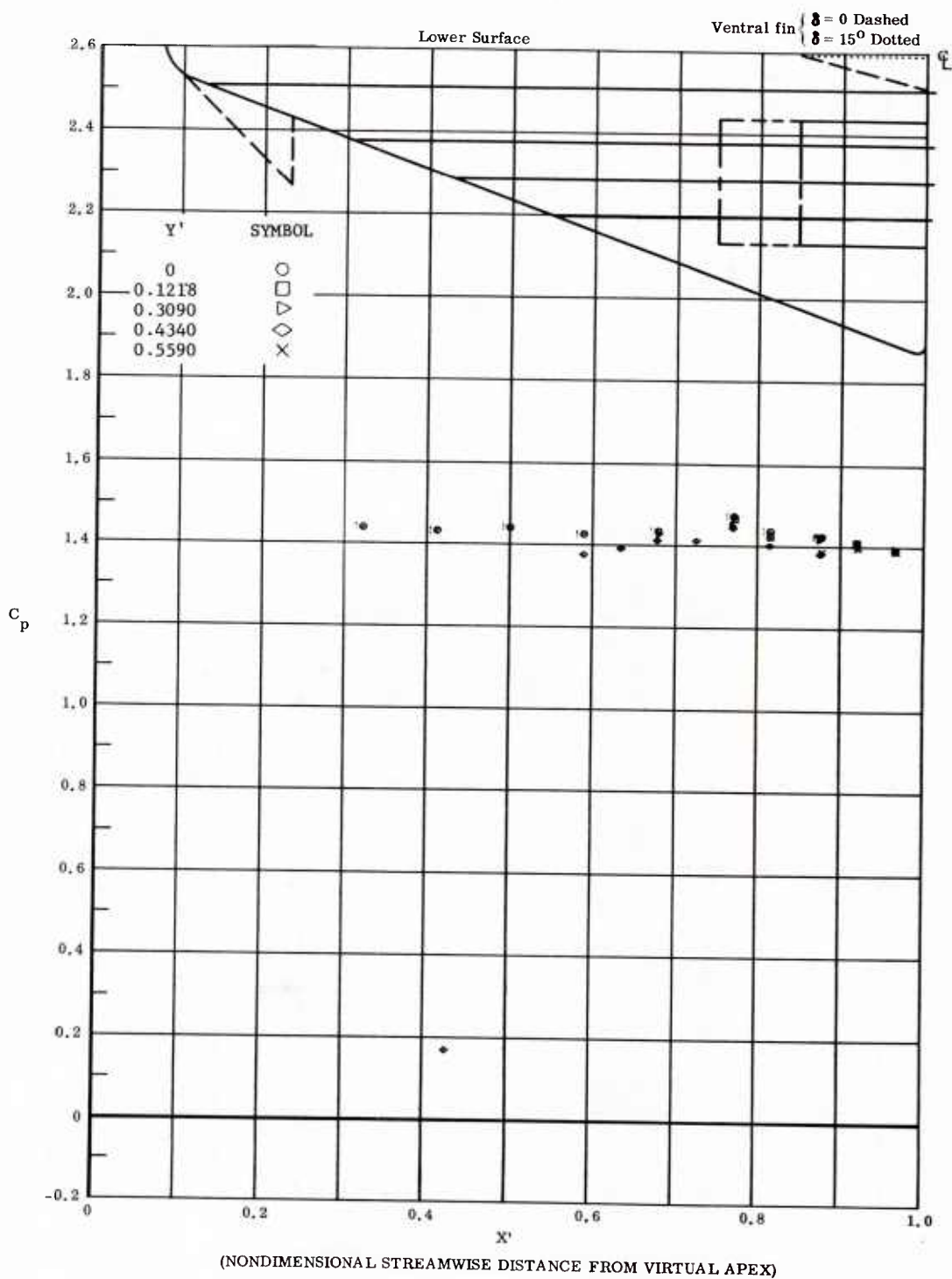


Fig. 99 Streamwise Distributions of Pressure Coefficients; Basic Configuration, Left and Right (Upper) Flaps Deflected  $-40^\circ$ ,  $\alpha = +54^\circ$ ,  $\beta = 0^\circ$ ,  $Re_\infty/ft = 3,300,000$ .

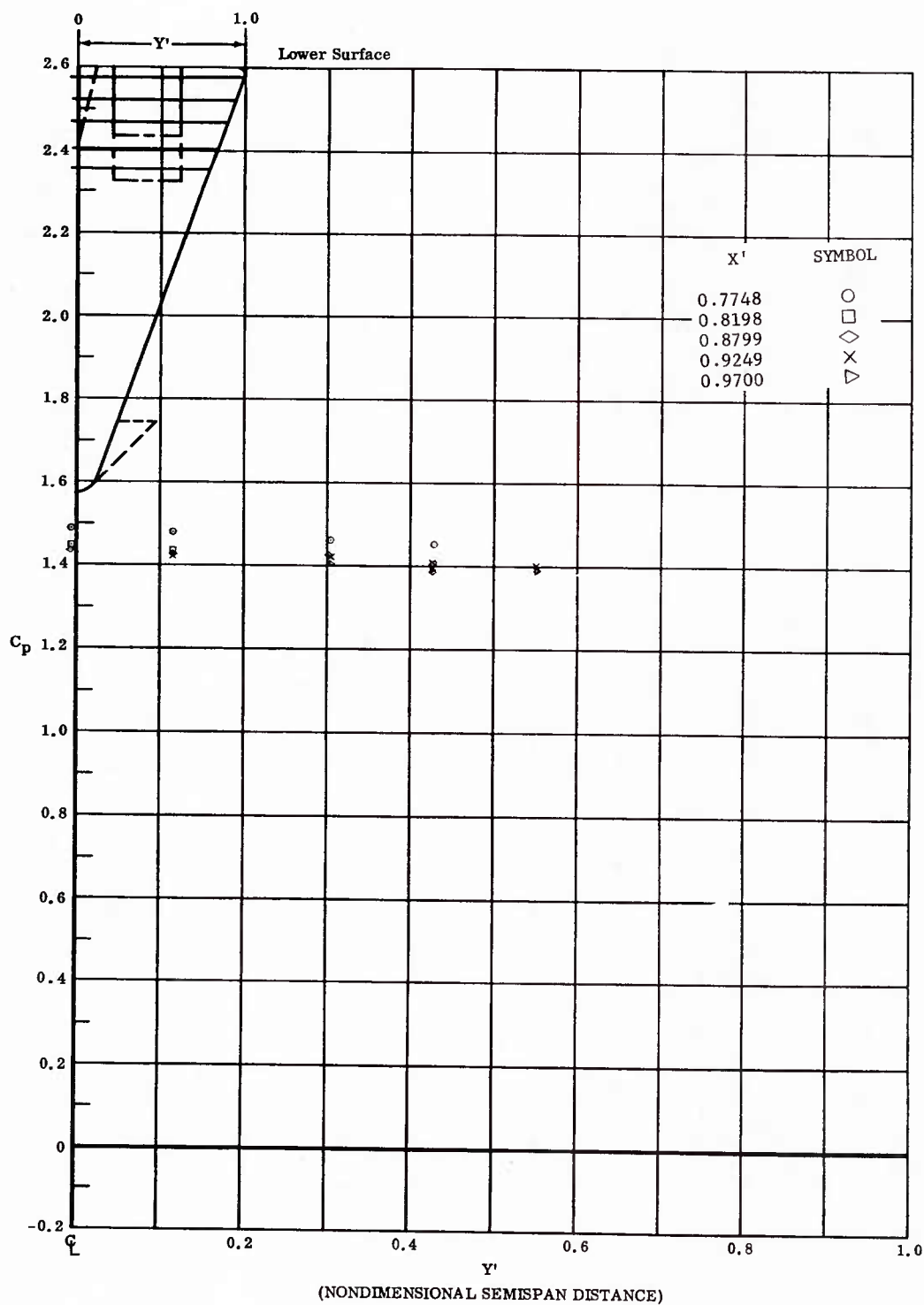


Fig. 99 Spanwise Distributions of Pressure Coefficients; Basic Configuration, Left and Right (Upper) Flaps Deflected  $-40^\circ$ ,  $\alpha = +54^\circ$ ,  $\beta = 0^\circ$ ,  $Re_\infty / ft = 3,300,000$ .

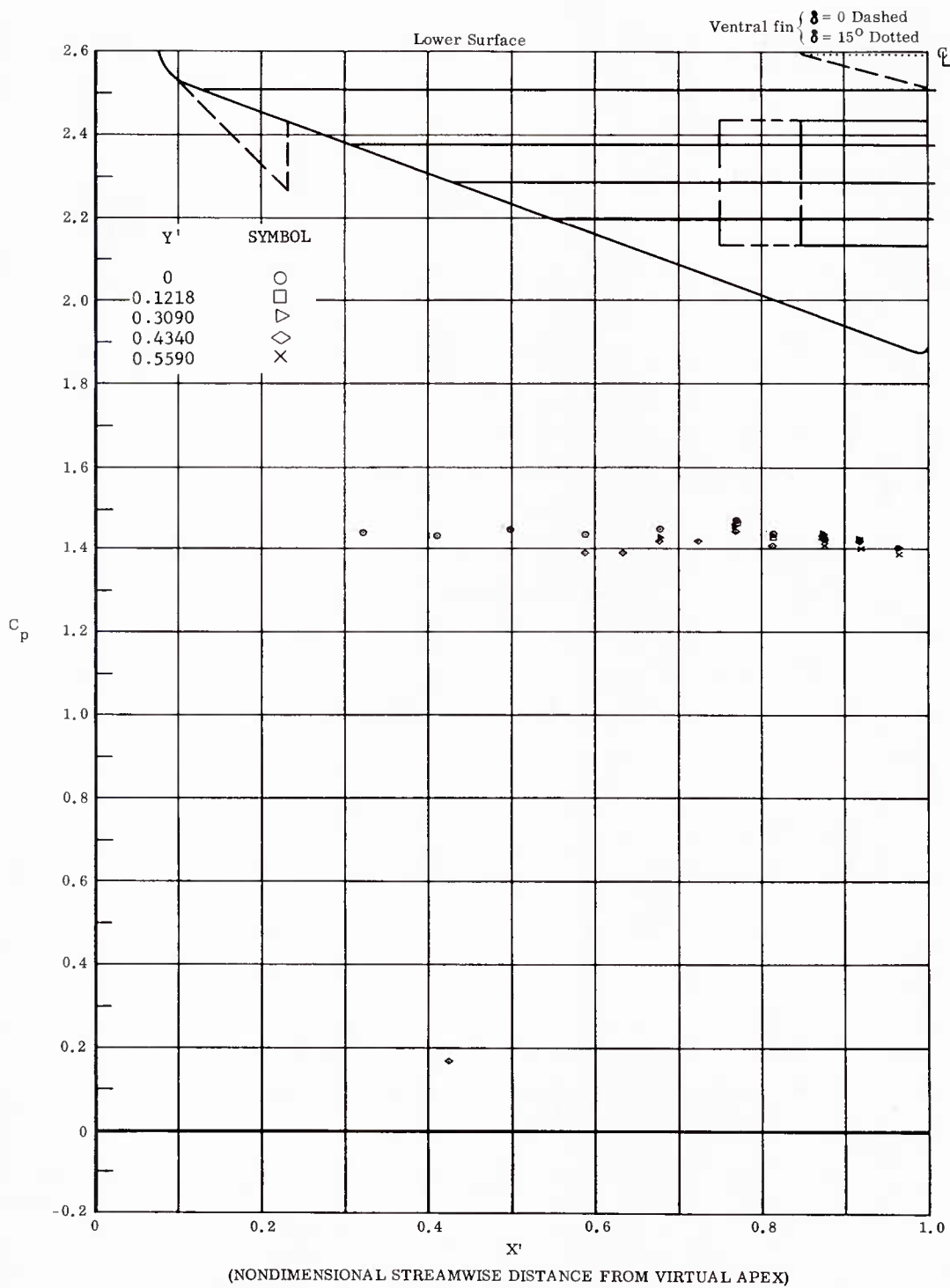


Fig. 100 Streamwise Distributions of Pressure Coefficients; Basic Configuration, No Flap Deflections,  $\alpha = +54^\circ$ ,  $\beta = 0^\circ$ ,  $Re_\infty / ft = 3,300,000$ .



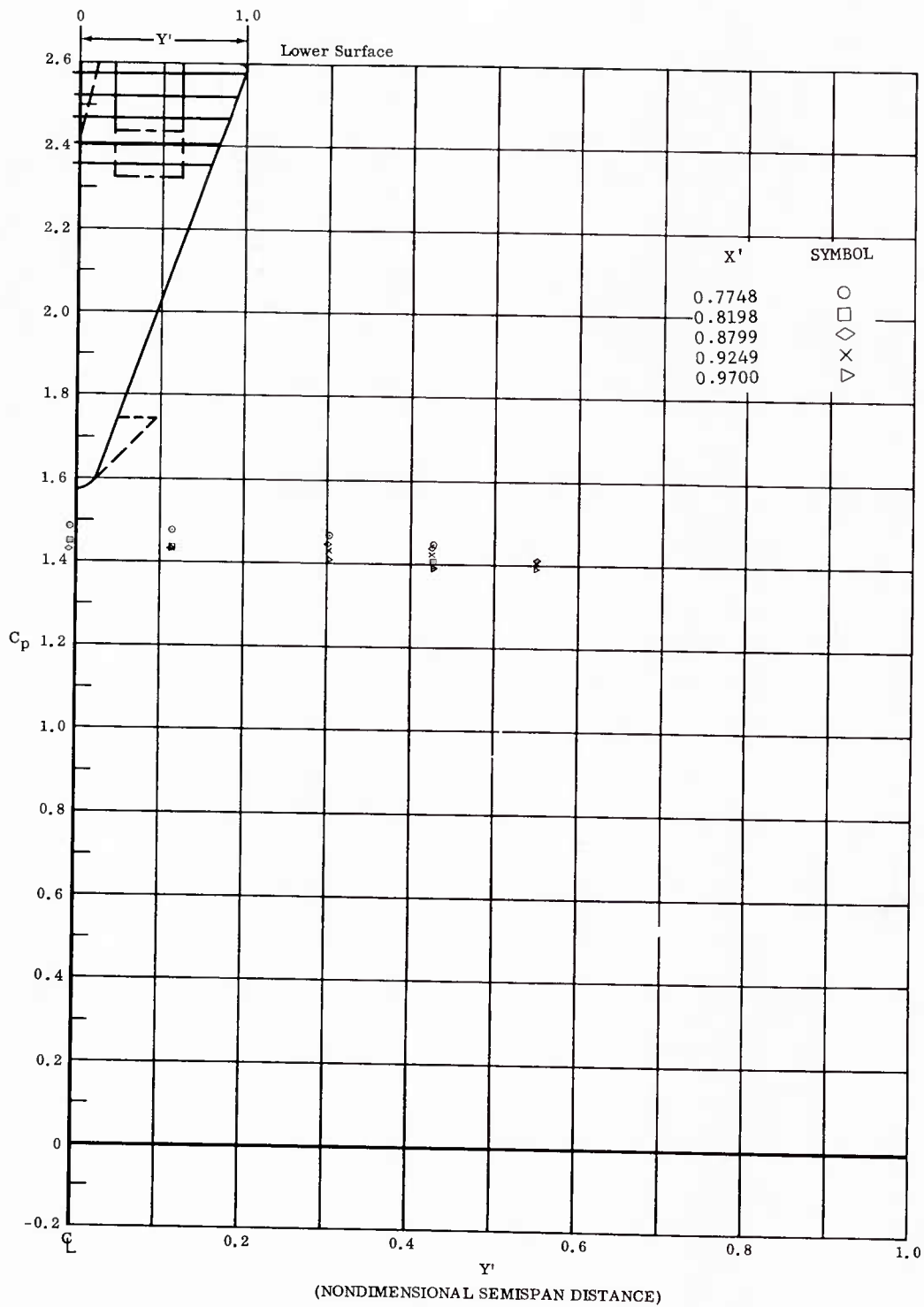


Fig. 100 Spanwise Distributions of Pressure Coefficients; Basic Configuration. No Flap Deflections,  $\alpha = +54^\circ$ ,  $\beta = 0^\circ$ ,  $Re_\infty/ft = 3,300,000$ .

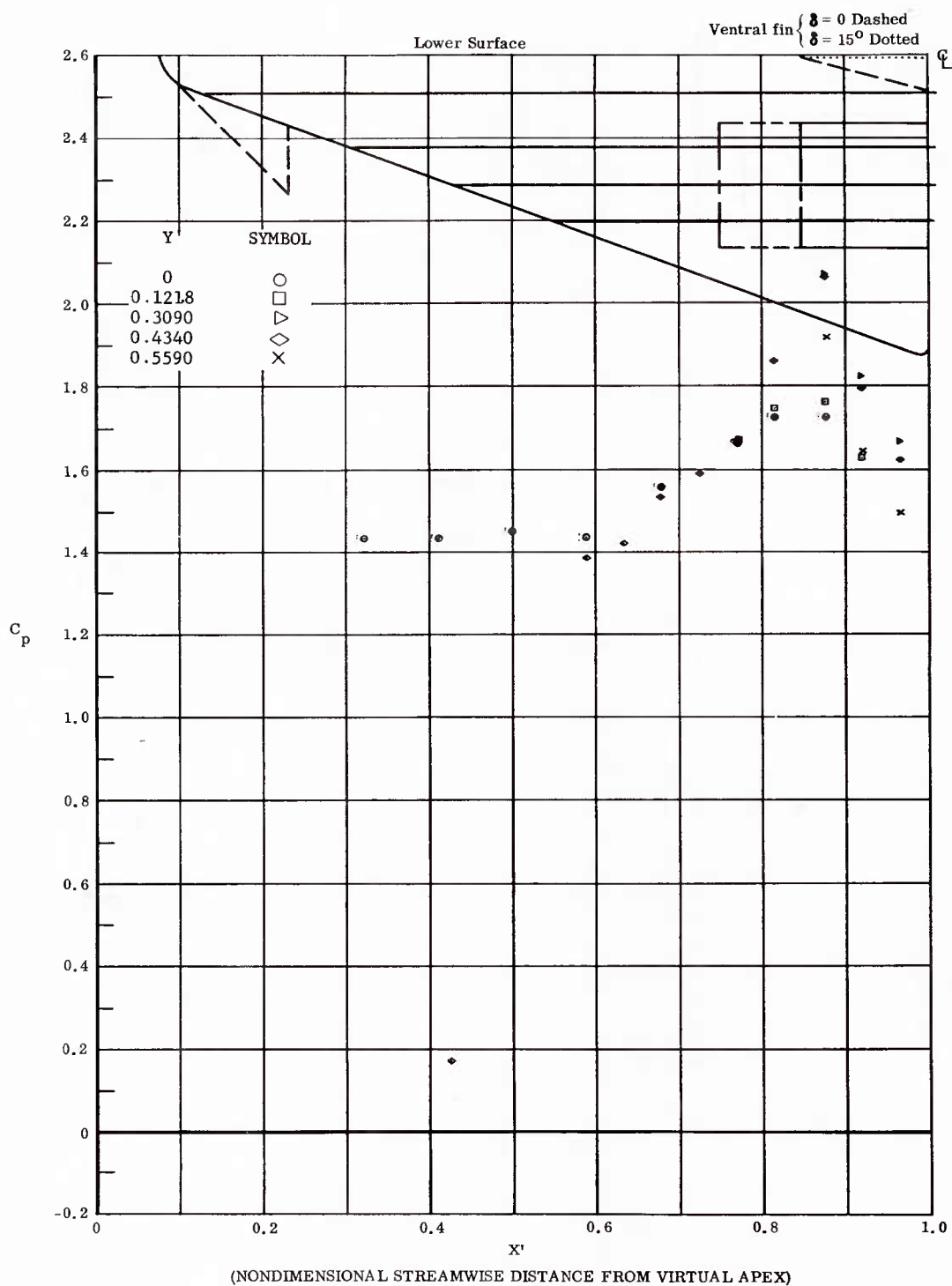


Fig. 101 Streamwise Distributions of Pressure Coefficients; Basic Configuration, Bottom Flaps Deflected  $+20^\circ$ ,  $\alpha = +54^\circ$ ,  $\beta = 0^\circ$ ,  $Re_\infty/ft = 3,300,000$ .

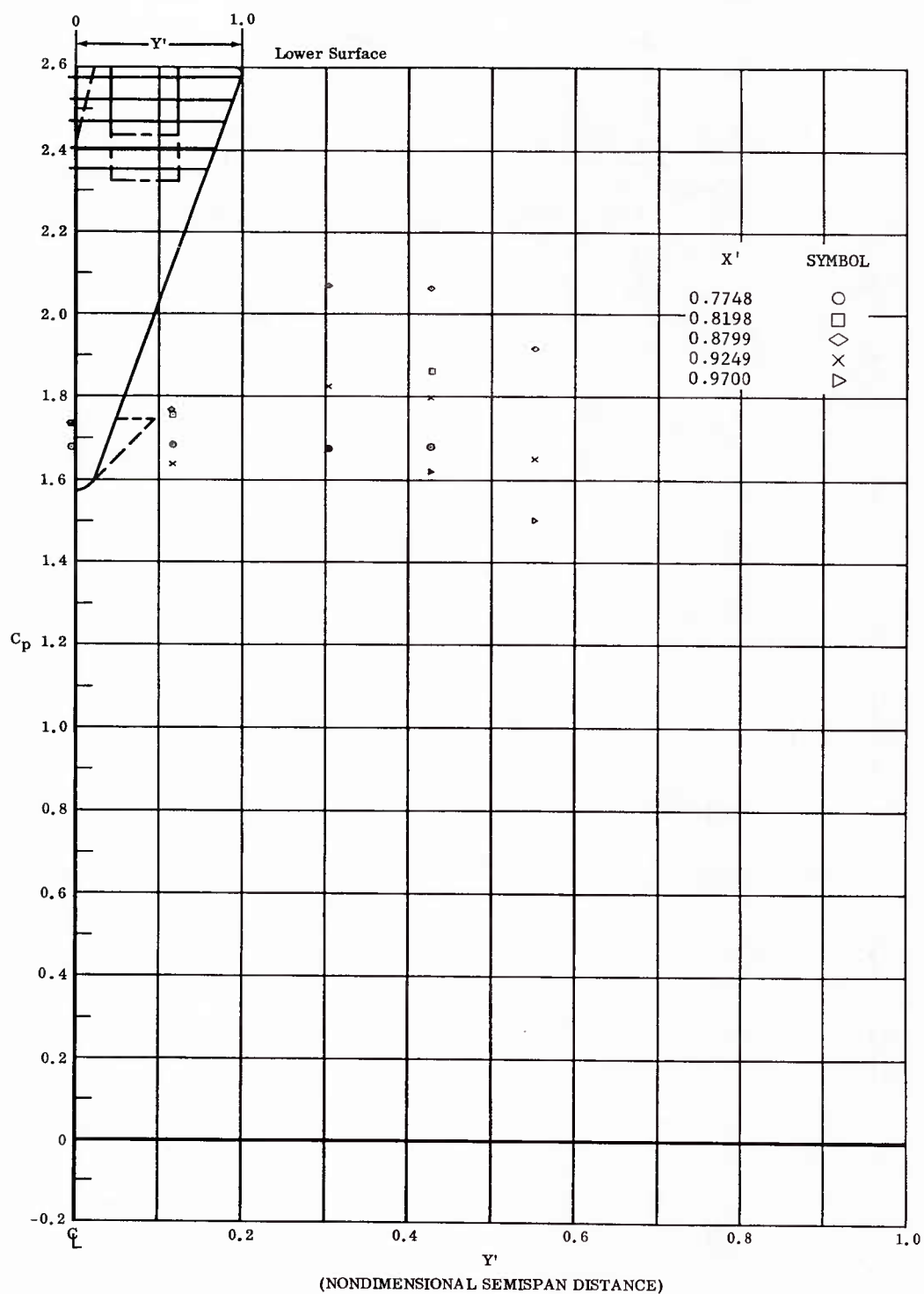


Fig. 101 Spanwise Distributions of Pressure Coefficients; Basic Configuration, Bottom Flaps Deflected  $+20^\circ$ ,  $\alpha = +54^\circ$ ,  $\beta = 0^\circ$ ,  $Re_\infty/ft = 3,300,000$ .

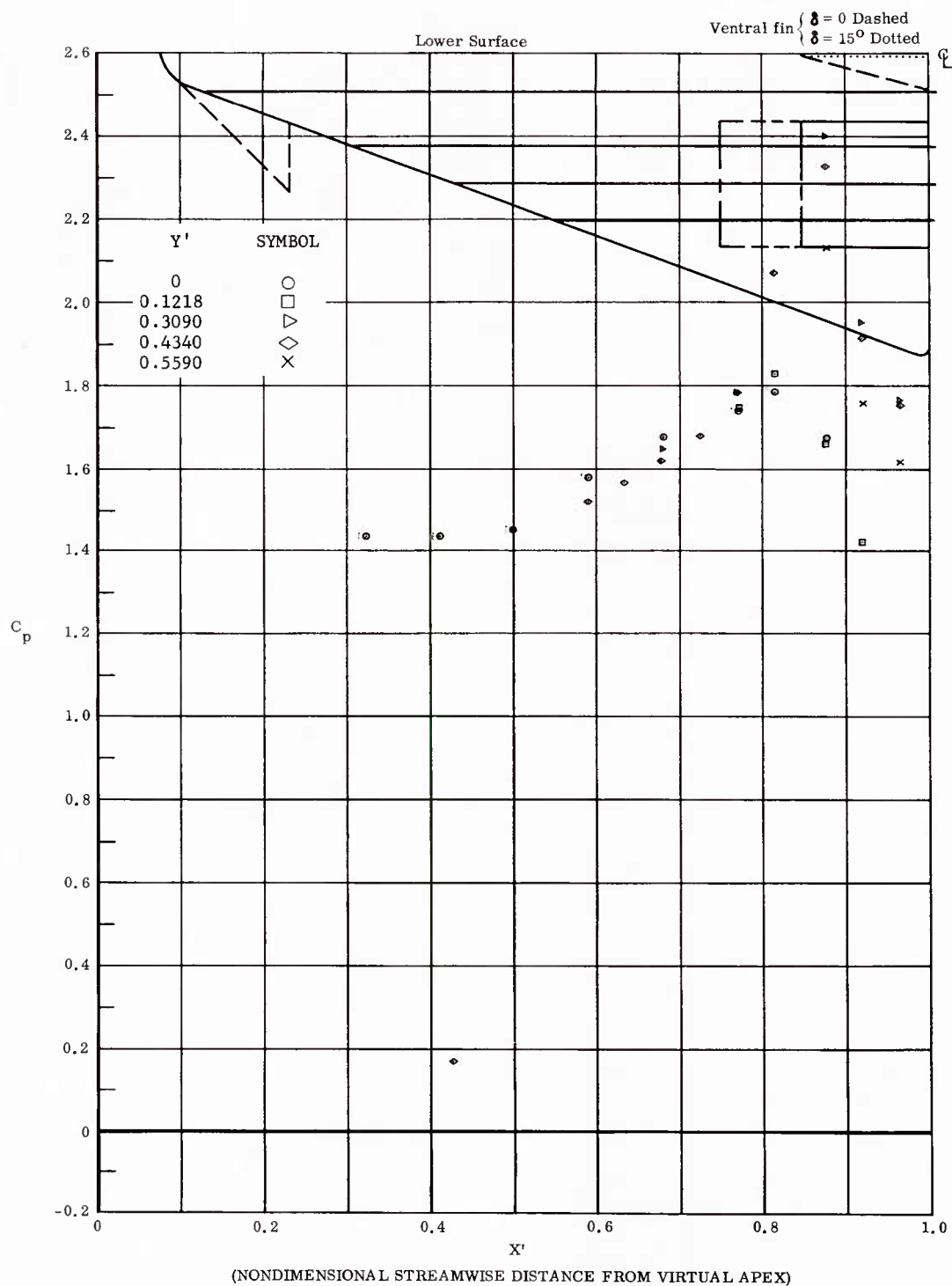


Fig. 102 Streamwise Distributions of Pressure Coefficients; Basic Configuration, Bottom Flaps Deflected  $+40^\circ$ ,  $\alpha = +54^\circ$ ,  $\beta = 0^\circ$ ,  $Re_\infty/ft = 3,300,000$ .

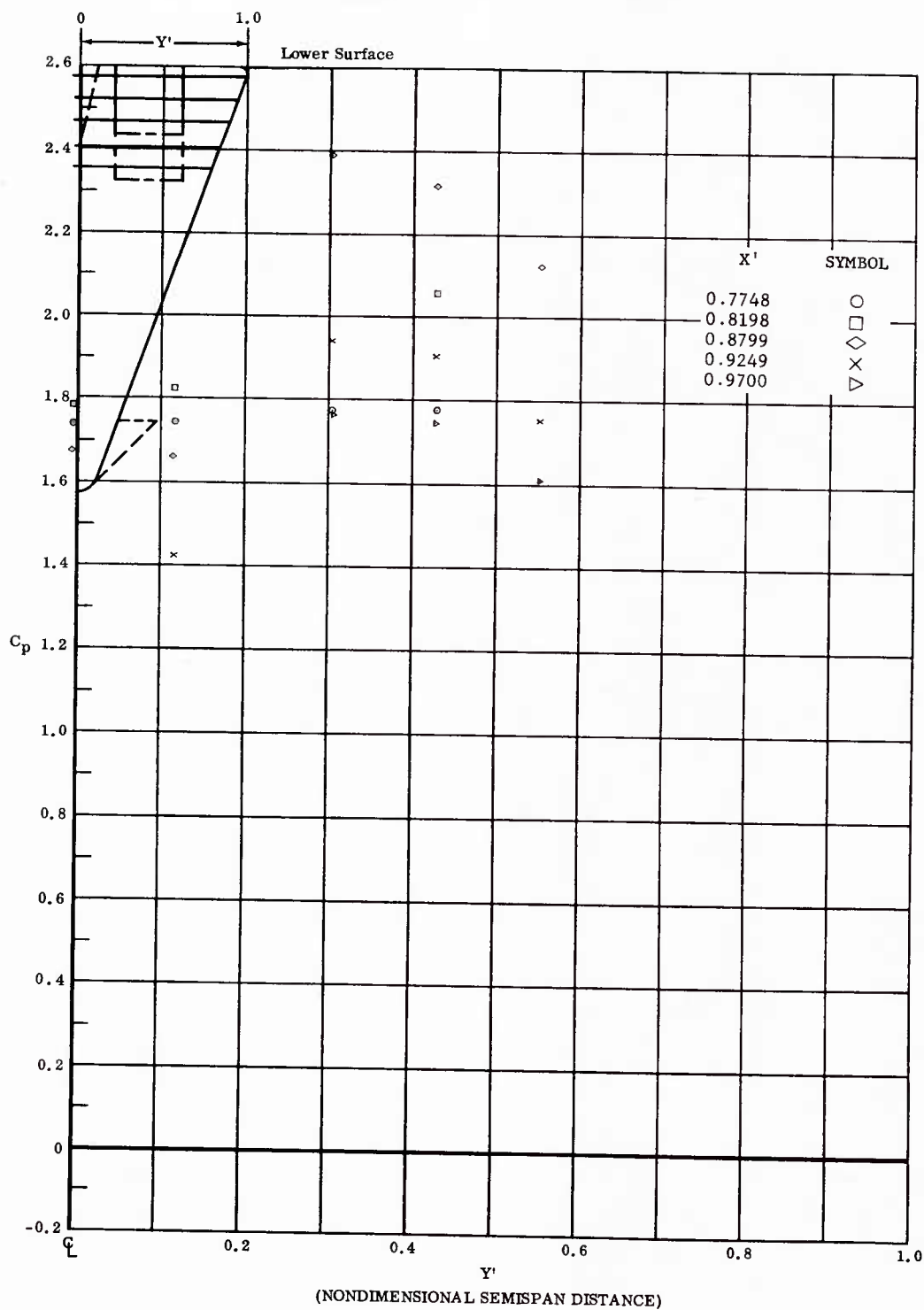


Fig. 102 Spanwise Distributions of Pressure Coefficients; Basic Configuration, Bottom Flaps Deflected  $+20^\circ$ ,  $\alpha = +54^\circ$ ,  $\beta = 0^\circ$ ,  $Re_\infty/ft = 3,300,000$ .